CONTENTS / OBSAH **3**

LIST OF REVIEWERS / ZOZNAM RECENZENTOV **5**

APPLICATION OF NON-DESTRUCTIVE TESTING METHODS TO IDENTIFY INHOMOGENEITY OF A SELECTED SAMPLE **6**
Pavol Višňovský, Peter Višňovský

A CRITICAL LITERATURE ANALYSIS BASED ON INVESTIGATION OF FRICTION STIR WELDING **11**
Pavol Višňovský, Peter Višňovský

NEGATIVE EFFECTS ACTING IN RENOVATION PROCESSES OF CLADDING **15**
Jozef Šutka, Andrej Zrak

MODIFYING NOZZLE ORIFICE TO IMPROVE CUTTING CAPABILITY OF PLASMA BEAM INVESTIGATED BY SIMULATION SOFTWARE **19**
Miloslav Málek, Miloš Mičian

SYNERGIC EFFECT OF TI AND ZR ON ALSI7MG0.3CU0.5 ALLOY FOR INVESTMENT CASTING TECHNOLOGY **23**
Michal Kuriš, Dana Bolibruchová, Marek Matejka, Martin Vicen

THE IMPACT OF COOLING MEDIA ON ALUMINUM ALLOY WITH INCREASED ZIRCONIUM CONTENT **31**
Lukáš Širanec, Elena Kantoríková, Dana Bolibruchová

EFFECT OF DIFFERENT WELDING PARAMETERS ON THE MECHANICAL PROPERTIES OF THE HSLA STEEL WELDED JOINT **36**
Martin Frátrik, Miloš Mičian

PLASMA NITRIDING OF TOOLS STEELS **40**
Elena Kantoríková, Denis Martinec, Richard Pastirčák

EVALUATION OF INFLUENCE OF FILTER MEDIA ON THE REOXIDATION PROCESSES WITH THE AID OF SIMULATION SOFTWARE **44**
Marek Galčík, Marek Brůna

ANALYSIS OF MEASURING SYSTEMS AND ITS THEORETICAL BASIS **48**
Ivan Litvaj

AUTOMATION OF INSPECTION PROCESSES BEFORE, DURING AND AFTER PRODUCTION PROCESS **53**
Aleš Mišura, Juraj Uríček

CLOUD COMPUTING **57**
Olha Kolesnyk, Peter Bubeník, Miroslav Rakyta

LOGISTIC SYSTEM SUPPORTED BY DIGITAL FACTORY **61**
Beáta Furmannová, Gabriela Gabajová, Marián Matys

FACTORIES OF THE FUTURE IN THE CONTEXT OF INDUSTRY 4.0 **65**
Patrik Grznár, Štefan Mozol, Marek Schickerle, Natália Buganová

ACOUSTIC PROPERTIES ANALYSIS OF A FREIGHT WAGON PROTOTYPE AT CONSTANT SPEED **69**
Pavol Šťastniak, Marián Moravčík, Vladimír Pavelčík, Erik Kuba

ANALYSIS OF FREIGHT TANK WAGON'S LONGITUDINAL FORCE TRANSMISSION ABILITY IN OPPOSITE TRACK CURVES **73**
Pavol Šťastniak, Marián Moravčík, Erik Kuba, Vladimír Pavelčík

METHODS FOR EVALUATION OF PASSENGERS' RIDE COMFORT IN VEHICLES **79**
Ján Dižo, Miroslav Blatnický, Stanislav Semenov, Evgeny Mikhailov

PRÍSPEVKY V SLOVENSKOM JAZYKU / ARTICLES IN THE SLOVAK LANGUAGE

SIMULÁCIA DILATÁCIE POTRUBIA POMOCOU EXPERIMENTÁLNEHO ZARIADENIA **86**
Juraj Drga, Michal Holubčík, Stanislav Gavlas

URČENIE TLAKOVEJ STRATY TLMIČOV HLUKU VO VZDUCHOTECHNIKE EXPERIMENTÁLNE A POMOCOU CFD METÓD **92**
Šimon Kubas, Andrej Kapjor, Martin Vantúch

MOŽNOSTI ÚPRAVY TVARU ROZTAVENEJ OBLASTI ZVARUPRI SIMULÁCIÍ OBLÚKOVÉHO ZVÁRANIA V PROGRAME SYSWELD **98**
Radoslav Koňár, Lukáš Petričko

POKROČILÉ POHONNÉ SYSTÉMY ELEKTROMOBILOV **102**
Laura Lichvajderova, Jaroslava Kádárová, Michal Puškár

NOVÝ OBRAZ BUDÚCNOSTI A TRENDY V GLOBÁLNEJ TRHOVEJ EKONOMIKE V 21. STOROČÍ, ADAPTÁCIA PODNIKU NA BUDÚCI VÝVOJ – ORGANIZAČNÝ ROZVOJ PODNIKU **107**
Ivan Litvaj

APLIKÁCIA CAD PROGRAMOV PRI TVORBE POČÍTAČOVÉHO MODELU PRE ZNÍŽENIE EMISIÍ HLUKU PREVODOVIEK **113**
Samuel Sivák, Silvia Maláková, Matúš Lavčák

NÁVRH VÝPOČTOVÉHO MODELU PRE ANALÝZU STAVU NAPÄTOSTI NA POVRCHU ZVARU S REÁLNOU GEOMETRIOU **119**
Peter Kopas, Marián Handrik, Milan Sága, Milan Vaško, Pavol Novák, Milan Uhríčik

NDT SKÚŠKA UMELÝCH SRDCOVÝCH CHLOPNÍ BSCC **125**
Milan Sapieta, Vladimír Dekýš, Peter Weis

VPLYV EXCENTRICITY ZVÁRACEJ TRAJEKTÓRIE A PREDOHREVU NA DEFORMÁCIU A ZVYŠKOVÉ NAPÄTIA HLINÍKOVEJ ZLIATINY ZVÁRANEJ ELEKTRÓNOVÝM LÚČOM **129**
Pavol Novák, Peter Kopas, Milan Vaško, Marián Handrik, Milan Sága

POROVNANIE SPÔSOBOV UMIESTNENIA MERACEJ TECHNIKY PRI POUŽITÍ OPTICKEJ LOCK-IN TERMOGRAFIE **134**
Ondrej Štalmach, Vladimír Dekýš, Václav Straka

KINEMATICKÁ ANALÝZA PRIESTOROVEJ VIAZANEJ MECHANICKEJ SÚSTAVY **139**
Alžbeta Sapietová, Vladimír Dekýš, Ondrej Štalmach, Milan Sapieta

List of Reviewers / Zoznam recenzentov príspevkov

doc. Ing. **Jozef BÍLIK**, PhD.

Ing. **Miroslav BLATNICKÝ**, PhD.

Ing. **Ján DIŽO**, PhD.

doc. Ing. **Ľuboslav DULINA**, PhD.

doc. Ing. **Patrik GRZNÁR**, PhD.

doc. Ing. **Michal HOLUBČÍK**, PhD.

Ing. **Elena KANTORÍKOVÁ**, PhD.

Ing. **Borislav MELO**, PhD.

doc. Ing. **Ján MORAVEC**, PhD.

doc. Ing. **Radovan NOSEK**, PhD.

doc. Ing. **Alena PAULIKOVÁ**, PhD.

doc. Ing. **Alexander SCHREK**, PhD.

Ing. **Andrej SUCHÁNEK**, PhD.

prof. Ing. **Pavol ŠVEC,** CSc.

doc. Ing. **Katarína TEPLICKÁ**, PhD.

Application of non-destructive testing methods to identify inhomogeneity of a selected sample

Pavol Višňovský, Ing., PhD.*
WELDING & TESTING OF MATERIALS, Ltd.,
Dlhá 1011/88 D, 010 09 Žilina, Slovak Republic.
E-mail: pavol.visnovsky@wtm.sk, Tel.: + 421 905 253 069

Peter Višňovský, Ing.
WELDING & TESTING OF MATERIALS, Ltd.,
Dlhá 1011/88 D, 010 09 Žilina, Slovak Republic.
E-mail: peter.visnovsky@wtm.sk, Tel.: + 421 907 853 172

Abstract: There are several methods for evaluating materials or components, and these methods inseparably include non-destructive methods with many possibilities within the application. The field of non-destructive testing (NDT) includes the identification and description of defects on the surface and inside materials without the material being cut or otherwise altered. Non-destructive testing refers to the process of evaluating and inspecting materials or components to identify errors and deficiencies compared to some standards without altering the original attributes or damaging the test object. NDT techniques provide a cost-effective way to test, whether it is testing a sample for individual purposes or can be used to test an entire material as part of a production quality control system. In this article, we focused on identifying the error on the pulley using three methods and then compare these methods and determine which can best identify the error. Three non-destructive testing methods were used, namely visual examination, ultrasonic testing and magnetic powder method.

INTRODUCTION

The field of non-destructive testing (NDT) includes the identification and description of damage or defects on the surface and inside materials without the material being cut or otherwise altered. It refers to the process of assessing or evaluating and inspecting materials or components to characterize or detect failures and deficiencies compared to standards without altering the original attributes or damaging the test object.

NDT techniques make available or provide a cost-effective means of testing a sample for individual examination and examination, or can be applied to all material for inspection in a production quality control system [1].

In many cases, the error detection approach requires more than the use of a single NDT test method. This may require a combination of methods.

A better understanding of the background, benefits and limitations of each NDT method is essential to ensure the success of the evaluation. Understanding one method of NDT alone may not be enough to ensure success in solving a problem [2].

A wide range of non-destructive testing methods play the most important role in testing composite materials.

NDT can be applied in many places, for example in production, in storage tanks, in aviation, in the military and defense, in the nuclear industry and in the description of compound defects.

Damage to composite materials can occur during material processing, component manufacturing, or activities such as cracking, porosity, and delamination [3].

Many techniques are used in the field of NDT, including:

- Radiographic testing.
- Visual testing (VT) or visual inspection (VI).
- Ultrasonic testing.
- Thermographic testing.
- Infrared thermographic testing.
- Acoustic emission (AE) testing.
- Electromagnetic testing.
- Shearographic testing.
- Optical testing.
- Liquid penetration testing.
- testing of magnetic particles and others.

This paper examines the various NDT methods for identifying and describing a specific defect in a selected sample, and then comparing the methods to determine the most effective method.

Defects can occur in composite materials during the manufacturing process or occur during normal life. The most common defects may be porosity, the presence of cavities and cracks in the matrix, and mostly delamination [4, 5, 6]. For these reasons, defect detection is becoming a critical activity to verify the integrity of structural parts [7, 8, 9].

There is a wide range of non-destructive techniques or methods, so here are some basic methods. The first three methods: VT, PT and MT were used to identify the discontinuity.

Visual testing (VT) or visual inspection, is one of the most common techniques, which involves the operator looking at a test specimen. The use of optical instruments, such as magnifiers or computer-aided systems, can help. This method allows the detection of corrosion, misalignment, damage, cracks and more. Visual testing is an integral part of most other NDT methods, as it will generally require the operator to look for discontinuities [10].

Penetration capillary testing (PT) involves the application of a low viscosity fluid to a test material. This fluid seeps into any defects, such as cracks or porosity, prior to developer application, which allows the penetrating fluid to seep upward and create a visible indication of a crack. Liquid penetration assays can be performed using solvent-removable penetrants, water-washable penetrants, or post-emulsifiable penetrants [11].

Magnetic powder testing (MT) uses magnetic fields to find discontinuities on or near the surface of ferromagnetic materials. The magnetic field can be formed by a permanent magnet or an electromagnet that requires a current supply. The magnetic field will accentuate any discontinuities because the magnetic flux lines cause leakage, which can be seen by the magnetic particles being drawn into the discontinuity [12].

Ultrasonic testing (UT) means the transmission of high frequency sound into a material to interact with the properties of the material that reflect or attenuate it. The pulse echo technique introduces a sound beam into the surface of the test material. The sound will move through the part, either reaching the back wall of the material and then returning to the transducer or returning earlier when it bounces off the discontinuity in the part. Transmission Testing uses separate transducers to transmit and receive audio [13]. The transmitting probe is located on one side of the test sample and the receiving transducer is located on the other side. When sound passes through a component, it is attenuated by elements in it, such as porosity. With this technique, it is usually not possible to measure the thickness. Ultrasonic testing with the PAUT phase system uses PAUT probes, which differ from conventional UT probes in that they consist of a set of individual elements that can be pulsed independently [14].

Acoustic emission (AE) is a passive NDT technique that relies on the detection of short ultrasound pulses emitted by active cracks under load. Surface-scattered sensors detect the structure of AE [15].

1 LITERATURE OVERVIEW

The issue is very current and is currently being addressed by many authors [16]. provided an overview of non-destructive testing (NDT) methods for composite evaluation. The review considers the possibilities of the most common methods in composite NDT applications, such as visual testing, ultrasound testing (UT), thermography, radiographic testing (RT), electromagnetic testing (ET), acoustic emission (AE), with regard to the advantages and disadvantages of these methods. Then, the methods were categorized based on their internal characteristics and their applications.

Kumar and Mahto [17] reported that non-destructive testing techniques typically use a form of sounding energy to determine material properties or to indicate the presence of material discontinuities (surface, internal, or hidden). It has also been found that most non-destructive testing techniques are mainly used in many places, such as the aerospace and engineering industries, and are likely to be used to evaluate civilian works and infrastructures. This document concludes that more research is needed to use these techniques in the field for civilian infrastructure. The authors seek to find the latest developments and trends available in industry and other areas in order to minimize damage, minimize overall equipment costs, and maximize the safety of equipment, machinery, structures, and materials.

M. Rojek et al. [18] explained fatigue and ultrasonic testing of epoxy glass composites. Epoxy glass composites are useful and are increasingly used as high-performance technical materials. They are used in areas such as construction, automotive, electronics, aerospace and many more. During the development and use of composites, many degradation processes occur. The main degradation effects are thermal aging, irradiation and chemical action, creep and fatigue. It shows the relationship between the degree of force degradation caused by fatigue and changes in the characteristics of ultrasonic waves, such as wave speed and damping coefficient [19]. A significant correlation was identified between the rate of propagation of ultrasonic waves and the degree of strength degradation of epoxy glass composites caused by fatigue. Ultrasound can be used as a useful tool to evaluate the fatigue degradation of polymer composites. This explains the mechanical properties such as flexural strength and the decrease in flexural modulus due to cyclic loading.

Aryan et al. [20] in their article provided an overview of state-of-the-art non-destructive testing (NDT) methods used to evaluate integrated circuit (IC) packaging. The review identifies the different types of defects and the capabilities of the most

common NDT methods used to detect defects. The main goal of their work is to provide a detailed overview of common NDT methods for IC packaging, which focus on their principles of operation, benefits, limitations and suggestions for improvement. Current methods such as X-rays, scanning acoustic microscopy (SAM), infrared thermography (IRT), magnetic current imaging (MCI) and surface acoustic waves (SAW) have been investigated. The uniqueness of the article lies in a comprehensive comparison of current NDT methods, recommendations for improvements and the introduction of new candidate NDT technologies that can be adopted for IC packaging.

Non-destructive testing (NDT) involves a wide range of techniques used in science and industry to evaluate material properties (e.g. residual stresses) without causing major damage. Because NDT does not cause any permanent changes in the controlled material, it is a valuable technique that can save money and time in evaluation and research. Therefore, non-destructive tests are often preferred over destructive ones. Shokrieh & Mohammadi [21] addressed this issue and in their article, they deal with the main methods that fall into the category of non-destructive methods for measuring residual stress.

Methods of non-destructive testing of wood are gaining in importance [22]. Online tools, such as production control, have been used for years. Based on the measurement system (physically active principle and important influencing factors), an overview of methods for the evaluation of cultural heritage objects is given. In order to adopt methods based on physical effects, a deep knowledge of wood physics is necessary, especially knowledge of interdependencies.

2 METHODOLOGY

This article provides an overview of the most common non-destructive testing (NDT) methods used by industry. The basics of NDT methods are explored in examining their potential, limitations, control techniques, and interpretations. Factors influencing the success of NDT methods are discussed and ways to mediate their impact are recommended. Reference is made to standard guidelines for the application and interpretation of the NDT methods discussed.

The aim of this paper was to analyze the selected sample and its inhomogeneity using three different NDT methods and then compare these three methods, in terms of interpretability of the results. Visual, penetration and magnetic powder methods were used for testing. The procedures were followed in accordance with the standards. The tests were performed by a technical worker of the company WELDING & TESTING OF MATERIALS, Ltd., who holds certificates in all three methods in level 2.

3 RESULTS

First, the positivity inhomogeneity was examined by visual testing. Visual inspection is particularly effective in detecting macroscopic defects such as bad welds.

Many welding defects are macroscopic, such as cracking, cutting, slag inclusion, incomplete penetration welds, and the like. Similarly, this method is also suitably used to detect deficiencies in composite structures and pipes of all types.

Bad welds or joints, missing fasteners or components, poor fit, wrong dimensions, wrong finish, large cracks, cavities, depressions, inadequate size, wrong parts, and more. In picture no. 1 we can see the investigated element and in picture no. 2, an error is highlighted in the yellow rectangular frame, which is also visible to the naked eye.

Fig. 1. Photographic recording from VT

Fig. 2. Indication of an error on the sample

Visual inspection revealed a linear inhomogeneity of 30 mm in laboratory conditions with artificial illumination of 1000 lux at a temperature of 20 °C. Simple measuring aids, a metal ruler, a caliper, a scale and a magnifier with 3x optical magnification were used. Standard EN 5817 was used.

The defect was documented and registered by the xyz spatial display.

A penetration check followed (Fig. 3 and Fig. 4). For comparison, the capillary test was performed on the given product at the same temperature values and illumination values.

At a development penetration time of 10 min. following wiping off the excess penetrant and applying the developer immediately after drying: the first evaluation was after 5 min., the second after 15 min., the inhomogeneity was shown at the same spatial values as in the visual test. Sprays from HELLING, U87, U88 and U89 were used. It was based on the general principles of EN 3452-1 and the degrees of acceptability at EN 23277 (degree of acceptability 1).

The wet fluorescence method was used in the magnetic test using a TIEDE pole magnetic instrument, Berthold scale, UV lamp (black light with an intensity of 20 lux), lux meter.

Fig. 3. Photographic record from NDT control by PT method

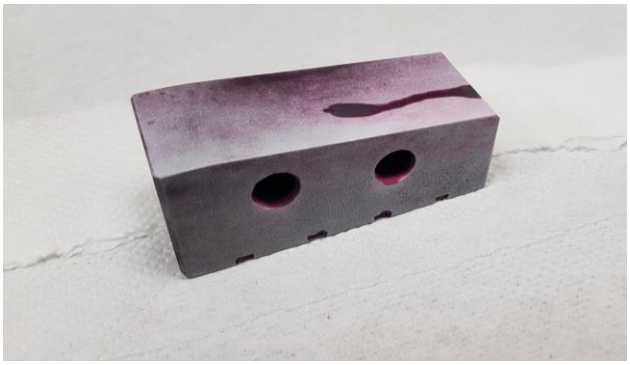

Fig. 4. Representation of the error by PT, evaluation after 5 min.

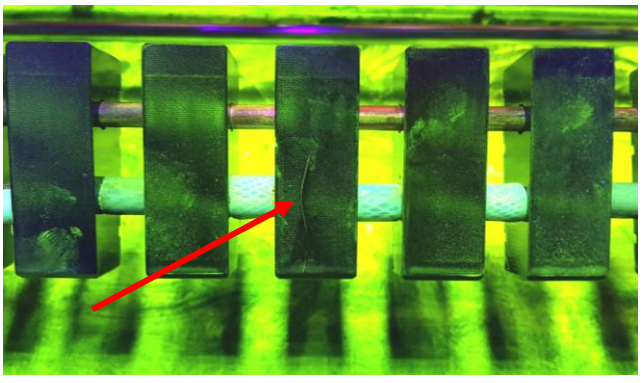

Fig. 5. Photographic record from MT with shown inhomogeneity

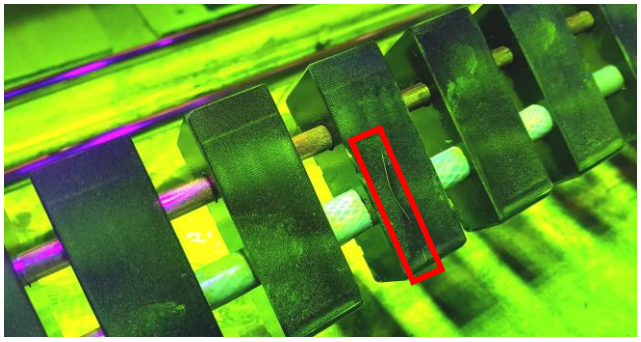

Fig. 6. Photographic record from NDT control by MT method

Linear inhomogeneity was found as in both previous methods (Fig. 5 and Fig. 6). The implementation was based on the standard EN 17638 and evaluated according to EN 23278, degree of acceptability 1.

The best results with the given methods were shown by the magnetic powder method, where the defect was best readable and interpretable.

CONCLUSION

Based on testing and review of the literature, we conclude that their various non-destructive techniques are applicable to the investigation of defects in materials.

These non-destructive techniques are used in various places, for example in the aerospace industry, the processing industry and civil infrastructure. These techniques have advantages and limitations depending on their use.

An overview of research conducted in the recent past shows that no non-destructive testing method gives us a sufficient result in the characterization of defects in a composite material, because they have their own limitations.

Therefore, a combination of two or more techniques is used to achieve a better result and increase the efficiency of the identification. The reliability and confidence level of a non-destructive test is usually increased by multiple test methods.

From the above research, we concluded that all methods used identified the error. However, the error was best seen with the magnetic powder method.

Acknowledgment

In this paper, we would like to thank the technical worker, Peter Planka, who participated in the implementation of individual tests and thus contributed to the creation of the contribution.

REFERENCES

[1] TIAN, G. Y., & SOPHIAN, A. (2005): *Reduction of lift-off effects for pulsed eddy current NDT*. NDT & E International, 38(4), 319-324.

[2] LIVITSANOS, G., SHETTY, N., VERSTRYNGE, E., WEVERS, M., VAN HEMELRIJCK, D., & AGGELIS, D. G. (2019): *Shear failure characterization in masonry components made with different mortars based on combined NDT methods*. Construction and Building Materials, 220, 690-700.

[3] CHAUVEAU, D. (2018): *Review of NDT and process monitoring techniques usable to produce high-quality parts by welding or additive manufacturing*. Welding in the World, 62(5), 1097-1118.

[4] BOLOTIN, E., SMOGORZEWSKA, M., SMITH, S., WIDMER, M., & WEINBERG, K. (1996): *Enhancement of thymopoiesis after bone marrow transplant by in vivo interleukin*-7.

[5] MALLICK, R. B., KANDHAL, P. S., & BRADBURY, R. L. (2008): *Using warm-mix asphalt technology to incorporate high percentage of reclaimed asphalt pavement material in asphalt mixtures*. Transportation Research Record, 2051(1), 71-79.

[6] GHOBADI, A., HAJIAN, H., GOKBAYRAK, M., DERESHGI, S. A., TOPRAK, A., BUTUN, B., & OZBAY, E. (2017): *Visible light nearly perfect absorber: an optimum unit cell arrangement for near absolute polarization insensitivity*. Optics Express, 25(22), 27624-27634.

[7] SHARP, T. D., ROTH, I. R. A., LIGGETT, U. M., & KESLER, J. M. (2012): *U.S. Patent No. 8,108,168*. Washington, DC: U.S. Patent and Trademark Office.

[8] HENDORFER, G., MAYR, G., ZAUNER, G., HASLHOFER, M., & PREE, R. (2007): *Quantitative determination of porosity by active thermography*. In AIP conference proceedings (Vol. 894, No. 1, pp. 702-708). American Institute of Physics.

[9] ALMOND, D. P. - PICKERING, S. G. (2012). *An analytical study of the pulsed thermography defect detection limit*. Journal of applied physics, 111(9), 093510.

[10] BECERRA, F. E. (2016): *Remote Visual Testing: NDT Initial Inspection of Turbines and Boilers*. Materials Evaluation, 74(12), 28-32.

[11] ROSHAN, C. C., RAGHUL, C., RAM, H. V., SURAJ, K. P., & SOLOMON, J. (2019). *Non-destructive testing by liquid penetrant testing and ultrasonic testing–A review*.

[12] WANG, Z. D., GU, Y., & WANG, Y. S. (2012): *A review of three magnetic NDT technologies*. Journal of Magnetism and Magnetic Materials, 324(4), 382-388.

[13] MA, H. W., ZHANG, X. H., & WEI, J. (2002). *Research on an ultrasonic NDT system for complex surface parts*. Journal of Materials Processing Technology, 129(1-3), 667-670.

[14] RAJ, B., SUBRAMANIAN, C. V., & JAYAKUMAR, T. (2000): *Non-destructive testing of weld*s.

[15] NAKAMURA, H., OHTSU, M., ENOKI, M., MIZUTANI, Y., SHIGEISHI, M., INABA, H. and SUGIMOTO, S. (2016): *Practical acoustic emission testing*. Springer, Society for Non-Destructive Inspection, Springer.

[16] GHOLIZADEH, S. (2016). *A review of non-destructive testing methods of composite materials*. Procedia Structural Integrity, 1, 50-57.

[17] KUMAR, S., & MAHTO, D. G. (2013): *Recent trends in industrial and other engineering applications of non destructive testing: a review*. International Journal of Scientific & Engineering Research, 4(9).

[18] ROJEK, M., STABIK, J., & WRÓBEL, G. (2005): *Ultrasonic methods in diagnostics of epoxy–glass composites*. Journal of Materials Processing Technology, 162, 121-126.

[19] VAVILOV, V. P. - BURLEIGH, D. D. (2015): *Review of pulsed thermal NDT: Physical principles, theory and data processing*. Ndt & E International, 73, 28-52.

[20] ARYAN, P., SAMPATH, S., & SOHN, H. (2018): *An overview of non-destructive testing methods for integrated circuit packaging inspection*. Sensors, 18(7), 1981.

[21] SHOKRIEH, M. M., & MOHAMMADI, A. G. (2014): *Non-destructive testing (NDT) techniques in the measurement of residual stresses in composite materials: an overview*. Residual stresses in composite materials (pp. 58-75). Woodhead Publishing.dd

[22] 21NIEMZ, P., & MANNES, D. (2012): *Non-destructive testing of wood and wood-based materials*. Journal of Cultural Heritage, 13(3), S26-S34.

A critical literature analysis based on investigation of friction stir welding

Pavol Višňovský, Ing., PhD.*
WELDING & TESTING OF MATERIALS, Ltd.,
Dlhá 1011/88 D, 010 09 Žilina, Slovak Republic.
E-mail: pavol.visnovsky@wtm.sk, Tel.: + 421 905 253 069

Peter Višňovský, Ing.
WELDING & TESTING OF MATERIALS, Ltd.,
Dlhá 1011/88 D, 010 09 Žilina, Slovak Republic.
E-mail: peter.visnovsky@wtm.sk, Tel.: + 421 907 853 172

Abstract: In the last two decades, we have witnessed increasingly intensive efforts to quantify scientific results in order to compare them. This is due to the growing importance of science in socio-economic development. This manifests itself primarily in the most developed parts of the world. An increasing amount of funding for science and research is forcing decision-makers to look for the clearest but also the simplest criteria that can help differentiate the prospects for scientific research, which deserves to strengthen funding from the dead ends of science, where money should not go. Despite the difficulty of objectively measuring phenomena which are as difficult to quantify as the quality of scientific outputs is undoubtedly, tools are emerging which make this possible with a greater or lesser degree of plausibility. One of them, on which a relatively large part of the representatives of science agree, is a bibliometric analysis, i.e. analysis of formal flows of scientific communication manifested primarily in professional publications. The area of friction stir welding is subject in this work to bibliometric analysis. We did not identify a similar article in our research, and therefore this analysis can be an asset in education and the technical sector as well as science and research.

INTRODUCTION

Friction Stir Welding (FSW) belongs to the group of solid-state welding and was developed by Thomas Wayne at The Welding Institute in Cambridge, UK in 1991. The principle of FSW welding is to push in a rotating tool with a special tool.) with an arm in the area of the contacting welded materials, which then moves in the direction of the line of the future weld. Heat is generated due to friction between the tool and the materials being welded (Fig. 1).

The authors in their publication [1] determine the effect of carbon content and conversion on mechanical properties and microstructures of FSW carbon steel joints were based on three types of carbon steels with different carbon content (IF steel, S12C, S35C) by friction welding under different welding conditions. Compared to IF steel, welding conditions are significantly affected by the microstructures and mechanical properties of carbon steel joints. The strength of the S12C steel joints increases with increasing welding speed, while the strength of the S35C steel joints shows a peak close to 200 $mm \cdot min^{-1}$. What they explain by the relationship between peak temperature and points A1 and A3. If friction welding is performed in the two-phase ferrite-austenite region, the microstructure is softened and the highest strength is achieved [1].

Friction welding (FSW) is a relatively new welding process that can have significant advantages over fusion processes: joining conventionally non-melting welded alloys, reducing distortion and improving the mechanical properties of weldable alloy joints due to pure solid state bonding of metals [3]. The Chen and Kovacovic model [3] includes the mechanical reaction of the tool and the thermomechanical process of the welded material.

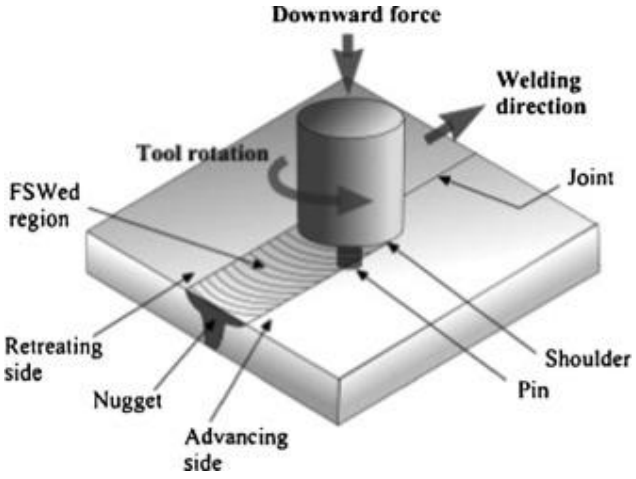

Fig. 1. Schematic drawing of FSW process [2].

The heat source built into the model involves friction between the material and the probe and arm. In order to provide a quantitative framework for understanding the dynamics of the thermomechanical FSW process, the thermal history and the development of longitudinal, lateral and transient stresses in the friction weld are simulated

numerically. The X-ray diffraction (XRD) technique is used to measure the residual stress of the welded plate and the measured results are used to verify the effectiveness of the proposed model. The relationship between the calculated residual weld stress and process parameters such as tool feed rate is given. It is expected that the model can be extended to optimize the FSW process to minimize residual weld stress [3].

Gibson et al. [4] also addressed this issue, and their article provides an introduction to the basic principles of friction mixing (FSW) as well as an overview of the latest research and applications in this field. The basic principles included include terminology, material flow, joint configuration, tool design, materials, and errors. The material flow is discussed from both an experimental and a modeling point of view. Process variants are also discussed, which include self-reactive (SR-FSW), stationary casting, friction mixing processing (FSP), friction spot welding (FSSW), assisted FSW, and pulsed FSW. Several aspects of robotic friction welding are included, including sensing, controlling, and monitoring joints. Methods for evaluating weld quality are also being investigated. The authors discuss the latest applications with an emphasis on recent advances in aerospace, automotive and shipbuilding. Finally, the direction of future research and potential applications are examined [4].

FSW was studied by Frigaard et al. [5] and in their present research, a numerical three-dimensional (3-D) heat flux model for friction stirring welding (FSW) based on the finite difference method was developed. The algorithm they implemented in MATLAB 5.2 is equipped with a separate module for calculating the development of the microstructure and the resulting hardness distribution. The process model is validated by comparison with in situ thermocouple measurements and experimental hardness profiles measured at specific time intervals after welding to reveal strength recovery during natural aging. They further characterized the grain structure in the plastically deformed region of the welded materials using the electron backscattered diffraction (EBSD) technique in a scanning electron microscope (SEM). Some practical applications of the process model are described at the end of the article [5].

Friction welding is a very complex process involving several highly related physical phenomena. The complex geometry of some types of joints and their three-dimensional nature make it difficult to develop an overall system of control equations for the theoretical analysis of the behavior of friction welded joints. Attempts are often time consuming and expensive. Numerical analysis has often been used since 2000 to overcome these problems. The paper by He et al. [6] provides an overview of the latest developments in the numerical analysis of friction welding processes, microstructures of friction welded joints and properties of friction welded structures. They address important numerical issues such as material flow modeling, networking process, and failure criteria. Numerical analysis of friction stir welding allows the simulation of many different welding processes to understand the effects of changes in various system parameters prior to physical testing, which would be time consuming or disproportionately expensive in practice. The main methods used in the numerical analysis of friction welding are discussed and illustrated by brief case studies. In addition, several important key issues related to numerical analysis of friction welding remain identified and opportunities for further research have been identified [6].

1 METHODOLOGY

The web of science database and the VosViewer technique were used to prepare this research paper, which was used for bibliometric analysis. We decided to analyze keywords that were 10 times higher in the 2019 articles on friction stir welding. A total of 768 articles were included in the analysis. Bibliometric analysis is very important and allows to create connections based on its outputs, which can lead to innovative thoughts and ideas.

The basic bibliometric analysis includes the results registered in the dataset of Web of Science in the year 2019. Due to the short time lag, the analysis does not work with bibliometric data relating to individual results (e.g. number of citations), but also with respect to the journals in which they are published. The basic bibliometric indicators are the Article Influence Score (AIS) for the WoS database and the Scimago Journal Rank (SJR) for the Scopus database. These indicators are created on the basis of the average number of citations of an article published in a given journal over the last 5 years (AIS) resp. 3 years (SJR) and unlike other indicators (eg impact factor) also take into account the quality of these citations. This analysis has different informative value for different fields - for some fields, publishing in impact journals is not a relevant quality measure - and the data provided are only evaluation criterion [7].

2 RESULTS

Figure 2 shows the most important keywords for 2019, which relate to the issue of friction stir welding and can point to new trends in this area. These are various models, methods and procedures, or other associations with this issue.

The next Figure 3 is the output of VosViewer and shows in which countries it is published the most on

this topic and what are the interconnections between countries.

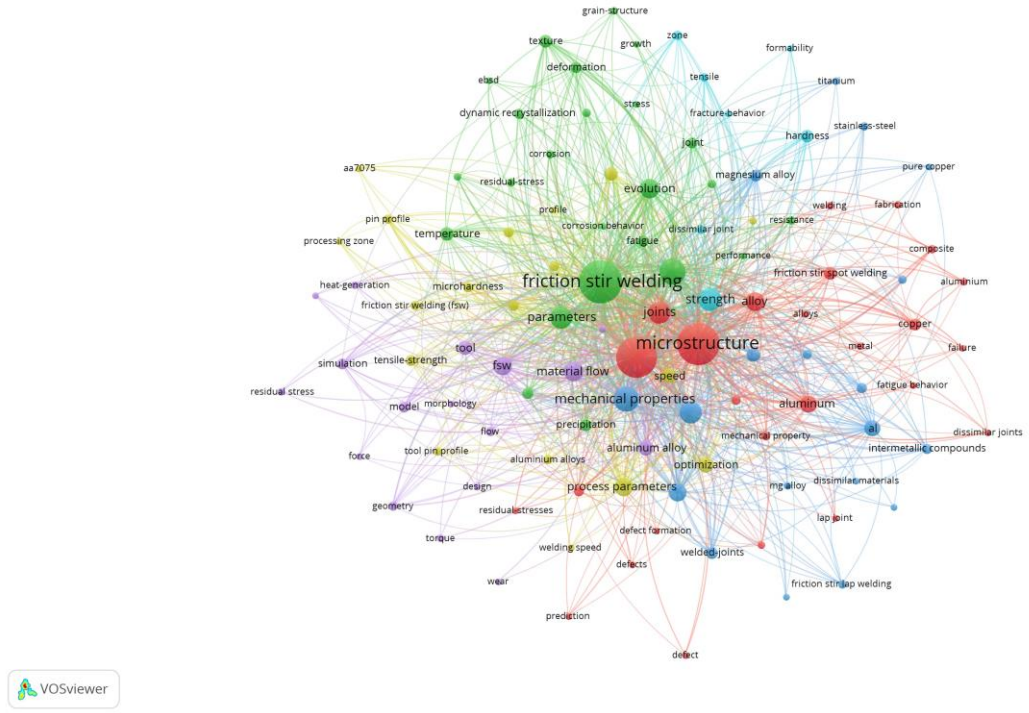

Fig. 2. Key words of friction stir welding

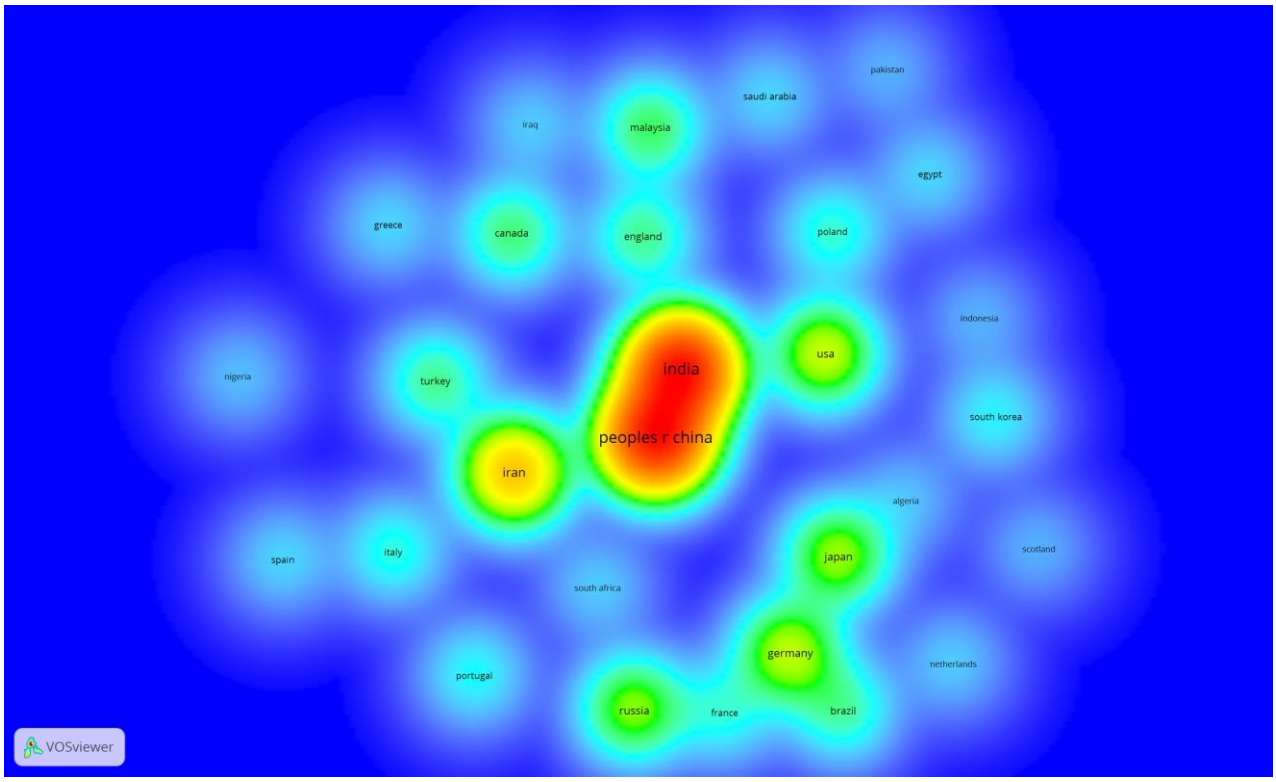

Fig. 3. Country´s connections through the friction stir welding

According to the analysis of countries, a total of 7 clusters were published and in the first largest cluster there are 11 countries that are interconnected. The first cluster includes Canada, Egypt, England, India Iraq, China, Malaysia, Pakistan, Saudi Arabia, Poland. The second cluster is Brazil, France, Germany, Algeria, Netherland, Russia, Scotland. The third cluster includes South Africa, Turkey, Nigeria, Iran. The fourth cluster is Italy, Portugal and Spain.

In the fifth cluster Japan and South Korea in the sixth is only Greece and in the seventh Indonesia. The strongest relationships are in the first cluster and this relationship is shown in red.

CONCLUSION

The field of friction stir welding is very interesting and constantly subject to innovation. Bibliometric analysis can help to reveal other connections and connections between. The results of a feasibility study of an innovative friction welding technique by mixing for the production of different metal-composite joints are presented. The new method uses the heat produced on the upper aluminum sheet by a rotating non-spindle tool to soften the composite thermoplastic matrix material. Cost-effective, long-lasting tools are available for aluminum and other soft alloys. They have been developed but are not currently available for the commercial application of FSW to high strength materials. Tool material properties such as strength, fracture toughness, hardness, thermal conductivity and coefficient of thermal expansion affect weld quality, wear and tool performance. It is necessary to constantly monitor current trends, and at the same time cross-border cooperation within other fields also contributes greatly to innovation.

REFERENCES

[1] FUJII, H. - CUI, L. - TSUJI, N. - MAEDA, M. - NAKATA, K. - NOGI, K. (2006). *Friction stir welding of carbon steels*. Materials Science and Engineering: A, 429(1-2), 50-57.

[2] GEMME, F. - VERREMAN, Y. - DUBOURG, L. - JAHAZI, M. (2010). *Numerical analysis of the dwell phase in friction stir welding and comparison with experimental data*. Materials Science and Engineering: A, 527(16-17), 4152-4160.

[3] CHEN, C. M. - KOVACEVIC, R. (2003). *Finite element modeling of friction stir welding—thermal and thermomechanical analysis*. International Journal of machine tools and manufacture, 43(13), 1319-1326.

[4] GIBSON, B. T. - LAMMLEIN, D. H. - PRATER, T. J. - LONGHURST, W. R. - COX, C. D. - BALLUN, M. C. - STRAUSS, A. M. (2014). *Friction stir welding: Process, automation, and control*. Journal of Manufacturing Processes, 16(1), 56-73.

[5] FRIGAARD, Ø. - GRONG, Ø. - MIDLING, O. T. (2001). *A process model for friction stir welding of age hardening aluminum alloys*. Metallurgical and materials transactions A, 32(5), 1189-1200.

[6] HE, X. - GU, F. - BALL, A. (2014). *A review of numerical analysis of friction stir welding*. Progress in Materials Science, 65, 1-66.

[7] BORNMANN, L. - MUTZ, R. (2015). *Growth rates of modern science: A bibliometric analysis based on the number of publications and cited references*. Journal of the Association for Information Science and Technology, 66(11), 2215-2222.

Negative effects acting in renovation processes of cladding

Jozef Šutka, Ing.*
Department of Technological Engineering, Faculty of Mechanical Engineering,
University of Žilina,
Univerzitná 8215/1, 010 26 Žilina, Slovak Republic.
E-mail: jozef.sutka@fstroj.uniza.sk, Tel.: +421 41 513 2771

Andrej Zrak, Ing., PhD.
Department of Technological Engineering, Faculty of Mechanical Engineering,
University of Žilina,
Univerzitná 8215/1, 010 26 Žilina, Slovak Republic.
E-mail: andrej.zrak@fstroj.uniza.sk, Tel.: +421 41 513 2760

Abstract: This paper presents an overview of renovation methods, which nowadays have wider application due to its wide applicability in repairing damaged machine parts. The main advantages of cladding as the process is mainly economical and time aspect. Post goes on to describe the advantages and disadvantages of the process itself, where the process entering factors are: automation, base and cladding material, thermal effect on the material and finishing machining. The final part of contribution focuses on the risks that may arise in the process of cladding and impact of these risks to the health of workers. These risks are prevented by extensive range of personal protective equipment, which at this technology is an integral part.

INTRODUCTION

In current industrial practice, we use welding processes, especially in the renovation of worn parts, where we require that the welded metal be of a similar or the same chemical composition. In practice, in order to increase the quality and service life of the repaired part, a weld metal of a higher quality than the base material is chosen. However, in the case of renovation of a worn object, it is first necessary to properly analyze the type of wear, environmental impact, working conditions and based on this analysis then choose the appropriate welding technology, suitable welded material, or decide whether renovation is possible at all or whether this process economically and temporally. In practice, the efficiency of welding renovation is up to about 70% of the price of a new spare part or tool. Creating or renovating various functional surfaces by welding is very useful and economical when used correctly, but it also has its advantages and disadvantages [1, 2].

1 RENOVATION BY WELDING

Welding can be defined as deposit welding, where the base material is melted by a metallurgical process at high temperatures, at the same time the applied welding material (additional material) is melted and added to the melting bath. The result is a homogeneous metal or alloy layer. When welding, the most common goal is to create a layer with a low mixing coefficient with the base material. It is an effort to eliminate the amount of heat introduced into the base material, thereby reducing internal stresses and deformations in the material during the welding process. The weld thus formed can form a protective layer with desired properties, such as resistance to corrosion, thermal stress, abrasive and adhesive wear, cavitation, erosion, and other adverse factors. The following two aspects are important for the successful implementation of the welding process. The first criterion concerns the melting point of the base material and the weld metal. It is very important that the melting point of the weld metal is the same, but preferably lower than the melting point of the base material. With this combination of materials, no problems arise during welding and the welding achieves the required properties. Extra care must be taken if the melting point of the base material is lower than the melting point of the weld metal, in which case welding is problematic, sometimes impossible. The basic and additional materials are melted by the action of an external heat source. The basic heat sources can be: - electric arc, - flame of flammable gas in a mixture with oxygen, - plasma, - laser, - electron beam.

Repairs and renovations of damaged machine parts are important technological operations. In FIG. 1 and 2 are components whose functional surfaces are renovated by welding methods. We recognize the following basic aspects of surface wear recovery: - shaped (repair of broken parts, addition of surface wear), - functional (wear resistance, friction properties, resistance to high temperatures), - operational capabilities-safety (reliability of the component under long-term load) [1, 2, 3].

Fig. 1. Renovation of flat surfaces - die welded by method 136

Fig. 2. Surface of freshly welded brake drum

2 ADVANTAGES AND DISADVANTAGES OF WELDING

One of the biggest advantages of welding technology is the possibility of process automation. In combination with the use of optimal types of weld metals and powerful heat sources, high productivity is achieved, which is applied in series production. The welded layer is compact, a diffusion joint is formed between the weld and the base material, the strength of which is at least equal to the strength of the base material or higher. By means of welding, the desired properties of the functional surface can be achieved by a suitable choice. Welds can be made in thicknesses up to several tens of millimeters. Subsequent heat treatment can then achieve suitable properties of the base material and the weld. Another equally important advantage is the fact that manual welding methods are in most cases inexpensive in terms of acquisition costs and can therefore be afforded by smaller repair and manufacturing companies, which do not have the capital of large multinationals [1].

The basic disadvantage of the welding technology is the thermal influence of the base material, where the structure of the material changes, especially in the heat affected zone between the base material and the weld metal. Depending on the welding technology used, a certain proportion of the base material is subsequently formed in the weld layer, which leads to the formation of internal stresses and deformations. In most cases, the welded layer must be further machined in order to achieve the required final dimensions and roughness. When welding on noble base materials, the base material must be preheated. The overall welding process is very energy-intensive in the case of the use of special metal welding technologies, where it also requires more expensive equipment, as well as higher demands on the abilities and skills of operators [1, 2].

Risks in the renovation process Welding renovations used in the restoration of functional surfaces and are realized mainly by arc methods MIG, MAG, TIG, manual arc welding, methods of submerged arc welding, resp. flame.

The following risks occur with these welding methods:

- Radiation.
- Smoke, fumes, aerosols.
- Liquid metal spray.
- Noise.
- Electric current.

2.1 Radiation

Welding processes are accompanied by electromagnetic radiation, which has a significant effect on the human body. The welding arc produces the following types of radiation: ultraviolet, visible and infrared. Ultraviolet radiation acts at wavelengths of 100–400 nm, which causes damage to the cornea, skin and skin of the eyelids. Visible light is light in the range of 400–700 nm, this type of radiation can damage the retina and in the worst case cause blindness. Infrared light covers the range from 700 nm to 1 mm wavelength. Prolonged exposure damages the retina and cornea, can lead to various inflammations and blindness. All negative effects can be effectively prevented by using suitable protective equipment, i. clothing, gloves, goggles, welding helmets, etc. [4, 5, 6].

2.2 Exhaust gases during welding

When eliminating the influence of exhaust gases and vapors, it is necessary to take into account in particular the harmfulness of individual chemical elements, which are found in renovated materials or. in welding consumables. In welding processes, emphasis is placed on an efficient system for the extraction of welding fumes, which can be toxic or carcinogenic [6, 7].

2.3 Components of welding smoke and their effect on health

Beryllium (Be) - Beryllium and its compounds are highly toxic and carcinogenic. Exposure to this substance causes irreversible changes in the lungs to death.

Cadmium(Cd) - Inhalation of cadmium or its compounds is a serious health hazard, including intercarcinogens. After heating and oxidation, cadmium leaves a dirty olive color and the effects of cadmium oxide emissions also act for several hours after exposure.

Carbon monoxide (CO) - The greatest danger occurs when this gas accumulates. CO is used as a protective atmosphere, is colorless and odorless. In low concentrations it causes fatigue, numbness and headaches. At higher concentrations, loss of consciousness and suffocation.

Chromium (Cr) - Exposure to chromium dust or fumes causes coughing, sneezing, breathing problems and headaches. Furthermore, eye irritation and in some forms is carcinogenic.

Copper (Cu) - Copper fumes and copper dust cause lung irritation, metallic taste in the mouth, also causes eye damage and skin irritation.

Manganese (Mn) - Manganese dust and its products irritate the eyes and mucous membranes. In chronic manganese poisoning, irritation, loss of appetite, headache, muscle weakness and joint pain can also cause death.

Zinc (Zn) - Zinc causes fever, which is manifested by bad taste in the mouth, weakness, fatigue, pain in muscles and joints. Inhalation of zinc fumes generated during welding or cutting of galvanized sheet metal, brass or other zinc alloys should be avoided [6].

Among the common gases used in welding, we include:

a) Oxygen - it is colorless, tasteless and odorless, it is heavier than air. It forms compounds with many substances, where a considerable amount of heat is released. There is also a violent reaction, from spontaneous combustion to explosion, due to various impurities and substances. When welding, pure is used very rarely.
b) Acetylene - is a flammable gas, smells of garlic, is lighter than air. This gas is transported in pressure vessels or produced in generators. They form explosive compounds with copper, mercury and silver.
c) Propane and butane - they usually live in a mixture, they are by-products in the production of synthetic gasolines, they are lighter and aerated, they are transported in containers in a liquid state, they are suitable mainly for cutting [3].

2.4 Noise

Noise intensity is given in decibels (dB). The range of noise that the human ear can distinguish starts at 0 dB, which is the weakest tones up to 190 dB, which is the intensity of the noise equal to the launch of the rocket. The noise level in the area of welding, brazing or cutting depends on the working environment and the method used. Conventional MIG/MAG welding achieves a noise level of 90 dB, plasma cutting with compressed gas 110 dB, the noisiest is the groove with a carbon electrode where the values are around 120 dB, which can already exceed the pain threshold [6].

2.5 Electric current

The greatest risks when working with electric current arise from faults on the electrical parts of welding machines, when the human body comes into contact with parts of the equipment or wiring that is live. Depending on the type of current (alternating, direct current), its intensity and exposure time, muscle stiffness, gastric nervousness, heart rhythm disorders and even heart failure may occur [8].

CONCLUSION

The paper presents the basic risk factors that negatively affect human health during the welding process, respectively. welding. The amount of harmful factors depends on the welding technology used, the chemical composition of the additional materials and the renovated base materials, the welding parameters used. The presented fusion welding methods require in particular the application of effective extraction systems, barriers to the spread of all types of radiation to the environment, with the exception of submerged arc welding methods, as well as anti-noise measures in operations with increased noise. Health and safety measures regulate the applicable directives and standards, which the employer is obliged to comply with in order to eliminate the risks and the negative impact of the above-mentioned effects on the health of workers.

REFERENCES

[1] BAJGA, M. (2007). Available on: https://www.hadyna.cz/svetsvaru/technology/Navarovani_complete.pdf

[2] HLAVATÝ, I. - JIŽÍ, H. - KREJČI. (2007). *Carbide welding*. World of welds (In Czech). Available on: http://www.hadyna.cz/svetsvaru/issue/SS07-3.pdf

[3] KUBÍČEK, J. (2006). *Technologies 2, Part: Wlding* (In Czech). Syllabus of lectures. Brno.

[4] KOSNÁČ, Ľ. (1998). *Health protection and safety during welding* (In Slovak). Bratislava.

[5] TURŇOVÁ, Z. (2006). *Health protection and safety during welding* (In Slovak). Welder, s. 29 - 30.

[6] DIMMEROVÁ, J. (2006). *Health risks during welding and cutting.*

[7] JAJCAY, A. (2006). Odsávanie a filtrácia zváračských dymov. *Zváranie – Svařování*, s. 321 - 325.

[8] *Welding: Safety provisions for metal welding, Design and preparation of workplaces* (2003). STN 05 0600 Standard.

Modifying nozzle orifice to improve cutting capability of plasma beam investigated by simulation software

Miloslav Málek, Ing.*
Department of Technological Engineering, Faculty of Mechanical Engineering,
University of Žilina,
Univerzitná 8215/1, 010 26 Žilina, Slovak Republic.
E-mail: miloslav.malek@fstroj.uniza.sk, Tel.: +421 41 513 2771

Miloš Mičian, doc. Ing., PhD.
Department of Technological Engineering, Faculty of Mechanical Engineering,
University of Žilina,
Univerzitná 8215/1, 010 26 Žilina, Slovak Republic.
E-mail: milos.mician@fstroj.uniza.sk, Tel.: +421 41 513 2768

Abstract: This research deals with modification of nozzle orifice geometry for plasma beam torch. Shape of the plasma beam affected by various modification of nozzle geometry is investigated via simulations software. The simulations focused to predict shape of plasma beam flow out of the nozzle. The best obtained modification serves for further research.

INTRODUCTION

Plasma jet and arc processes are widely used for cutting, welding and coating of metals. The shielding gases as well as their flow profiles near the arc have a decisive influence on the machining results (Fig. 1) [1]. One of the modern technologies widely used is Plasma Arc Cutting (PAC) which is a far better metal cutting technique in some aspects when compared to conventional cutting techniques [2]. In this process, an inert gas (in some units, compressed air) is blown at high speed out of nozzle, at the same time an electrical arc is formed through that gas from the nozzle to the surface being cut, turning some of that gas to plasma [3]. Plasma is a jet or beam of ionized gas capable of conducting electricity. This ionized jet or beam produces extreme heat of around 33000 °C by recombination of ions and electrons into atoms and atoms into molecules. This heat is sufficiently high to melt and remove the metal [4]. Plasma looks and behaves like a gas but has distinctive difference, it conducts electrical charge [2]. The role of working fluid is to make the protection for the outer core of the PAC torch for the safe and protected operation. Hence the working fluid is very much in PAC and there are many fluids available and compatible for the PAC [5].

On of the biggest problems in plasma arc cutting is dross formatiuon on the worse side of cut. The amount of dross depends of lot parameters i.e. types of materials, cutting speed, currents, nozzle and flow rate [4]. The geometry of the nozzle causes significant increase in inert gas speed and temperature [2]. The plasma is sufficiently hot to melt the metal being cut and moves sufficiently fast to blow molten metal away from the cut [3]. The gas pressure and current required to cut a work piece is dependent on various factors for example scanning speed, gas pressure and cutting height [2].

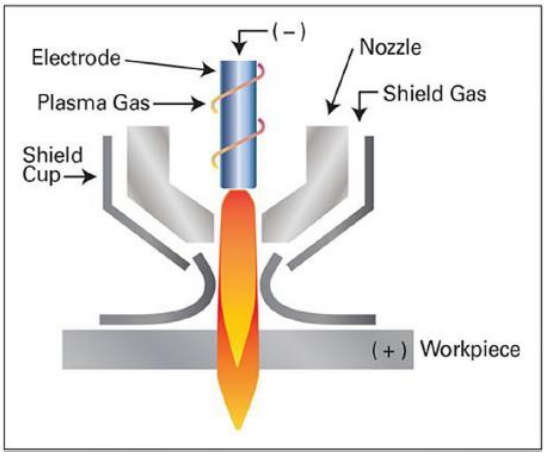

Fig. 1. The plasma arc cutting process [1]

A laval nozzle is a convergent-divergent nozzle that was invented by Gustav Patrik de Laval in 1888 for steam engine applications to produce a supersonic flow in the divergent section. The expansion state and internal flow line of the Laval nozzle are important parametrs that determine the structure of the air jet flow field as shown in Fig. 2. The expansion state is characterized by the nozzle pressure ration n, i.e., the ratio of the nozzle outlet static pressure Pe to atmospheric pressure. When $n < 1$, it corresponds to an overexpanded jet, and $n = 1$ correspond to an full-expansion jet. Additionally, $n > 1$ corresponds to an underexpanded

jet wherein $1 < n < 1.15$ corresponds to a low underexpanded jet and $n \geq 2$ corresponds to a highly underexpanded jet [6].

Ansys Fluent is the industry-leading fluid simulation software used to predict fluid flow, heat and mass transfer, chemical reactions and other related phenomena. Known for delivering the most accurate solutions in the industry without compromise, Fluent´s advanced physics modeling capabilities include cutting-edge turbulence models, multiphase flows, heat transfer, combustion, shape optimization, multiphysics and much more [7].

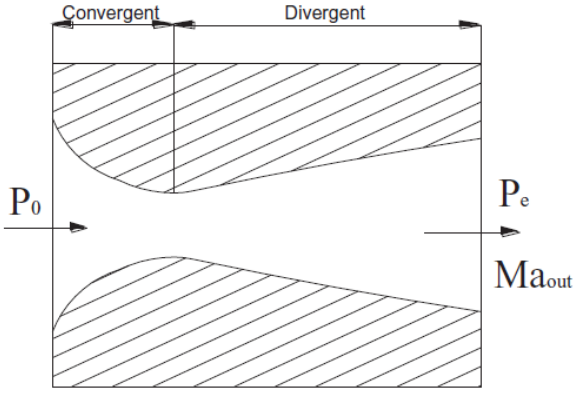

Fig. 2. Structure of the Laval nozzle [7]

1 PREPARATION OF SIMULATED MODELS

First of all, plasma torch was measured and then 3D model was created. For simulations was used simplified model consist of nozzle and electrode, in 2D shape (Fig. 3).

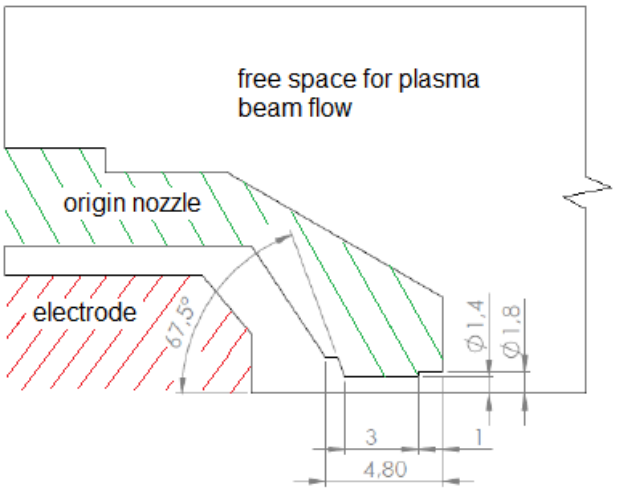

Fig. 3. A 2D schematic model of a nozzle with an electrode for simulation of a plasma flow

The experiments consist of simulating a plasma flow using 8 different modified nozzle orifice shapes. Shape modification of the nozzle orifice kept these rules:

- The easiest manufactured way by conventional technologies.
- Low production/modification time.
- Low financial costs of manufactured.

For simplified and reduced computing time were used mentioned 2D models. Moreover, the task had symmetrical character, so the axis symmetry was placed identically with axis of nozzle and electrode, which means even more reduction in computing time.

Automatically generated net of finite elements was coarse and inaccurate. The modification of finite elements net consists of adding more finite elements, modify function "Skewness" and significant increasing finite elements in critical area. Sharp or significant dimensional changes and wall were marked as critical area (Fig. 4). The "Bias" function was used to modify net around the wall. After appropriate adjustment of finite elements net was model prepared to define boundary conditions. Modified net has 33.8-times more finite elements compared to an automatically generated net (Fig. 5).

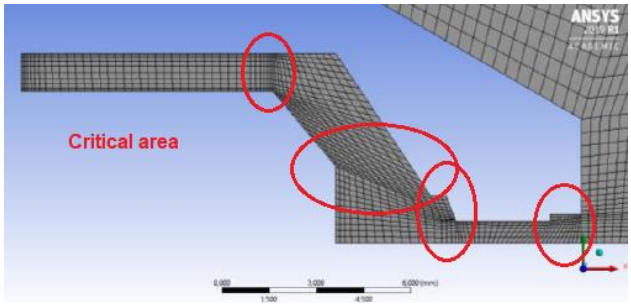

Fig. 4. Identification of critical areas on the model (circle marks)

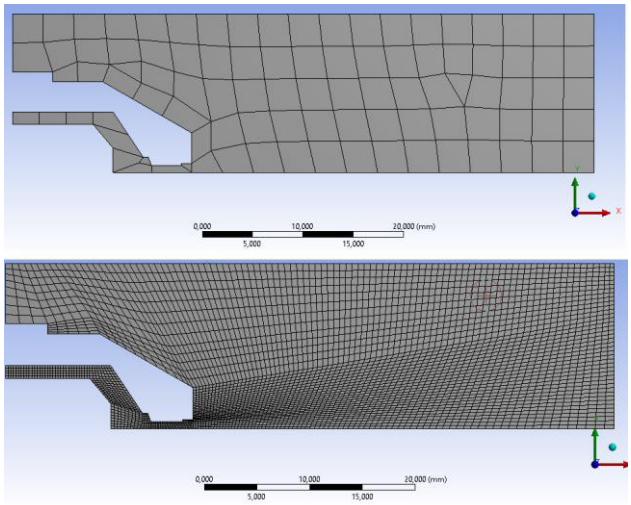

Fig. 5. Comparison of an automatically generated mesh and an adjusted mesh

The boundary condition, as wall, axis symmetry, inlet and outlet, were set up (Fig. 6). Properties of plasma i.e. heat conductivity, density (electron density), effect of magnetic field, plasma beam frequency, viscosity (Newtonian or non-Newtonian fluid), plasma beam flow affected by electric arc and others is complex issue. In this research, the

simulations were simplified as much as possible in order to obtain relevant results for further investigation. Inlet pressure and temperature were set up at 2.26 MPa and 1200 K. The outlet pressure and temperature were set up at 39.4 kPa and 273.2 K. The number of iteration was 4500 and fluid medium was ideal gas with Sutherland model viscosity.

Fig. 6. Boundaries for the simulation of flow: 1 – flow input, 2 – impenetrable walls, 3 – axes of symmetry, 4 – flow output

2 RESULTS OF SIMULATIONS

Flow simulation is focused to achieve plasma beam shape flow out of modified nozzle orifice and then compared with origin nozzle shape.

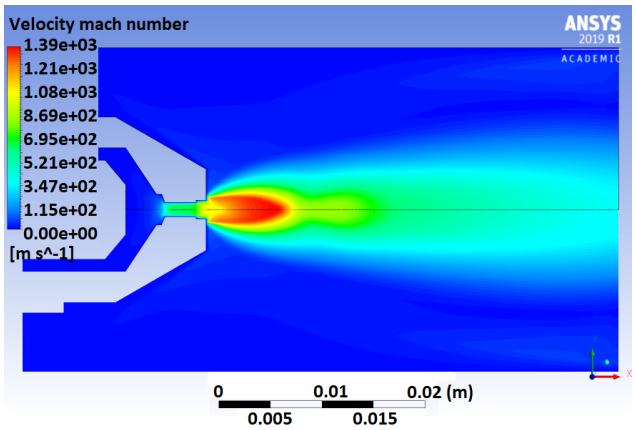

Fig. 7. Reference nozzle flow simulation

Figure 7 shows results of flow simulation investigated on the origin nozzle shape (reference

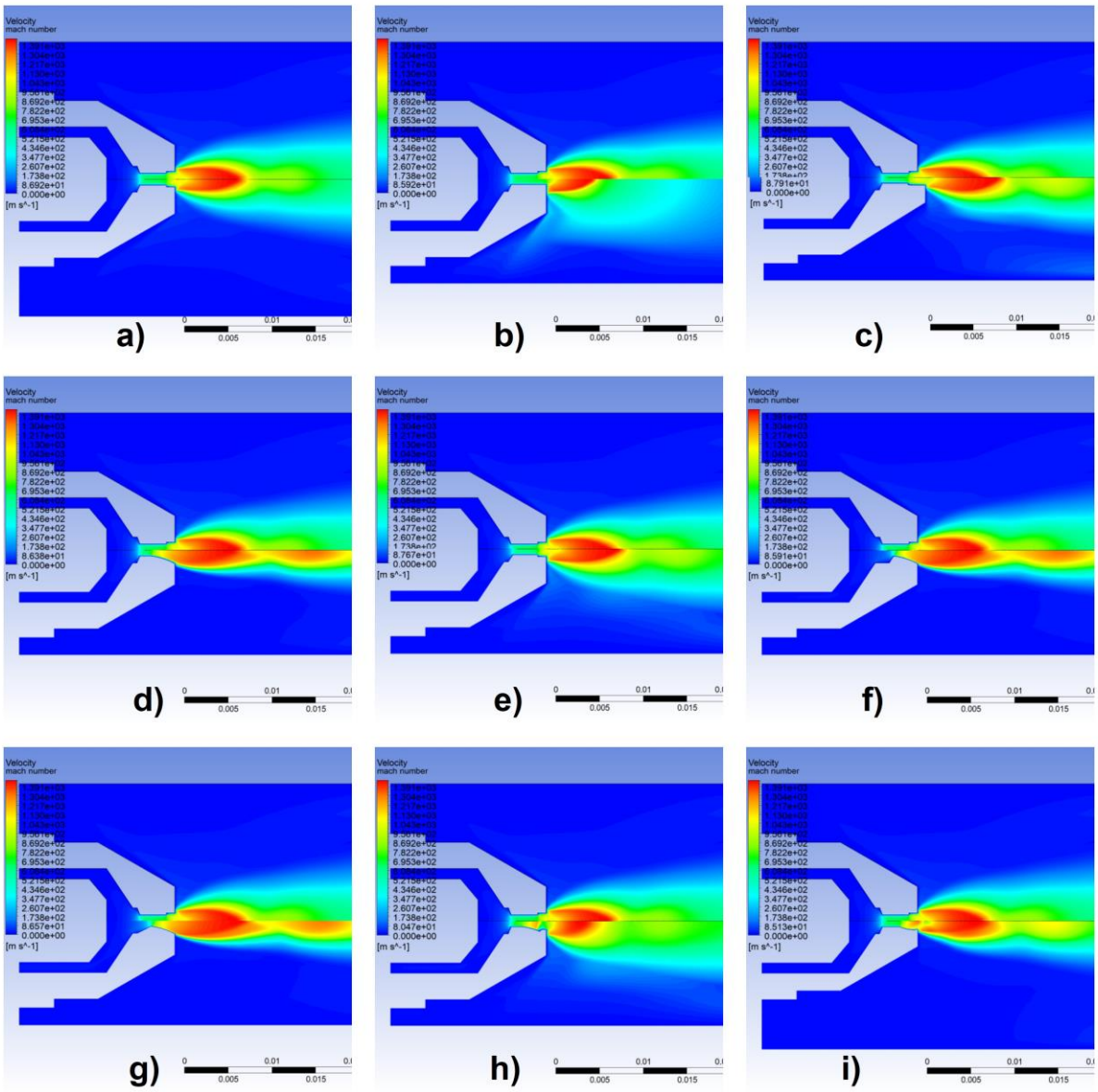

Fig. 8. Results of comparison of flow simulation: a) reference nozzle; b) to i) modified nozzles (upper half of picture is reference nozzle and lower half is modified nozzle)

sample). Core formation of fluid medium represented by yellow outline was observed. All modified nozzles were simulated and compared with reference nozzle. Every modification of nozzle orifice kept the rules mentioned above expect last two modifications. Figure 8 **s**hows all simulated results compare to the reference nozzle (Fig. 8a to Fig. 8i upper half of picture).

From the results of the simulation calculations and based on a comparison with the plasma beam flow in the reference nozzle, the most suitable shape for the cutting process is the modified shape marked as No. 7 (Fig. 8f). The plasma beam shape for this modification had significant different shape against reference nozzle. The core of the plasma beam (yellow outline) had longer range, moreover there was observed second and third core area, which could help to blow dross out from cutting gap (fig. 9). This modification fulfils manufacture requirements.

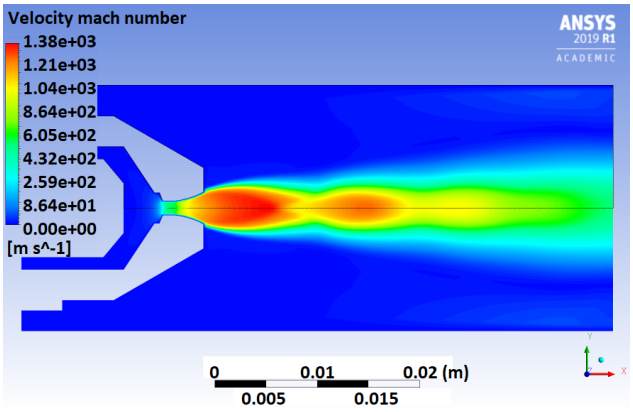

Fig. 9. Modified nozzle No. 7 flow simulation

CONCLUSION

Flow simulation of gas fluid through nozzle with electrode affected by different nozzle orifice modifications was investigated in this paper. This research served to further investigation, to predict suitable design for real experiments. Modified nozzle No. 7 indicated the best results from all 8 modified shape of nozzle orifice. This modification fulfilled requirements as easy manufacture by conventional technology, low production time and costs, and moreover it is an easily repeatable process. The simulation confirmed the prediction that Laval nozzle shape is suitable for supersonic flow which is an accompanying phenomenon of every plasma arc cutting.

Acknowledgment

This research was funded by KEGA, grant number KEGA 009ŽU-4/2019; and VEGA, grant number VEGA 1/0951/17. The authors hereby thank these agencies for their support.

REFERENCES

[1] ANSYS (2018). ANSYS. Available on: https://www.ansys.com/products/fluids/ansys-fluent

[2] LIU, Y. - ZHANG, J. - WEI, J. - LIU, X. (2020): *Optimum structure of a laval nozzle for an abrasive air jet based on nozzle pressure ratio*. Powder Technology 364, pp.343-362

[3] MOARREFEYADEH, A. (2011): *Numerical simulation of workpiece thermal profile in Plasma Arc Cutting (PAC) Process.* WSEAS Transactions on Applied and Theoretical Mechanics 6, pp.160-166

[4] RAJESHKANNAN, A. - ALI, M. - PRAKASH, R. - JEEVANANTHAM, A. K. - JAYARAM, K. (2020): *Optomizing the process parameters in plasma arc cutting using Taguchi approach for the case industry in Fiji.* Materials Today: Proceedings 24, pp. 1122-1131

[5] SCHNICK, M. - FÜSSEL, U. - ZSCHETZSCHE, J. (2006): *Simulation of plasma and shielding gas flows in welding and cutting arcs with Ansys CFX.* Modelling for Material Processing, pp. 143-148

[6] SHARMA, D. N. - KUMAR, J. R. (2020): *Optimazation of dross formation rate in plasma arc cutting process by response surface method.* Materials Today

[7] SURESH, A. - DIWAKAR, G. (2020): *Optimization of process parameters in plasma arc cutting for TWIP steel plates.* Materials Today

Synergic effect of Ti and Zr on AlSi7Mg0.3Cu0.5 alloy for investment casting technology

Michal Kuriš, Ing.*
Department of Technological Engineering, Faculty of Mechanical Engineering,
University of Žilina,
Univerzitná 8215/1, 010 26 Žilina, Slovak Republic.
E-mail: michal.kuris@fstroj.uniza.sk, Tel.: + 421 41 5132771

Dana Bolibruchová, prof. Ing., PhD.
Department of Technological Engineering, Faculty of Mechanical Engineering,
University of Žilina,
Univerzitná 8215/1, 010 26 Žilina, Slovak Republic.
E-mail: danka.bolibruchova@fstroj.uniza.sk, Tel.: +421 41 513 2757

Marek Matejka, Ing., PhD.
Department of Technological Engineering, Faculty of Mechanical Engineering,
University of Žilina,
Univerzitná 8215/1, 010 26 Žilina, Slovak Republic.
E-mail: marek.matejka@fstroj.uniza.sk, Tel.: +421 41 513 2771

Martin Vicen, Ing., PhD.
Department of Technological Engineering, Faculty of Mechanical Engineering,
University of Žilina,
Univerzitná 8215/1, 010 26 Žilina, Slovak Republic.
E-mail: martin.vicen@fstroj.uniza.sk, Tel.: +421 41 513 2626

Abstract: The article is focused on the synergic effect of constant content of *Zr* and higher content of *Ti* on mechanical properties of AlSi7Mg0.3Cu0.5 aluminium alloy. The *Ti* additions were in gradual increase from 0.1, 0.2 and final 0.3 wt. % *Ti*. The *Zr* additions is in constant content 0.15 wt. % where we get the best mechanical parameters. The casting process was carried out in ceramic molds, created for the investment casting technology by AluCAST company. After casting and finishing operation half of the experimental samples were heat treatment by precipitation curing T6. The measured results were compared with primary aluminium alloy AlSi7Mg0.3Cu0.5 and experimental aluminium alloy AlSi7Mg0.3Cu0.5Zr0.15. In variant with addition of *Ti* 0.1 wt. %, the tensile strength R_m increased by 1.5 % but the elongation A_M decreased to 40 %. Variants with addition of *Ti* 0.2 and 0.3 wt. % achieved similar R_m but approximately 40 % decrease in A_M. However, it is interesting that yield strength $R_{p0.2}$ increased for all variants by approximately 14 to 20 %. The results point out the possibility of developing a more sophisticated alloy for automotive and airplanes industry.

INTRODUCTION

The automotive and aerospace industries require a constant need to improve the properties of the materials originally used. The development in the given field includes also *Al* alloys, but focuses on improving not only their mechanical properties but also the heat resistance of *Al* alloys in applications above 300 °C. Very interested field of casting where we can use this development are cylinder heads, gearboxes and engine blocks. Here the emphasis is on the lowest casting weight possible and the ability to function at high performance and temperatures. The application of a more sophisticated alloy with improved mechanical properties and heat resistance increases material savings by reducing the dimensions of engine blocks, improving the environmental aspect by reducing fuel consumption, and increasing performance due to the improved resistance of *Al* castings to operating pressures and heat load during the device operation (Fig. 1.). AlSi7Mg0.3 *Al* alloy is frequently used in the manufacture of castings where good casting properties, corrosion resistance, pressure tightness and weldability are required. It is therefore often used in the manufacture of components for internal combustion engines. Improvement of the strength properties of the AlSi7Mg0.3 Al alloy can be ensured by the addition of various elements, with copper being particularly important. The addition of *Cu* provides increased strength, hardness or creep resistance by eliminating the curable Al_2Cu phases. These can be excluded either as small oval grains

with a high *Cu* concentration or as a ternary Al-CuAl2-Si eutectic. However, increasing *Cu* content in the AlSi7Mg0.3 *Al* alloy decreases ductility, adversely affects corrosion resistance and increases solidification interval. The combination of *Mg* and *Cu* allowed the development of commercial alloys such as AlSi7MgCu0.5, AlSi8Cu3 and AlSi7Mg0.3Cu. The AlSi7Mg0.3Cu alloy is the one used most frequently in the manufacture of components for internal combustion engines. The main characteristic of the above-mentioned alloys is the crystallization of two eutectics: primary Al-Si and secondary Al-Si-Cu. The introduction of *Zr* into the alloy is important in order to increase the strength, while the strengthening effect is induced by the elimination of the Al_3Zr or AlSiZr intermetallic phases. Primarily, *Zr* is excluded in the form of Al_3Zr during the peritectic reaction, with a *Zr* content of ≥ 0.1 wt. %. The Al_3Zr phase is excluded in two different crystallographic morphologies. The first is the tetragonal DO_{23} system, the second is the cubic coherent metastable $L1_2$ system (Fig. 2.) [1-12].

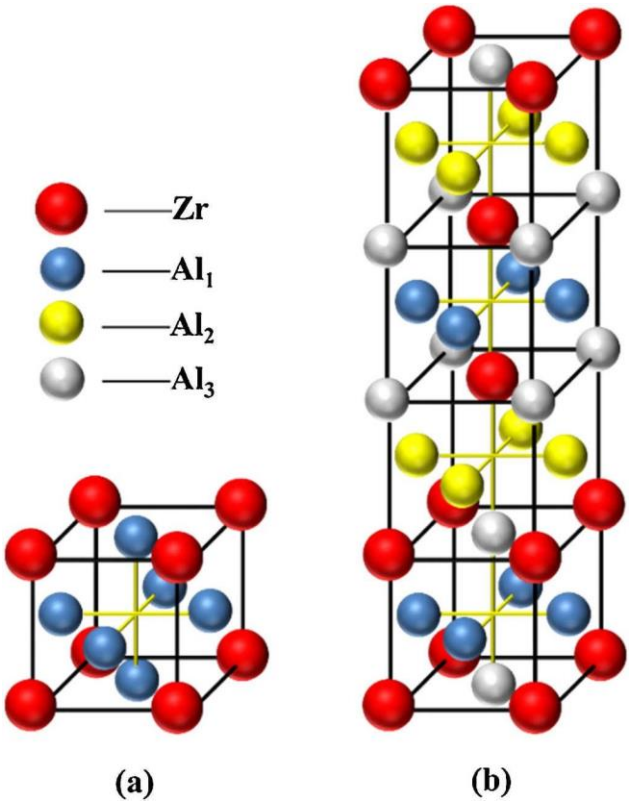

Fig. 1. Al_3Zr phase crystallographic lattices: a) $L1_2$ b) DO_{23}

Zr is characterized by the lowest diffusion in *Al* compared to other elements such as *Mn*, *V* or *Sc*. *Zr* atoms have high binding energy with unoccupied *Al* sites. The Al_3Zr particles are resistant to dissolution and roughening, they regulate the development of grains and sub-grains in the metal matrix of the Al-Si alloy. This makes it possible to increase and maintain the strength of the *Al* alloy even after precipitation hardening, above 250 °C. DO_{22} and DO_{23} tetragonal lattices influence the strength characteristics of construction materials. However, these phases are too fragile due to the low symmetry of the tetragonal lattice. A more preferred variant is the L_{12} cubic lattice, which better compensates for the negative aspect of the DO_{22} and DO_{23} tetragonal lattices. The Al_3Zr intermetallic phases in an Al-Si-based alloy can be excluded either in the form of long acicular (needle-like) formations or in a square-like (angular) form. *Zr* can positively influence the properties of Al-Si alloys, therefore the more advantageous is the combination of *Zr* with other elements such as *Ti*, *Sr*, *Sc*, *Mo* or lanthanides. As confirmed by the work of Nabawy and Voncina [7-8], *Ti* in combination with *Zr* can induce primary grain and sub-grain refinement in an *Al* alloy. *Ti* has a significant inoculant effect on the alloy under investigation. It also causes an increase in the number of nucleation nuclei for the Al_3Zr phase at a higher *Ti* content. At a higher *Ti* content it replaces the *Zr* atoms in the Al_3Zr phase, thereby enhancing the smoothening and strengthening effect on the Al alloy. At temperatures above 300 °C, phases with a higher *Ti* content are characterized by increased stability. Intermetallic phases containing *Zr* and *Ti* provide higher resistance and strengthening characteristics than Al_2Cu or Mg_2Si phases, which become unstable at temperatures above 250 °C. The market growth and demand for electric vehicles (EV) also have a significant impact on Al casting manufacturers. The main focus is on the possibility of producing low-weight components that allow less power consumption from battery cells and thus increase EV range on a single charge. At the same time, highly favourable mechanical properties combined with high corrosion resistance, electrical permeability and resistance to higher temperatures represent a very interesting material in the construction of modern EVs [8-16].

1 METHODS AND GOALS

The aim of the experiments was to determine the impact of the synergistic effect of *Zr* and *Ti* on selected properties of the AlSi7Mg0.3Cu alloy which was cast by investment casting technology. The ceramic mold consists of three layers ensuring the formation of a contact, insulating and reinforcing cover (Tab. 1). After melting and cooling for at least 24 hours the ceramic mold (Fig. 3a) of approximately 3 mm thickness was annealed at 750 °C for at least 1.5 hours. The ceramic mold temperature was 510-540 °C before casting. The samples were cast at a rate of 0.3 $kg \cdot s^{-1}$ from a casting height of 500 mm.

The casting temperature was 750 ± 10 °C. After casting, the ceramic mold was cooled on air for one hour.

Tab. 1. Ceramic mold material composition

	1. Layer	2. Layer	3. Layer	4. Layer	5. Layer
Binder	Primcot cote plus	SP-Ultra 2408	Matrixsol 30	Matrixsol 30	Matrixsol 30
Grain	Cerabed DS 60	Rancosil A	Molochite 30-80 DD	Molochite 30-80 DD	Molochite 30-80 DD

The AlSi7Mg0.3Cu primary alloy was supplied by the manufacturer in a pre-inoculated and pre-modified condition. The AlSi7Mg0.3Cu alloy represents a new type of alloys not standardized according to STN EN 1706 (Tab. 2).

Tab. 2. Ceramic mold material composition

Variant	*Si*	*Fe*	*Cu*	*Mn*	*Mg*	*Zn*	*Ti*	*Zr*	*Al*
P	6.88	0.12	0.54	0.07	0.37	0.07	0.13	-	rest
R	6.86	0.12	0.55	0.07	0.37	0.07	0.13	0.15	rest
***E*1**	6.96	0.13	0.55	0.07	0.37	0.01	0.23	0.12	rest
***E*2**	6.68	0.13	0.54	0.07	0.35	0.01	0.28	0.14	rest
***E*3**	6.51	0.13	0.52	0.07	0.34	0.01	0.37	0.13	rest

P - chemical composition of AlSi7Mg0.3Cu alloy; *R* - reference alloy AlSi7Mg0.3Cu with addition of *Zr* 0,15 wt. %; *E*1, *E*2, *E*3- experimental alloys AlSi7Mg0.3Cu with constant addition of *Zr* 0.15 hm. % and gradual increasing of *Ti* o 0.1 wt. %

A total of 3 experimental melts were prepared, characterized by a constant *Zr* content of 0.15 wt. % and a gradual addition of *Ti* by 0.1 wt. %. The AlSi7Mg0.3Cu experimental alloys were not degassed or refined throughout the experiment. The AlZr15 master alloy featured impaired melt solubility. The melt had to be preheated up to a temperature of 770 ± 10 °C, thus creating suitable conditions for increasing hydrogen gasification. After casting the experimental samples with a constant addition of 0.15 wt. % *Zr* and a gradual addition of *Ti* in the range of 0.1 to 0.3 wt. % (Tab. 2), the process was followed by heat treatment ("*HT*") in the form of T6 precipitation curing. *HT* was performed on 5 pcs of a total of 10 experimental samples (Fig. 2) from each experimental variant. Subsequently, the individual samples were evaluated for mechanical properties before and after the *HT* process, whereby the arithmetic mean was determined from the mechanical characteristics and a graph was made for each experimental variant.

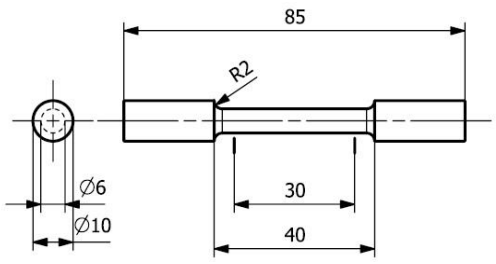

Fig. 1. Scheme of the test specimen

The highest mechanical characteristic values obtained were selected in order to evaluate the microstructure before and after *HT*. The samples were prepared using a conventional metallographic procedure. For the Zr-phase distinguishability and unmistakability, these samples were etched with a ferric-phase etch (H_2SO_4). Primarily, the results of the mechanical properties were confronted with the values of the AlSi7Mg0.3Cu primary alloy ("*P* alloy"), and the AlSi7Mg0.3CuZr0.15 reference alloy ("*R* alloy"). The *R* alloy represents an alloy with the most preferred addition of Zr. In the above-mentioned alloy, an optimum increase of selected mechanical properties such as $R_{p0.2}$, *E* or *HBW* was observed for the alloy in the alloying range from 0.05 wt. % to 0.3 wt. % *Zr*.

2 RESULTS AND DISCUSSION

Based on the values obtained we can assume that the *Zr* phases are excluded even before the *α*-phase and the eutectic. In experimental alloys with an addition of *Ti* 0.1 wt. % and 0.3 wt. % there is no higher level of super-cooling compared to the *R* alloy with an addition of 0.15 wt. % *Zr*. A partial change compared to the R alloy occurs in the variant with an addition of 0.2 wt. % *Ti*. Mechanical characteristics are improved with an increase in *Ti* addition, which in many cases exceed the best measured results in experimental alloys alloyed only using *Zr*. From the viewpoint of evaluating the tensile strength R_m (Fig. 3) before *HT*, the *E*1 experimental samples achieved the best results.

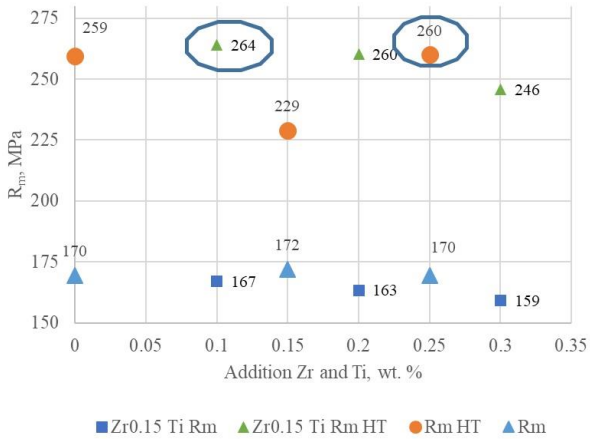

Fig. 3. Dependence of R_m before and after *HT* for investigation alloys AlSi7Mg0.3Cu

Before *HT*, the *E*1 samples reached R_m of about 167 MPa, which represents a lower value compared to the P samples by 2 % and compared to the R alloy by 3 %. After *HT*, samples of *E*1 again made the best values, reaching 264 MPa. The given value is significant precisely because the previous samples, with the addition of only *Zr*, reached the highest value up to 260 MPa. This value is considered by the STN EN 1706 standard to be the minimum R_m value of the AlSi7Mg0.3 alloy. The *E*1 samples reached a R_m value that is 2 % higher than that of the P alloy, and 2 % higher than that of the *R* alloy. The best results of the agreed $R_{p0.2}$ yield strength were achieved by the *E*3 sample with an addition of 0.3 wt. % *Ti* (Fig. 4).

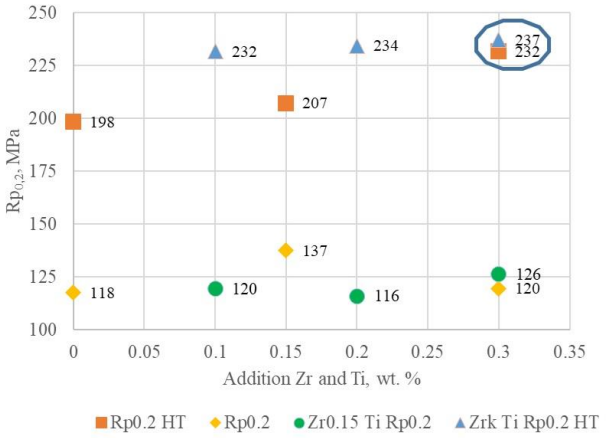

Fig. 4. Dependence of $R_{p0.2}$ before and after *HT* for investigation alloys AlSi7Mg0.3Cu

The increase achieved was by 20 % compared to the *P* alloy, 15 % compared to the *R* alloy, and compared to the experimental alloy with the addition of 0.3 wt. % *Zr* by 2.2 %. Increased plasticity during engine operation ensures better adaptation of the cylinder head to temperature changes and operating pressure exerted during operation, thus extending the service life. Positive results, similar to $R_{p0.2}$, were also measured at the *E* – modulus of elasticity (Fig. 5).

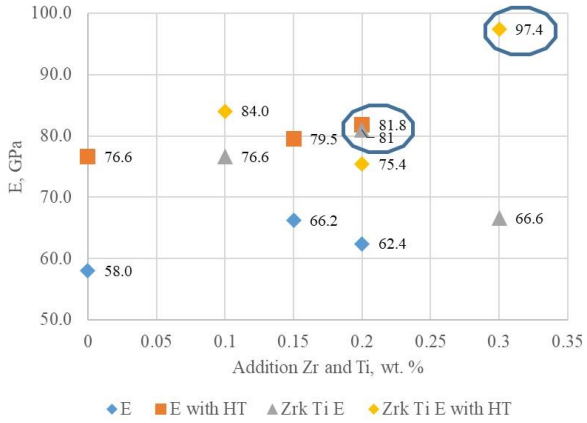

Fig. 5. Dependence of *E* before and after *HT* for investigation alloys AlSi7Mg0.3Cu

Best results were obtained in the case of *E*3 samples with a constant addition of 0.15 wt.% *Zr* and 0.3 wt% *Ti*. Compared to the *P* alloy, the increase in *E* is up to 21 %, and compared to the *R* alloy it is by up to 18 %. The best experimental alloy with a constant addition of 0.2 wt.% *Zr* achieves approximately 10 % lower *E* than the *E*3 experimental alloy. Based on the given parameters we can conclude that the examined samples are able to withstand higher operating loads during the device operation. By increasing $R_{p0.2}$ and *E* we obtained an AlSi7Mg0.3Cu alloy, which is able to withstand the same or, eventually, higher operating loads even when the functional cross-sections of the casting walls (e.g. cylinder heads) are narrowed. Of all the mechanical properties, a decrease was observed at ductility *A* (Fig. 6).

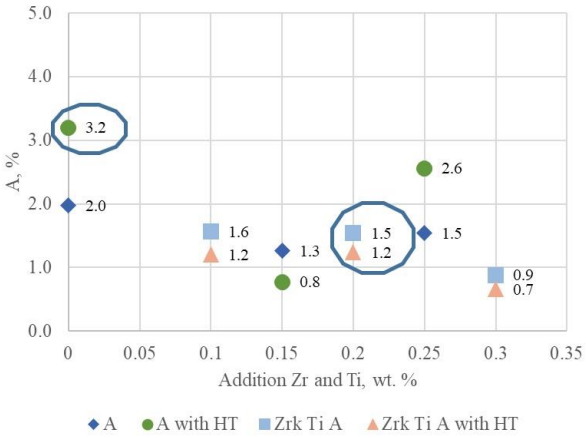

Fig. 6. Dependence of *A* before and after *HT* for investigation alloys AlSi7Mg0.3Cu

In contrast to the *P* alloy, the results of the *A* alloy are slightly better than those of the *R* alloy with an addition of 0.15 wt. % *Zr*. Although the *E*3 samples with the addition of 0.3 wt. % *Ti* reach lower values before *HT* by 30 % and after *HT* by 13 %, other variants *E*1 and *E*2 achieved a significant improvement in ductility. For *E*1 experimental samples, this is an increase by 23 % before *HT* and by almost 50 % after *HT*. The *E*2 samples achieved an improvement of 15 % before and after *HT* similar to *E*1 up to 50 %. The significance of ductility (elongation) is especially important for the motor parts of the engine during its operation. In the case of reduced ductility, some components such as e.g. the engine cylinders could not react flexibly and plastically enough to the desired extent during the temperature change in the combustion chamber. This would reduce the service life of any internal combustion engine. When evaluating the hardness, its increase compared to the *P* alloy was between 9 and 15 %, and compared to the *R* alloy the value was between 6 % and 12 % (Fig. 7). The best values were obtained from E3 experimental samples with a value achieved of 102 *HBW*. The increase compared to the

P alloy is by 15 %, compared to the *R* alloy by 12 %, and compared to the best experimental variant with an addition of *Zr* 0.05 % by 7 %. However, a positive increase is noticeable in all experimental alloys with a combination of *Zr* and *Ti*. The microhardness of the *Zr* phases was evaluated as the arithmetic mean of the 10 test punctures, reaching a value of about 265 *HM*5 achieved by the *E*3 experimental samples (Fig. 7). The microhardness of *Zr* phases is between the hardness of Al_4Ca and Al_6CuMg phases, which are characterized by microhardness in the range of 200 to 300 *HM*5.

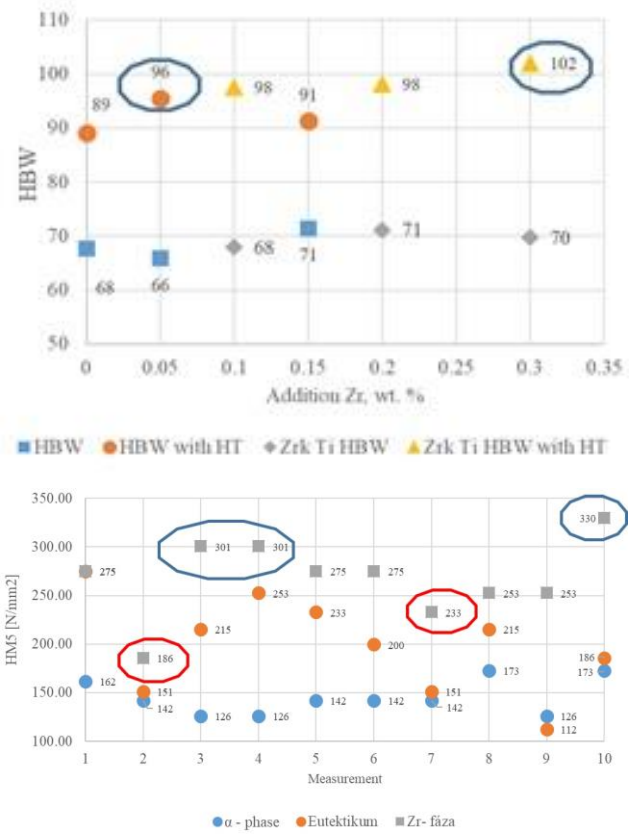

Fig. 7. *HBW* for investigation alloys AlSi7Mg0.3Cu and *HM*5 microhardness for *E*3 alloy

In the evaluation of microhardness, a decrease was observed in *Zr* phases in interaction with other phases, e. g. on *Mg* or *Fe* base (Fig. 7). This can be seen with punctures 3, 4 and 10, which were performed into *Zr* phases without interaction with other phases. In contrast, punctures 2 and 7 were performed in *Zr* phases in strong interaction with other phases. A similar phenomenon was observed in experimental alloys with the addition of only *Zr*. In metallographic evaluation, the experimental AlSi7Mg0.3Cu alloy can be defined as a sub-eutectic alloy containing primary *α*-phase dendrites and globular eutectic consisting of *α*-phase and *Si*. In addition to the base phases, it also contains the curing phases Mg_2S and Al_2Cu. Based on the content of elements in the alloys such as *Fe* and *Mn*, there can occur their exclusion in the form of ferric intermetallic phases in various morphological shapes. The effect on the resulting structure is closely related to the chemical composition and casting technology. In the mold casting technology, a quicker cooling and the formation of a fine dendritic structure can be expected, as opposed to the investment casting technology, which is characterized by much slower heat dissipation. Because the alloy is pre-modified, the acicular morphology of eutectic *Si* is transformed into a finer, globular morphology. *Zr* is excluded in the metal matrix as *Zr* phases in the form of longer needles with a smooth surface and cleaved ends, respectively it occurs in a more compact shorter morphology without cleaved ends. The *Zr* phases observed on microstructures are intermetallic phases of the Al_3Zr and AlSiZr type. Similar phase morphology is identified by Vončina in his work [9]. *Zr* is characterized by the least diffusion to the *α* matrix and is therefore excluded preferably as Al_3Zr. From previous experiments it was found that *Zr* phases bind not only *Fe*, thus suppressing the negative effect of *Fe*-based phases in the metal matrix of the experimental AlSi7Mg0.3Cu alloy, but also increase the interaction with Mg_2Si phases (Fig. 8).

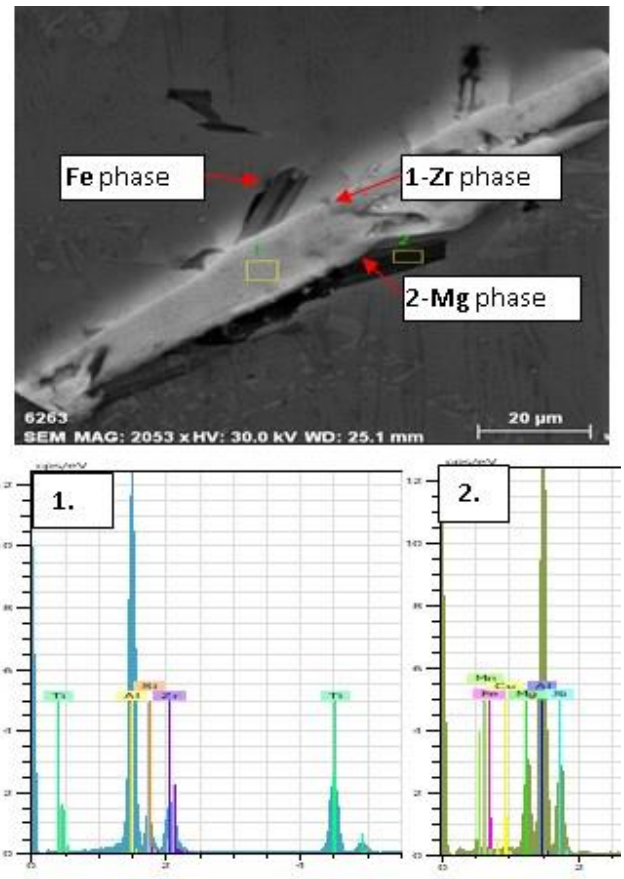

Fig. 8. EDX analysis of the *Zr* phase in the AlSi7Mg0.3CuZr0.15 *R* alloy

A high presence of *Ti* in the respective *Zr* phases was found after evaluation by EDX analysis. When comparing the *E*1, *E*2, and *E*3 sample microstructure with the *R* alloy it can be concluded that the amount of excluded *Zr* phases has increased (Fig. 9).

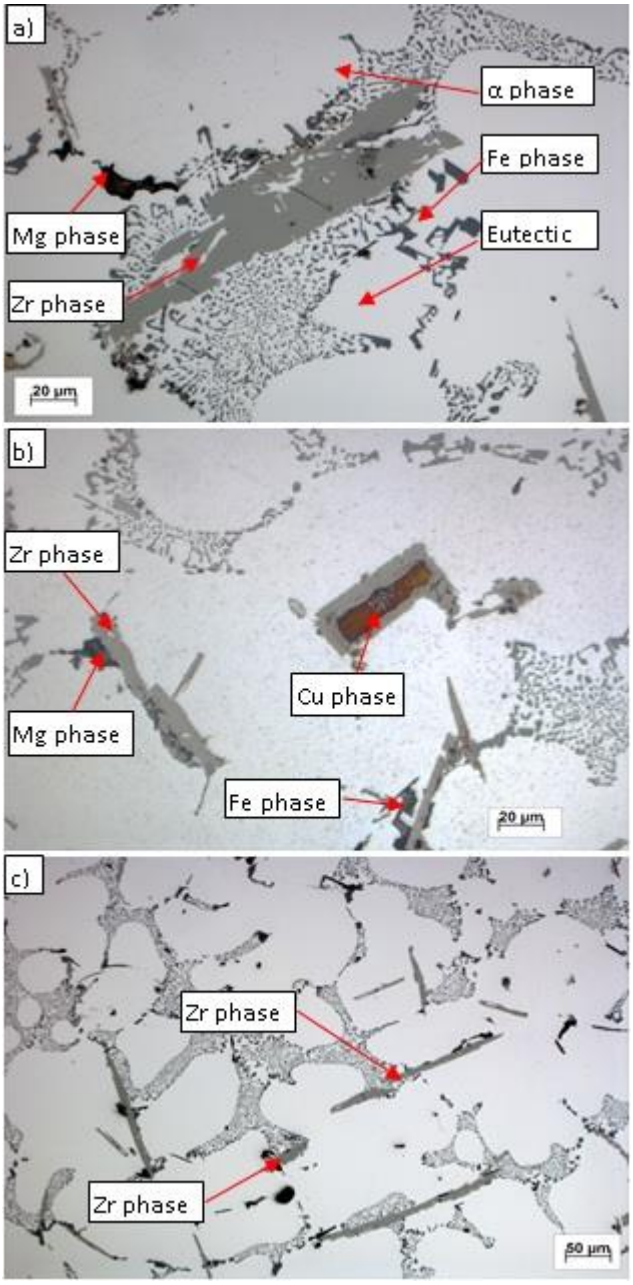

Fig. 9. Microstructure of the alloys before *HT*: a) *R* alloy, b) *E*1 alloy, c) *E*2 alloy, H_2SO_4 etch

This phenomenon doubles with increasing *Ti* content in the alloy under investigation compared to the *R* alloy (Fig. 9a). When evaluating the microstructure, we can observe a uniform ratio of excluding *Zr* phases in the form of longer acicular morphology with a sharp edge ending and more consistent angular morphology.

The *Zr* phases were excluded in some cases in the form of large structures in the eutectic region (Fig. 10a), or at an increased concentration of *Zr* phases in the subsurface region of the sample under investigation (Fig. 9c). After exceeding the *Ti* content ≥ 0.25 wt. % in the experimental samples, there was a sharp increase in the amount of precipitated *Zr* phases, with the preferential elimination being mainly in the subsurface area of the investigated sample.

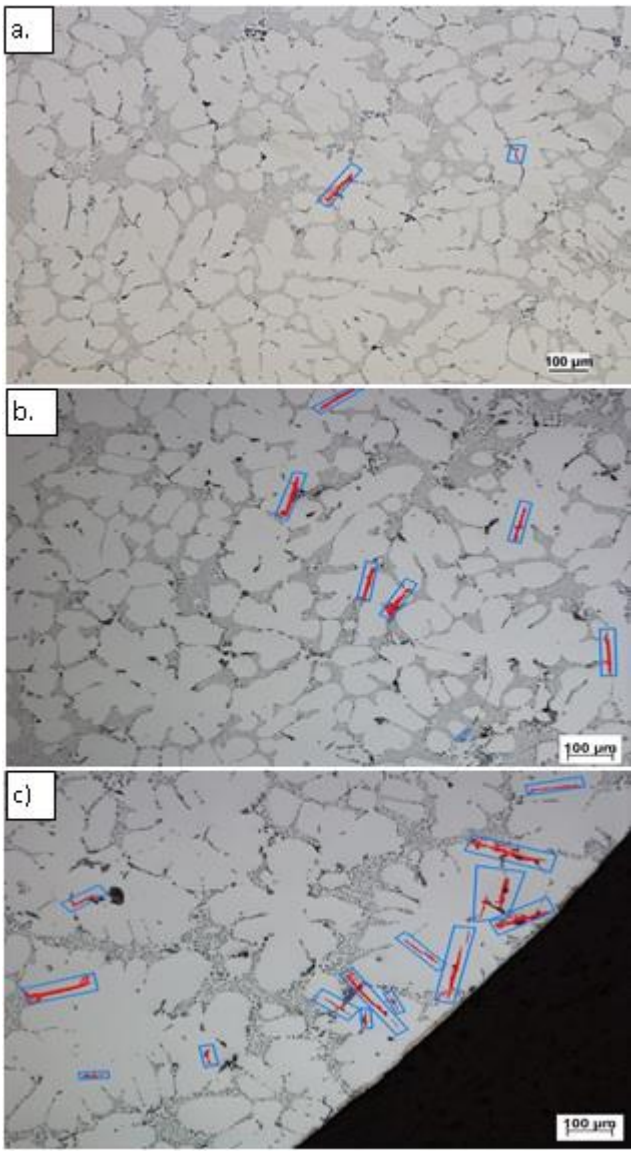

Fig. 10. Microstructure of *E*1, *E*2, and *E*3 alloys before *HT*: a) 0.1 wt.% *Ti*, b) 0.2 wt.% *Ti*, c) 0.3 wt.% *Ti*, H_2SO_4 etch

This condition is probably related to the slow cooling of the alloy in ceramic molds. At the same time, with the increased *Ti* content represented by samples *E*2 and *E*3, *Zr* phases were formed with presumed *Cu* enrichment (Fig. 10b). Excluded *Zr* phases of acicular morphology can be observed in samples *E*3 (Fig. 10c). *HT* caused partial breakdown of larger Zr phases in acicular morphology. All samples after *HT* show a slight increase of R_m and a significant increase of $R_{p0.2}$ and *E*. In contrast to the *R* alloy, the *Zr* phases were excluded in the form of long acicular-shaped formations and consequently more pronounced disintegration after *HT*. In the experimental samples, the *Zr* phases retained their morphology even after *HT* without significant changes.

CONCLUSIONS

A decrease in mechanical properties was recorded in ductility, where in the experimental sample's ductility exceeded the values of *R* alloys. A

significant decrease in ductility may be related to an increase in the *Zr* phase content in the form of longer acicular formations that reduce plasticity of the metal matrix of the experimental AlSi7Mg0.3Cu alloy. The increase in mechanical properties was observed in $R_{p0.2}$, *E* and partly also R_m. A significant increase in $R_{p0.2}$, *E* and partly also R_m may be related to an increase in the number of *Zr* phases of smaller dimensions. These increase the strength of the metal matrix while not increasing the brittleness of the metal matrix. A significant effect of the synergies of *Zr* and *Ti* induces the refinement of the grains and sub-grains and hence a fine-grained structure. This fact positively affects the increase in mechanical properties such as $R_{p0.2}$ or *E*. The combination of *Zr* and *Ti* induces an increase in the number of *Zr* phases of angular morphology. The most preferred ratio was about 0.25 wt. % *Ti*. Above the given content, a larger volume of longer acicular formations has been excluded lowering the R_m. *Zr* phases induced an increase in the interaction between curable Mg_2Si and Al_2Cu phases. At the same time, it was observed Fe interaction with *Zr* phases occurred. A similar phenomenon was also observed in samples with the addition of *Zr* only (Fig. 8.). On this basis, we can assume the ability of *Zr* phases to reinforce the metal matrix when binding with curing phases, and reducing negative effect of Fe like corrector. When evaluating the hardness, the most significant increase was in the experimental samples *E*3. In the evaluation of microhardness, the best values were also measured in samples of *E*3, in which a higher number of *Zr* phases was observed without interaction with other phases. This may be related to the increased hardness of the *E*3 samples because the metal matrix, in addition to the *Zr* phase content in interaction with other phases, contains an increased number of *Zr* phases without a given interaction.

Acknowledgment

The article was written as part of the VEGA 1/0494/17 Grant Agency project. The authors thank the Agency for their support. Our gratitude also goes to Alucast s.r.o. and Nemak Slovakia Ltd. for the technical coverage of experiments.

REFERENCES

[1] TILLOVÁ, E. - CHALUPOVÁ, M. (2009): *Štruktúrna analýza zliatin Al-Si*. Žilina: EDIS - vydavateľstvo ŽU, ISBN 978-80-554-0088-4.

[2] PISAREK, B. P. - RAPIEJKO, C. - SZYMCZAK, T. - PAYNIAK, T. (2017): *Effect of Alloy Additions on the Structure and Mechanical Properties of the AlSi7Mg0.3 Alloy*. Lódź : Archives of Foundry Engineering, Vol.: 17, 2017, ISSN: 1897-3310, pp. 137-142

[3] HERMANDEZ-SANDOVAL, VALTIIERRA, S. (2017):, *Thermal Analysis for Detection of Zr-Rich Phases in Al-Si-Cu-Mg 354-Type Alloys.* Québec: International Journal of Metalcasting, 2017, ISSN: 1939-5981, DOI: 10.1007/s40962-016-0080-0.

[4] BOLIBRUCHOVA, D. - KURIŠ, M. - MATEJKA. (2019): *Effect of Zr on Selected Properties and Porosity of AlSi9Cu1Mg Alloy for the Purpose of Production of Hight-precision Castings*a iní.. Žilina: Manufacturing Technology, Vol.: 19, 2019, ISSN: 552-558, DOI: 10.21062/ujep/333.2019/a/1213-2489/MT/19/4/552

[5] WANG, F. - QIU, D. - LIU, Z. - TAYLOR, J. A. - EASTON, M. A. - ZHANG. M. (2013): *The grain refinement mechanism of cast aluminium by zirconium.* St. Lucia: Acta Materialia, Vol.: 61, 2013, ISSN: 5636-5645, DOI: 10.1016/ j.actamat.2013.05.044, pp- 5636-5645.

[6] TSIVOULAS, D. - ROBSON, J. D. (2015), *Heterogeneous Zr solute segregation and Al_3Zr dispersoid distributions in Al-Cu-Li alloys*. Manchester: Acta Materialia, Vol.: 93, 2015,. DOI: 10.1016/j.actamat.2015.03.057, pp. 73-86.

[7] NABAWY, A. - M., SAMUEL, F. H. - DOTY, H. W. (2011): *Investigation of Chemical Additives on the Microstructure and Tensile Properties of Al-2 wt. % Cu Based Alloys.* Québec: American Foundry Socienty, AFS Proceedings, 2011, pp. 1-17.

[8] VONČINA, M. - MEDVED, J. (2018): *Effect of Molybdenum and Zirconium on Aluminium Casting Alloys.* Ljubljana: University of Ljubljana, Faculty of Natural Science and Engineering, 2018, ISSN: 552-558, DOI: 10.21062/ujep/333.2019/a/1213-2489/MT/19/4/552.

[9] RAKHMONOV, J. - TIMELLI, G. - BONOLLO, F. (2017): *Characterization of the solidification path and microstructure of secondary Al-7Si-3Cu-0,3Mg alloy with Zr, V and Ni additions*. Padova: University of Padova, Department of management and engineering, 2017, ISSN:1044-5803.

[10] MEDVED, J. - KORES, S. - VONČINA, M. (2018): *Development of Innovative Al-Si-Mn-Mg Alloys with Hight Mechanical Properties*. Ljubljana: University of Ljubljana, Faculty of Natural Science and Engineering, 2018, DOI: 10.1007/978-3-319-72284-9_50.

[11] LI, J. - H., OBERDORFER, B. - WURSTER, S. (2014): *Impurity effects on the nucleation and growth of primary $Al_3(Sc, Zr)$ phase in Al alloys.* Journal of Material Science, Vol.: 49, 2014, DOI: 10.1007/s10853-014-8315-z, pp. 5972-5977.

[12] BARADARANI, B. (2006): *Precipitation hardening of cast Zr-containing A356 aluminium alloy*. Tehran: University of Tehran - Faculty of Engineering, 2006, ISSN: 2606-2610, DOI: 10.1016/j.matlet.2006.01.046

[13] BOLIBRUCHOVÁ, B. (2019): *Trendy vo výrobe náročných hliníkových odliatkov s dôrazom na ekológiu.* Žilina: Žilinská univerzita v Žiline – Katedra technologického inžinierstva, Technológ, Vol: 5, 2019.

[14] FISCHER, E. - COLINET, C. (2015): *An Updated Thermodynamic Modeling of the Al-Zr System*. Journal of Phase Equilibria and Diffusion, Vol.: 35, 2015,. ISSN: 1547-7037.

[15] TSIVOULAS, D. - ROBSON, J., D. (2015): *Heterogeneous Zr solute segregation and Al_3Zr dispersoid distributions in Al-Cu-Li alloys*. Manchester: Acta Materialia, Vol.: 93, 2015,. DOI: 10.1016/j.actamat.2015.03.057, pp. 73-86.

[16] 17FULLER. CH., B., SEDMAN, D., N., DUNAND, D., C. (2003): *Mechanical properties of Al(Sc, Zr) alloys at ambient and elevated temperatures*. Ewaston: Acta Materialia, Vol.: 51, 2003, ISSN: 4803-4814, DOI: 10.1016/S1359-6454(03)00320-3, pp. 4803-4814.

The impact of cooling media on aluminum alloy with increased zirconium content

Lukáš Širanec, Ing.*
Department of Technological Engineering, Faculty of Mechanical Engineering,
University of Žilina,
Univerzitná 8215/1, 010 26 Žilina, Slovak Republic.
E-mail: lukas.siranec@fstroj.uniza.sk, Tel.: +421 41 513 2771

Elena Kantoríková, Ing., PhD.
Department of Technological Engineering, Faculty of Mechanical Engineering,
University of Žilina,
Univerzitná 8215/1, 010 26 Žilina, Slovak Republic.
E-mail: elena.kantorikova@fstroj.uniza.sk, Tel.: +421 51 513 2763

Dana Bolibruchová, prof. Ing., PhD.
Department of Technological Engineering, Faculty of Mechanical Engineering,
University of Žilina,
Univerzitná 8215/1, 010 26 Žilina, Slovak Republic.
E-mail: danka.bolibruchova@fstroj.uniza.sk, Tel.: +421 41 513 2772

Abstract: This article deals with the description of different cooling media used in hardening of aluminum alloys. The choice of suitable cooling environment is important in terms of achieving optimal mechanical properties (strength, ductility, hardness, etc.) and low internal stresses causing deformation of castings. In the experimental part, the influence of different cooling media on the mechanical properties of the AlSi7Mg0.3 alloy alloyed with zirconium was studied.

INTRODUCTION

Aluminum alloys are widely used construction materials applied mainly in the automotive and aerospace industry. The main advantage of using these alloys as construction materials are their good strength-to-weight ratio, satisfactory physical (thermal and electrical conductivity), chemical (corrosion resistance) or technological properties (e. g. formability).

Parts made of aluminum alloys (body parts, wheels, aircraft fuselages etc.) must meet a number of criteria for safe operation - they are required to have very good hardness, strength, corrosion and fatigue resistance, but also the ability to maintain their properties at negative and elevated temperatures. This combination of properties can be achieved by alloying alloys with suitable chemical elements or using age hardening heat treatment. Age hardening can effectively influence mainly the mechanical properties of aluminum alloys due to the precipitation of very small, evenly distributed particles of the hardening phases inside the alloy matrix [1]. The age hardening process consists of several steps (Fig. 1):

1. **Solution treatment**. During which the segregate (intermetallic phases precipitated at grain boundaries) being dissolved during heating to a specified temperature. After solution treatment, a homogeneous solid solution of α (*Al*) is obtained.
2. **Quenching**. The aim of quenching is to suppress elimination of coarse equilibrium intermetallic phases, resulting in the loss of mechanical properties. The purpose of quenching is to obtain a supersaturated solid solution at ambient temperature.
3. **Aging**. Characterized by precipitation of dispersed particles (θ phase) in the alloy matrix, which is accompanied by an increase in alloy´s hardness and strength. Depending on the type of aluminum alloy, aging can take place at ambient temperature (natural age hardening) or at elevated temperature (artificial age hardening).

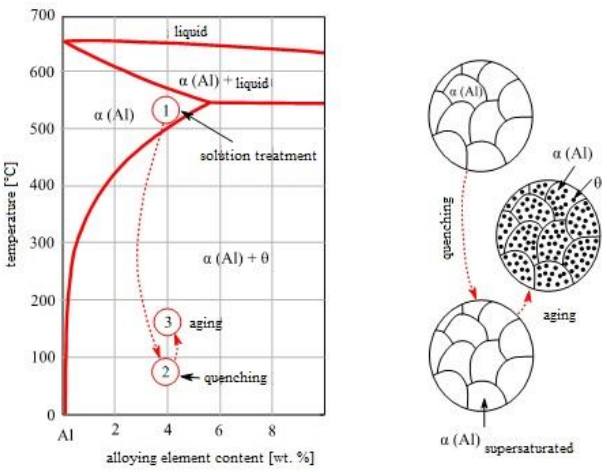

Fig. 1. Age hardening steps

As already mentioned above, coarse intermetallic phases eliminated at grain boundaries are being dissolved during solution treatment. These phases can cause a decrease in mechanical properties (especially ductility). The purpose of rapid cooling after solution treatment is to suppress the diffusion of alloying elements atoms to potential nucleation sites (grain boundaries, undissolved particles, etc.), thus preventing the re-elimination of such intermetallic phases [3]. Cooling after solution treatment must be realized by critical or supercritical speed. The critical cooling speed is the lowest speed at which a solid solution does not yet decompose during cooling from the solutionizing temperature [4, 5].

1 COOLING MEDIA

The intensity of heat dissipation of particular cooling medium is described by Grossmann´s factor *H*, defined as:

$$H = \frac{h}{2 \cdot k}, \tag{1}$$

where h – interfacial heat transfer coefficient [$W \cdot m^{-2} \cdot K^{-1}$],

k – thermal conductivity of cooled material [$W \cdot m^{-2} \cdot K^{-1}$]

Higher value of Grossmann´s factor *H* means that the material is more intensively cooled in a given cooling medium. The H value depends not only on the type of cooling medium, but also on its temperature and flow rate. Table 1 shows *H* values for water with different temperature and flow rate [5].

Tab. 1. Grossmann´s factor *H* for alloy AlZn5,5MgCu with 75 mm thickness [5]

Cooling medium	Cooling medium temperature [°C]	Cooling medium flow rate [$m \cdot s^{-1}$]	*H*
Water	27	0.0	1.07
Water	27	0.5	1.55
Water	38	0.0	0.99
Water	38	0.5	1.48
Water	60	0.0	0.86
Water	60	0.5	1.33

The mechanism of cooling can be described by three stages (Fig. 2):

1. **Vapor blanket stage**. In which the intensity of cooling is slow, since after immersion of the part in the cooling medium, a so-called vapor blanket that slows down the cooling process is being formed. Heat transfer is realized only by radiation through the vapor blanket. Cooling intensity in this stage is slow and in technical practice it is required that the period of existence of the vapor blanket should be as short as possible. For this reason, the circulation of the cooling medium is used to disrupt the vapor blanket [6].
2. **Nucleate boiling stage**. It is characterized by the disruption of the vapor blanket, allowing the contact of the cooling medium with the surface of the part. During contact, a large number of bubbles are formed and the cooling medium boils, which at the same time supports mixing of the cooling medium. Cooling intensity is the most intense at this stage [7].
3. **Convection stage**. When boiling no longer occurs. The intensity of cooling is slow, as the heat transfer is realized only by convection [7].

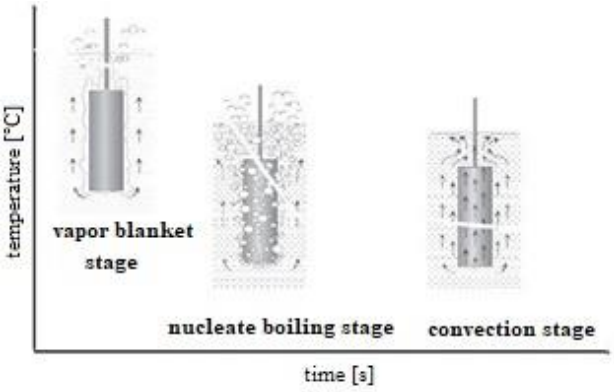

Fig. 2. Cooling stages [7]

There are several types of cooling media used in aluminum alloys age hardening process – media without change of state during cooling (e. g. air) and with the change of state (water, polymer solutions ...):

1. **Air**. Air is characterized as a cooling medium with relatively low cooling intensity (Grossmann´s factor $H \approx 0.02$ for calm air). Air cooling after solution treatment is rarely done – in most cases only with aluminum alloys, which are characterized by a very stable solid solution (e. g. AlMgSiCu0.3).
2. **Water**. It is the most frequently used cooling medium used in heat treatment of aluminum alloys. Cooling intensity can be controled by changing the flow rate ($H \approx 1$ for calm water and $H \approx 1.50$ for circulating water with 0.5 $m \cdot s^{-1}$ flow rate at 20 °C), or by changing its temperature. Table 2 shows correlation between water temperature and cooling rate.

Tab. 2. Correlation between water temperature and cooling rate [5]

Cooling medium	Cooling rate in range from 300 to 200 °C [$°C \cdot s^{-1}$]
Water 18 °C	600
Water 26 °C	500
Water 50 °C	100

1.1 Aqueous solutions

The adverse phenomenon of vapor blanket formation around the cooled part can be solved by using salt/hydroxide aqueous solutions. The principle of increasing cooling rate of aqueous solution is to brake up the vapor blanket by salt/hydroxide crystals forming during the water evaporation from the surface of the part. The most commonly used are 10 % NaOH and NaCl solutions [2, 3]. For illustration, Tab. 3 compares cooling rate of water and aqueous solutions.

Tab. 3. Cooling rate of water and aqueous solutions [5]

Cooling medium	Cooling rate in range from 300 to 200 °C [°C·s^{-1}]
Water 18 °C	600
10 % aqueous solution NaOH	1200
10 % aqueous solution NaCl	1100

1.2 Polymers

These cooling media are used as aqueous polymer solutions, ranging the polymer concentration in water from 5 to 30 %. Compared to water, cooling rate of such media is lower, which reduces internal stresses and deformation of the material – according to [8], based on experience from the aviation industry, using aqueous polymer solutions as cooling media can reduce the straightening cost of deformed parts by 60 % (compared to water cooling).

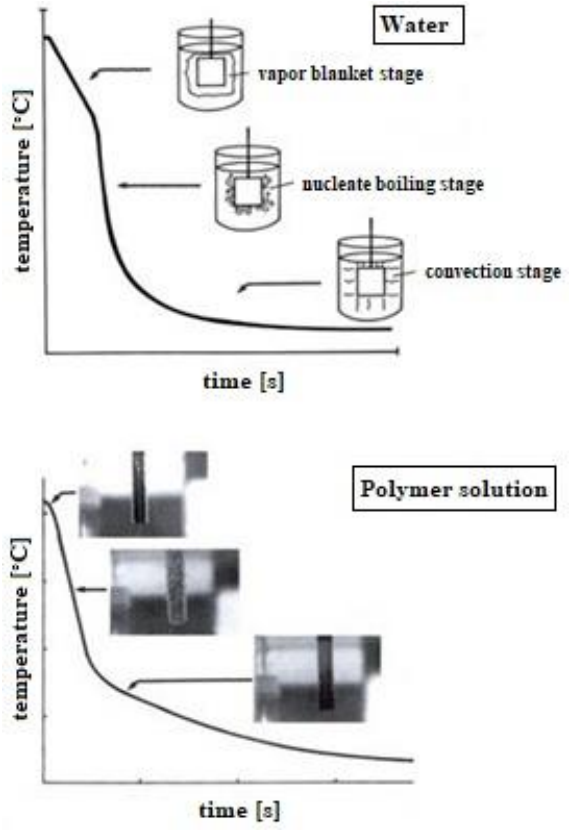

Fig. 3. Water and polymer solution cooling process [8]

The main disadvantage of polymer solutions is their gradual degradation, characterized by decomposition of the polymer chain under the thermal load. This phenomenon is called polymer aging and can be treated by increasing the polymer concentration in water up to 30 % [6].

Quenching the alloy into the polymer solution is characterized by the formation of a thin film of polymer on the surface of cooled part, which reduces the cooling rate. As can be seen in Fig. 3, the vapor blanket stage duration during polymer quenching is reduced, so the cooling is much more uniform compared to water cooling, resulting in temperature gradient reduction and reduction in the deformation rate of the cooling part.

In the heat treatment of aluminum alloys, two types of polymers are most commonly used: polyalkylene glycol (PAG) and polyvinylpyrrolidone (PVP), which are used dissolved in water in 5 to 30 % concentration.

1.3 Polyalkylene glycol (PAG)

It is characterized by a specific feature – inverse solubility. At ambient temperature, PAG is fully soluble in water. As the cooled part is immersed in PAG solution, with increasing temperature the polymer becomes insoluble, creating a thin layer on the surface of the cooled part that serves as an insulator and regulates the intensity of heat dissipation from the part [7]. This makes it possible to achieve more uniform cooling and eliminates the occurrence of high internal stresses causing deformations. After a certain time from immersion of the part in the polymer solution as the temperature of the part gradually decreases, the polymer redissolves in water (a thin layer on the surface of the part disappears) and cooling takes place at an increased rate [7].

1.4 Polyvinylpyrrolidone (PVP)

Compared to PAG, PVP polymer does not have the ability to regulate the intensity of heat dissipation due to reverse solubility by forming a thin layer on the surface of the part. In this case, the cooling rate is reduced by evaporation of water on the surface of the cooled part, whereby a viscous polymer shell with a higher concentration is formed. As temperature of the component decreases, the polymer concentration in the viscous shell decreases and the cooling rate begins to increase [8].

2 EXPERIMENTAL PART

The aim of the experiment was to compare the impact of different cooling media on mechanical properties of the aluminum alloy with increased zirconium (*Zr*) content. *Zr* forms an Al_3Zr intermetallics, which are stable at elevated temperatures and make it possible to increase the mechanical properties of the alloy

during age hardening and prevent their decrease in the environment with elevated temperature. Aluminum alloys alloyed with *Zr*, or other chemical elements creating thermodynamically stable intermetallic phases, can be used in the development of new materials designed e. g. for electric vehicles.

In the experiment, aluminum alloy AlSi7Mg0.3 alloyed with 0.2 wt. % *Zr* was used. In this alloy, the titanium content was also increased to 0.27, 0.37 and 0.47 wt. % *Ti*. Table 4 shows the values of mechanical properties of the reference alloy AlSi7Mg0.3 given in the STN EN 1706 standard. Mechanical properties of the experimental alloy alloyed with *Zr* were subsequently compared with these values.

Tab. 4. Mechanical properties of AlSi7Mg0.3 according to STN EN 1706 standard (permanent mold, T6 state)

Minimal mechanical properties	
Tensile strength R_m [MPa]	290
Ductility *A* [%]	4
Hardness *HBW*	90

The experimental alloy was artificially age hardened with following parameters:

- Solution treatment: 540 ± 5 °C/12 h.
- Quenching: 3 different cooling media – 20 °C water, 65 °C water and 5 % aqueous polymer solution at 20 °C (hereinafter referred as „polymer solution“).
- Aging: 155 ± °C/3 hours, air cooling.

2.1 Tensile test

Tensile test bars of circular cross-section made in accordance with STN EN ISO 6892-1 standard were placed in the testing machine and slowly extended until creating fracture. During the test, the correlation between the loading force and elongation was recorded. Using PC software, the measurement of tensile strength R_m and ductility *A* of each specimen was determined. The average values of R_m and *A* depending on the cooling medium used are given in Tab. 5.

2.2 Hardness

After the tensile test, cylindrical specimens were taken from the tensile test bars, on which the Brinell hardness was measured using Innovatest Nexus 3000 measuring device. Hardness measurement was performed with following parameters:

- Indenter: carbide ball with 5 mm diameter.
- Load: 250 kp (2451.6 N).
- Load time: 10 s.

Five hardness measurements were made on each specimen at different locations. Figure 4 shows the average hardness values of tested specimens depending on the type of cooling medium.

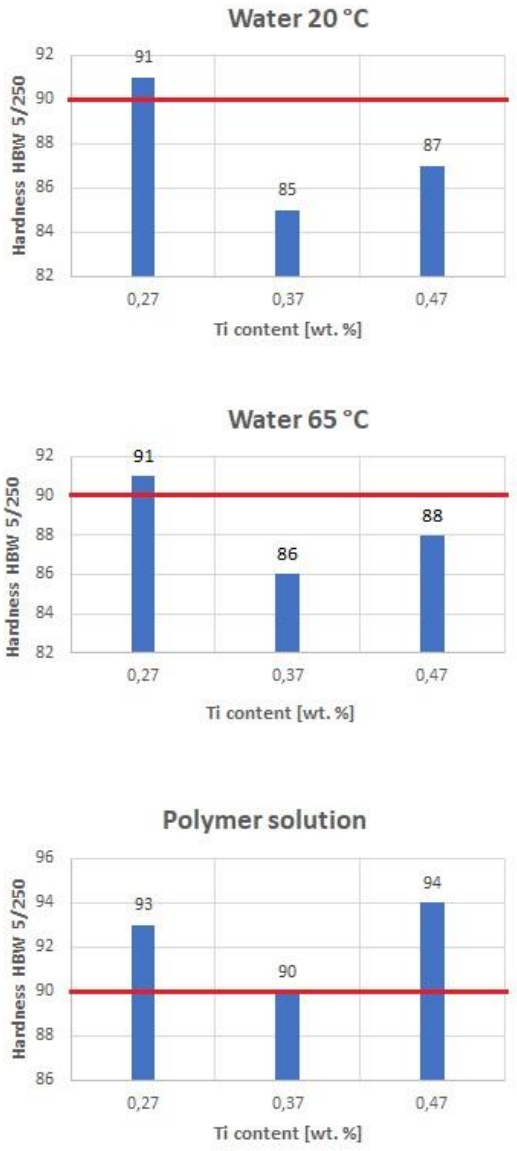

Fig. 4. Hardness values

Tab. 5. Average values of R_m and *A* depending on the type of cooling medium

Cooling medium	Specimen [wt. % *Ti*]	R_m [MPa]	*A* [%]
Water 20 °C	0.27	227	1.9
	0.37	250	3.7
	0.47	280	4.8
Water 65 °C	0.27	251	3.7
	0.37	244	3.4
	0.47	252	4.4
Polymer solution	0.27	222	1.1
	0.37	238	2.5
	0.47	253	2.8

3 SUMMARY OF RESULTS

As can be seen in Tab. 5, none of the tested specimen of the experimental alloy reached at least the same or higher values of R_m compared to the reference alloy AlSi7Mg0.3, which $R_{m\,min}$ = 290 MPa. Specimen with R_m = 280 MPa (alloyed with 0.47 wt. % *Ti*, quenched into 20 °C water) was closest to this value. The failure to achieve increased values of tensile strength might be caused by imperfect dissolution of Zr alloying element, possibly affecting only limited hardening effect after heat treatment of the alloy.

From the measured ductility values (Tab. 5) of specimens, it can be stated that there was a decrease in ductility in most of the tested specimens (compared to ductility of the reference alloy with A_{min} = 4 %). The increase in ductility values occurred only in two specimens (probably due to the formation of fine-grained structure of the α phase due to the presence of a higher amount of *Ti*):

- A specimen with 0.47 wt. % *Ti*, cooled in 20 °C water, with 20 % increase in ductility compared to the reference alloy.
- A specimen with 0.47 wt. % *Ti*, cooled in 65 °C water, at with 10 % increase in ductility compared to the reference alloy.

An increase in the hardness values of the experimental alloy specimens compared to the reference alloy, whose HBW_{min} = 90 (red line in Fig. 4), was recorded in 4 tested specimens (Fig. 4). The highest increase was recorded in the specimens quenched into polymer solution, where the hardness value increased from 90 *HBW* to 93 and 94 *HBW* (3.3 and 4.4 % increase).

CONCLUSION

The aim of the experiment presented in this paper was to compare the influence of different cooling media on mechanical properties of the experimental aluminum alloy AlSi7Mg0.3 with increased zirconium content.

Despite the fact that most of the specimens failed to reach the improvement in mechanical properties after age hardening, it can be concluded that the best combination of mechanical properties (tensile strength, ductility, hardness) among all tested specimens in the experiment reached specimen alloyed with 0.47 wt. % Ti cooled into 20 °C water, and thus this cooling medium appears to be the most suitable for the heat treatment of this alloy.

As this medium had the highest cooling rate among the all media used in the experiment, by high cooling rate after the solution treatment a solid solution with sufficient degree of supersaturation was produced, from which the hardening phases subsequently precipitated during age hardening.

Acknowledgment

This article was created within the project of the grant agency VEGA 1/0494/17. The authors would like to thank VEGA agency for support.

REFERENCES

[1] MACKENZIE, D.S. - BOGH, N. - CROUCHER, T. (2016): *Quenching of aluminum alloys.* [online]. 2020 [cit. 2020-09-15]. Available at: http://www.boghindustries.com/articles/QuenchingAluminum%20Alloys%20161219.pdf.

[2] Precipitation hardening of aluminum alloys (2002): [online]. 2020 [cit. 2020-09-22]. Available at: https://imechanica.org/files/handout4.pdf.

[3] GÁBRIŠOVÁ, Z. - BRUSILOVÁ, A. (2019): *Tepelné spracovanie. Návody na cvičenia.* Bratislava: Vydavateľstvo SPEKTRUM STU. ISBN: 978-80-227-4894-0.

[4] MICHNA, Š. - Michnova, L. (2014): *Neželezné kovy*. Praha: PrintPoint s.r.o.. ISBN: 978-80-260-7132-7.

[5] POLMEAR, I. J. (2004): *Aluminium Alloys – A Century of Age Hardening.* [online]. 2020 [cit. 2020-09-16] Available at: https://core.ac.uk/download/pdf/160256824.pdf.

[6] FABIAN, P. - KEČKOVÁ, E. - BETÁK, P. (2007): *Tepelné spracovanie kovov.* Žilina: Tlačiareň svidnícka, s.r.o. ISBN: 978-80-969-5927-3.

[7] Heat treating (2002): [online]. 2020 [cit. 2020-09-24] Available at: https://shorturl.at/elyTZ.

Effect of Different Welding Parameters on the Mechanical Properties of the HSLA Steel Welded Joint

Martin Frátrik, Ing.
Department of Technological Engineering, Faculty of Mechanical Engineering,
University of Žilina,
Univerzitná 8215/1, 010 26 Žilina, Slovak Republic.
E-mail: martin.fratrik@fstroj.uniza.sk , Tel.: +421 910 576 568

Miloš Mičian, doc. Ing., PhD.*
Department of Technological Engineering, Faculty of Mechanical Engineering,
University of Žilina,
Univerzitná 8215/1, 010 26 Žilina, Slovak Republic.
E-mail: milos.mician@fstroj.uniza.sk , Tel.: +421 41 513 2768

Abstract: This article deals with the use of various welding parameters for butt welding of HSLA steel S960MC. The subject of the research is a steel sheet used for production of cranes, arms, load-bearing structures, etc. Based on mechanical testing and macrostructural analysis is assessed weldability of researched steel. The obtained values are compared to assess the effect of heat input on mechanical properties. The results show that the strength of welded joints decreases with increasing heat input.

INTRODUCTION

In today's industrial production there is a growing demand for weight reduction of structures. This requirement has accelerated the development and production of new types of high-strength steels such as HSLA steels, which are characterized by high strength with a low carbon and alloys content. Therefore, it is improvement in properties of HSLA steels associated with different strengthening mechanism, which are not based only on the carbon content. The most important is grain refinement whereby both strength and toughness are improved at the same time [1]. Steel is also strengthened by precipitation strengthening with nanoscale precipitates of different types and size together with solid solution strengthening. All those strengthening mechanisms can be achieved in the thermo-mechanical controlled process (TMCP), which includes controlled rolling with accelerated cooling. The investigated steel S960MC was also produced in this way. When welding TMCP steels, the strength of the welded joint decreases due to softening in HAZ. This decrease is due to the exceeded heat input, which adversely affects the cooling rate and the resulting HAZ microstructure [2,3,4]. For this reason, it is recommended to minimize heat input when welding such steels [7,8]. In the case of GMAW, the reduction of the heat input is performed by using different modes of metal transfer such as pulse or CMT (Cold Metal Transfer). Those modes provide lower heat input during welding. Another way to reduce heat input is to use FCAW. Tubular wire offers a higher deposition rate, which allows an increase in welding speed and thus a decrease in heat input [6].

This work deals with the application of various welding parameters and welding methods in the welding of S960MC butt welds. Therefore, short arc, pulse and CMT welding modes were applied. Welds made by metal-cored wire were only welded in short arc. The effect of the applied heat input on the welds was evaluated. For comparison, a macroscopic analysis, tensile test, and hardness test were performed.

1 MATERIALS AND METHODS

1.1 Materials

A 3 mm thick Strenx960MC (SSAB, Sweden) steel sheet was used as the base material. Steel was made by thermo-mechanical controlled process, which provided a fine-grained microstructure composed by martensite, tempered martensite and retained austenite with additions of dispersive precipitates. Chemical composition is shown in Tab. 1 and mechanical properties in Tab. 2.

Tab. 1. Chemical composition of steel S960MC (wt. %)

C	*Si*	*Mn*	*P*	*S*	*Al*	*Nb*	*V*
0.085	0.18	1.06	0.01	0.003	0.036	0.002	0.007
Ti	***Cu***	***Cr***	***Ni***	***Mo***	***N***	***B***	
0.026	0.01	1.08	0.07	0.109	0.005	0.0015	

Tab. 2. Mechanical properties of steel S960MC

$R_{p0.2}$ [MPa]	R_m [MPa]	A_{min} [%]	*CET/CEV*	*KV –40 C*
960	1000-1250	7	0.28/0.51	27

Used filler materials, Union X96 classified as G89 5 M21 Mn4Ni2.5CrMo according to STN EN ISO 16834-A and Böhler X96 L-MC with classification T89 4 TMn2NiCrMo M M21 1 H5 according to STN EN ISO 18276-A (both Voestalpine, Austria) are intended for welding fine-grained high-strength steels and guarantee good deformability in spite of very high strength values. Chemical compositions according to manufacturer are given in Tab. 3.

Tab. 3. Chemical composition of filler materials (wt.%)

	C	*Si*	*Mn*	*Cr*	*Mo*	*Ni*
Union X 96	0.12	0.80	1.90	0.45	0.55	2.35
Böhler X96 L-MC	0.06	0.70	1.90	0.60	0.50	2.20

1.2 Mechanical testing

All welded joints were subjected to a tensile test in accordance with the standard STN EN ISO 4136 on the ISTRON 5985 device. Two test specimens were taken from each welded joint, from which the average values of yield strength, tensile strength and elongation were calculated.

Samples for the bending test were taken in accordance with STN EN ISO 7438. The test is used to determine the ability of the welded joint to deform plastically. The essence of the test is the bending deformation of the test specimen by means of the loading mandrel up to the prescribed angle, or until the appearance of cracks. 2 samples were loaded from the root side (TRBB) and 2 samples from the face side (TFBB).

Hardness measurements were performed to assess the microstructural changes in HAZ due to the welding process. Measurements were made in a line 1.5 mm from the top edge of the sheet by the Vickers method with a load of 1 kg (HV1). A total of 87 indents with a distance of 0.25 mm were made. The line thus recorded the hardness distribution across all zones of the welded joint (BM, HAZ, WM) (Fig.).

1.3 Macrostructural analysis

Macrostructural analysis was performed using a stereo microscope Olympus SZX 16. Cross-sectional samples were etched with 2 % Nital.

2 WELDING PROCEDURE

For the purposes of the experiment, I-shaped butt welds were made. A Fronius TPS2700 welding machine was used. The welding torch was clamped in the Fronius FDV 15/MF positioning device during GMAW (135) welding. During FCAW (138), the torch was clamped on the arm of the KUKA VKR250/2 industrial robot. Welded sheets with dimensions 3x150x300 mm were clamped on the work table using clamps as shown in Fig. 1.

Fig. 1. Welded parts clamped on the working table

Welding parameters for all welded joints are shown in Tab. 4.

Tab. 4. Welding parameters for various welded joints

Weld	v_{wire} [m·mm^{-1}]	I_m [A]	U_m [V]	v_w [mm·s^{-1}]	Q_p [kJ·cm^{-1}]
135 short arc	3.8	102	16.6	3.7	3.69
135 pulsed	3.2	61	19.7	3.7	2.62
135 CMT	5.3	131	13.1	8.3	1.65
138 short arc	3.0	86	14.7	4.0	2.53
138 cooled	3.0	86	14.7	4.0	2.53

3 RESULTS AND DISCUSSION

The macrostructures of all welds were analysed to compare the effect of heat input on the width of the HAZ. Figure 2 shows macrostructural images of the investigated welds with the indicated HAZ width (both HAZ zones together with the width of the weld metal). Based on these macrostructural images, it is possible to observe the effect of heat input on the HAZ width. Lower heat input reduces the width of the total HAZ, applies to solid wire. When using a metal-cored electrode, the trend of decreasing the HAZ width continues, with the heat input increasing.

The average values of yield strength and tensile strength are shown in Fig.3. The values are also shown in Tab.5.

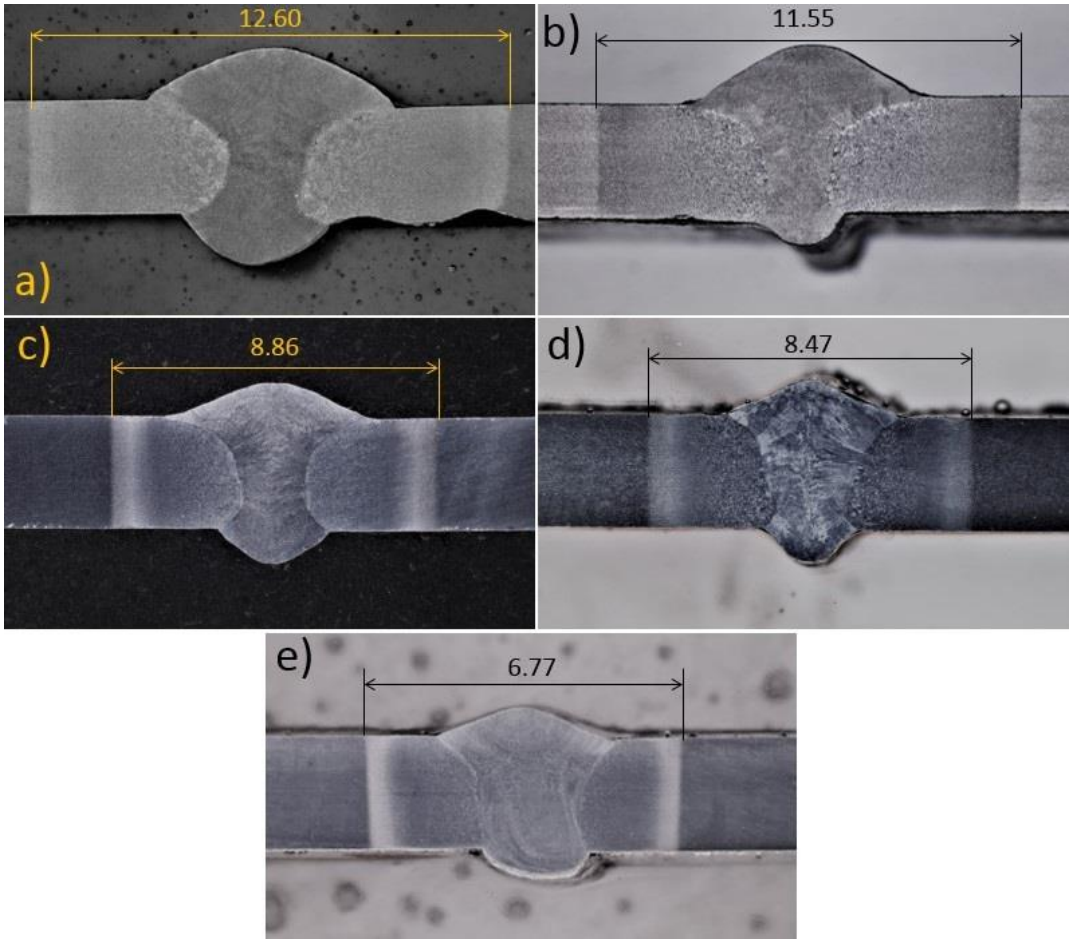

Fig. 2. Cross-sectional images of investigated welds welded by various methods: a) 135 – short arc, b) 135 – pulsed, c) 135 – CMT, d) 138 – short arc, e) 138 – short arc (cooled)

Tab. 5. Mechanical properties of various welded joints

Weld	Average $R_{p0,2}$ [MPa]	Average R_m [MPa]	Average A [%]
135 short arc	883	921	3,3
135 pulsed	915	940	2,2
135 CMT	927	945	2,2
138 short arc	951	969	2,2
138 cooled	955	972	1,7

It can be observed that the strength of welded joints increases with decreasing heat input. This is due to the increase in the cooling rate, which significantly affects the resulting decay structures in the HAZ, especially in the inter-critical heat affected zone (ICHAZ).

The above graph also shows that neither the value of the yield strength nor the value of the yield strength corresponds to the values specified in the standard STN EN ISO 10149. The standard requires a minimum tensile strength of 980 MPa. The strength also does not comply with the standard STN EN ISO 15614-1, which is used to approve welding procedures.

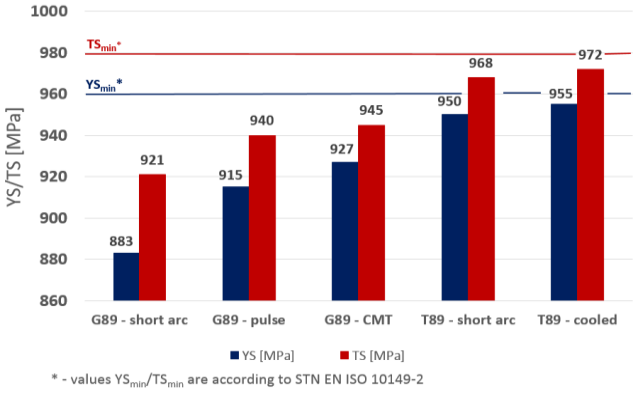

Fig. 3. YS/TS values for various welding parameters

This decrease is caused by the phenomenon of softening. Due to the thermal effect from the welding process, the strength in a certain part of the HAZ decreases. The hardness distribution on the cross section of the FCAW welded joint shows the mentioned phenomenon (Fig. 4). A similar significant drop in hardness is found on each of the welded joints considered. The decrease in hardness at the most softened zone compared to base material (360 HV1) varies from 70 HV1 to 110 HV1. This decrease does not correspond to the measured

strength values, which means that the decrease in strength is not affected only by the decrease in hardness but by the width of the soft-zone. The main cause of the hardness drop was excessive overheating of the material and low cooling rate, which caused the formation of tempered martensite, ferrite and coarsening of precipitates in the area.

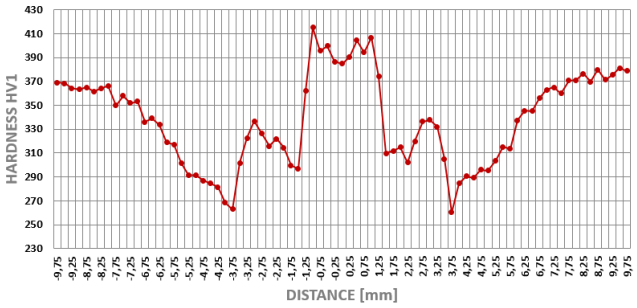

Fig. 4. Cross-sectional hardness distribution on FCAW welded joint in short arc mode

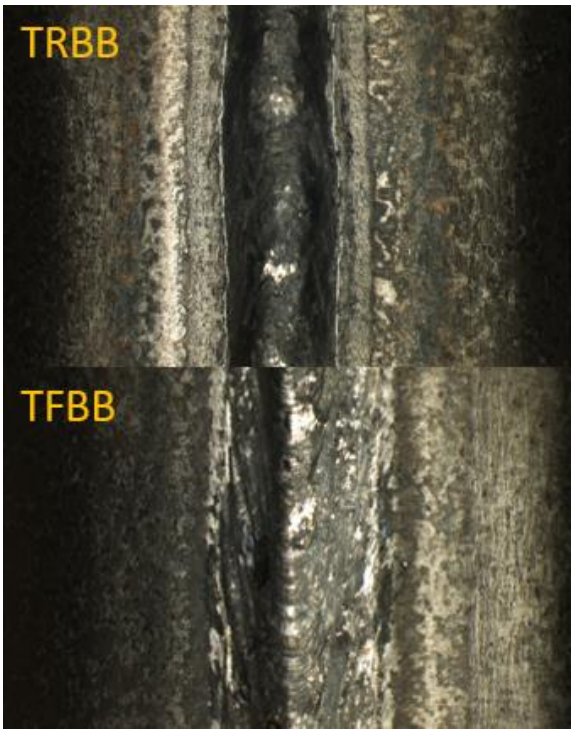

Fig. 1 Detailed images of the specimens after the bending test

The bending test showed sufficient plastic properties of the welded joint. Specimens after the test are shown in Fig. 5.

CONCLUSIONS

Based on macroscopic analysis, it is possible to observe the effect of heat input on the width of HAZ. Mechanical testing also showed a change in mechanical properties depending on heat input. The observed results can be summarized in the following points:

- The use of pulse and CMT mode in MAG welding resulted in a decrease of heat input.
- With decreasing heat input, the width of the HAZ decreases significantly.
- The strength of welded joints increases with decreasing heat input.
- With increasing YS/TS, elongation decreases significantly.
- Compared to the FCAW method in the short arc mode, a lower heat input was measured on welds welded by GMAW in the CMT mode, which, however, did not result in an increase in strength. The strength depended on the width of the soft zone, which was narrower in the case of FCAW.

Acknowledgement

The research was supported by KEGA agency no. 009ŽU-4/2019 and APVV agency with project no. APVV-16-0276.

REFERENCES

[1] LIU, Y. - ZHU, F. - LI, Y. - WANG, G. (2005): *Effect of TMCP Parameters on the Microstructure and Properties of an Nb-Ti Microalloyed Steel*. ISIJ International, Vol. 45 (2005), No. 6, pp. 851-857.

[2] PISARSKI, H.G. - DOLBY, R.E. (2003): *The significance of Softened HAZs in High Strength Structural Steels.* Welding in the World, Vol. 47 (2003), No. 5/6, pp. 32-40.

[3] HOCHHAUSER, F. - ERNST, W. - RAUCH, R. - VALLANT, R. - ENZINGER, N. (2012): *Influence of the Soft Zone on the Strength of Welded Modern HSLA Steels*. Welding in the World, Vol. 56 (2012), pp. 77-85.

[4] de MEESTER, B. (1997): *The Weldability of Modern Structural TMCP Steels*. ISIJ International, Vol. 37 (1997), No. 6, pp. 537-551.

[5] JAMBOR, M. - NOVÝ, F. - MIČIAN, M. - TRŠKO, L. - BOKUVKA, O. - PASTOREK, F. - HARMANIAK, D. (2018): *Gas Metal Arc Welding of Thermo-mechanically Controlled Processed S960MC Steel Thin Sheets with Different Welding Parameters*. Communications, Vol. 20 (2018), No. 4

[6] MYERS, D. (2020): *Advantages and Disadvantages of Metal Cored Wires* [Online]. 2020. [Cit. 2020-04-16]. Available at: https://www.esabna.com/us/en/education/blog/advantages-and-disadvantages-of-metal-cored-wires.cfm

[7] KAH, P. - PIRINEN, M. - SUORANTA, R. - MARTIKAINEN, J. (2014): *Welding of Ultra High Strength Steels*. Advanced Materials Research, Vol. 849 (2014), pp. 357-365.

[8] SCHNEIDER, CH. - ERNST, W. - SCHNITZER, R. - STAUFER, H. - VALLANT, R. - ENZINGER, N. (2018): *Welding of S960MC with Undermatching Filler Material*. Welding in the World, Vol. 62 (2018), No. 4, pp. 801-809.

Plasma nitriding of tools steels

Elena Kantoríková, Ing., PhD.*
Department of Technological Engineering, Faculty of Mechanical Engineering,
University of Žilina,
Univerzitná 8215/1, 010 26 Žilina, Slovak Republic.
E-mail: elena.kantorikova@fstroj.uniza.sk, Tel.: + 421 41 513 2763

Denis Martinec, Ing.
Department of Technological Engineering, Faculty of Mechanical Engineering,
University of Žilina,
Univerzitná 8215/1, 010 26 Žilina, Slovak Republic.
E-mail: denis.martinec@fstroj.uniza.sk, Tel.: + 421 41 513 2753

Richard Pastirčák, doc. Ing., PhD.
Department of Technological Engineering, Faculty of Mechanical Engineering,
University of Žilina,
Univerzitná 8215/1, 010 26 Žilina, Slovak Republic.
E-mail: richard.pastircak@fstroj.uniza.sk, Tel.: + 421 41 513 2767

Abstract: Plasma nitriding is one of the modern methods of nitriding layer formation, but it is still under observation. The article compares the mechanical properties of steels, which were produced by powder metallurgy and on which a nitridation layer was formed by plasma. The results presented that the formation of the layer depends on the chemical c composition of the material.

INTRODUCTION

There are still high demands on the mechanical properties of the tools. The aim is to constantly improve the quality of the tool. Tools must have a long service life and must retain their properties such as hardness, toughness, dimensional stability, wear resistance even at high operating temperatures, pressures, and forces [1]. Tools produced by powder metallurgy meet all quality requirements. The principle of powder metallurgy is in pressing metallic or non-metallic powder into the desired shape and its subsequent sintering. During production, the greatest emphasis is placed on the shape, dimensions, and weight of the moulding. The biggest advantages of powder metallurgy include the ability to combine different materials and good chemical uniformity. The components are excellently resistant to wear and abrasion. No waste is generated during production. Powder metallurgy can only be used for series production. With the right combination of chemical composition and very fine grain, which is characteristic of this method, we achieve very advantageous mechanical properties. We can increase them by using suitable thermal and chemical-thermal treatment [2, 3]. High demands are placed on tool steels, which include hardness, tempering resistance, toughness, cutting ability, wear resistance, hardenability, and dimensional stability. Due to these requirements, a high carbon content and proper heat treatment, hardening and subsequent tempering are usually required [4]. During heat treatment, there are always reactions between the processed product and the surrounding environment. The exchange of matter on the surface of the product with the surrounding environment can take place spontaneously or by chemical-thermal treatment [5].

Plasma nitriding known as ion nitriding or radiant discharge nitriding. It is nitriding in a gaseous atmosphere, amplified by a plasma discharge on the parts we want to nitride. Plasma is a gas into which, when we bring in an electric potential, it begins to ionize and glow. The nitrided parts and the walls of the furnace are connected by means of a cathode and an anode. The cathode is located on the nitrided parts and the anode on the furnace walls. The size of the supplied electric potential is between 0.3 - 1 kV. The particles begin to accelerate and strike the cathode (nitrided parts), transferring all their kinetic energy and generating heat. The magnitude of the kinematic energy of the particles depends on the size of the mean distance between the particles and the free path. As a result, the particles can reach the highest possible speed they need before colliding with the workpiece and subsequent collision with another gas particle. For this reason, plasma nitriding is most often performed in a vacuum [6].

Advantages of plasma nitriding - gases (nitrogen, hydrogen and argon) are environmentally friendly. There is no danger of fire, because the process takes place in a vacuum. Increases nitrogen storage rate and heating time. The possibility of automation increases the reliability of production and

repeatability of the process. Ability to process stainless steels. Unlike a salt bath, with plasma nitriding, only the parts we need can be nitrided very easily. Low decarburization when working in a vacuum and low operating costs.

Disadvantages of plasma nitriding - the biggest disadvantage of plasma nitriding compared to nitriding in salt baths or in a gaseous atmosphere is the price. While the operating costs of plasma nitriding are among the advantages, the purchase price of the devices needed for this technology is very demanding. Another disadvantage of the process is the formation of a hollow cathode. The hollow cathode is an area of low vacuum pressure where the flame glow seam does not follow the contour of the nitrided part. This effect usually occurs in blind holes where electrons are trapped and begin to flow through the walls of the holes. There is a large ion bombardment of the steel and its overheating, which causes the steel to burn or sputter.

1 METHODS AND TEST SAMPLES

The main goal of the research was to compare the mechanical properties of tool steels after plasma nitriding. The work is devoted to monitoring the influence of plasma nitriding on changes in the structure of tool steels. Seven samples with different chemical compositions were prepared. The samples were made by powder metallurgy and subjected to heat treatment before nitriding. The nitriding was performed at 490 ° C for 2 hours. The samples were evaluated for hardness and the thickness of the nitriding layer was measured. For CPM 3V and Vancron samples, it was not possible to measure the thickness of the niridation layer, therefore only the microstructure of the given steel is given. The individual steels are described below.

1.1 CPM 3V steel

CPM 3V is a newly developed ultra-hard and high-performance tool steel.

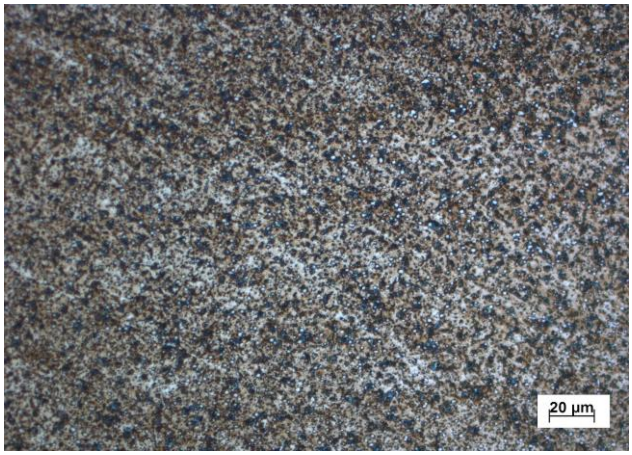

Fig. 1. Microstructure after nitriding (incr. 1000x) CPM 3V

It is characterized by high resistance to wear, breakage and splitting of the tool, wear resistance. It is used for cutting and punching tools for thicker sheets, tools for fine edging, pressing, and forming tools, for rolling tools and threads, cutting and industrial knives. Figure 1 shows the wet structure of nitrided steel, the surface layer could not be measured.

1.2 CPM 15V steel

This steel was developed in 2007. CPM 15V contains more vanadium carbides, which ensures better wear resistance and longer tool life. Compared to conventionally produced steel, it has excellent dimensional stability, grindability and toughness. It is most often used for cutting and punching tools for thinner sheets, drawing tools, knives for cutting foil and paper, rotary cutters, machine parts for highly abrasive plastics, etc. Figure 2 shows the thickness of the nitriding layer about 593 µm.

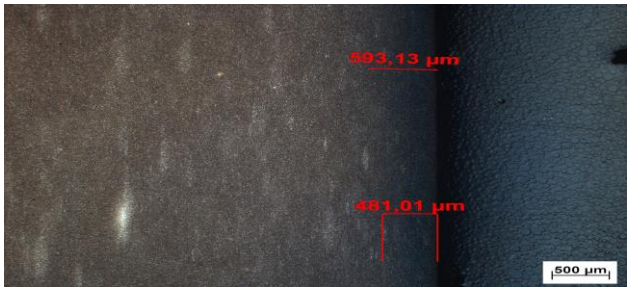

Fig. 2 Nitriding layer thickness CPM 15V.

1.3 TSP1 steel

This tool steel is produced by powder metallurgy. It is characterized by extremely high and exceptional toughness. It has good wear resistance and compressive strength due to the presence of *Nb*, and increased hot hardness due to the presence of *Co*. These properties are the result of a unique production process. TSP1 also has a very high dimensional stability after heat treatment. It is used for high-performance tools such as cutting tools, punching tools, stamping tools and dies, calibration tools, cold forming tools and forging tools. The thickness of the niridation layer is about 633 µm (Fig. 3).

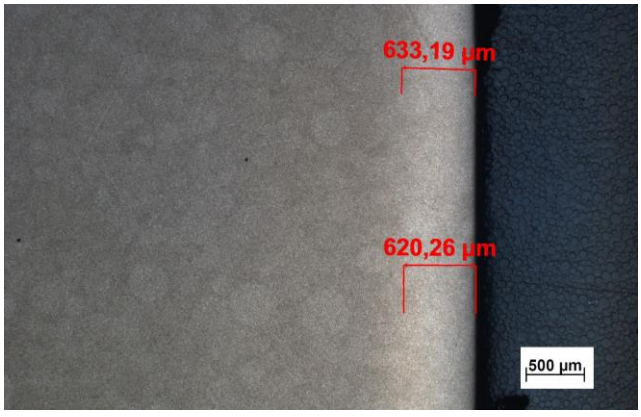

Fig. 3. Nitriding layer thickness TSP1

1.4 S390 tool steel

S390 tool steel is a high-speed steel produced by powder metallurgy. It is characterized by good hardness, compressive strength, and wear resistance. Thanks to powder metallurgy production, the S390 has excellent toughness and machinability. It is most often used to produce twist drills, taps, milling cutters, stretchers or for cold work. The thickness of the niridation layer is about 428 μm (Fig. 4).

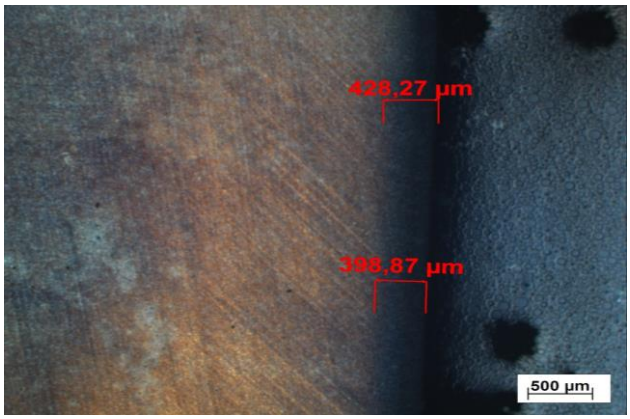

Fig. 4. Nitriding layer thickness S390

1.5 M390 tool stainless steel

M390 is a tool stainless steel. It is characterized by extremely high wear resistance, excellent corrosion resistance, excellent mirror finish, high toughness, minimal dimensional changes, better resistance to vibration and mechanical shock. It is used for the production of CD and DVD molds, molds for processing chemically aggressive plastics containing highly abrasive fillers, molds for processing duraplasts, molds for injection molding machines, check valves, linings for injection rollers, machine parts for the paper and food industries. The thickness of the niridation layer is approx. 603 μm (Fig. 5).

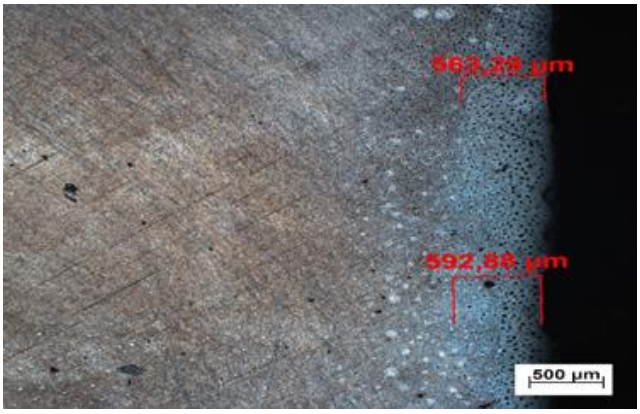

Fig. 5. Nitriding layer thickness M390

1.6 CALDIE tool steel

Caldie is a chromium-molybdenum tool steel alloyed with vanadium, which is characterized by very good crush resistance, high hardness (> 60 *HRC*) at high temperature, good dimensional stability during heat treatment and operation, excellent hardening properties, polishability, good tempering resistance, good machinability and sandability. This steel has been developed with the focus on use in demanding cold work applications. It is used for forging and cold forming, tool knives, substrate for surface coatings, knives for fragmentation of plastics and metals. The thickness of the niridation layer is about 295 μm (Fig. 6).

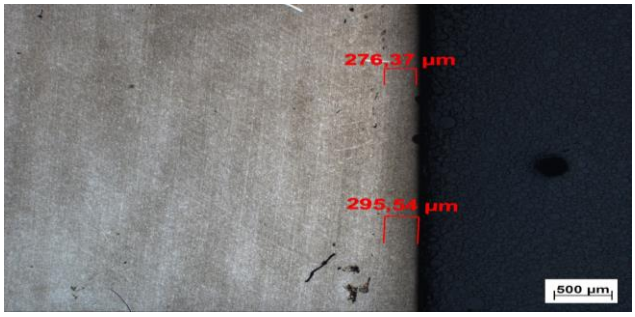

Fig. 6. Nitriding layer thickness CALDIE

1.7 VANCRON SUPERCLEAN tool steel

Vancron SuperClean is a Cr-Mo-V-N cold-rolled tool steel, which is characterized by very high resistance to wear and seizure, good resistance to tearing, cracking and tempering, high compressive strength and good dimensional stability during hardening. It is used for cutting, forming, cold working and powder metallurgy. Figure 7 shows the wet structure of nitrided steel, the surface layer could not be measured.

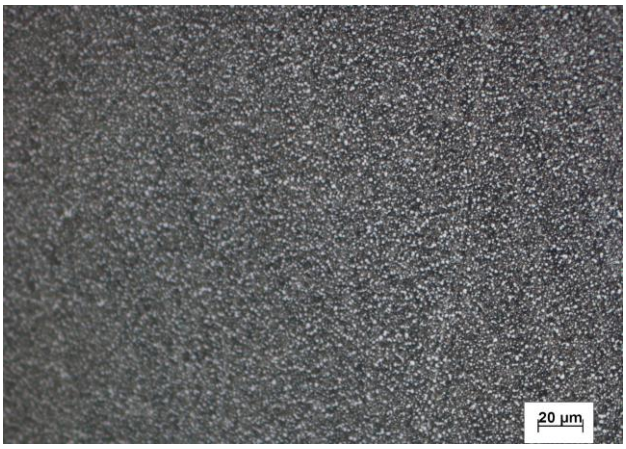

Fig. 7. Microstructure after nitriding (incr. 1000x) Vancron SuperClean

2 DISCUSSION OF RESULTS

The work deals with the influence of plasma nitriding on changes in the structure of tool steels. The biggest advantages of plasma nitriding include a shorter nitriding process time, the ability to nitride stainless steels and environmental friendliness. Plasma nitriding is used mainly to increase the hardness of the surface layer and the abrasion resistance properties of materials. All steels are high alloy, have high hardness, toughness, and wear

resistance. Figure 8 shows the difference in the chemical composition of individual samples. The carbon content is in the range of 0.7 - 3.4 %. The Cr content in M390 is 2% and the Vanadium content in CPM 15V (14.5 %) and Vancron (10 %) is significant. S390 steel surpasses others with vanadium and cobalt content.

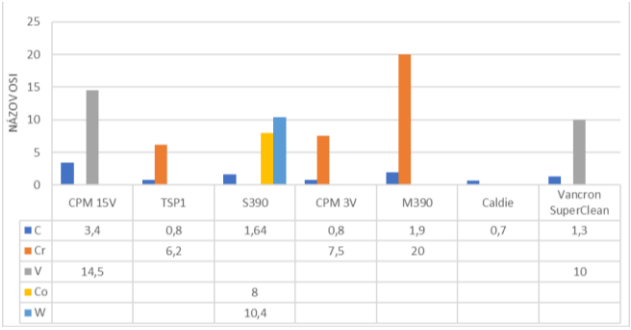

Fig. 8. Comparison of chemical composition [%]

There were performed five measurements on each sample, gradually from the edge to the core of the sample. These hardnesses differed only minimally since the nitriding layer is very thin. The highest average hardness was measured for Vancron SuperClean steel (62 *HRC*) and the lowest for TSP1 steel (57 *HRC*). The hardness of the samples is presented in Fig. 9.

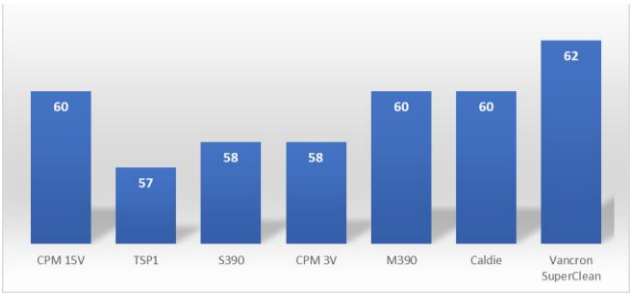

Fig. 9. Average hardness of samples [HRC]

The thicknesses of the nitriding layers are compared in Fig. 9. The largest layer was achieved on TSP1 steel (633 µm) and the lowest on Caldie steel (295 µm). CPM 3V steels and Vancron supercliens failed to determine the nitriding layer thickness.

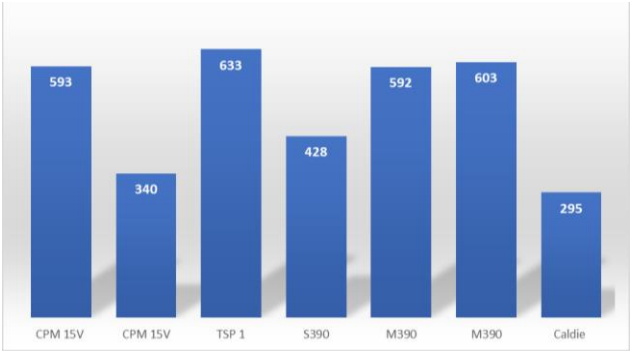

Fig. 10. Maximum measured value of the nitriding layer thickness of the samples [µm]

REFERENCES

[1] CZERWIEC, T. - RENEVIER1, N. - MICHEL, H., (2000): *Low-temperature plasma-assisted nitriding*. Droitwich SPA: Teer Coatings Ltd, 2000. Surf. Coating Technology 131, 267-277.

[2] KOCH, H. - FRIEDRICH, L. J. - HINKEL, V. - LUDWIG, F. - POLITT, B. - SCHURIG, T. (1991): *Hollow cathode discharge sputtering device for uniform large area thin film deposition*. J. Vac. Sci. Technol., A 9, 2374.

[3] BOLIBRUCHOVÁ, D. - PASTIRČÁK, R. (2018): *Foundry metallurgy of non-ferrous metals* (In Slovak). Žilina: EDIS – Publishing house. ISBN: 978-80-554-1463.

[4] FUNATANI, K. (2004): *Low-temperature salt bath nitriding of steels*. Nagoya: Metal Science and Heat Treatment, 2004. Vol. 46, Nos. 7 – 8.

[5] KRAUS, V. (2013): *Heat treatment and sintering* (In Czech). Plzeň, ISBN 978-80-2610-260-1.

[6] PULC, V. - HRNČIAR, V. - GONDÁR, E. (2004): *Material science* (In Slovak). Bratislava: STU v Bratislave, 333 pages, ISBN 80-2272-8478.

Evaluation of influence of filter media on the reoxidation processes with the aid of simulation software

Marek Galčík, Ing.
Department of Technological Engineering, Faculty of Mechanical Engineering,
University of Žilina,
Univerzitná 8215/1, 010 26 Žilina, Slovak Republic.
E-mail: marek.galcik@fstroj.uniza.sk, Tel.: + 421 41 513 2771

Marek Brůna, doc. Ing., PhD.*
Department of Technological Engineering, Faculty of Mechanical Engineering,
University of Žilina,
Univerzitná 8215/1, 010 26 Žilina, Slovak Republic.
E-mail: marek.bruna@fstroj.uniza.sk, Tel.: + 421 41 513 2756

Abstract: Reoxidation is one of the main problems in the casting process of aluminium alloys. The oxide layer created on the melt surface during reoxidation process is entrained into the metal liquid volume and bifilms are created. Bifilms decrease internal homogenity and quality of final casting. The aim of paper is to clarify influence of filter media on melt velocity and amount of oxides created in non-pressurized and naturally pressurized gating system. The evaluation of influence of filter media is observed by visualization with the aid of ProCAST numerical simulations software.

INTRODUCTION

In the foundry industry, the demands on the aluminium alloys quality are increasing. It is related to the effort to eliminate as many casting defects as possible. The key issue in the production of castings from aluminium alloys is reoxidation process, which significantly affects the quality of liquid metal [1, 2].

Melt reacts with the surrounding atmosphere which leads to the formation of Al_2O_3 oxide layer on its surface. This phenomenon is called primary oxidation. Reoxidation is considered to be the secondary oxidation that occurs from the beginning of the casting process until the moment when the mold cavity is filled, as well as tertiary oxidation that occurs during solidification process [3, 4].

The result of reoxidation processes are „bifilms“ (Fig. 1), which are formed and entrained into the bulk of liquid metal by turbulence. Due to their compact dimensions, bifilms can pass through entire gating system and they often cannot be removed even with filter media. Bifilms can grow and thus regain their original dimensions after the filling of mold cavity, when the melt is relatively calm. This phenomenon acts as nucleation sites of various casting defects. The quality of input material affects the castings quality also. However, if turbulence occurs during the filling of the mold, even a good quality input material will not prevent the formation of bifilms [3, 5].

The amount of oxides and the melt velocity are among the most important parameters during the filling of the gating system, which affect the final quality of the castings. According to prof. Campbell, the critical melt velocity in the gates is 0.5 ms^{-1}. Higher melt velocity causes turbulence which increases the amount of entrained bifilms. The formation of bifilms is also influenced by a poorly designed geometry of the gating system [2, 5].

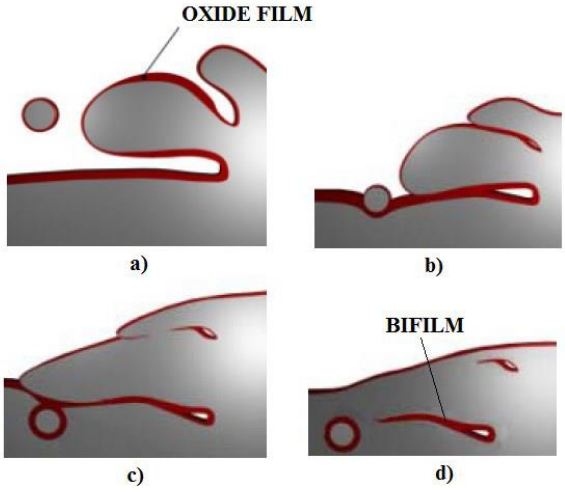

Fig. 1. Bifilm formation [7]

During filling of the gating system and mold cavity vortices are formed. Vortices cause the formation of turbulence, and thus reoxidation, bifilms and various defects. By using filter media melt velocity is decreased. The filter media ensures a more stable and calmer course of filling the gating system and the mold cavity and quality of castings is increased [1, 6].

Nowadays, there are few studies on the effectiveness of filters media with respect to their effect on

reoxidation. Experimental work deals with the design of non-pressurized and naturally pressurized gating system with using filter in order to determinate affect the melt velocity and amount of oxides in the castings. Reoxidation cannot be removed in the casting process. The aim is to reduce their quantity to a minimum. By using a suitable gating system is one of the way to achieve the aim.

1 EXPERIMENTAL PROCEDURES

The experimental work is focused on the evaluation of influence of filter media on the melt velocity and amount of oxides with the aid of ProCAST numerical simulation software. Two construction designs of gating systems was used for numerical simulation. One of the construction designs is commonly used non-pressurized gating system which is typically used for aluminum alloys with 1:4:4 ratio (Fig. 2a). The second one construction design is naturally pressurized gating system with 1:1:1 ratio (Fig. 2b).

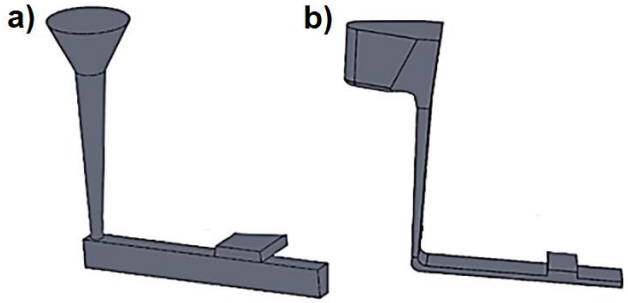

Fig. 2. Gating system design for numerical simulation: a) non-pressurized gating system, b) naturally pressurized gating system

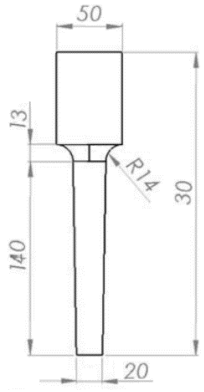

Fig. 3. Design of casting

Such a design minimizes presence of turbulence in gating system because the melt is in all places in direct contact witch mold walls. Naturally pressurized gating system is preferable because of the area exposed to further reoxidation is significantly smaller and it promotes the natural melt flow. Although this type of gating system has been known for a long time. Its use in practice is rare because of the melt velocity is critical in gates area which leads to splashes, and thus extensive reoxidation. To reduce the melt velocity in naturally pressurized gating system were used 30 ppi ceramic foam filters.

For the purpose of experiments was designed casting which exact dimensions are according to Fig. 3. Casting design was intended for mechanical properties evaluation (tensile strength, elongation).

2 SIMULATIONS, RESULTS AND DISCUSSION

Analysis of melt velocity during mold filling and amount of oxides were evaluated by the numerical simulations. For the purpose of experimental work was used aluminum alloy AlSi7Mg0.3. The melt temperature was 720 ± 5 °C poured to a mold with temperature 20 °C. Casts were poured by gravity sand casting method.

2.1 Analysis of the melt velocity

The result of the melt velocity in the non-pressurized gating system showed a reduction of the melt velocity in the choke area (Fig. 4), which ensures calm filling in the gates area. By using filter media the melt velocity is decreased especially in the first casting (Fig. 5).

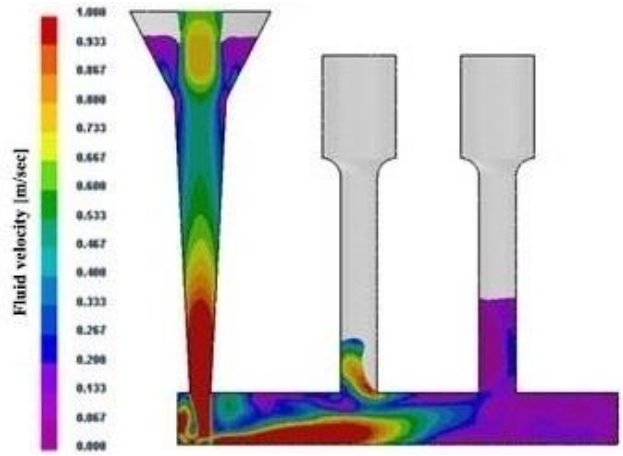

Fig. 4. Analysis of the fluid velocity in the non-pressurized gating system without filter media

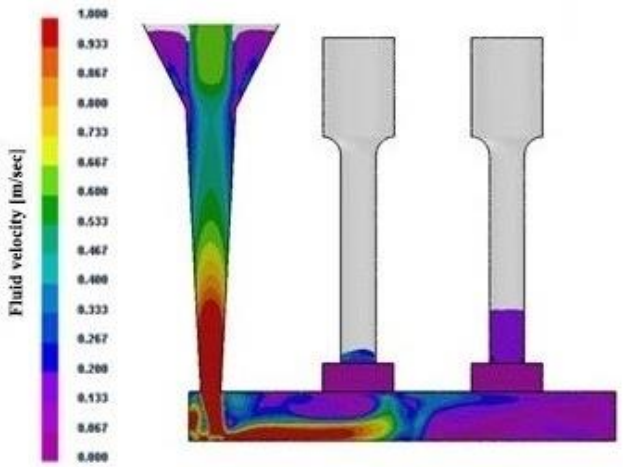

Fig. 5. Analysis of the fluid velocity in the non-pressurized gating system with filter media

In the naturally pressurized gating system is the critical melt velocity exceeded (Fig. 6) due to absence of mechanism to reduce it. Velocity energy at the end of the runner is transferred to the gate area, where the splashes are formed which resulting in the extensive reoxidation. At this point, all benefits of naturally pressurized gating system are lost. Filters ensure a significant reduction of the melt velocity in the gates area (Fig. 7).

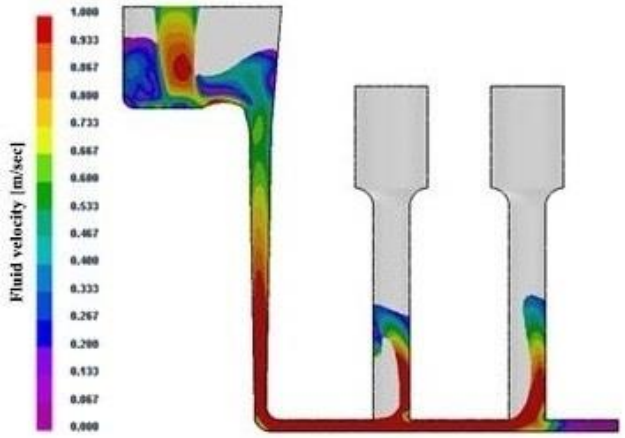

Fig. 6. Analysis of the fluid velocity in the naturally pressurized gating system without filter media

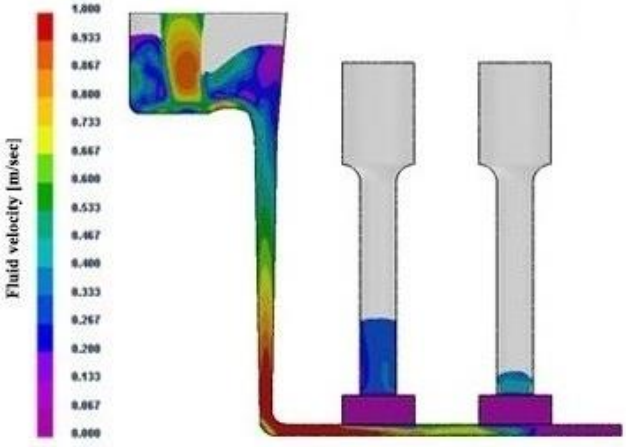

Fig. 7. Analysis of the fluid velocity in the naturally pressurized gating system with filter media

2.2 Analysis of the amount of oxides

The melt velocity rate affects the reoxidation process and the amount of oxides. The amount of oxides is unsuitable in the non-pressurized gating system (Fig. 8). Due to imperfectly filled runner in non-pressurized gating system, a large space for surface oxide layer entraining is available, also bounce wave can occur at the end of the runner. It results to fold and join two surfaces and thus to creation a large amount of bifilms. This phenomenon also leads to a large amount of oxides in concept with filter (Fig. 9). The melt velocity in the gates area is reduces by filters, but the bifilms formed in the runner can pass through filter media due to their compact dimensions.

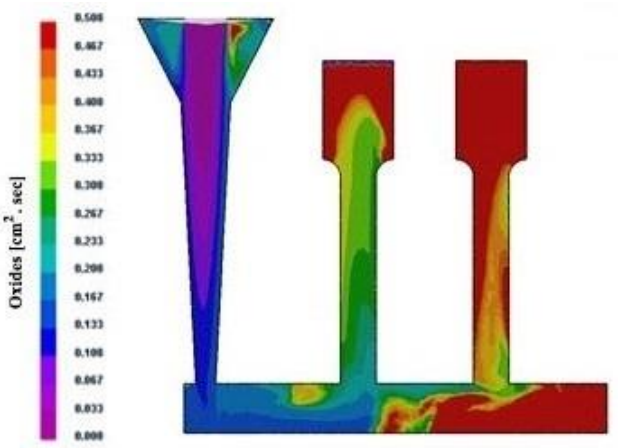

Fig. 8. Analysis of the amount of oxides in the non-pressurized gating system without filter media

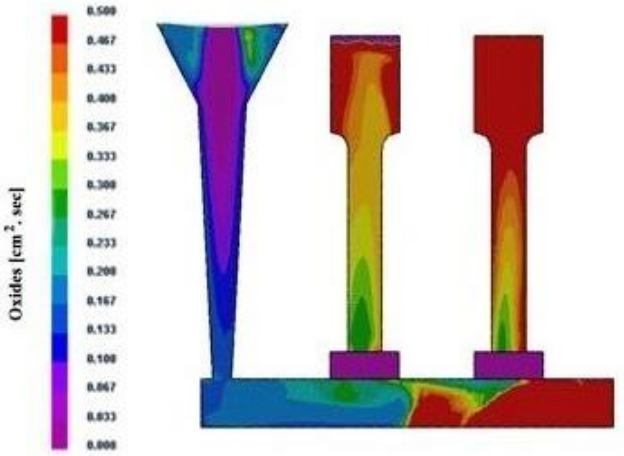

Fig. 9. Analysis of the amount of oxides in the non-pressurized gating system with filter media

The amount of oxides in the naturally pressurized gating system gains significantly better results (Fig. 10). Critical melt velocity in this concept of gating system in the gates area is exceeded and splashes leads to extensive reoxidation. Melt velocity in the gates area is reduced by using of filter media and reoxidation process is limited (Fig. 11).

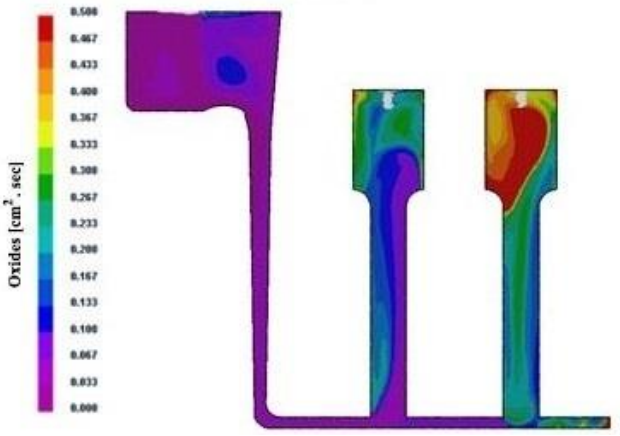

Fig. 10. Analysis of the amount of oxides in the naturally pressurized gating system without filter media

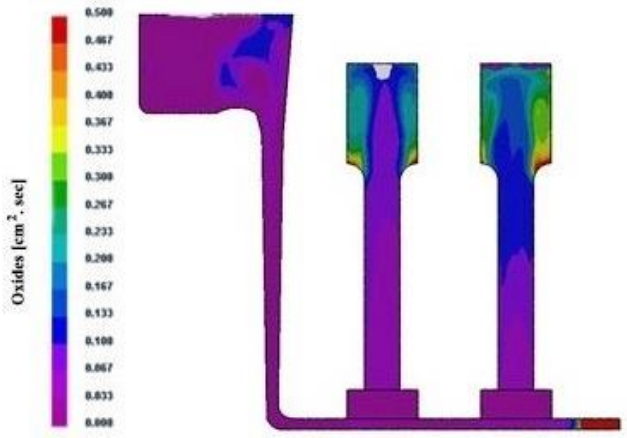

Fig. 11. Analysis of the amount of oxides in the naturally pressurized gating system with filter media

CONCLUSION

The beneficial effect of filter media on reoxidation process is proven by numerical simulation. Using of filter media reduces the critical melt velocity in which the melt enters the mold cavity through the gates and also minimizes the oxide occurrence. A choice of suitable gating system is also importance. Bifilms formed in the runner in the non-pressurized gating system can pass through filter media because of their compact dimensions and the amount of oxides is unsatisfactory in castings. Naturally pressurized gating system eliminates the conditions for the formation of oxides in the runner, but the critical melt velocity in the gates area is exceeded which leads to splashes and reoxidation. By using naturally pressurized gating system in combination with filter media the best results of the amount of oxides are achieved.

Acknowledgement

This article was made under support of project V-1/0706/18 Concept and realization of modern centre of diagnostics and quality control for castings and weldments.

REFERENCES

[1] CAMPBELL, J. (2015): *Complete Casting Handbook 2nd edition.* Oxford: Elsevier Ltd. 1054 s. ISBN 978-0-444-63509-9.

[2] BRŮNA, M. - BOLIBRUCHOVÁ, D. - PASTIRČÁK, R. (2017): *Analýza reoxidačných procesov vo vtokovej sústave pri odlievaní Al zliatin.* Slévárenství, 9-10, pp. 300-303, ISSN 0037-6825.

[3] CAMPBELL, J. (2006): *An Overview of the Effects of Bifilms on the structure and Properties of Cast Alloys.* s.l. : Metallurgical and Materials Transactions B-Physical Metallurgy and Materials Science, 2006.

[4] BOLIBRUCHOVÁ, D. - PASTRIČÁK, R. (2018): *Zlievarenská metalurgia neželezných kovov.* Žilina: Edis, 2018. 167 s. ISBN 978-80-554-1463-8.

[5] CAMPBELL, J. (2004): *Castings Practice, the 10 Rules of Castings, 1st ed.* Oxford : Elsevier Butterworth-Heinemann.

[6] DISPINAR, D. - CAMPBELL, J. (2004): *Metal Quality in Secondary Remelting of Aluminium.* Foundry Trade J. 2004. pp. 78-81.

[7] BRŮNA, M. - BOLIBRUCHOVÁ, D. - PASTIRČÁK, R. (2017): *Reoxidation Process Prediction in Gating System by Numerical Simulation for Aluminium Alloys.* Archives of Foundry Engineering. 23-26, ISSN 2299-2944.

Analysis of measuring systems and its theoretical basis

Ivan Litvaj, Ing, PhD.*
Department of Power Systems and Electric Drives, Faculty of Electrical Engineering and Information Technology,
University of Žilina,
Univerzitná 8215/1, 010 26 Žilina, Slovak Republic.
E-mail: ivan.litvaj@feit.uniza.sk, Tel.: + 421 41 513 2168

Abstract: Measurement, measurement processes are important parts of business processes. Measurement accuracy is constantly increasing and the requirements for ensuring the competence of measurement and measuring processes are also growing. Measurements are an important part of determining the true state of the production of products. By measuring, we confirm whether or not the requirements of internal or external customers have met. The variance, variability of a product parameter can be caused either by the product or by the measurement itself, the measurement system. Measurement Systems Analysis (MSA) is a tool we use to evaluate the capability of a measurement system.

INTRODUCTION

Metrology is the science of measurement, metrology has an irreplaceable place in business processes. Metrology, the company's metrology system, provides us with evidence of whether customer requirements have met because today's global economy is highly dependent on reliable measurements that meet all requirements that are credible and internationally recognized. Company metrology deals with: measurement, units of measurement, methods, means of measurement (gauges, measuring devices) to ensure the uniformity and accuracy of measurements in the company. We currently know of two ways to evaluate the measurement. The first method is "Measurement uncertainty" and the second method is "Measurement system analysis". [1] I deal in detail with the analysis of measuring systems, I define its meaning, I describe this analysis, I describe its procedure and evaluation.

1 MSA MEASUREMENT SYSTEM ANALYSIS

1.1 Description: Measurement system analysis (MSA)

It uses scientific tools to determine the amount of variation contributed by the measurement system. It is an objective method to assess the validity of a measurement system and minimize the factors contributing to process variation that is actual stemming from the measurement system.

Objective: Validate the measurement system used to collect the data and quantify the:

1. Process variation.
2. Appraiser variation and the total measurement system variation. [2]

Key terms and definitions:

- Attribute data – data that can be counted for recording and analysis (sometimes referred to as go/ no go data).
- Variable data – data that can be measured; data that has a value that can vary from one sample to the next; continuous variable data can have an infinite number of values.
- Bias – difference between the average or mean observed value and the target value.
- Stability – a change in the measurement bias over a period of time.
  - A stable process would be considered in "statistical control."
- Linearity – a change in bias value within the range of normal process operation.
- Resolution – smallest unit of measure of a selected tool gage or instrument; the sensitivity of the measurement system to process variation for a particular characteristic being measured.
- Accuracy – the closeness of the data to the target or exact value or to an accepted reference value.
- Precision – how close a set of measurements are to each other.
- Repeatability – a measure of the effectiveness of the tool being used; the variation of measurements obtained by a single operator using the same tool to measure the same characteristic.
- Reproducibility – a measure of the operator variation; the variation in a set of data collected

by different operators using the same tool to measure the same part characteristic [3].

1.2 Measurement system as process

The measurement and analysis activity is a process – a measurement process. Any and all of the management, statistical, and logical techniques of process control can be applied to it. This means that the customers and their needs must first be identified. The customer, the owner of the process, wants to make a correct decision with minimum effort. Management must provide the resources to purchase equipment which is necessary and sufficient to do this. But purchasing the best or the latest measurement technology will not necessarily guarantee correct production process control decisions. Equipment is only one part of the measurement process. The owner of the process must know how to correctly use this equipment and how to analyze and interpret the results. Management must therefore also provide clear operational definitions and standards as well as training and support. The owner of the process has, in turn, the obligation to monitor and control the measurement process to assure stable and correct results which includes a total measurement systems analysis perspective – the study of the gage, procedure, user, and environment, i. e. normal operating conditions [4].

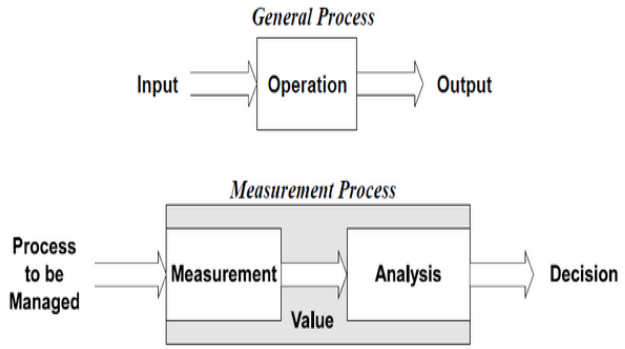

Fig. 1. Measurement system as process (Measurement System Analysis) [4]

2 MEASUREMENT SYSTEM ANALYSIS

2.1 Introduction to measurement system analysis (MSA)

Everyday our lives are being impacted by more and more data. We have become a data driven society. In business and industry, we are using data in more ways than ever before. Today manufacturing companies gather massive amounts of information through measurement and inspection. When this measurement data is being used to make decisions regarding the process and the business in general it is vital that the data is accurate. If there are errors in our measurement system, we will be making decisions based on incorrect data. We could be making incorrect decisions or producing non-conforming parts. A properly planned and executed Measurement System Analysis (MSA) can help build a strong foundation for any data based decision making process.

2.2 What is measurement system analysis

MSA is defined as an experimental and mathematical method of determining the amount of variation that exists within a measurement process. Variation in the measurement process can directly contribute to our overall process variability. MSA is used to certify the measurement system for use by evaluating the system's accuracy, precision and stability. Before we dive further into MSA, we should review the definition of a measurement system and some of the common sources of variation. A measurement system has been described as a system of related measures that enables the quantification of particular characteristics. It can also include a collection of gages, fixtures, software and personnel required to validate a particular unit of measure or make an assessment of the feature or characteristic being measured.

The sources of variation in a measurement process can include the following:

- Process – test method, specification.
- Personnel – the operators, their skill level, training, etc.
- Tools/Equipment – gages, fixtures, test equipment used and their associated calibration systems.
- Items to be measured – the part or material samples measured, the sampling plan, etc.
- Environmental factors – temperature, humidity, etc.

All of these possible sources of variation should be considered during Measurement System Analysis. Evaluation of a measurement system should include the use of specific quality tools to identify the most likely source of variation. Most MSA activities examine two primary sources of variation, the parts and the measurement of those parts. The sum of these two values represents the total variation in a measurement system.

2.3 Why Perform Measurement System Analysis

An effective MSA process can help assure that the data being collected is accurate and the system of collecting the data is appropriate to the process. Good reliable data can prevent wasted time, labor and scrap in a manufacturing process. A major

manufacturing company began receiving calls from several of their customers reporting non-compliant materials received at their facilities sites. The parts were not properly snapping together to form an even surface or would not lock in place. The process was audited and found that the parts were being produced out of spec. The operator was following the inspection plan and using the assigned gages for the inspection. The problem was that the gage did not have adequate resolution to detect the non-conforming parts. An ineffective measurement system can allow bad parts to be accepted and good parts to be rejected, resulting in dissatisfied customers and excessive scrap. MSA could have prevented the problem and assured that accurate useful data was being collected [3].

Measurement System Analysis is the underlying principle and methodology for ensuring a measurement system is capable of producing accurate results. The goal of MSA is to ensure that the measurement method poses little variation as compared to the entire process variation. The system must be capable of accurate and reliable measurements. According to the Automotive Industry Action Group (AIAG) standards (Fig. 2), a measurement system is acceptable when the variation is less than 10 percent of the total process variation. This ensures that the measurements obtained from the measurement device are mainly driven by the part to part variation and not the measurement device or gage used to measure.

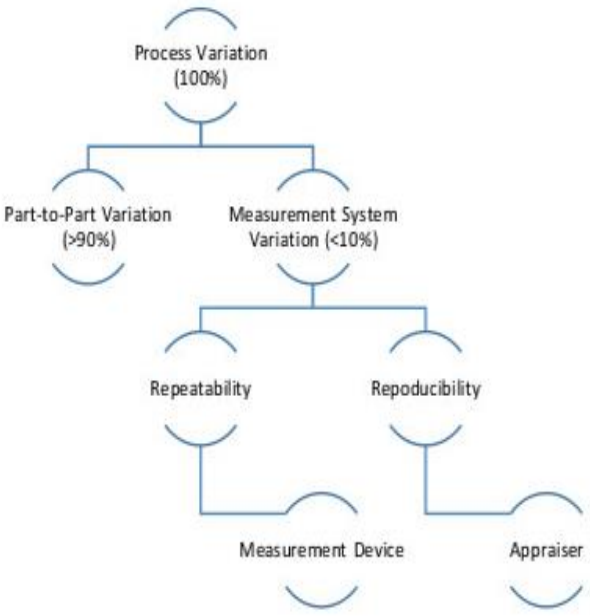

Fig. 2. MSA Process variation [5]

2.4 How to Perform Measurement System Analysis

MSA is a collection of experiments and analysis performed to evaluate a measurement system's capability, performance and amount of uncertainty regarding the values measured. We should review the measurement data being collected, the methods and tools used to collect and record the data. Our goal is to quantify the effectiveness of the measurement system, analyze the variation in the data and determine its likely source. We need to evaluate the quality of the data being collected in regards to location and width variation. Data collected should be evaluated for bias, stability and linearity. During an MSA activity, the amount of measurement uncertainty must be evaluated for each type of gage or measurement tool defined within the process Control Plans. Each tool should have the correct level of discrimination and resolution to obtain useful data. The process, the tools being used (gages, fixtures, instruments, etc.) and the operators are evaluated for proper definition, accuracy, precision, repeatability and reproducibility.

3 DATA CLASSIFICATIONS

Prior to analyzing the data and or the gages, tools or fixtures we must determine the type of data being collected. The data could be attribute data or variable data. Attribute data is classified into specific values where variable or continuous data can have an infinite number of values. More detailed definitions can be found below.

3.1 The Master Sample

To perform a study, you should first obtain a sample and establish the reference value compared to a traceable standard. Some processes will already have "master samples" established for the high and low end of the expected measurement specification.

3.2 The Gage R&R Study

For gages or instruments used to collect variable continuous data, Gage Repeatability and Reproducibility (Gage R & R) can be performed to evaluate the level of uncertainty within a measurement system. To perform a Gage R & R, first select the gage to be evaluated.

Then perform the following steps:

- Obtain at least 10 random samples of parts manufactured during a regular production run.
- Choose three operators that regularly perform the particular inspection.
- Have each of the operators measure the sample parts and record the data.
- Repeat the measurement process three times with each operator using the same parts.
- Calculate the average (mean) readings and the range of the trial averages for each of the operators.

- Calculate the difference of each operator's averages, average range and the range of measurements for each sample part used in the study.
- Calculate repeatability to determine the amount of equipment variation.
- Calculate reproducibility to determine the amount of variation introduced by the operators.
- Calculate the variation in the parts and total variation percentages.

The resulting Gage R & R percentage is used as a basis for accepting the gage. Guidelines for making the determination are found below:

- The measurement system is acceptable if the Gage R & R score falls below 10%.
- The measurement system may be determined acceptable depending upon the relative importance of the application or other factors if the Gage R & R falls between 10% to 20%.
- Any measurement system with Gage R & R greater than 30% requires action to improve
    - Any actions identified to improve the measurement system should be evaluated for effectiveness.

When interpreting the results of a Gage R & R, perform a comparison study of the repeatability and reproducibility values. If the repeatability value is large in comparison to the reproducibility value, it would indicate a possible issue with the gage used for the study. The gage may need to be replaced or re-calibrated. Adversely, if the reproducibility value is large in comparison with the repeatability value, it would indicate the variation is operator related. The operator may need additional training on the proper use of the gage or a fixture may be required to assist the operator in using the gage.

Gage R & R studies shall be conducted under any of the following circumstances:

- Whenever a new or different measurement system is introduced.
- Following any improvement activities.
- When a different type of measurement system is introduced.
- Following any improvement activities performed on the current measurement system due to the results of a previous Gage R & R study.
- Annually in alignment with set calibration schedule of the gage.

3.3 Attribute Gage R & R

Attribute measurement systems can be analyzed using a similar method. Measurement uncertainty of attribute gages shall be calculated using shorter method as below:

- Determine the gage to be studied.
- Obtain 10 random samples from a regular production run.
- Select 2 different operators who perform the particular inspection activity regularly.
- Have the operators perform the inspection two times for each of the sample parts and record the data.
- Next, calculate the kappa value.
- When the kappa value is greater than 0.6, the gage is deemed acceptable
    - If not, the gage may need to be replaced or calibrated.

The attribute gage study should be performed based on the same criteria listed previously for the Gage R & R study. During MSA, the Gage R&R or the attribute gage study should be completed on each of the gages, instruments or fixtures used in the measurement system. The results should be documented and stored in a database for future reference. It may be required for a PPAP submission to the customer. Furthermore, if any issues should arise, a new study can be performed on the gage and the results compared to the previous data to determine if a change has occurred. A properly performed MSA can have a dramatic influence on the quality of data being collected and product quality [3].

CONCLUSION

I focused on one topic, the analysis of measuring systems. The aim of this paper was to answer basic questions related to the analysis of measuring systems, for example: why we use the analysis of measuring systems, what is the justification of this method, what is the procedure of application of this method, etc. Finally, I will briefly summarize the most important reasons for the application of the analysis of measuring systems in practice. The company must prove to the customer compliance with the specification from this customer, this is a necessity, it is the basis of the business relationship that is between the customer and the company, the company must meet all the requirements of the customer and other stakeholders, e.g. legislation, standards. For these reasons, the company is interested in the capability of all processes (including the measurement process), because the product is the output of business processes. In terms of the capability of the measurement system, the company is interested in the variability of the measurement system it uses, the magnitude of the variability of the measurement system, the sources of variability. All

this has a single goal - the company must know whether its measurement system is capable, whether it is can meet customer requirements. The company must be sure that all measured values are correct, the company must have reliable information about how the production process works. The company must have a functional analysis of measuring systems.

REFERENCES

[1] *Measurement System Analysis (MSA)* (2003): Praha 2003. ISBN 80-02-01562-2.

[2] *MSA Measurement System Analysis - Six Sigma Material* (2020): Available on: http://www.six-sigma-material.com.

[3] *Measurement System Analysis (MSA)* (2020): Available on: https://quality-one.com/msa/.

[4] *Measurement system as process (Measurement System Analysis)* (2020): http://isoconsultantpune.com/measurement-system-analysis/).

[5] SEALY, W. (2020): *Metrology Series II: The Effects of Measurement System Analysis on Type I and II Errors*. Available on: http://caristem.org/20-engineering/40-metrology-series-ii-the-effects-of-measurement-system-analysis-on-type-i-and-ii-errors.

Automation of inspection processes before, during and after production process

Aleš Mišura, Ing.
topNDT, s.r.o.
Hálkova 31, 01001 ŽIlina, Slovak Republic.
E-mail: misura@topndt.sk , Tel.: + 421 41 37 002 37

Juraj Uríček, doc. Ing., PhD.*
Department of Automatization and Production Systems, Faculty of Mechanical Engineering,
University of Žilina,
Univerzitná 8215/1, 010 26 Žilina, Slovak Republic.
E-mail: juraj.uricek@fstroj.uniza.sk, Tel.: + 421 41 513 2813

Abstract: This article presents an overview of various pre-production, production and post-production inspection processes, which are often required to ensure the final production quality. We will also present various practical examples of automated, or semi-automated inspection technologies, that are aimed to ensure the input material quality, processed material quality and final product quality.

INSPECTION SYSTEMS DESCRIPTION

The automation of material inspection processes in production itself expanded hand in hand with digitalization. Digitalization of the inspection equipment allows today to build up sophisticated software around the hardware. This in combination with the skilled inspection workforce enables much higher throughput during the inspection phase of production.

For the simple repetitive tasks, the inspection can be basically fully automated with the OK / NO OK system, where system itself decides, if the tested specimen is or is not in line with required quality levels.

When it comes to more complex tasks, or inspection processes, where more variables come into consideration, the software usually is doing so called "evaluation assistance". This means, that software is proposing its programmed view based on the input, which is compared with the stored reference data. In this case, the operator is the one, who makes the final decision – he either accepts or reject the proposed system evaluation.

1 BASIC SEGMENTATION

Based on the system capabilities, we can divide these automation processes to:

a) Fully automated solutions with simple logic OK or NO OK.
b) Semi-automated solutions providing evaluation assistance (OK or NO OK decision proposal).

Based on the production phase, where these automated system can be deployed, we can divide them to:

a) Pre-production automated/semi-automated inspection systems.
b) Production automated/semi-automated inspection systems.
c) Post-production automated/semi/automated inspection systems.

We will now refer to both, automated and semi-automated systems, as systems.

Pre-production systems ensure, that the production process is entered only with the input material, that fulfills the required quality level, avoiding the use of defective material in production process. This is mostly inspection of raw material, but also input materials in form of finalized parts from other suppliers. For example it can be the inspection of steel plates for homogeneity, inspection of parts for porosity, cracks, hardness, but also very simple indirect visual inspection (RVI = Remote Visual Inspection.

Production systems are usually deployed to critical phases of the production process, where the risk, that the defect can occur is the highest. Typical example can be the eddy current inspection of wheel hubs for cars, or spot weld inspection on car bodies to ensure the car body strength and durability).

Post-production systems are used to check the quality of the final product after it finished, before it enters the final phase of processing (painting, etc.) or durin gits lifetime. This is aimed very often not only to detect possible flaws in material, but also for example to test leakage (pressure vessels, storage tanks, etc.). So we can say, that this phase is already testing the material properties and product functions, that it will be used for.

Another division of systems can be done based on the used inspection method, which we call modalities. RT - X-Ray inspection

a) UT - Ultrasonic inspection.
b) VT - Visual inspection (direct VT or indirect RVI).
c) MT - Magnetic particle testing.
d) PT - Penetrant testing.
e) ACFM - Alternating Current Field Measurement.
f) EC - Eddy Current Testing (EC, ECA - Eddy Current Array, ECT - Eddyc current tangential, PEC - Pulsed Eddy Current, PECA - Pulsed Eddy Current ARray).
g) MFL - Magnetic Flux Leakage.
h) HT - Hardness testing (Note: destructive type of test).

All of above mentioned can be today integrated to robotic automated or semi-automated systems systems.

As we can see, there are a lot of various inspection possibilities. Before selecting one, there has to be conducted a feasibility study, that clearly confirms, if the selected option is suitable for the reuired production process and detection requirements.

2 SELECTED PRACTICAL EXAMPLES

Existing vast portfolio of various system, that can be, or are already used in the production processes to maintain the reuired production quality levels are offered by many known vendors. There are standardised solutions, but also custom solutions designed on demand. Vendors quite often just offer only the robotic part of the solution and there has to be additional integration with the inspection hardware by customer, or 3rd party supplier. So it is quite complex and not always easy task.

One of the main benefit of these systems is so called high PoD (Probability of Detection). This advantage comes with the automation of some human made tasks, that usually could influence the inspection itself. As an example a very simple thickness measurement can be done by qualified technician in grid mode. But if we would like to get more resolution (more detailed view on the inspected specimen), e. g. 0.5x0.5 mm, it would be impossible to make by hand. Such mapping can be effective only with the automated solution (Fig. 2). This solution enables not only fast mapping in grid modes from 0.5x0.5 mm up to 10x10 mm, but in highest resolution it gives us in graphical representation the view on shape of the defect under the surface.

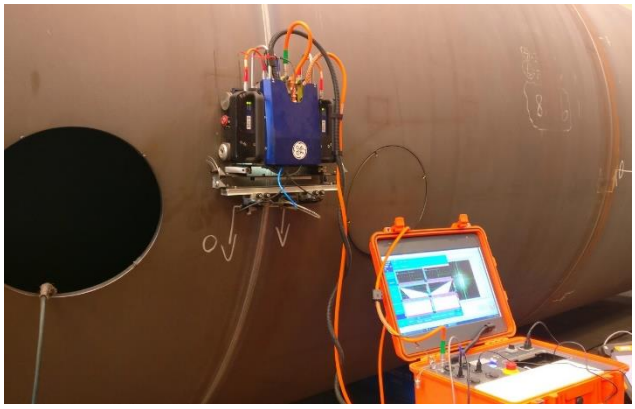

Fig. 1. Ultrasonic Phased Array Inspection System - Inspection of LPG pressure tanks with the automated weld laser following, to maintain the proper distance of the probes from the weld. System scanning speed depends on the selcted UT hardware. Can be adjustaed from 1 cm·s^{-1} up to 5 cm·s^{-1} Such system can reduce the inspection time almost by 75 % compared to X-Ray inspection, thus speeding up the production process.

Fig. 2. Ultrasonic (conventional|) corrosion mapping system. Useful to inspect walls of storage tanks to size the remaining wall thickness, but also to detect material changes by selecting the attenuation option interpretation for scanned data. Can work through coatings.

Fig. 3. RVI system used to inspect inner parts of the storage tanks. Combined with the laser system and CAD drawing, system knows and remembers position of robot, but also the position of viewed area. Data are automatically recorded so the operator next time just send the unit to selected position to compare the changes if any.

We could continue further with many other examples. There is no doubt, that robotics stepped in to the inspection of the production rocesses also to areas, where it was before not imaginable because of high cost or simply that the inspection equipment, that should be combined with the robotic platforms was either too big, heavy or simply in development. Today there is a wide choice of option. Ready made

solutions, but also platforms ready to be integrated with virtually any NDT (Non destructive testing) equipment.

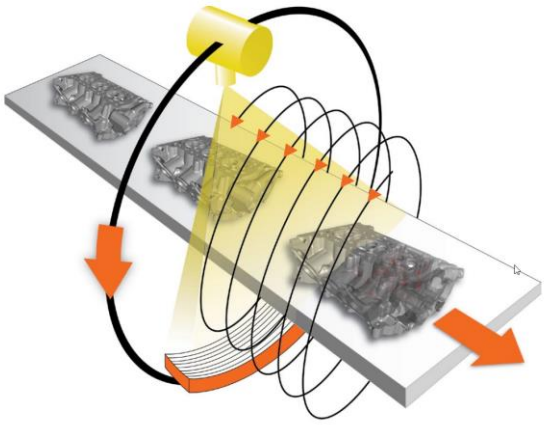

Fig. 4. Automated CT inspection system in Automotive industry. Detects defects over the defined level of threshold. Can be used also for dimensional analysis. Can be combined with the conveyor belts and robotic arms to sort OK and NO OK parts [6].

Fig. 5. Automated high-resolution CT inspection system in Automotive industry. Detects defects over the defined level of threshold. Can be used also for dimensional analysis. Can be combined with the conveyor belts and robotic arms to sort OK and NO OK parts. X-Ray cabinet solution [6].

3 WHO ARE THE ROBOTIC COMPANIES IN NDT?

During the SPRINT Robotics 2019 world conference (see more for this colaborative robotics initiative - https://www.sprintrobotics.org) in Rotterdam, we could visit some major players presenting their solutions. Even the conference was aimed quite strongly for Oil&Gas industry, but not only, it represented present state of the technology used to automate the inspection processes.

Some major players in the field:

- **GE Inspection Robotics** – company based in Zurich, Switzerland [https://inspection-robotics.com/].
- **Eddyfi Technologies (Inuktun)** – Canada based company recently acquired Inuktun. Their goal is to integrate their existing products with Inuktun robotic platforms [https://eddyfi.com/en].
- **ANYbotics** – Swiss based company oferring specific mobile platform to indirectly support the production process. The main task of their solution is to replace the humans in the risky and dangerous areas. The main task is to detect any problems on production assets, eliminating the risks for human life [https://www.anybotics.com].
- **FLYABILITY SA** – Swiss based company focused on flying drones, with many safety features. Branches in China and USA [https://www.flyability.com].
- **Standlee Starnes Robotics –** US based company focused on custom solution [https://standleestarnesrobotics.com].
- **ExRObotics –** company based in Netherland providing certified robotic solution for explosive environments (ATEX/IECEx Zone ! certification). Their solutions are aimed for production assets inspection [https://exrobotics.global].
- **Waygate Technologies (Baker Hughes business, previously GE Inspection Technologies) –** integrated solution for CT inspection in automotive industry, electronics [https://www.bakerhughesds.com/waygate-technologies].

There are many others, a lot of start-ups. The development in this field is so fast, that from year to year the changes are significant. Especially in software development, where software side of the robotic unit creates more than 50 % of their succes.

CONCLUSION

High demand for quality assurance in production today creates a new market opportunity for robotics and new demand from producers. New technologies come hand in hand with new problems during the production, that have to be reduced to minimum. No solution is universal in terms of usability and there are a lot of tasks unresolved in various industrial areas, where technology and human knowledge has not yet found a suitable solution, but we can clearly see a significant shift from manual inspection in production to semi-automated, or fully automated solutions. This is already not only privilege of big and rich companies, but it also enters step by step the area of common NDT service providers where most small and medium enterprises are active. This shift also creates a need for more skilled and adaptable workforce, capable of absorbing the new technologies.

There are a lot of feasibility studies each year performed to check on various inspection tasks in various industrial areas such as Automotive, Oil &

Gas, Aviation, Casting, Welding, etc. Companies are constantly looking for new options in NDT.

No system is perfect, there is always some kiind of trade-off, which comes from the used modality, system limitations and real world conditions, but overall the higher PoD, possible automated, or semi-automated evaluation brings much more advantages and speed to production process itself.

Acknowledgment

This article was made under support of project: STIMULY MATADOR 1247/2018. Project title: Research and development of modular reconfigurable production systems using Smart Industry principles for automotive with pilot application in MoBearing Line industry.

REFERENCES

[1] REGAZZO, R. - REGAZZOVÁ, M. (2013): *Ultrasound – fundamentals of ultrasound defectoscopy*. Praha: BEN, 2013. 292 s. ISBN 978-80-7300-466-8.

[2] ATG (2014): *Company ATG*. [online]. [cit. 2014-11-14]. Available at: <http://www.atg.sk>.

[3] BINDT (2014): *The British Institute of Non–Destructive Testing*. [online]: [cit. 2014-07-30]. Available at: <http://www.bindt.org>.

[4] KOVÁČIK, M. (2010): *Materials testing by ultrasound* (In Slovak). Bratislava: s.n., 2010.

[5] FATURÍK, M. - VRZGULA, P. - MIČIAN, M. (2016): *New inspection technologies for identification of failure in the materials and welded joints for area of gas industry*. Manufacturing technology: Journal for science, research and production. Vol. 14, No. 3, s. 487-492, ISSN 1213- 2489.

[6] EBERHARD, A. - VON GUERICKE, O. - BRUNKE, O. - NEUBER, D. - STUKE, I. - BESSER, W. - ZIESEMANN, M. - HOYM, D. - HEIKEL, CH. - HUXOL, A. (2012): *High-speed computer tomography employed in pressure die casting*. Casting Plant & Technology, Vol. 03, pp. 42-51.

Cloud computing

Olha Kolesnyk, Ing.*
Department of Industrial Engineering, Faculty of Mechanical Engineering,
University of Žilina,
Univerzitná 8215/1, 010 26 Žilina, Slovak Republic.
E-mail: olha.kolesnyk@fstroj.uniza.sk, Tel.: +421 41 513 2713

Peter Bubeník, doc. Ing., PhD.
Department of Industrial Engineering, Faculty of Mechanical Engineering,
University of Žilina,
Univerzitná 8215/1, 010 26 Žilina, Slovak Republic.
E-mail: peter.bubenik@fstroj.uniza.sk, Tel.: +421 41 513 2719

Miroslav Rakyta, doc. Ing., PhD.
Department of Industrial Engineering, Faculty of Mechanical Engineering,
University of Žilina,
Univerzitná 8215/1, 010 26 Žilina, Slovak Republic.
E-mail: miroslav.rakyta@fstroj.uniza.sk, Tel.: +421 41 513 2737

Abstract: Cloud calculations have revolutionized many areas that require enough computing power. Cloud platforms can also provide tremendous support for analysis, mainly through the disclosure of scalable resources of different types. In the cloud, these resources are available as services, making it easier to allocates and release them. This feature is especially useful in analysing large amounts of data, such as data produced by next-generation sequential experiments that require not only enhanced storage space, but also a distributed computing environment. But at the same time, at the same time, the global volume of data is growing very fast. And yet we have a limitation in data mobility.

INTRODUCTION

Global data volumes are growing very fast. While cloud calculations are now mostly held in large data centres, by 2025 this trend will reverse: 80% of all data is expected to be processed in smart devices closer to the user (edge computing). The availability of both peripheral and cloud calculations is essential in the computer continual to ensure that data is processed as efficiently as possible. Energy-efficient and trustworthy border and cloud infrastructure will serve to finance the sustainable use of cloud and peripheral computing technologies. Cloud calculations make an important contribution to achieving the objectives of the data strategy, digital strategy and industrial strategy.

Cloud computing is one of modern computing technologies that can help address the challenges of dynamic data growth and need growth in computing units that will be able to process and analyse data within a reasonable time. Cloud calculations provide a lot of storage space, computing networks, hardware and software resources as a service, without the need for extensive configuration, and on demand, if necessary. There are now several commercially available cloud platforms on the market that provide various services for sophisticated purposes and can be used on a public subscription basis, allowing for elastic scaling of the analyses performed according to current requirements.

The real economic benefits come from the widespread use of cloud solutions by businesses and the public sector, thanks to a significant reduction in IT costs. Cloud computing will help access future and emerging technologies such as artificial intelligence, the Internet of Things and blockchain. It plays a key role in promoting a competitive and innovative European economy in the digital age.

The cloud provides:

- Computing storage capacities on which all types of digital services can run, for all sectors of the economy.
- Purchase the necessary computing resources on demand without risking a return on hardware investment.
- Start-ups and small and medium-sized enterprises using simple computing equipment to acquire new business models and to thrive.

1 CLOUD FEATURES THAT SUPPORT DATA ANALYSIS

Cloud calculations have several features that significantly distinguish this model of providing computer resources from computer systems stored locally. According to the National Institute of Standards and Technology (NIST), the cloud computing model defines five basics [1]:

- On-demand self-service - if necessary (on request) and without further interaction with cloud provider employees, various computer resources needed to perform analyses can be provided.
- Wide network access - data analytics in cloud services can be done on the network and through thin clients, including laptops, tablets and workstations.
- Pooling resources - The sources and services used for data analysis are collected and can be used independently on request by several scientists in their analyses.
- Rapid elasticity - data scientists can allocate more resources when they are needed, e.g. in the field of data. When they need to process more data, and release these resources when they complete their analysis, which reduces the cost of using the cloud.
- Measured service - measures, monitors and controls the use of cloud resources allocated to data analysis, and researchers receive reports on the number of resources used and the cost of their use.

In other words, cloud platforms allow for rapid magnification or magnification of analyses, the provision of resources needed to speed up investigations in a remote data centre with minimal effort over the network, and the management of their allocation in order to minimise costs. Use. This avoids the need to purchase large computer clusters that may remain idle for some time and avoid costs related to the purchase and maintenance of hardware [1].

2 CLOUD-BASED DATA ANALYTICS SERVICES

Thanks to the cloud, researchers can also operate across different models of cloud services. These models define how cloud resources will be used and who will manage the resources that underpin the analysis services used or created. There are three general and generally accepted cloud service models (Figure 1) [2]:

1. Software as a Service (SaaS) - Analysis services should be available as a software application running on the cloud infrastructure and the capabilities of this application are provided through a program interface (e.g. Web application). The researcher does not manage the underlying cloud infrastructure and its capabilities are limited, such as uploading data that should be analysed using software located in the cloud or customizing program execution settings.
2. Platform as a Service (PaaS) - analysis services developed by the researcher can be implemented using programming languages, libraries, software packages and tools supplied by the cloud provider. The researcher deploys services to the cloud, controls and manages services, but does not control the cloud infrastructure (storage, servers, network).
3. Infrastructure as a Service (IaaS) - A researcher can directly allocate the various sources needed to analyse data, such as storage and computing power (e.g. Virtual Machines), and deploy and execute the software used for the analysis. At the same time, the researcher manages and controls the.

In other words, a data researcher who provides a collection of virtual machines and installs his own software to perform his analyses works in the Infrastructure as a service model. Conversely, a researcher who connects to a cloud-hosted web application designed to analyse data, upload data, provide execution parameters, and view results, works as a service in the software model [2].

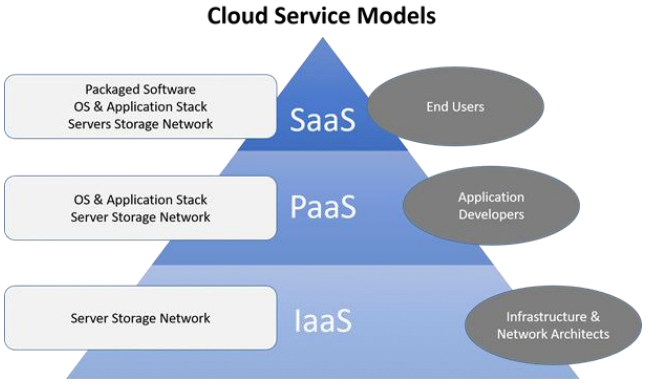

Fig. 1. Cloud service models mapped to researchers' competencies [1].

Higher service models, such as SaaS, limit the amount of administrative work related to the analyses performed and are more convenient for an end-user who works using the prepared software interface. Lower service models leave more freedom to build your entire system and provide more configuration options, but at the same time require more administrative skills in it and software development and deployment.

3 CLOUD ANALYTICS RESOURCES

Cloud platforms are constantly evolving and providing new services for sophisticated purposes. Many standard resources, such as AWS, Azure, and GCP, are available on public cloud platforms, which are versatile in nature. Those that serve to address specific tasks are also provided by third-party companies or institutions through a marketplace. Taking into account scientific calculations, some

resources are directly used in experiments carried out. For example, a researcher working with a set of virtual machines with preinstalled software and running a script to perform their calculations in parallel directly consumes the computing resources of the selected cloud platform. Other resources are often used indirectly. For example, the same researcher searches for his virtual machines and works on a virtual network with a subnet, a set of virtual network interfaces, a group of public and private IP addresses. Sometimes he doesn't even know about it, because these resources are virtualized and abstract for him. Among the wide range of resources that can be provided from the cloud, the following can be used in general data analysis cases [3]:

- Calculate resources.
- Storage.
- Web applications.
- machine learning models.
- Big Data platform.

4 FUTURE DATA STORAGE AND PROCESSING MODEL

The cloud offers an alternative model for storing and processing data on demand. Users can access their data and apps on the device of their choice over the Internet. Many services, such as web-based e-mail, use computing cloud technologies because they are faster, cheaper, and more flexible than conventional computing methods [3].

The real economic benefits come from the widespread use of cloud solutions by businesses and the public sector, thanks to a significant reduction in IT costs. Cloud computing will help access future and emerging technologies such as artificial intelligence, the Internet of Things and blockchain. It plays a key role in promoting a competitive and innovative European economy in the digital age.

5 LIMITATIONS IN DATA MOBILITY

Currently, only 1 in 4 businesses and 1 in 5 SMEs use the cloud for their day-to-day operations in Europe. If the increase in cloud use increases, it will also strengthen the competitiveness of the European economy and its innovation potential [4].

Cloud calculations mean a huge flow and data exchange. For a booming cloud market, data should be able to move in a credible and secure way within the Digital Single Market [4].

The Regulation on the free flow of non-personal data, together with the General Data Protection Regulation (GDPR), provided for the unrestricted movement of all data throughout Europe. By 30 May 2021, any existing unjustified restrictions on data localisation must be removed. As a result, companies will now be able to store and process their data anywhere in the EU [4].

Regulation of the free flow of non-personal data:

No data localisation restrictions: data can be stored in any EU Member State. Restrictions on data localisation by Member States' public authorities: 62 % of respondents said that data localisation restrictions should be removed.

Competent authorities in each Member State continue to have the right to access data stored across the EU.

Codes of conduct in the self-regulatory industry so that clients can seamlessly transfer their data from one cloud provider to another. Legal uncertainty leading to market caution as regards cross-border storage and processing of data. A complex EU legal mix valid in different sectors or situations, but the general principle of the free flow of non-personal data is lacking. 55 % of respondents believe that legislative action is needed.

Mistrust due to security risks and concerns about cross-border availability of data for regulatory purposes [4].

6 DISADVANTAGES CLOUD COMPUTINGOM

Clouds offer users a variety of benefits. One of the most important is to reduce the cost and complexity of owning and using computers and networks. Cloud users don't have to invest in the information infrastructure, buy hardware, or pay for software licenses. In addition, there are cloud providers that specialize in specific areas (such as email) that can provide useful and advanced services to companies.

Cloud computing is often considered effective because it allows organizations to free up resources and use them to innova program and develop products. In addition, information from the cloud is not easy to lose [5].

Below is a list of some of the most important benefits of using cloud computing [5]:

- Select an app. This allows cloud users to choose and test what best suits their needs. Cloud computing also allows businesses to use, access and pay only for what they use, with fast implementation time.
- Cooperation. Users are starting to see the cloud as a way to collaborate with common data and information.
- Reduce costs. Unlike pay-per-usage, the pay-per-usage model allows an organization to pay only for the resources it needs, virtually without investing in the physical resources available in the cloud.

- Flexibility. The provider transparently manages the client's use of resources based on dynamically changing needs.
- Reduce the risk. Organizations can use the cloud to test ideas and new concepts before investing heavily in technology.
- Scalability. Users have access to a large number of resources that are reduced to suit their needs.
- Up-to-date software. The cloud provider is able to update the software while providing feedback on previous versions of the software.
- Virtualization. Each user has their own view of the resources available, no matter what physical devices are organized. Therefore, the provider can serve more users with fewer physical resources [5].

On the contrary, there are several issues that can prevent an organization from using cloud computing. This is a list of such restrictions [5]:

- Interoperability. Universal standards and/or interfaces have not yet been defined, which may lead to the risk of blocking a single provider.
- Delay. All access to the cloud happens over the Internet, resulting in delays in any communication between the user and the provider.
- Platform or language restrictions. Some cloud providers only support selected platforms and languages.
- Regulation. There are concerns in the cloud computing community, particularly for organisations managing sensitive data, about jurisdiction, data protection, fair handling of information and international transmission.
- Reliability. Many existing cloud infrastructures use cheaper hardware that may crash unexpectedly.
- Control resources. The amount of control a user has over a cloud provider and its resources varies considerably from provider to provider.
- Safety. The main concern is the protection of personal data; users have no control or awareness of where their data is actually stored. However, from a forensic security perspective, the use of cloud computing can provide specialized forensic images of virtual machines that are available without disconnecting infrastructure, in pay-per-use. This leads to a shorter disconnection time required for forensic analysis. Audit records can also be kept more efficiently and therefore a more detailed analysis of audit records is possible without affecting performance [5].

CONCLUSION

Cloud computing is an evolving and rapidly evolving model with new capabilities and uses. Cloud computing is a cloud alternative to something that an organization would normally manage with its own resources using dynamically scalable and often virtualized resources provided both over the Internet or intranet. For example, webmail is a cloud-based alternative to hosting on your own e-mail server.
Most cloud computing services can be accessed through the web browser of the connected device (mobile device, tablet, personal computer ...). Therefore, cloud services do not require users to have a sophisticated computer capable of software. With a user-oriented interface, there is a cloud infrastructure and support for transparent applications for users.
One of the main concerns is security and privacy. These concerns depend on the type of company. In the case of large organizations with significant resources that can provide an information security programmed, it is necessary to overcome in the areas of security, privacy and cooperation.

Acknowledgment

This work was supported by the Slovak Research and Development Agency under the Contract no. APVV-14-0752.

REFERENCES

[1] European Commission. Available at: https://ec.europa.eu/info/strategy/priorities-2019-2024.

[2] DARIUSZ, M. (2020): *A review of Cloud computing technologies for comprehensive microRNA analyses*. Computational Biology and Chemistry.

[3] FUSKO M. - BUČKOVÁ M. - VAVRÍK V. - MARTINKOVIČ M. (2020): *Logistics and Technical service in Industry 4.0 concept*. Daily automation, No. 6, May, ISSN 2453-8175.

[4] BUČKOVÁ M. - VAVRÍK V. - GAŠO M. (2019): *Future of the manufacturing systems.* Průmyslové inženýrství, Plzeň.

[5] YANG, B. - CAO, J. - LIU, X. - WANG, N. - LV, J. (2018): *Edge computing based real-time passenger counting using a compact convolutional neural network.* Neural Comput. Appl., pp. 1-13, 10.1007/s00521-018-3894-2.

Logistic system supported by the Digital Factory

Beáta Furmannová, Ing., PhD.*
Department of Industrial Engineering, Faculty of Mechanical Engineering,
University of Žilina,
Univerzitná 8215/1, 010 26 Žilina, Slovak Republic.
E-mail: beata.furmannova@fstroj.uniza.sk, Tel.: + 421 41 513 2711

Gabriela Gabajová, Ing., PhD.
Department of Industrial Engineering, Faculty of Mechanical Engineering,
University of Žilina,
Univerzitná 8215/1, 010 26 Žilina, Slovak Republic.
E-mail: gabika.gabajova@fstroj.uniza.sk,Tel.: + 421 41 513 2731

Marián Matys, Ing.
Department of Industrial Engineering, Faculty of Mechanical Engineering,
University of Žilina,
Univerzitná 8215/1, 010 26 Žilina, Slovak Republic.
E-mail: marian.matys@fstroj.uniza.sk, Tel.: + 421 41 513 2740

Abstract: This paper is focused on application of digital factory tools in the logistics planning process. We have used software Tecnomatix Process Designer which represents complex PLM solution for digital factory. Environment of logistics module, main workflow and basic functionalities of this module are described here.

INTRODUCTION

Logistics is increasingly the motor of success of industrial organisations on global markets. Globalisation brought not only the potential of global market, disturbance of market barriers and free movement of capital, but also global competition and so far unknown speed by which market turbulences appear. Design of the logistics system represents an important part of the production system design. Production can`t exist without supply of material from the warehouse to the workplace and transport of products from the workplace to the warehouse of finished products. Therefore, it is necessary to create appropriate routes, to define appropriate transported quantities, to choose the technology to be used in warehouses for transport, etc. New technologies are developed rapidly and enterprises have to think about their implementation into the strategy.

1 THE SITUATION IN LOGISTICS

The current effort of modern logistics systems projectants is, when designing to build into their features the ability of fast adaptation to changing market conditions. Reconfiguration of logistics, as well as adaptability, is based on the current need to project logistics concepts in smart factories. Extraction of information and knowledge from data brings the new era of knowledge engineering, when the knowledge is not created by a man, but they are also the result of data processing by information systems. Designing such logistics operations uses a huge amount of data [1].

Software and software services and their development became the condition for the further development of logistics. Software services represent nowadays the crucial factor of competition ability of logistics solutions. It can be seen literally on every step. Pallets, containers, conveyors, robots, mobile robotics, reservoirs, storages - these all become intelligent and able to mutually communicate and make decision. Software therefore gradually becomes the thing which decides about the amount of added value which is created by logistics and which becomes the part of added value of product. Software and software services therefore directly become to affect the quality and price of products [2].

2 TECNOMATIX – TOOL OF DIGITAL FACTORY

Digital Factory represents one of the most progressive, integrated approaches to the design of new products, production processes and systems. Digital Factory entitles virtual picture of a real production. It represents the environment integrated by computer and information technologies, in which the reality is replaced by virtual computer models. Such virtual solutions enable to verify all conflict

situations before real implementation and to design optimized solutions. Figure 1 shows an example of a digital factory [3].

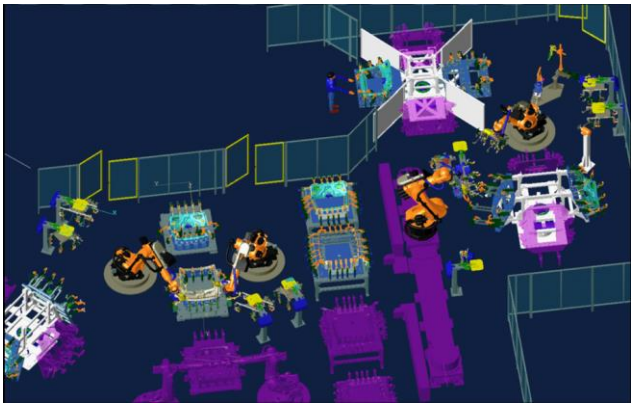

Fig. 1. Demonstration of digital factory [3]

Tecnomatix is aimed at increasing the effectiveness of work planning, optimization the layout of production facilities and material flows in the enterprise. The use of a company can achieve a sustained increase in productivity through the implementation and optimization of robotic and automation systems [4].

Tecnomatix is a complete portfolio of digital manufacturing solutions that bring innovation by linking all manufacturing disciplines with manufacturing and engineering to the design and planning, simulation and verification through to actual production. Tecnomatix is built on an open product lifecycle management (PLM), called Teamcenter manufacturing platform and provides the most versatile set of manufacturing solutions on the market today. Tecnomatix consists of basic parts: Process Designer, Process Simulate, Factory CAD, Factory Flow, Robcad, Plant Simulation.

Tecnomatix product portfolio can be used to represent a "digital factory" on the computer. This is not just about controlling individual machine tools. The interaction of all manufacturing resources in production is what is important –for instance, whether robots work together smoothly and can easily access all tools. Long before the manufacturing begins, Tecnomatix users are able to simulate the material flow and figure out the optimal assembly line speed [4, 5].

Tecnomatix Process Designer is a digital manufacturing solution for manufacturing process planning and validation in a 3D environment. Process Designer is a major enabler of speed-to-market by allowing manufacturing organizations to bridge product and process design with integrated authoring capabilities that leverage digital product development. An example layout is shown in the following figure (Fig. 2).

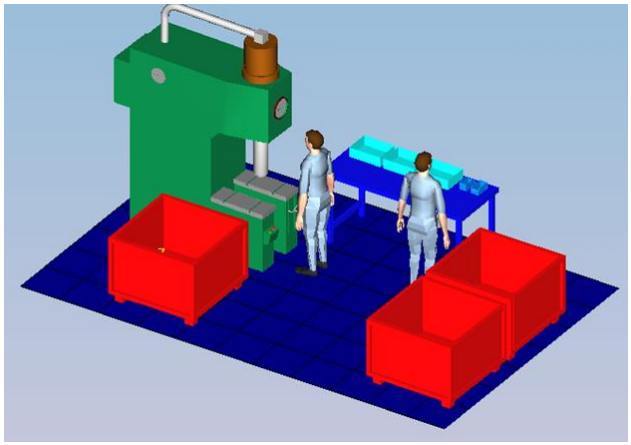

Fig. 2. Example layout in Texnomatix

Its main features are: process modelling and verification (pert and Gantt charts, schematic and table views, time estimation, cost estimation and tracking, line design, alternative planning, process variants management, documentation authoring, application customizations), integrations with time standards systems, automatic generation of assembly structure or assembly process, line balancing, tasks management and collaboration, 2D\3D system integrations, natively supported JT visualization standard, quotation, manufacturing features management, 3D simulation, static and dynamic collision detection, 2D and 3D sections, 3D measurements, sequencing of operations, assembly and robotic path planning.

3 TECNOMATIX PROCESS DESIGNER IN LOGISTICTS

Tecnomatix Process Designer is a digital manufacturing solution for manufacturing process planning in a 3D environment. Process Designer is a major enabler of speed-to-market by allowing manufacturing organizations to bridge product and process design with integrated authoring capabilities that leverage digital product development resulting in faster launch and higher production quality.

Tecnomatix Process Designer facilitates the authoring and validation of manufacturing processes from concept and detailed engineering through production planning. Process Designer enables manufacturers to develop, capture and re-use process plans. Furthermore, process design teams can compare alternatives to develop and select best manufacturing strategies that meet specific business requirements. In a 3D virtual environment, Process Designer is a collaborative platform that enables distributed enterprise teams to evaluate process plans and alternatives, optimize and estimate throughput and costs, plan for variants and changes and coordinate production resources [5, 6].

Part of this solution is the Logistics module, which provides users with a basic data model of logistic

objects, allowing them to build logistics-specific planning projects and manage the relevant data.

You need to start planning your network. In this phase logistics planners are allowed to define logistic networks and to calculate production rates per part family. This requires taking a few steps. First, setup the network structure. Setup the part structure (BOM). As we can see in Fig. 3, setup one resource per logistic plant. Then assign the resource which represents the logistic plant to the logistic plant of the network structure. Assign the produced parts to the logistic plant project and define the production rate. As the last to create part families automatically out of the BOM. One part family is created for each part in the BOM, and the relevant part is assigned to the part family.

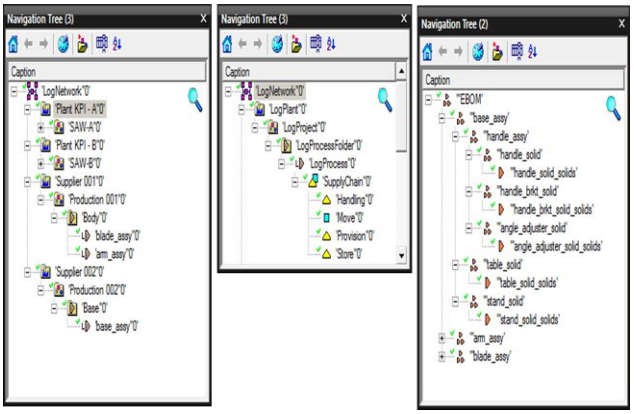

Fig. 3. Network and part structure (BOM)

Alternatively, the part families can be defined in a library and copied below the logistic project. Based on the information you defined, the system calculates the required transportation relations between the plants. The calculated transportation relations include the calculated number of products and required parts.

Logistics planners can open the Process Check tab (Fig. 4) to view progress of the logistic planning.

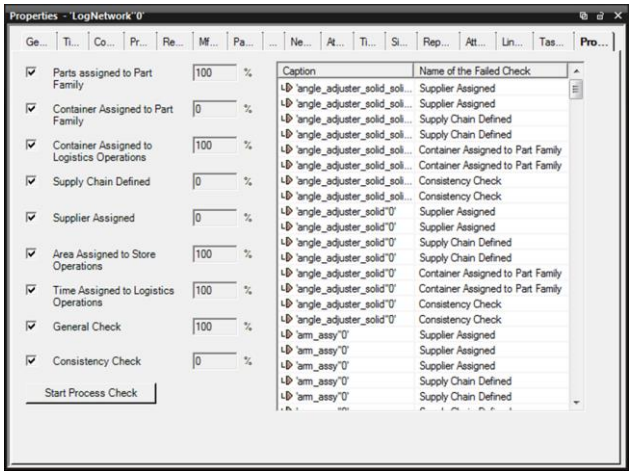

Fig. 4. Process Check tab

The Process Check tab offers the following predefined checks:

- Parts assigned to LogProcess: Is there at least one part assigned to the LogProcess object?
- Container assigned LogProcess: Is there exactly one Container assigned to the LogProcess object?
- Container assigned to logistics operations: Is there exactly one Container assigned to the Move/Store operations of the supply chain of the LogProcess?
- Supply Chain defined: Is there a supply chain defined for the LogProcess?
- Supplier assigned: Is a supplier assigned to the LogProcess?
- Areas assigned to store operations: Are there LogAreas assigned to the store operations of the supply chain?
- Times assigned to logistics operations: Are there times assigned to the logistics operations (do all logistic operations of the supply chains have an allocated time > 0).
- General check that assigned container, supplier, areas, etc., are from the correct defined library: The system checks whether all assigned resources of the following types - LogArea, LogContainer, Supplier, Vehicle, Transporter, SupplyChains (for linked supply chains) belong to the respective library of the plant, under which the LogProcess resides. The libraries are taken from fields such as LogPlant, LibrarySuppliers, etc.
- Consistency check to verify the logistics plan against the production plan to find any inconsistencies. The check is based on the use of the same parts and logistics areas by both production planning and logistics planning. A logistics plan is consistent if the parts and the corresponding logistics areas are assigned to the same station as in the production plan.

Logistics areas and tracks features enable to build a logistic path network and logistics areas. Logistics planners can describe full area and path networks by drawing areas and tracks and connecting them, using connection points, to other logistic areas or tracks. Using these commands logistics planners can define the direction of the tracks, and to set them as one-way or two-way. Defined path networks can be used as the basis for calculations of route and transport time.

Using basic commands for drawing, deleting, showing and hiding all logistics areas and logistics tracks they can be seen and designed directly in the 3D layout of production system (Fig. 5).

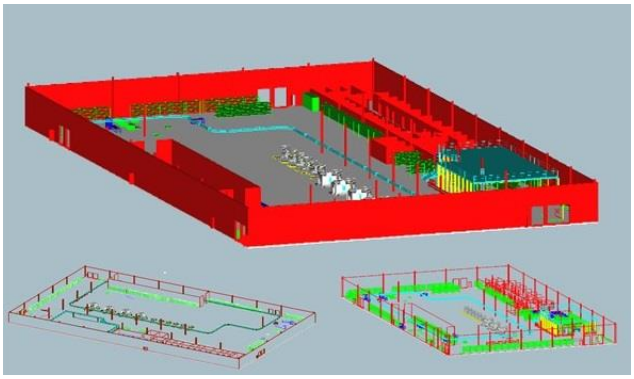

Fig. 5. 3D layout of production systems with logistics areas and tracks

After conceptual solution has been proposed, we can start with detailed design of logistic and production system. In this phase, we use software Tecnomatix Factory CAD and Factory FLOW.

Tecnomatix Factory CAD is a facility layout application that gives you everything you need to create detailed, intelligent warehouse models.

Factory FLOW enables you to optimise your warehouse layout based on material flow distances, traffic Congestion and cost.

CONCLUSION

The 21st century is typical by development and implementation of "intelligent solutions" in all areas of human life. Production and technologies become intelligent. Only countries, which maintain top technological development, will succeed in the future.

Competitive advantages in the global environment make possible to increase. Competitive advantages, then quality, costs, time, flexibility, productivity, innovation, are essential for every producer. Time is now the most important element, how to gain a customer.

Although many different software applications for the field of logistics exist, human with his knowledge is still the most important element for the successful design and planning of logistics systems. His early logistics analysis and optimal definition of supply chain is a key to the effective logistic processes. But using these technologies, companies can prevent unintended failure in case of improper design of material flows and verify their designs before it`s integration into reality.

In today's robust competitive environment and worsened economic environment, most factories need to readjust their strategy to produce as many products as possible at a minimal cost. The goal is to make the production process more efficient, encouraging workers to increase sustainability.

Acknowledgments

This work was supported by the KEGA Agency under the Contract no. KEGA 020ŽU-4/2019.

REFERENCES

[1] PLINTA, D. - KRAJČOVIČ, M. (2016): *Production system designing with the use of digital factory and augmented reality technologies.* Advances in Intelligent Systems and Computing, Vol. 350, pp. 187-196, ISSN 2194-5357.

[2] MIČIETA, B. - BIŇASOVÁ, V. - HALUŠKA, M. (2014): *The approaches of advanced industrial engineering in next generation manufacturing systems.* Communications: scientific letters of the University of Žilina. Vol. 16, no. 3A, pp. 101-105, ISSN 1335-4205.

[3] Matador Group (2020): *Digital factory.* [online] [cit. 2020-10-05]. Available at: https://www.matador-group.eu/produkty-a-sluzby/priemyselna-automatizacia/digital-factory/.

[4] SIEMENS (2020): *Tecnomatix.* [online] [cit. 2020-10-01] https://www.plm.automation.siemens.com/global/en/products/tecnomatix/

[5] HOREJŠÍ, P. - POLCAR, J. - ROHLÍKOVÁ, L. (2016): *Digital Factory and Virtual Reality: Teaching Virtual Reality Principles with Game Engines.* Virtual Learning; Cvetkovic, D., Ed.; InTech, https://doi.org/10.5772/65218.

[6] DULINA, Ľ. - BARTÁNUSOVÁ, M. (2015): *CAVE Design Using in Digital Factory.* Procedia Engineering, Vol. 100, pp. 291-298. https://doi.org/10.1016/j.proeng.2015.01.370.

Factories of the Future in the context of Industry 4.0

Patrik Grznár, doc. Ing., PhD.*
Department of Industrial Engineering, Faculty of Mechanical Engineering,
University of Žilina,
Univerzitná 8215/1, 010 26 Žilina, Slovak Republic.
E-mail: patrik.grznar@fstroj.uniza.sk, Tel.: + 421 41 513 2733

Štefan Mozol, Ing.
Department of Industrial Engineering, Faculty of Mechanical Engineering,
University of Žilina,
Univerzitná 8215/1, 010 26 Žilina, Slovak Republic.
E-mail: stefan.mozol@fstroj.uniza.sk, Tel.: + 421 41 513 2713

Marek Schickerle, Ing.
Department of Industrial Engineering, Faculty of Mechanical Engineering,
University of Žilina,
Univerzitná 8215/1, 010 26 Žilina, Slovak Republic.
E-mail: kpi@fstroj.uniza.sk, Tel.: + 421 41 513 2713

Natália Burganová, Ing.
Department of Industrial Engineering, Faculty of Mechanical Engineering,
University of Žilina,
Univerzitná 8215/1, 010 26 Žilina, Slovak Republic.
E-mail: natalia.burganova@fstroj.uniza.sk, Tel.: + 421 41 513 2713

Abstract: Today's world is undergoing a digital transformation based on the implementation of new advanced technologies based on Industry 4.0. Old manufacturing systems are facing increasing instability in markets where speed is becoming an important competitive advantage. As manufacturing lead time and costs increase, manufacturers are starting to look at new technologies and organizational concepts that will bring sustainability to their companies. These new concepts for manufacturing will be used in Factories of the Future in which manufacturing will better cope with the shortcomings of current systems. The article deals with the Factories of the Future in the context of Industry 4.0 therefore with new Industry 4.0 technology and new manufacturing concepts.

INTRODUCTION

The current market world, which is characterised by instability and the need to react rapidly, the old manufacturing systems become inefficient. This is reflected in the increase of manufacturing costs and manufacturing lead time. That's why new manufacturing concepts are being developed around the world that can respond quickly to changes thanks to Industry 4.0 technologies, giving companies a competitive advantage. These new concepts such as reconfigurable manufacturing systems, competency islands and adaptive logistics system are the systems within of Factories of the Future. Old manufacturing systems will only be applied where it is effective and new concepts will be applied where there is a demand for reaction in speed today. The article describes in its core technologies of Industry 4.0 used in Factories of the Future and new concepts which is developed within of this trends.

1 INDUSTRY 4.0 AND TECHNOLOGIES USED IN FACTORIES OF THE FUTURE

According to prof. Gregor [1] will further develop new concepts of manufacturing systems in the field of intelligent, reconfigurable manufacturing systems, in which advanced technologies will become the central element of the manufactured product and the basis for innovation will become advanced technologies. Prof. Gregor's forecast is based on theoretical and practical knowledge, which has been concentrated in CEIT for almost 20 years.

Future factories will be based on the basic principles of Industry 4.0, which is built on two main pillars [2]:

- Digitisation.
- Application of exponential technologies.

The basic technologies currently being linked with Industry 4.0 is [2]:

Cyber-physical systems (CPS) - physical devices with built-in tools for digital data collection, processing and distribution, and over the Internet are connected to each other online.

Internet of Things (IoT) - a network of physical objects - devices, vehicles, machinery and other objects with built-in electronics, software, sensors and network connectivity (CPS), which allows these objects to collect and exchange data. The Internet of Things allows connected objects to be controlled remotely through existing network infrastructures, and create opportunities for further direct integration of the physical world into computer systems.

Internet of Services (IoS) - an area that is cross-cutting for all areas of Industry 4.0. It presents as an infrastructure that uses the Internet as a medium for offering and selling services. As a result, services become tradable goods. IoS provides a business and technical basis for advanced business models, focused on the provision and use of services.

Big Data (BD) - the term for data files that are so large or complex that traditional data processing applications are inadequate. The solution includes analysis, capture, data management, search, sharing, storage, transmission, visualization, search, etc. BD provide infrastructure for transparency in the industry, which is the ability to detect uncertainties and sources of inconsistent performance and availability.

Cloud Computing (CC) - provide services or programs stored on servers on the Internet, where users can access them, for example, using a web browser or client of a given application, and use them from virtually anywhere.

Product Lifecycle Management (PLM) [3] - a system designed to manage detailed information about its design, characteristics, method of manufacture and use. It allows to integrate data, processes, business systems and also people in vertical interconnection inside the company, as well as horizontal integration of suppliers, manufacturer and customers. PLM software allows you to effectively and efficiently manage this information throughout the life cycle of the product, from initial idea, design and manufacturing through service and disposal.

Digital Manufacturing (DM) - represents the use of an integrated computer system composed of simulation, three-dimensional (3D) visualization, analysis and various tools designed to collaborate in product creation and manufacturing process simultaneously. Simulation of manufacturing processes can be carried out with the intention of reusing existing knowledge and optimising processes before products are manufactured. Digital manufacturing also allows feedback on actual manufacturing operations to be integrated into the product design process, allowing companies to take advantage of the actual layout of workshops at the planning stage.

Digital Twin (DT) - represents a digital copy of a physical object (product and/or manufacturing) that can be used for a variety of purposes. DT processes data from sensors installed in physical objects, which it usually uses to optimize the activity of these physical objects. It is also used to manage manufacturing processes (PLM and DM tools create a digital manufacturing model, it is simulated, all processes and activities are optimised in detail, and physical manufacturing is created on this basis. When manufacturing starts, data from the manufacturing process is collected, evaluated, continuously optimised, and progressively iteratively streamlined.) and is an essential tool of Industry 4.0 for increasing the operational efficiency of manufacturing.

Exponential Technologies (ET) - it is one of the fundamental pillars of Industry 4.0. Exponentials are called because they bring rapid productivity and efficiency growth. Some of the exponential technologies are still more in laboratory conditions, and their practical applications are expected in the order of years, and some in turn become a daily part of today's industry. ET include: biotechnology, neurotechnology, nanotechnology, new energy, ICT and mobile technologies, 3D printing, sensor, artificial intelligence, advanced robotics, drones, etc.

Key elements in the implementation of basic technologies in the construction of Industry 4.0 pillars include [4]:

- Autonomous Robots.
- Simulation.
- System Integration.
- Internet of Things.
- Cybersecurity.
- Cloud Computing.
- Additive Manufacturing.
- Augmented Reality.
- Big Data.

2 NEW MANUFACTURING CONCEPTS IN FACTORIES OF THE FUTURE

According to [5], all new manufacturing concepts strive to achieve one main objective, which is adaptability, the ability to react immediately to rapid changes in the environment, also referred to as turbulence. Adaptive manufacturing systems are currently the culmination of scientists' efforts to formulate the contours of the future manufacturing

environment. To meet the adaptability requirement, it is possible to approach several paths, which is why scientists have developed, developed and tested a whole group of new manufacturing concepts, such as reconfigurable manufacturing systems, competency islands, multi-agent control systems, etc.

In new manufacturing concepts, the manufactured product will act as a smart entity, able to communicate with its surroundings and able to organize its processing completely autonomously. Such a product will determine its own sequence of processing, allocate the required capacity in the respective competency islands and summon mobile robotic systems to transport it in manufacturing. In order for such an organisation system to work safely and reliably and perform the required tasks, this will require new ways of planning and control manufacturing. In the future seemingly 'chaotic' world of manufacturing, the current pressure management systems will no longer work. With a very large number of intelligent elements (entities) in the manufacturing system, there will be complicated relationships and situations that today's hierarchical control can no longer deal with effectively. Complex relationships between individual entities will create a condition known as emergence, a condition in which it will be difficult to predict the future behaviour of such complex systems. That's why researchers are experimenting with new control approaches based on the relative autonomy of individual elements of the manufacturing system and their behaviour, which will resemble the behaviour of intelligent, living organisms. In addition to real objects, there will therefore be virtual representatives in the manufacturing, whom we now refer to as digital twins. Such dual representation of manufacturing is also referred to as virtual manufacturing.

2.1 Reconfigurable manufacturing systems

The Reconfigurable Manufacturing System (RMS) is a manufacturing system whose structure is easily adjustable with the possibility of scaling capacity and flexibility limited to the selected product family [6].

Reconfigurable manufacturing systems represent the evolutionary phase of development of manufacturing systems, they are a continuation of developmental evolution. Their application requires a new approach in which reconfigurable machines, preparations, tools, logistics and a reconfigurable management system play a dominant role [7].

RMS are built to allow easy and quick reconfiguration. This property moves reconfigurable manufacturing systems to adaptive systems. Conversions make it possible to adapt the manufacturing system to new product types (functionality) and to new manufacturing quantities (capacity) [8]. Reconfigurability has thus become a new technology that can better meet market fluctuations and turbulence through the gradual rebuilding of the manufacturing system.

Reconfigurability is the operational capability of a manufacturing system to adapt its functions and capacities to a specific product family. This results in the required flexibility of the manufacturing system. Unlike reconfigurability in the manufacturing system, flexibility is firmly defined. Reconfigurability and flexibility make the adaptive capacity of the manufacturing system, which is achieved through a change in its structure, subject to a change in its structure. Such structural change makes it possible to adapt (adapt) the functions and capacity of the manufacturing system to new requirements. Effective reconfigurability is conditional on a requirement to minimise the effort deployed and to reduce the maximum time needed to implement the changes [9].

2.2 Competency islands

The existing large-scale manufacturing method, organized rhythmically in manufacturing halls, working in a manufacturing tact, will no longer be able to respond to future customer demands. Today's "hard" manufacturing and assembly lines will be replaced by a set of autonomous workplaces, the so-called competency islands (Fig. 1). These can be imagined as virtual manufacturing lines, formed dynamically, virtually, based on real need. The competency islands will be equipped with technologies and cooperative robots capable of working safely and reliably with humans [10].

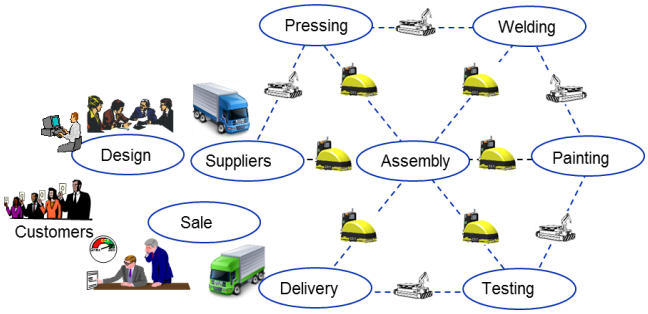

Fig. 1. Competency islands [1]

New manufacturing systems should therefore be conceived as small, highly flexible manufacturing units, which will be deployed where there is sufficient real demand. Such manufacturing systems will be designed for the manufacturing of a selected product family, which requires their concept to be built on the principles of reconfigurable manufacturing systems.

CONCLUSION

The activities of future manufacturing systems will be organised in a completely different way. Classic manufacturing and assembly lines will only be maintained where it will still benefit the economy. Future manufacturing will feel like total chaos to the outside observer. It will seem to him that the material, blanks, work in process, or mobile robots move unplanned, chaotically. Each of them, however, will follow the strict logic of the superior level, which will allow it to conduct relatively autonomously. In fact, it will therefore be organised chaos. For the management of manufacturing will be used principles observed from nature, which offer evolution-proven, optimal procedures.

Smart mobile robots, mobile robotic systems and platforms will gain a strong position in future factories. Thousands of such robots will ensure the movement of work in-process products and their processing in a seemingly chaotic world.

Manufacturing will be organized as a living organism, resembling an anthill, in which the ants seem to run chaotically, but are strictly organized, specialized, and each of them performs well-defined tasks that require the survival of the anthill.

The product, manufacturing facilities, technologies and the entire manufacturing system will change. Manufactured products, manufacturing facilities and means of mobile logistics will become intelligent and communicate with each other. They will exchange and share all necessary data and information in real time.

Mobile robots transporting the work in process will move between the competency islands, with the product itself determining the required operations and planning their order. The observer will not see the classical manufacturing line, it will observe the apparent physical chaos, behind which will be hidden virtual line (its digital and virtual data model), formed from the competency islands, necessary for the manufacturing of the customer product.

Future manufacturing will not be structured according to the manufacturing rhythm of the line, as is the case today, but according to the content of the work to be carried out. Functional relationships, not fixed cycle times, will play a decisive role. This type of manufacturing environment will be suitable not only for small manufacturing enterprises, but will be particularly advantageous for those types of manufacturing that operate with high volumes, highly variant manufacturing and which aim at high flexibility and efficiency. Such systems will be able to respond much more efficiently to fluctuations in demand, rapid changes in manufactured models, requiring different manufacturing technologies.

Acknowledgments

This work was supported by the KEGA Agency under the Contract no. KEGA 020ŽU-4/2019.

REFERENCES

[1] GREGOR, T. et al. (2017): *Future factories. Technological changes and their impact on future production system*s (In Slovak). CEIT, University of Žilina, Study CEIT-Š001-05-2017, 47pages, ISBN 978-80-971684-6-9.

[2] Industry 4.0 (2020): [cit. 2020-30-09]. Available at: <http://industry4.sk/>

[3] HNAT, J. - GRZNÁR, P. (2013): *Use of virtual reality tools as a part of PLM*. InvEnt 2013: modern technologies - way to higher productivity: proceedings of the international conference: June, 19-21, Lopušná dolina, Žilina: University of Žilina, pp. 78-81, ISBN 978-80-554-0658-9.

[4] Industrie 4.0 (2020): [cit. 2020-30-09]. Available at: https://www.plattform-i40.de/PI40/Navigation/EN/Home/home.html

[5] GRZNÁR, P. (2019*)*: *Modelling and simulation of processes in future factories* (In Slovak). Habilitation thesis. Department of Industrial Engineering, Faculty of Mechanical Engineering, University of Žilina, 158 pages.

[6] HALUŠKA, M. - GREGOR, M. (2017). *Reconfigurable logistics system* (In Slovak). Research report No. CEIT-V009-06-2017, 33 pages.

[7] WESTKÄMPER, E. (2006). *Digital Manufacturing in the global era.* 3rd International CIRP Conference on Digital Enterprise Technology. Setúbal, Portugal, September 18.-20.

[8] HALUŠKA, M. (2014): *Reconfigurable production systems* (In Slovak). Written work for the dissertation exam. Department of Industrial Engineering, Faculty of Mechanical Engineering, University of Žilina, 65 pages.

[9] BAUERNHANSL, T. (2014). *Die Vierte Industrielle Revolution – Der Weg in ein wertschaffendes Produktionsparadigma*. BAUERNHANSL, T., TEN HOMPEL, M., VOGEL-HEUSER, B. (Hrsg.) (2014): Industrie 4.0 in Produktion, Automatisierung und Logistik. Anwendung, Technologien, Migration. Springer Fachmedien Wiesbaden, pp. 5-35, ISBN 978-3-658-04681-1.

[10] GREGOR, M. - KRAJČOVIČ, M. - GREGOR, T. - GRZNÁR, P. - HALUŠKA, M. - ĎURICA, L. (2015): *Smart Logistics. New technologies for logistics.* Study No. 04-2015 APVV. CEIT, University of Žilina, 68 pages, ISBN 978-80-971684-8-3.

Acoustic properties analysis of a freight wagon prototype at constant speed

Pavol Šťastniak, Ing., PhD.*
Department of Transport and Handling Machines, Faculty of Mechanical Engineering,
University of Žilina,
Univerzitná 8215/1, 010 26 Žilina, Slovak Republic.
E-mail: pavol.stastniak@fstroj.uniza.sk, Tel.: + 421 41 513 2562

Marián Moravčík, Ing., PhD.
Tatravagónka, Inc.,
Štefánikova 887/53, 058 01 Poprad, Slovak Republic.
E-mail: marian.moravcik@tatravagonka.sk

Vladimír Pavelčík, Ing.
Department of Transport and Handling Machines, Faculty of Mechanical Engineering,
University of Žilina,
Univerzitná 8215/1, 010 26 Žilina, Slovak Republic.
E-mail: vladimir.pavelcik@fstroj.uniza.sk

Erik Kuba, Ing.
Department of Transport and Handling Machines, Faculty of Mechanical Engineering,
University of Žilina,
Univerzitná 8215/1, 010 26 Žilina, Slovak Republic.
E-mail: erik.kuba@fstroj.uniza.sk

Abstract: The article is focused on verification of noise characteristics of a prototype tank wagon Zans 95 m3 during operation. In the first part, the problematics of noise created by railway vehicles is described. The testing requirements were defined for the test of the tank wagon. The proper measurement setup was selected for weighted equivalent acoustic pressure level observation. Based on the TSI requirements, the measurement stand was assembled on the testing track, repeated measurements were performed, and the results were compared to the limit value related to wagon category.

INTRODUCTION

One of the current trends in the development of any kind of vehicle is decreasing emissions. The category of emissions contains not only emissions created by fuel combustion in power units, but noise emissions as well. So, it is necessary to test each newly developed vehicle also from the acoustic point of view. In order to reach this goal, the computer-aided simulation of acoustic effects can be made, however, the best reality-related results can be obtained via experiments. There is a wide range of reasons – combustion, wheel-rail contact, aerodynamical noise – which can be created either with the airflow around the vehicle or with the function of some vehicle parts (air conditioning, engine cooling, etc.) Noise creation shall be avoided as much as possible, mostly because of people working on, using or simply being in insufficient distance away from vehicles.

To be able to compare the results of experiments like these, it is necessary for them to be somehow specified, for example via TSI standards. These tests are conducted by a certified testing institute. After receiving the prototype vehicle, the institute performs every single step described in the standards. Based on the customer's order, additional measured parameters can be added. The results of the tests are the measured values recorded in the testing protocol, which can contain the calculations of parameters needed for final evaluation.

The results of noise experiment have an informative character for the design engineers. Based on the results, they can make design modifications decreasing the noise pollution – either change the aerodynamic shape of the vehicle or anything else. On the contrary, these experiments can confirm the correctness of the design or design modifications and prove, that that the noise limitations are obeyed in the vehicle surroundings.

1 MEASUREMENT METHOD AND METHODOLOGY

The verification of noise properties during passing was made for four-axle tank wagon Zans with the tank

volume of 95 m^3 at constant speed velocity according to TSI 2011/229/EU. The test was performed on the reference section of the testing track in Żmigród, Poland, designated for the measurements of acoustic parameters of vehicles.

Tab. 1. Technical parameters of tested wagon

Max. speed of empty wagon	120 km·h^{-1}
Track gauge	1 435 m
Length over buffers	16 880 mm
Swivel pivot distance	11 040 mm
Mass of empty wagon	24 840 kg
Mass of loaded wagon	90 000 kg
Wheelset diameter	ø 920 mm
Type of bogie	Y25 Ls1-K
Wheelbase of bogie	1 800 mm
Brake	KNORR KE-GP (K)
Brake blocks	Bg 320, JURID 816M

1.1 Test requirements

The test requirements were defined according to TSI-noise, which is the source of following requirements:

- The microphone must be positioned perpendicularly to the track in the distance of 7.5 m from the track axis and in the height of 1.2 m over the top of the rail.
- The test station must be in the free sound field, another rail must not be between microphone and test track.
- The measurement takes place during passing of a wagon at the reference velocity 80 km·h^{-1} and at the maximum velocity, in this case 120 km·h^{-1} ± 5 km·h^{-1},
- The wheel surfaces must be bedded-in (min. 1000 km),
- The descriptor of the measurement is the equivalent noise level $L_{pAeq,Tp}$ dB(A).
- At least three measurements for every defined velocity must be done and the condition of dispersion less than 3 dB(A) must be satisfied.
- One-third octave analysis must be measured when tonal noise is expected.

Tested vehicle does not contain any power unit, which could emit noise, when the velocity is zero. Therefore, the test was restricted on non-stationary vehicle only.

The limit value on noise emitted during passing at constant velocity is defined in TSI - noise using the descriptor $L_{pAeq,Tp}$ (weighted equivalent acoustic pressure level measured in time interval T_p). The limit value can be calculated according to boundaries defined in eq. (1), where A_{pl} is the number of axles on one unit of a length scale, n is the number of axles and L_n is the vehicle's length over buffers [m].

$$Apl = \frac{n}{l_n} \cdot \tag{1}$$

The tested wagon is in the category of new wagons with an average number of axles on one length unit from 0.15 m^{-1} to 0.275 m^{-1} and the limit value of $L_{pAeq,Tp}$ (80 km·h^{-1}) = 83 dB(A). From the results measured at velocity 120 km·h^{-1}, eq. (2) can be used to calculate the final value related to the reference velocity 80 km·h^{-1}. Such value can be compared with the one mentioned above.

$$L_{pAeq,Tp}(80\mathrm{km\cdot h^{-1}}) = L_{pAeq,Tp}(v) - 30 \cdot \log(v / 80\mathrm{km\cdot h^{-1}}) \tag{2}$$

1.2 Measured quantities and instruments used

Equivalent noise level $L_{pAeq,Tp}$ [dB(A)] is defined by equation (3), where $L_{pAeq,Tp}$ is A-weighted equivalent noise level [dB(A)], $t_2 - t_1$ is time interval of the measurement T_p [s], $p_A(t)$ is A-weighted instant acoustic pressure [Pa] and p_0 is reference value of acoustic pressure (p_0 = 20 μPa).

$$L_{pAeq,Tp} = 10\log\left[\frac{1}{t_2 - t_1}\int_{t1}^{t2}\frac{p_A^2(t)}{p_0^2}dt\right] \tag{3}$$

For pressure level measurement, Modular Precision Sound Analyzer Type 2260 from Brüel & Kjaer containing:

- Sound level meter Investigator 2260.
- Condenser microphone Brüel & Kjaer type Falkon 4189 for free sound field, sensitivity 50 mV/V, without external polarization, with frequency range 6 Hz – 20 kHz,
- For calibration purposes Brüel & Kjaer type 4220.
- Actual atmospheric pressure correction was gained using Brüel & Kjaer UZ 003.

All values from the sound level meter were postprocessed by weight filter A and expressed in dB(A). The entire measurement setup met the requirements of EN 60804 for devices type 1.

The following devices were also used:

- A pair of optical sensors type IDEC SA1U-B02MW – for synchronization and independent measurement of the speed of the vehicle.
- Weather station Davis Vantage Pro 2 for temperature, relative humidity, atmospheric pressure, and wind direction detection.
- MDK device for acoustic roughness measurement.

2 TEST PROCEDURE

The following section describes tested train set, test track and measuring station.

2.2 Train set

The prototype wagon was placed at the end of the train set (Fig. 1). The train set consists of an electric locomotive ET 22-037, a measuring wagon (MV), a freight wagon of the Tagnpps series and a tested wagon Zans 95 m^3. Wagon was tested in a fully loaded condition, which represents a maximum load of 90 t.

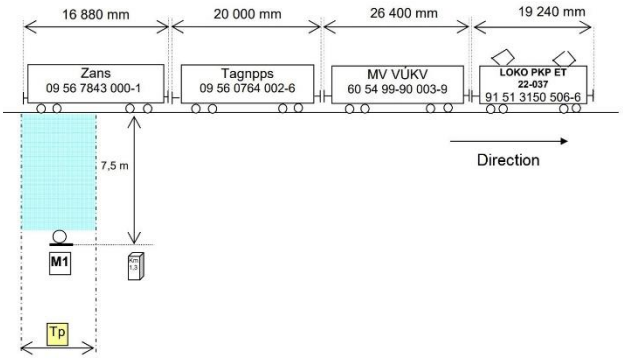

Fig. 1. Composition and orientation of the test set

2.2 Test track

The test was performed on the reference section of the test track of the Instytut Kolejnictwa in Żmigród in the place designated for performing acoustic test. The track parameters are in Tab. 2.

Tab. 2. Track parameters

Geometric	
Track	Straight
Cant [mm]	0
Track gauge [mm]	1435
Rail inclination	1:40
Measuring station [km]	6.5
Structural	
Subgrade	Natural ground
Height of ballast [m]	0.8 – 1
Type of sleepers	concrete
Rail profile	UIC 60
Sleepers spacing	1733 pcs·km^{-1}
Fastening system	K and S

The actual acoustic roughness of the rail surface (Fig. 2 and Fig. 3) was measured at the noise measurement station before the test.

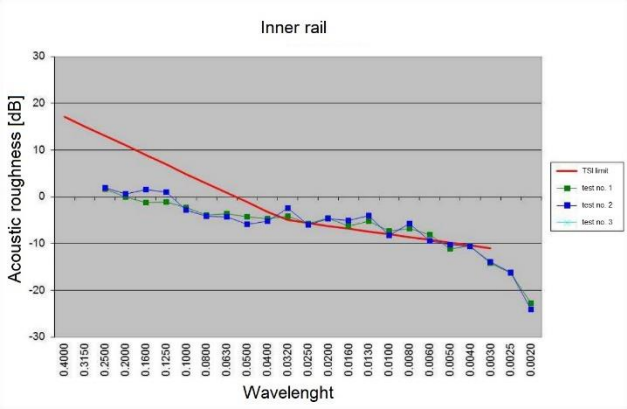

Fig. 2. Acoustic roughness of the inner rail

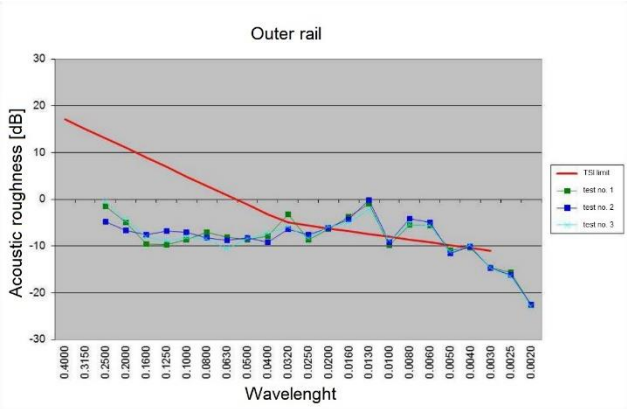

Fig. 3. Acoustic roughness of the outer rail

Dynamic attenuation parameters were not recorded in this section during this test.

2.3 Measuring station

The placement of the M1 and M2 microphones met the condition of a free sound field. The microphone was placed horizontally perpendicular to the track at a distance of 7.5 m from the track axis and at a height of 1.2 m above the top of the track. The appearance of the entire measuring station is shown in Fig. 4.

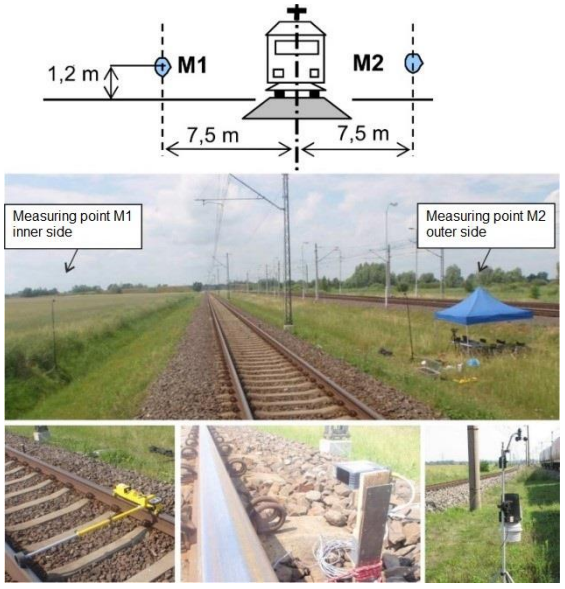

Fig. 4. Measuring station

3 MEASUREMENT RESULTS

The tests were performed in almost clear weather, dry track and surrounding. Overall, the meteorological conditions during the test can be considered satisfactory from the point of view of the requirements of the TSI – noise. By observing all conditions, it was possible to determine the measurement error $UAB = \pm 2$ dB, which, for the normal distribution, corresponds to a coverage probability of approximately 95 %.

3.1 Measurement interval T_p

The measurement interval T_p [ms] is based on TSI – noise for testing a single unit at the end of the train. It corresponds to the passing time of half of the unit, i.e. it starts at the moment when the center of the tested wagon passes in front of the microphone and ends at the moment when the rear bumpers of the wagon pass. This time can be theoretically determined by the equation:

$$T_p = \frac{L}{2}.\frac{1}{v}, \quad (4)$$

where L is length of the wagon over buffers and

v is speed of the vehicle when passing the measuring station.

The measuring interval T_p is equal to 380 ms for vehicle speed of 80 km·h^{-1} and 253 ms for vehicle speed of 120 km·h^{-1}.

The real measurement interval T_p was determined by data from optical sensors.

3.2 Background noise and control of the acoustic neutrality of the adjacent wagon

Background noise expressed using the A-weighted acoustic pressure descriptor was measured before each pass. Acoustic pressure L_{pAeq} did not exceed 53.1 dB(A) for the M1 microphone and 52.7 dB(A) for the M2 microphone.

The principle of verifying the acoustic neutrality of the adjacent wagon was to compare the noise levels $L_{pAeq,T1}$ and $L_{pAeq,Tp}$ for the time intervals T_p and T_1, the difference in none of the measurements exceeded 2 dB(A). The T_1 interval is the time from the passage of the center of the wagon placed in front of the test wagon to the passage of the center of the test wagon.

3.3 Equivalent noise level

Table 3 summarizes the measured values of the A-weighted equivalent noise level $L_{pAeq,Tp}$. For a speed of 120 km·h^{-1} values are converted to reference speed of 80 km·h^{-1}. The occurrence of tonal or impulse noise was not detected during any measurement.

Tab. 3. Values of the A-weighted equivalent noise level $L_{pAeq,Tp}$

Speed [km·h^{-1}]	80		120			
			Measured values		Converted to reference speed of 80 km·h^{-1}	
Measuring place	M1	M2	M1	M2	M1	M2
Height above top of the track [m]	1.2	1.2	1.2	1.2	1.2	1.2
Distance from the axis of the track [m]	7.5	7.5	7.5	7.5	7.5	7.5
Measurement no. 1 [dB(A)]	81.6	82.0	86.7	87.3	81.4	82.0
Measurement no. 2 [dB(A)]	81.8	81.7	86.8	87.3	81.6	82.1
Measurement no. 3 [dB(A)]	81.4	81.7	86.7	87.2	81.6	82.1
Arithmetic mean [dB(A)]	81.6	81.8	-	-	81.5	82.1
The resulting value [dB(A)]	82	82	-	-	82	82

CONCLUSION

The article is focused on the assessment of the acoustic properties of a tank wagon. Test conditions have been established, then three measurements were made at a speed of 80 km·h^{-1} and three measurements at a speed of 120 km·h^{-1} and recalculated for the reference speed. Based on the measured values and their comparison with the limit value of the weighted equivalent acoustic pressure level, it has been demonstrated that the wagon meets the requirements for permissible noise levels.

Acknowledgement

„This publication is the partial result of the Research & Development Operational Program for the project Development of two types of freight wagons with bogies for non-standard track gauge or wheelbase, meeting the criteria for interoperability, environmentalism, safety and reliability, ITMS 26220220070, supported by the Operational Program funded by the ERDF."

REFERENCES

[1] GORBUNOV, M. - GERLICI, J. - KRAVCHENKO, K. - DIŽO, J. - LACK, T. - BLATNICKÝ, M. (2019): *Method of the detection of a defective damper*. Current problems in rail vehicles: Proceedings of the conference, University of Žilina, pp. 153-160, ISBN 978-80-89276-58-5.

Analysis of freight tank wagon's longitudinal force transmission ability in opposite track curves

Pavol Šťastniak, Ing., PhD.*
Department of Transport and Handling Machines. Faculty of Mechanical Engineering.
University of Žilina.
Univerzitná 8215/1. 010 26 Žilina. Slovak Republic.
E-mail: pavol.stastniak@fstroj.uniza.sk, Tel.: + 421 41 513 2562

Marián Moravčík, Ing., PhD.
Tatravagónka. Inc..
Štefánikova 887/53. 058 01 Poprad. Slovak Republic.
E-mail: marian.moravcik@tatravagonka.sk

Erik Kuba, Ing.
Department of Transport and Handling Machines. Faculty of Mechanical Engineering.
University of Žilina.
Univerzitná 8215/1. 010 26 Žilina. Slovak Republic.
E-mail: erik.kuba@fstroj.uniza.sk

Vladimír Pavelčík, Ing.
Department of Transport and Handling Machines. Faculty of Mechanical Engineering.
University of Žilina.
Univerzitná 8215/1. 010 26 Žilina. Slovak Republic.
E-mail: vladimir.pavelcik@fstroj.uniza.sk

Abstract: The article deals with investigation of longitudinal force transmission ability in opposite track curves. The vehicle being investigated is newly designed tank wagon. The investigation took place by the means of experiment on a test track. Recorded wheel lifts and mutual transverse displacements were evaluated in accordance with the UIC leaflet. The achieved results reflect both proper design solutions of separate parts of the railway vehicle and the vehicle as a whole.

INTRODUCTION

Nowadays. tank wagons are important parts of railway transport. During casual traffic of a tank wagon as well as any other railway vehicle. an extraordinary situation can occur. In such situation. it is necessary for the vehicle construction to prove its relevancy.

One of those situations might be a wagon passing through opposite track curves. where one of the most important properties a railway vehicle needs to secure unconditionally is its ability to transmit longitudinal forces. Whether this criterion is met or not is a result of suitable design solution of various railway

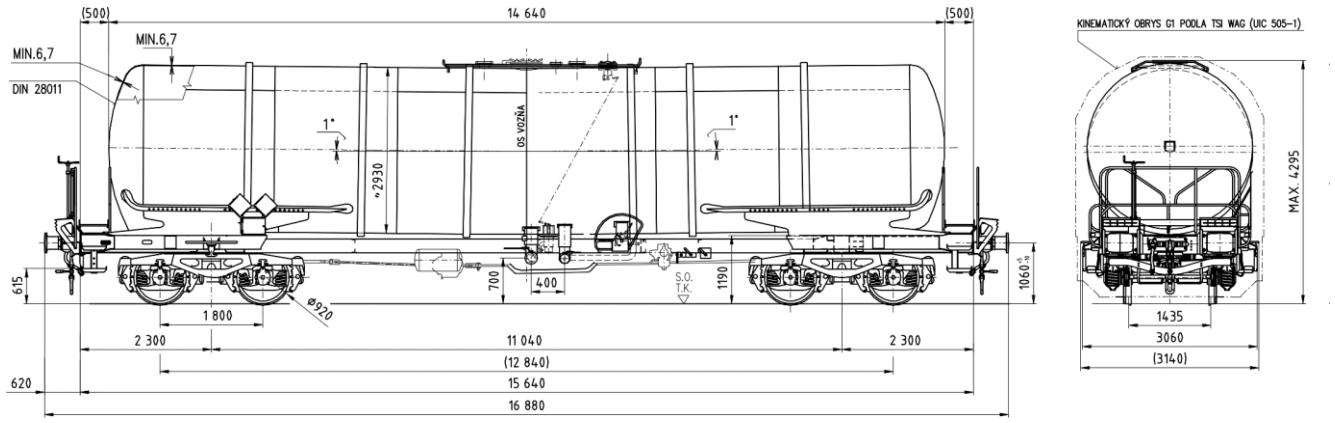

Fig. 1. Scheme of the tested tank wagon Zans 95 m^3

vehicle's parts and of the design of the vehicle as a whole.

The suitability assessment of design of the wagon for the transmission of longitudinal forces follows paragraphs of leaflet UIC 530-2. Based on the requirements stated in this leaflet. the geometry of the test track is given. which contains two opposite curves of exact radiuses and a shorter straight section between them. Next. the interval of speeds is given. which are acceptable during the test itself. and the minimum tractive force exterted in the frame during the test. The result of the test is an evaluation of geometrical parameters. such as wheel lift on the outer and inner side of the curve. transverse movement of the buffers and their dependency on the tractive force. The measured quantities need to be compared to limit values given either by the UIC leaflet or the contract between customer and test executor. Based on this comparison. the suitability of the design of the railway vehicle can be either accepted or rejected.

The goal of the test is to verify the tested wagon's ability to transmit longitudinal forces in the train set during pushing through opposite track curves with radiuses 150 m.

Traffic safety was verified at constant longitudinal tractive force 240-280 kN at the speed of 4-8 km·h^{-1}. In case of wheel lifted higher than 50 % of the limit value. the measurement of H-forces needed to be done. Final evaluation of this test was meant to be done according to the leaflet mentioned above.

The tested wagon is tank wagon Zans 95 m^3. schematically drawn in Fig. 1. Its technical parameters are in Tab. 1.

Tab. 1. Technical parameters of tested tank wagon

Wagon type	Zans 95 m^3
Track gauge [mm]	1 435
Length over buffers [mm]	16 880
Swivel pivot distance [mm]	11 040
Max. axle load [t]	22.5
Tare [t]	25 ± 1%
Mass of loaded wagon [t]	90
Height of buffers of new empty wagon over top of the rail [mm]	1 060 +5/-10
Operational overpressure [MPa]	0.3
Type of bogie	Y25 Ls1-K
Wheelbase of bogie [mm]	1 800

1 MEASUREMENT METHOD AND METHODOLOGY

Measured quantities are presented in Tab. 2 followed by Tab. 3. where assessed quantities are compared with limit values.

Tab. 2. Measured quantities

Quantity	Symbol and unit	Method of measurement
Longitudinal pushing force	$F_{LX(1.2)}$ [kN]	Tensometric force-measuring sensors under buffers on the buffer beam of cover wagon $F_{LX} = F_{LXn(1)} + F_{LXn(2)}$
Wheels' lifts	$d_{z(i.\,j)}$ [mm]	Potentiometric distance sensors
Crosswise buffers movements	$d_{y(A.\,B)}$ [mm]	Draw wire potentiometric distance sensors
Speed of train set	v [m·s^{-1}]	GPS sensor
Position of train set	s [m]	GPS sensor (distance measured from the original position)
Bogie rotation	$\alpha_{A.\,B}$ [mm]	Draw wire potentiometric distance sensors

Tab. 3. Assessed quantities and their limit values

Quantity	Criterion	Limit value
Longitudinal pushing force [kN]	$F_{LX} \geq F_{LXmin}$	min. 240 kN
Min. overlap of buffer heads [mm]	$d_{y(A.B)i} \leq$ $\leq d_{yp.MAX}$ $d_{yp.MAX}$	max. mutual crosswise movement of wagons in the plane of buffers heads 467 mm
Wheels lifts over the inner rail of the track curve[mm]	$d_{zi(2m).(i.j)} \leq d_{max\ zi(2m)}$	max. 50 mm
Wheels lifts over the outer rail of the track curve[mm]	$d_{ze(2m).(i.j)} \leq d_{max\ ze(2m)}$	max. 5 mm

Measuring equipment is summarized in Tab. 4. In Fig. 2. one of the sensors of the wheel lift is presented.

Fig. 2. Sensor of wheel lift

Tab. 1. Measuring equipment used during measurement

Amount	Device
2	Electric tensometric dynamometer
4	Draw wire sensor type WDS-750-Z60-S-U
4	Potentiometric distance sensor TR50
1	Sensor Garmin GPS 18X-5Hz
1	Measuring amplifier EMS 5V – 231
1	PC measuring board AD14 with original software VÚKV – AD Anal

3 TEST PROCEDURE AND RESULTS

At the beginning of the description of the measurement process. it is appropriate to specify the composition of the test set – Tab. 5 and Fig. 3 and parameters of the cover wagons – Tab. 6.

Tab. 5. Composition of the test trainset

Vehicle order in the direction of travel	Vehicle	Type
1 and 2	Braking wagons	Rmms
3	Braking wagon	Eas
4	Cover wagon 1	Fcc^{210}
5	Tested wagon	Zans 95 m^3
6	Cover wagon 2	Rs^{680}
7	Pusher locomotive	731.058-4
8	Pusher locomotive	720.099-1
9	Pusher locomotive	721.549-4

Tab. 2. Cover wagons parameters

	Bogie platform wagon	Discharge wagon with 2 wheelsets
Wagon type	Rs680	Fcc210
Swivel pivot distance[mm]	13 000	-
Wheelbase of bogie [mm]	2 000	-
Wheelbase of wagon[mm]	-	6 000
Length over buffers [mm]	19 900	9 800
Buffers	category A (590 kN). *R* = 1 500 mm	

The static characteristic of the cover wagon buffers that were in contact with the tested wagon were measured by Výzkumný Ústav Železniční (VUZ). The buffer characteristics of the tested wagon were checked by the manufacturer and practically correspond to the type characteristics of this type of buffer. The test was carried out in the premises of VUZ Velim on a special track with track geometry corresponding to the requirements of the UIC leaflet 530-2 – two opposite curves R = 150 m with an added straight section 6 m long. Before and after the test. track gauge values were recorded at selected locations. The required value should be in the range of 1450 – 1465 mm. The measured value ranged from 1455 to 1457 mm. The control measurement of the

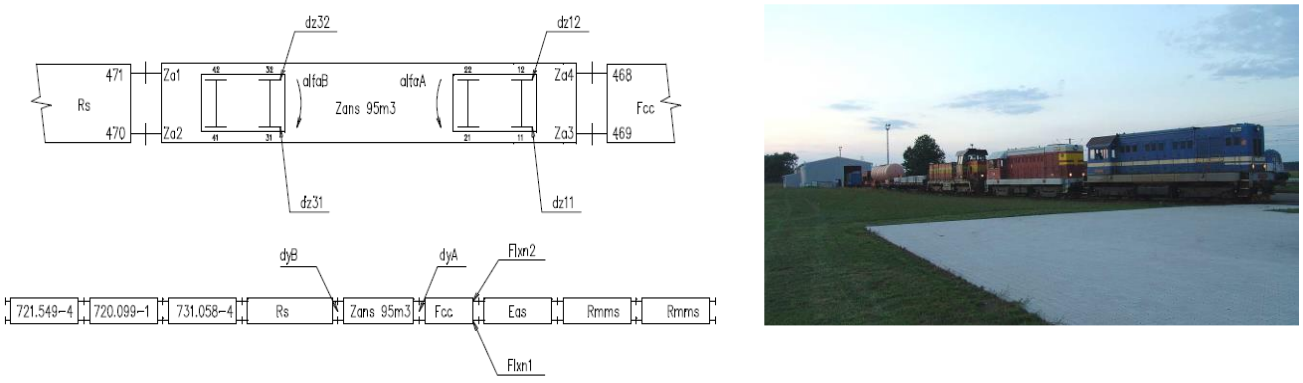

Fig. 3. Scheme of test set and measuring points

Both cover wagons were in a fully loaded condition during the test. On the opposite front of the cover wagon – not adjacent to the tested wagon. the measuring inserts necessary for measuring the tractive force were mounted under the buffers. thus extending the length of these buffers by 50 mm. Since the Rs wagon had new wheels. the overlap of the buffers was not sufficient even when wagon was fully loaded. it was necessary to reduce the position of the bumpers by means of reduction plates.

position of the track before the test and after the test did not reveal its displacement. The wagon was equipped with sensors and subsequently the condition of the buffer heads was documented. An adequate amount of lubricant was applied to the buffer heads. The test train set was checked in terms of parameters crucial for the test – train formation. condition of screw coupling. measuring the difference in height of the buffers of the cover wagon and the tested wagon. where the bumpers overlap in the range of 90 to

Tab. 7. Results and parameters of test runs

Tractive force	Speed	Wheel lift in the inner side of the track curve				Transversal movement of buffers		Wheel lift in the outer side of the track curve			
F_{Lx}	v	d_{z11}	d_{z12}	d_{z31}	d_{z32}	d_{yA}	d_{yB}	d_{z11_e}	d_{z12_e}	d_{z31_e}	d_{z32_e}
[kN]	[km·h^{-1}]	[mm]	[mm]	[mm]	[mm]	[mm]	[mm]	[mm]	[mm]	[mm]	[mm]
257.4	5.2	1.0	0.3	1.0	0.8	135.1	224.1	0.1	0.4	1.3	0.5
263.5	5.0	0.8	0.5	0.8	1.4	130.5	232.7	1.3	0.8	1.1	0.4
282.2	6.0	0.8	0.5	0.9	0.4	136.2	237.9	1.4	0.8	1.2	0.6
281.1	6.1	0.8	0.5	0.9	0.4	136.4	236.0	1.4	0.7	1.2	0.5
273.6	4.3	0.8	0.5	1.6	1.0	135.1	232.9	1.4	1.0	1.6	0.5
275.2	6.9	0.8	0.4	1.7	1.3	130.9	237.3	1.4	0.8	1.7	0.6
285.2	4.9	0.8	0.5	1.8	1.4	132.7	235.1	1.4	0.8	1.7	0.5

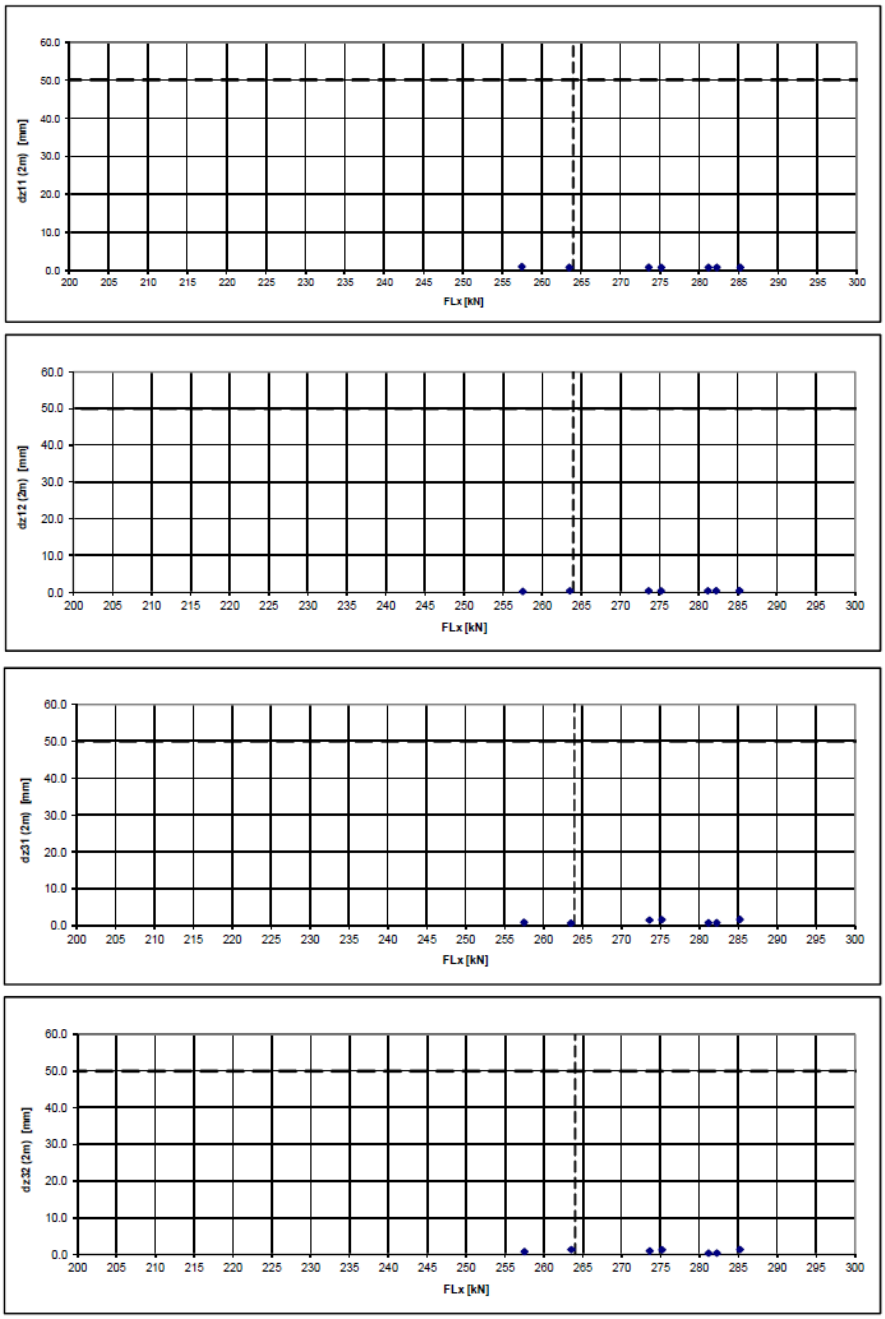

Fig. 4 The dependence of the wheel lift on the longitudinal tractive force at the inner rail of the curve

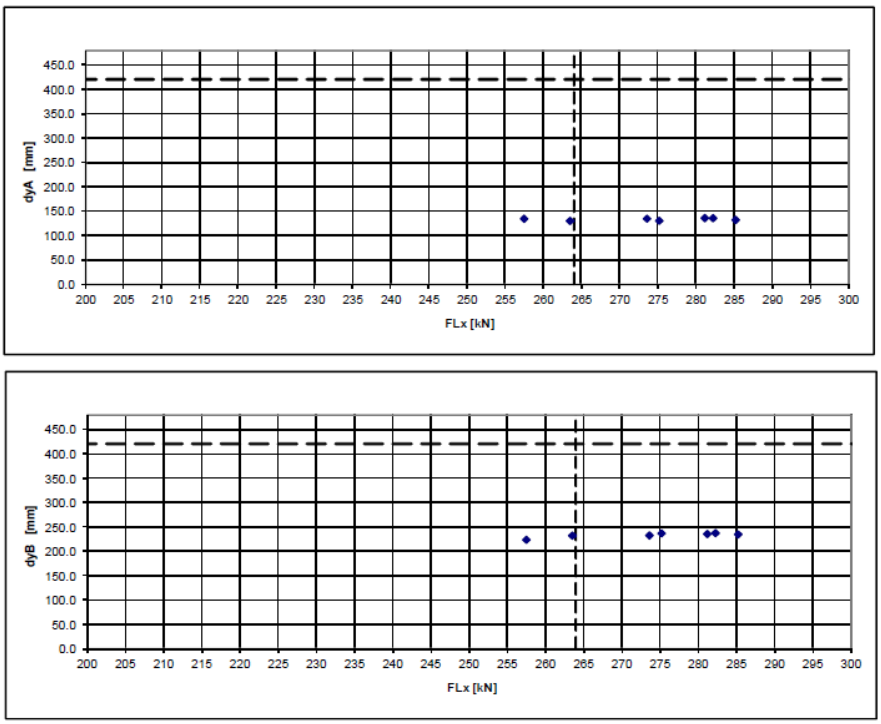

Fig. 5 Dependence of mutual transverse displacements of buffer heads on longitudinal tractive force

105 mm. The screw coupling between the test wagon and cover wagons has been adjusted in accordance with the requirements so that the buffers of these wagons touch without preload on a straight track. The test was performed by moving the test train at a constant sped in the range of 4 to 8 km.h^{-1} through the test section of the track under the action of an approximately constant tractive force. A total of 7 measuring runs were performed in the range of tractive forces from 257 to 285 kN.

A total of 7 measurements were performed with the Zans 95 m^3 wagon. of which 5 measured runs were performed with a tractive force greater than 264 kN (the required minimum transmissible tractive force is 240 kN + 10%). the remaining two runs were performed with a tractive force close to 264 kN. All test runs were performed immediately after each other without refilling the buffer head lubricant and without the need for buffer repairs.

The highest value of the tractive force was 285 kN. No visible wheel lifts of the tested wagon were observed during any of these tests. the maximum vertical movements up to 2 mm were evaluated on the measured wheels. The dependence of the wheel lift on the longitudinal tractive force at the inner rail of the curve is shown in fig. 4. The evaluated transverse movements are significantly lower than the limit value 25 mm stated for the maintaining the transverse overlap of the buffer heads. The buffers of the Zans 95 m^3 wagon did not show any signs of damage after the test. The dependence of the mutual transverse displacements of the buffer heads on the longitudinal tractive force is shown in fig. 5. The post-test inspection did not reveal any change in track gauge or displacement of the test track rail.

CONCLUSION

To verify the ability of the tank wagon Zans 95 m^3 to transmit longitudinal tractive forces in the trainset. a test was performed by pushing wagon in opposite curves with radius of 150 m. Test runs were performed with the wagon on a special track corresponding to the requirements of UIC 530-2 leaflet. The test runs were performed with a longitudinal tractive force ranging from 257 to 285 kN. The recorded wheel lift and mutual transverse displacements were evaluated in accordance with UIC 530-2 Appendix G. All evaluated quantities are significantly lower than the limit values set by UIC 530-2 leaflet. In this respect. the Zans 95 m^3 tank wagon meets the safety requirements to be put into operation.

Acknowledgement

„This publication is the partial result of the Research & Development Operational Program for the project Development of two types of freight wagons with bogies for non-standard track gauge or wheelbase. meeting the criteria for interoperability. environmentalism. safety and reliability. ITMS 26220220070. supported by the Operational Program funded by the ERDF "

REFERENCES

[1] DIŽO, J. - BLATNICKÝ, M. - KRAVCHENKO, A. (2018): Substantiation of replacement of the block brake on the disc brake in the bogie of articulated platform wagon for intermodal transport. Advances in mechanical engineering and transport: scientific journal, Vol. 11, No. 2, pp. 11-17, ISSN 2313-5425.

[2] DIŽO, J. - BLATNICKÝ, M. - NOZHENKO, O. - KRAVCHENKO, K. (2017): *Computer analysis of influence of the flexible body in multibody system of the rail vehicle bogie on outputs parameters* Visnyk schidnoukrajinskogo nacionaľnogo universytetu imeni Volodymyra Daľa: naukovyj žurnal, Vol. 4., No. 234, pp. 14-20, ISSN 1998-7927.

[3] DIŽO, J. - BLATNICKÝ, M. (2015): *Analysis of vehicle system dynamics by means of computer simulation.* Logistyka, No. 4, ISSN 1231-5478.

[4] GERLICI, J. - GORBUNOV, M., I. - KRAVCHENKO, K. - PROSVIROVA, O. - LACK, T. (2020): *Evaluation of innovative methods of modern rolling stock brake systems efficiency increase.* Zaliznyčnyj transport Ukrajiny, No. 2, pp. 33-40, ISSN 2311-4061.

[5] GERLICI, J. - LACK, T. (2014): *Modified strip method specification for wheel / rail contact stress evaluation*. Prace Naukowe. Transport: Analiza i ocena elementów systemów transportowych, Z. 101, pp. 63-82, ISSN 1230-9265.

[6] GERLICI, J. - LACK, T. (2006): *Profiles synthesis through radii variation of arcs profile.* Archives of Transport = Archiwum Transportu, Vol. 18, No. 3, pp. 37-56, ISSN 0866-9546.

[7] SUCHÁNEK, A. - HARUŠINEC, J. - LOULOVÁ, M. (2017): *The downhill braked railway wheel structural analysis.* Visnyk Schidnoukrajinskoho nacionaľnoho universytetu imeni Volodymyra Daľa: naukovyj žurnal, No. 4, No. 234, pp. 37-42, ISSN 1998-7927.

[8] SUCHÁNEK, A. - LOULOVÁ, M. - HARUŠINEC, J. (2017): *Evaluation of passenger riding comfort of a rail vehicle by means dynamic simulations.* 23rd Polish-Slovak scientific conference on machine modelling and simulations, London: Édition Diffusion Presse Sciences, pp. [1-10], ISSN 2261-236X.

[9] STRÁŽOVEC, P. - HARUŠINEC, J. - SUCHÁNEK, A. - KURČÍK, P (2018): *Hydrostatic powertrain of a mining locomotive* (In Slovak). Dynamics of rigid and deformable bodies 2018: proceedings, Ústí nad Labem, Univerzita J.E. Purkyně Ústí nad Labem, pp. 1-8, ISBN 978-80-7561-142-0.

Methods for evaluation of passengers' ride comfort in vehicles

Ján Dižo, Ing., PhD.*
Department of Transport and Handling Machines, Faculty of Mechanical Engineering,
University of Žilina.
Univerzitná 8215/1, 010 26 Žilina, Slovak Republic.
E-mail: jan.dizo@fstroj.uniza.sk, Tel.: + 421 41 513 2560

Miroslav Blatnický, Ing., PhD.
Department of Transport and Handling Machines, Faculty of Mechanical Engineering,
University of Žilina.
Univerzitná 8215/1, 010 26 Žilina, Slovak Republic.
E-mail: miroslav.blatnicky@fstroj.uniza.sk, Tel.: + 421 41 513 2570

Stanislav Semenov, Ing., PhD.
Department of Logistics and Traffic Safety, Educational and Scientific Institute of Transport and Building,
Volodymyr Dahl East Ukrainian National University.
Central Avenue 59A/303, 93400 Severodonetsk, Ukraine.
E-mail: semenov@snu.edu.ua

Evgeny Mikhailov, doc. Ing., PhD.
Department of Logistics and Traffic Safety, Educational and Scientific Institute of Transport and Building,
Volodymyr Dahl East Ukrainian National University.
Central Avenue 59A/303, 93400 Severodonetsk, Ukraine.
E-mail: mihajlov@snu.edu.ua

Abstract: Comfort for passengers in a vehicle is one of the most important issue when a vehicle is designed and evaluated. The contents of this article presents some methods, which are used for evaluation and assessment of the passengers ride comfort in vehicle, both for road and rail vehicles. The fundamentals of methods consist in evaluation of accelerations measured in given points. Accelerations signals are processed by the corresponding methods, filtered and finally, the ride comfort index is calculated. Resulted processed acceleration signals are compared with generalized values of accelerations. They were observed by tests.

INTRODUCTION

The ride comfort for passengers is one of the most important and investigated issue of the means of transport. It represents the complex term, which includes the set of components specifying heating, acoustic comfort, air quality, however mainly effects of vibration to passengers. Senses, which relates with ride comfort, depend on more factors, i. e. vibration – amplitude, frequency, time of exposition, etc. For evaluation of ride comfort of passengers in vehicles, ride comfort indices are used.

Although factors mentioned above have the significant effect on the ride comfort for passengers, vibration and shocks are crucial for it. They can even lead to very negative health problems.

Quantification of ride comfort is performed either by the direct method, i. e. by evaluation of ride comfort level on a real vehicle (road or railway vehicle) or by the indirect method, which is based on knowledge of accelerations in analyzed locations.

When vibrations act, some parts of a human body of the entire human body can vibrate. It depends on the way of transmission of vibration on a human organisms and on physical properties of vibrations (time-period and frequency). If the excitation frequency and natural frequency are closed to each other, some parts of a human body can resonate. It can lead to severe resonance phenomena. In case of the vertical vibration, natural frequencies of a human body are in the frequency range of 4 to 6 Hz. In this frequency range, not only thorax is exposed to the resonance, but also to resonance of vertebras and a stomach. For the horizontal direction of total vibration, resonance vibrations occur about frequency range of 1 to 3 Hz. Generally, a human body is able to withstand horizontal vibration (i. e. perpendicularly to a back bone) better than vibration in the vertical direction (i. e. parallel with a back bone). A dynamic model of a human body with marking of natural frequencies of individual parts is shown in Fig. 1.

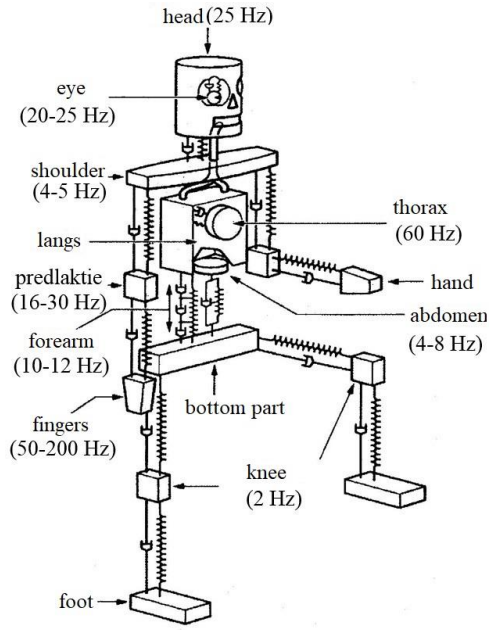

Fig. 1. A dynamic model of a human body

Accelerations acting to a human body during ride are the main parameter, based on which ride comfort for passengers relating to vibrations is determined and evaluated.

In primary studies focused on evaluation of vibrations acting on a passenger, limits of comfort related with influence of vibrations on a human body were considered in a frequency range of 1 to 12 Hz. Sperling later developed the method for evaluation of ride comfort for passengers. He has introduced the ride comfort index W_z. This index has been used for long time in Europe as the criteria of ride comfort for passengers.

1 DEFINITION OF PASSENGER RIDE COMFORT

The ride comfort for passenger is the entire sense, which is excited in a human body by vehicle body movements and they are transmitted to the entire human body through contact points. This sense is classified as:

- Average sense, which is influenced by vibrations acting during longer time interval (several minutes).
- Quasistatic lateral sense, which is evaluated during vehicle moving in a curve.
- Immediate sense, which is characterized by the instant change of the average sense due to short-time event.

Quantification of ride comfort of passengers is most often performed by the indirect method, i. e. measurement and processing of relevant data (accelerations of a vehicle body).

2 EVALUATION OF PASSENGER RIDE COMFORT BY THE WEIGHED METHODS

Evaluation of ride comfort for passenger by the spectral method consists in determining of effective values of accelerations $a_{j,rms}$ in third octave band (for horizontal and vertical direction) and their comparing for every band with limit values, which define boundaries of reduced comfort and of limit reduced performance in the ISO 2631-1:1985 standard. It defines limited values for effective accelerations in various directions x, y and z (Fig. 1).

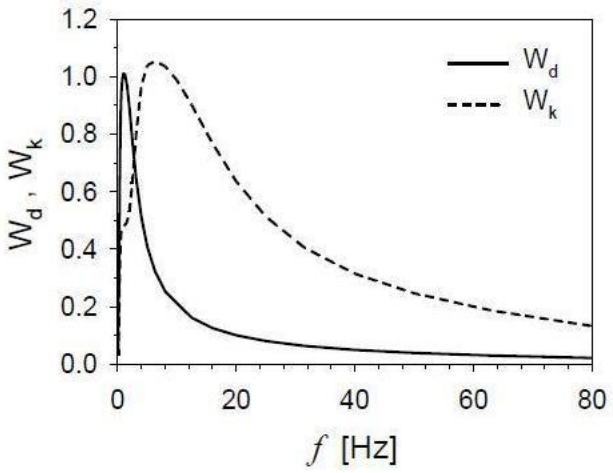

Fig. 1. Boundaries of reduced comfort (dash line), limit of reduced performance (solid line) for effective values of accelerations in the third octave band for horizontal direction

2.1 The method of the ISO standard

The method based on the ISO 2631 standard is the basic method for evaluation of vibration effect on a passenger during moving. This method consists in the spectral analysis of individual directions and comparing of effective values. It is necessary to calculate the modified weighed value of acceleration $a_{rms\text{-}w}$, which represents the synthetic ride comfort index. The effective value of the acceleration $a_{j,rms}$ in the third octave band is calculated as following:

$$a_{j,rms-w} = \sqrt{\sum_{i=1}^{n} \left[w_j(f_i) \cdot a_{j,rms}(f_i) \right]^2}, \quad j = x, y, z, \qquad (1)$$

where $w_j(f) = W_d(f)$ is identical for the x and y direction, $w_j(f) = W_k(f)$ is valid for the z direction.

The ISO standard recommends to include the third octave band with the middle frequency f_i within the frequency range of 1 to 80 Hz.

The value of the total weighed value of acceleration is calculated as following:

$$a_{rms-w} = \sqrt{a_{x,rms-w}^2 + a_{y,rms-w}^2 + a_{z,rms-w}^2}. \qquad (2)$$

This calculated value is compared with the scale in Tab. 1.

Tab. 1. The scale for evaluation of the ride comfort according to the ISO 2631

$a_{rms\text{-}w}$ [m·s^{-2}]	Ride comfort level
less than 0.315	comfortable
0.315 to 0.63	less comfortable
0.50 to 1.00	uncomfortable
0.80 to 1.60	quite uncomfortable
1.25 to 2.50	very uncomfortable
more than 2.00	extremely uncomfortable

2.2 The method based on the EN standard

Evaluation of the ride comfort by means of the EN 12299 standard is based on the indirect method. Movements of the vehicle body is measured by means of accelerometers located in a vehicle in the required locations.

This method is most often used for evaluation of ride comfort for passengers in a rail vehicle. A human body is exposed in a rail vehicle to vibrations, which are transmitted to a human organism by contact points (Fig. 2):

- In standing position.
- In seating position.

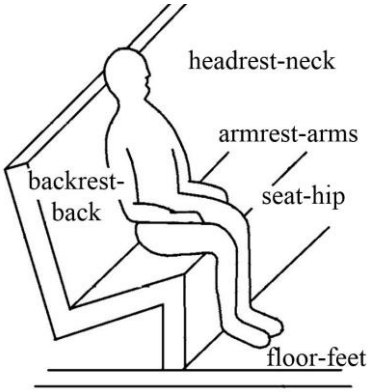

Fig. 2. Contact points

The calculation of the ride comfort includes values of measured accelerations in individual directions a_x, a_y a a_z (for ride comfort indices N_{MV}, N_{VA}, N_{VD}, P_{CT}, P_{DE}) or velocity of a wagon body yaw (for the index P_{CT}).

2.3 Average comfort – standard method N_{MV}

Average comfort is calculated by the standard method and it is marked by the N_{MV} index. It qualifies the ride comfort index on the floor for a seating passenger. It is necessary to know values of accelerations in the longitudinal x, lateral y and vertical z direction for evaluation. Values of accelerations are frequency weighed by the weighted functions W_b and W_d (Fig. 3) in the frequency range of 0.4 to 100 Hz.

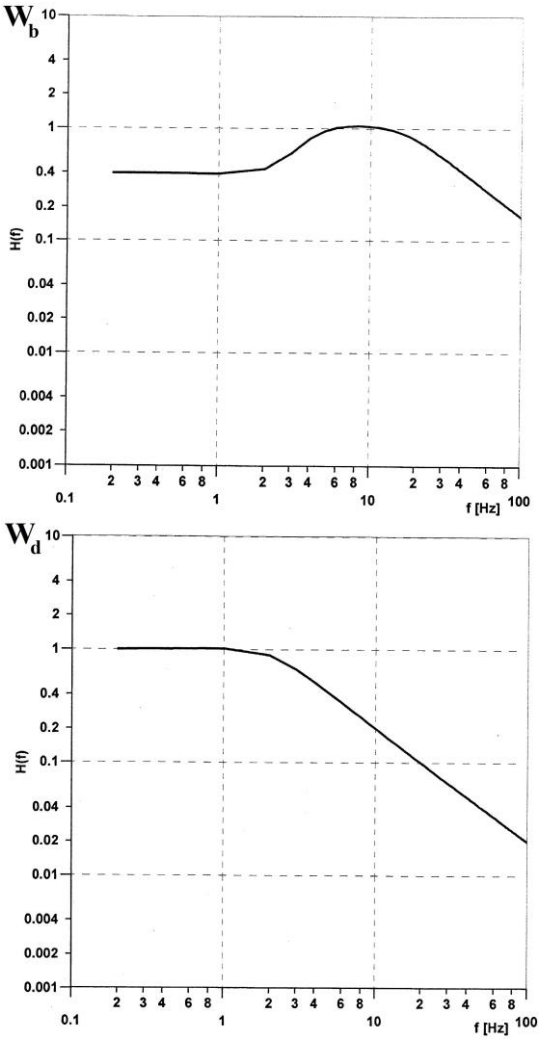

Fig. 3. Weighed functions W_b and W_d

The average quadratic values of these accelerations are calculated as following:

$$a_{j\eta}^{Wi}(t) = \sqrt{\frac{1}{T} \cdot \int_{t-T}^{T} \left[\ddot{x}_{W_i}^{*}(\tau) \right]^2 \cdot d\tau}, \quad j = x, y, z, \qquad (2)$$

where T = 5 s and it is a multiple of 5 s.

Modified accelerations values is statistically evaluated in corresponded directions and sum functions are determined in histograms. Finally, there are determined 95-percetiles of distribution function in 5-second weighed average quadratic values calculated in time period of 5 min. The procedure of processing of acceleration signals and calculation of the N_{MV} ride comfort index is shown in Fig. 4.

The resulting value of the average ride comfort index for passenger on the wagon floor N_{MV} is:

$$N_{MV} = 6 \cdot \sqrt{\left(a_{xP95}^{W_d}\right)^2 + \left(a_{yP95}^{W_d}\right)^2 + \left(a_{zP95}^{W_b}\right)^2}. \qquad (3)$$

The calculated ride comfort index is compare with the scale in Tab. 2.

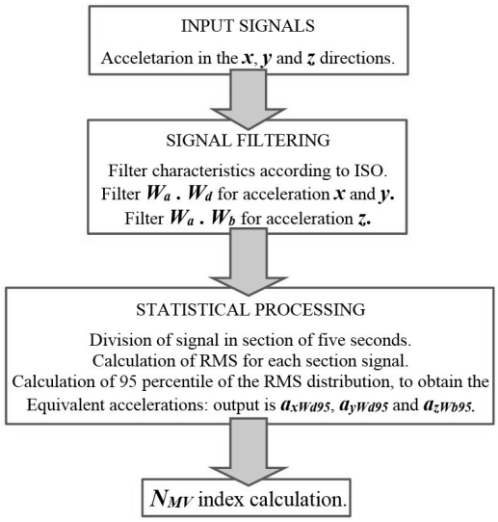

Fig. 4. Procedure of processing and calculation of ride comfort index

Tab. 2. The scale for evaluation of the ride comfort index N_{MV} according to the EN 12299 standard

Value of N_{MV}	Ride comfort level
$N_{MV} < 1.5$	very comfortable
$1.5 \le N_{MV} < 2.5$	comfortable
$2.5 \le N_{MV} < 3.5$	average comfortable
$3.5 \le N_{MV} < 4.5$	uncomfortable
$N_{MV} \ge 4.5$	very uncomfortable

Evaluation of ride comfort by the EN method is very similar to the ISO standard. The problem of the N_{MV} method is, that the calculated index of ride comfort is not possible to assign to particular vehicle position on a track and to corresponding track irregularities.

2.4 Average comfort – complete method N_{VA}, N_{VD}

Complete methods N_{VA} and N_{VD} quantify comfort during continuous five-minute running of a rail vehicle.

The N_{VA} method is based on measurements of accelerations not only on a floor in the vertical direction, but also in contact points between a seating passenger body and a seat in the lateral direction and in the vertical direction as well as in the longitudinal direction. By this reason, this method is more difficult both for real tests on a rail vehicle and for computer simulations. For calculation of ride comfort, the 95-percentile is used and its value is determined by the relation:

$$N_{VA} = 4 \cdot a_{zP95}^{W_b} + 2 \cdot \sqrt{\left(a_{yP95}^{W_d}\right)^2 + \left(a_{zP95}^{W_b}\right)^2} + \\ +4 \cdot a_{xP95}^{W_c}. \quad (4)$$

For values of accelerations in the x direction, the weighed function W_c is applied (Fig. 5).

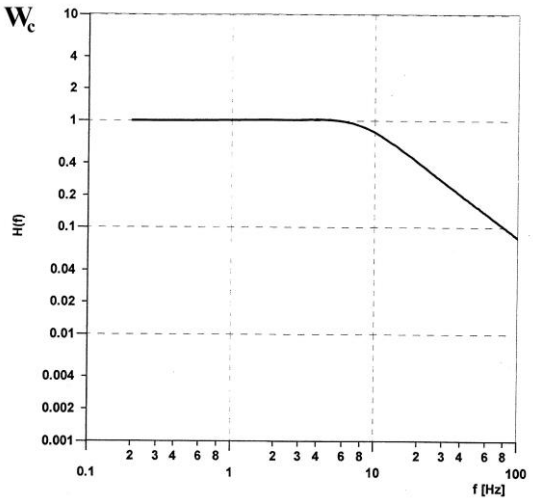

Fig. 5. Weighed functions W_c

The N_{VD} method is used for evaluation of ride comfort for a standing passenger. Accelerations are measured only on a floor. A calculation of ride comfort is based on determination of 50-percetil of measured accelerations in all three directions (x, y and z) and 95-percetile in the lateral direction (y). The calculation formula is as following:

$$N_{VD} = 3 \cdot \sqrt{16 \cdot \left(a_{xP50}^{W_d}\right)^2 + 4 \cdot \left(a_{yP50}^{W_d}\right)^2 + \left(a_{zP50}^{W_b}\right)^2} + \\ +5 \cdot a_{yP95}^{W_d}. \quad (5)$$

Both complete methods for evaluation of average ride comfort are characterized, that there is not possible to assign the calculated values N_{VA} and N_{VD} to particular position of a rail vehicle in a track.

2.5 Continuous comfort, C_{Cx}, C_{Cy} and C_{Cz} methods

As the N_{MV} method uses 95-percentle of measured acceleration signals for ride comfort indices calculation, many information related with level of vibrations are lost. Therefore, the standard suggests to take into account all effective values of accelerations in five-second intervals.

Tab. 3. The scale for evaluation of the ride comfort index $C_{Cy}(t)$ and $C_{Cz}(t)$

Value of comfort indices [m·s^{-2}]	Ride comfort level
$C_{Cy}(t)$, $C_{Cz}(t) < 0.20$	very comfortable
$0.20 \le C_{Cy}(t)$, $C_{Cz}(t) < 0.30$	comfortable
$0.30 \le C_{Cy}(t)$, $C_{Cz}(t) < 0.40$	average comfortable
$C_{Cy}(t)$, $C_{Cz}(t) > 0.40$	uncomfortable

This way would allow to perform other analyses and their comparison with results of measurements of rail vehicle vibrations. These five-second effective

values of accelerations define time series for *x*, *y* and *z* directions, which are marked as C_{Cx}, C_{Cy} and C_{Cz}.

2.6 Comfort in curves, P_{CT} method

The method of ride comfort for passengers during rail vehicle running in curves P_{CT} is used, when a number and shape of transverse track sections can significantly affect the comfort sense. There is observed, that a passenger is exposed to lower comfort level, when a rail vehicle enters a curve track section as well as values of accelerations in the lateral direction are higher, when a rail vehicle runs through multiple curves. Moreover, there has been observed, that lover comfort level relates with the maximal lateral acceleration, maximal lateral jerk as well as with the maximal angular velocity of a rail vehicle body.

The comfort index is calculated by means of following equation, while the member in squares is taken in consideration, when its value is higher or equals to nought:

$$P_{CT} = \left(A \cdot \ddot{y} + B \cdot \dddot{y} - C\right) + D \cdot \dot{\varphi}^{E}, \tag{6}$$

where $\ddot{y}$ is a maximal value of the lateral acceleration of a rail vehicle in the interval of entering a curve to its end, the value 1.6 s is added to it,

$\dddot{y}$ is a maximal value of jerk evaluated as the maximal deviation of two values of lateral acceleration in a row in the time interval beginning one second before entering a curve or an opposite curve until its end,

$\dot{\varphi}$ is a maximal value of an angular velocity of a rail vehicle body measured one tenth of a second before entering a curve until its end,

A, *B*, *C*, *D* and *E* are values of coefficients introduced in the standard.

A higher value of the calculated ride comfort index always means lower ride comfort level.

For evaluation of ride comfort, it is necessary to obtain values of lateral accelerations in a rail vehicle body and its angular velocity, at which, the vehicle movement must take at least two second in the prescribed section.

2.7 Comfort at the discrete events, P_{DE} method

This method is based on the British standard. Ride is evaluated during tests according to the following scale:

- Very comfortable.
- Comfortable.
- Average comfortable.
- Uncomfortable.
- Very uncomfortable.

There has been found out, that the ride comfort level is decreased during running on a track with large irregularities and curves transitions. Two variables are evaluated:

Average lateral accelerations (due a track curvature and a track inclination).

Value of the lateral acceleration obtained by the method of peak addition.

Ride comfort is evaluated for both a standing and seating person.

The ride comfort index P_{DE} for discrete events is calculated by means on following formulation:

$$P_{DE} = A \cdot \ddot{y}_P + B \cdot \ddot{y}_M - C, \tag{7}$$

where $\ddot{y}_P$ is a difference between a maximal and a minimal value measured in the time interval of two seconds, while the low pass filter W_d with the minimal frequency of 10 Hz is used,

$\ddot{y}_M$ is an average value of as acceleration signal $\ddot{y}$ filtered by the low pass filter in the same time interval of two seconds,

A, *B* and *C* are values of coefficients introduced in the standard.

The value of the PDE index represents percentage of passengers, who evaluate the ride as uncomfortable or very uncomfortable.

CONCLUSION

Analysing of passengers ride comfort is still actual topic. Subjective sense of comfort, which a passenger feels in during travelling in a vehicle, often influences choice of a transport mean. In case of evaluation of passenger ride comfort by means of simulation computations, an indirect method is used. It consists in measuring and identification of accelerations in corresponding locations. Processed and calculated values of the resulting acceleration signals give the ride comfort index. Finally, them are compared with values in scales.

The first official method focused on the effect of vibrations on a human body, the ISO 2631 standard was. It substituted the W_z criteria. The ISO standard defines the average comfort for passengers based on total effective value of acceleration, which is weighed in the frequency range by using weighed functions.

Because of various methods and ambiguous adopting of weighed functions, the European Committee for

Standardisation has established the standard for evaluation of passengers ride comfort.

Acknowledgment

This work was supported by the Cultural and Educational Grant Agency of the Ministry of Education of the Slovak Republic in the project No. KEGA 023ŽU-4/2020: Development of advanced virtual models for studying and investigation of transport means operation characteristics.

The work was supported by the Slovak Research and Development Agency of the Ministry of Education, science, Research and Sport of the Slovak Republic in Educational Grant Agency of the Ministry of Education of the Slovak Republic in the project No. VEGA 1/0558/18: Research of the interaction of a braked railway wheelset and track in simulated operational conditions of a vehicle running in a track on the test bench.

REFERENCES

[1] KARDAS-CINAL, E. (2010): *Ride comfort for various passenger positions in a railway vehicle - Simulation study*. Archives of Transport, Vol. 22, No. 2, pp. 189-199, ISSN 0866-9546.

[2] SPERLING, E. - BETZHOLD, C. (1957): *Contribution to evaluation of comfortable running of railway vehicles*. Bulletin of the International Railway Congress Association.

[3] ISO 2631–1 (1985 and 1997): *Mechanical vibration and shock. Evaluation of human exposure to whole-body vibration*. Part 1: General Requirements. International Organization for Standardization.

[4] KARDAS-CINAL, E. (2006): *Analysis of ride comfort ans safety of a railway vehicle*. Proceedings of the Institute of Vehicles [online], Vol. 60, No. 1, 45-52, ISSN 1642-347X.

[5] UIC 513R (1994): *Guidelines for evaluating passenger comfort in relation to vibration in railway vehicles*. International Union of Railways.

[6] EN 12299 (2009): *Railway applications. Ride comfort for passengers. Measurement and evaluation*, Comite Europeeen de Normalisation.

[7] LACK, T. - GERLICI, J. (2007): *Vehicles dynamical properties analysis from the point of view of comfort for passengers*. Archives of Transport, Vol. 19, No. 1-2, pp. 91-110, ISSN 0866-9546.

[8] BS 6841 (1985): *Guide to measurement and evaluation of human exposure to whole-body mechanical vibration and repeated shock*. British Standard Institution, London.

[10] DIŽO, J. - GERLICI, J. - LACK, T. (2013): *The passenegr car ride comfort assessment by means of ADAMS/Rail software utilization*. TRANSCOM 2013: 10th European conference of young researchers and scientists, Žilina: University of Žilina, pp. 67-70, ISBN 978-80-554-0695-4.

[11] DIŽO, J. - BLATNICKÝ, M. (2017): *Assessment of passenger ride comfort of rail vehicle running using simulation tools*. Dynamical problems in rail vehicles 2017: Slovak-Polish Scientific Workshop, Žilina: University of Žilina, pp. 8-17, ISBN 978-80-554-1347-1.

[12] LOULOVÁ, M. – SUCHÁNEK, A. – HARUŠINEC, J. (2017): *Evaluation of the parameters affecting passenger riding comfort of a rail vehicle*. Manufacturing Technology, Vol. 17, No. 2, 224-231, ISSN 1213-2489.

[13] ŠŤASTNIAK, P. (2015): *Freight long wagon dynamic analysis in S-curve by means of computer simulation*. Manufacturing technology: journal for science, research and production, Vol. 15, No. 5, 930-935, ISSN 1213-2489.

[14] GERLICI, J. - GORBUNOV, M. - NOZHENKO, O. - PISTEK, V. - KARA, S. - LACK, T. - KRAVCHENKO. K. (2017): *About creation of bogie of the freight car*. Communications – Scientific Letters of the University of Zilina, Vol. 19, No. 2, pp. 29-35, ISSN 1335-4205.

[15] LACK, T. - GERLICI, J. - HARUŠINEC, J. (2007): *Accurate calculation of contact stresses of railway wheel/rail contact* (In Slovak). Dynamics of rigid and deformable bodies 2007, Proceedings of the 5th international conference, Ústí nad Labem, Fakulta výrobních technologií a managementu, Univerzta Jana Evangelity Purkyně, pp. 127-136, ISBN 978-80-7044-914-1.

[16] GERLICI, J. - LACK, T. - ŠŤASTNIAK, P. (2019): *Wheelset/rail geometric characteristics and contact forces assessment with regard to angle of attack*. 23rd Polish-Slovak scientific conference on machine modelling and simulations, Londýn: Édition Diffusion Presse Sciences, pp. 1-8, ISSN 2261-236X.

[17] SUCHÁNEK, A. - HARUŠINEC, J. - LOULOVÁ, M. - KURČÍK, P. (2018): *Proposal of stiffness of triple spring of a passenger railway vehicle*. Horizons of Railway Transport 2018, Londýn: Édition Diffusion Presse Sciences, pp. 1-5, ISSN 2261-236X.

[18] VLK, F. (2003): *Dynamics of engine vehicles* (In Czech). Brno: Nakladatelství a vydavatelství František Vlk, ISBN 80-239-0024-2.

PRÍSPEVKY V SLOVENSKOM JAZYKU

ARTICLES IN THE SLOVAK LANGUAGE

Simulácia dilatácie potrubia pomocou experimentálneho zariadenia

Juraj Drga, Ing.*
Katedra energetickej techniky, Strojnícka fakulta,
Žilinská univerzita v Žiline
Univerzitná 1, 010 26 Žilina, Slovenská republika.
E-mail: juraj.drga@fstroj.uniza.sk, Tel.: +421 41 513 2860

Michal Holubčík, doc. Ing., PhD.
Katedra energetickej techniky, Strojnícka fakulta,
Žilinská univerzita v Žiline
Univerzitná 1, 010 26 Žilina, Slovenská Republika.
E-mail: michal.holubčík@fstroj.uniza.sk, Tel.: +421 41 513 2855

Stanislav Gavlas, Ing., PhD.
Katedra energetickej techniky, Strojnícka fakulta,
Žilinská univerzita v Žiline
Univerzitná 1, 010 26 Žilina, Slovenská republika.
E-mail: stanislav.gavlas@fstroj.uniza.sk, Tel.: +421 41 513 2853

Simulation of pipeline expansion by an experimental device

Abstract: The essence of this article was the design of an experimental device, which has the task of simulating the effect of thermal expansion on the proposed compensating elements of selected materials. This device will later be constructed and used at the Department of Power Engineering at the University of Žilina, as a teaching aid. The calculations in the article were processed in the form of numerical calculations of selected compensation sections and calculations performed in the calculation program CAE Pipe.

ÚVOD

Tepelná dilatácia zapríčiňuje vznik napätí, ktoré môžu eskalovať k prekročeniu dovoleného napätia potrubného materiálu. Sila, ktorá vzniká ako tlaková sila pri dilatácii a ťahová pri zmršťovaní materiálu, je rovnako namáhavá pre spoje a uloženia potrubia. Preto je veľmi dôležité tepelnú dilatáciu potrubia vyrovnávať buď vlastnou pružnosťou potrubia alebo kompenzátormi [1]. Návrh potrubnej siete musí okrem toho pozostávať z výpočtov hrúbky steny rúry a dovoleného napätia potrubia, pričom sa jedná o komplexné výpočty zahŕňajúce v sebe vplyvy zaťažovacích stavov, prevádzkových podmienok, vlastností použitých materiálov, a pod. [2]. Téme dilatácie potrubia sa venovalo už množstvo prác, pričom najčastejšie sa zaoberali návrhom potrubnej trasy, vplyvmi tepelnej dilatácie na potrubnú sieť, skúmaním tepelnej rozťažnosti rôznych materiálov, prípadne aj dilatáciou potrubia na naše pomery v nekonvenčných podmienkach [3-5].

Riešenie práce spočívalo v návrhu experimentálneho zariadenia na simuláciu dilatácie potrubia a jeho možných variant, ktoré bude slúžiť ako učebná pomôcka pri výučbe danej problematiky. Inšpirácia autorov z hľadiska vypracovania práce pramenila z princípu spracovania práce o využití tepelných trubíc na prenos tepla zo spalinového priestoru [6]. Použité kompenzačné prvky v experimentálnom zariadení predstavovali tri druhy prirodzeného kompenzátora („L“ kompenzátor, „Z“ kompenzátor a „U“ kompenzátor) a jeden variant axiálneho vlnovcového kompenzátora. Prirodzené kompenzátory boli navrhované pre 3 druhy materiálov (pozinkovaná oceľ, polyetylén a meď), pre variant s axiálnym vlnovcovým kompenzátorom sa uvažovalo potrubie z pozinkovanej ocele. Pre všetky varianty kompenzátorov sa uvažovalo s výpočtovou dĺžkou dilatačného úseku 2 m. Výpočty v práci boli rozdelené do dvoch častí na numerické výpočty, založené na základných vzťahoch pre definovanie dilatačných posunov a k nim prislúchajúcich rozmerov daných kompenzačných prvkov, a výpočty vykonané vo výpočtovom programe CAE Pipe, pre získanie presnejších údajov o dilatačných posunoch, veľkostiach síl na pevné body a napätiach pôsobiacich na potrubné úseky. Hlbšej analýze pôsobenia napätí na potrubie sa nevenovala pozornosť. Ak by boli kladené nároky na skúmanie potencionálnych deformácií potrubia, v kontexte práce by takéto riešenie mohlo pôsobiť kontra-produktívne, v dôsledku komplikovanosti

celého procesu a účelu práce [7]. Výhodu programového prostredia CAE Pipe predstavovala možnosť získania daných údajov v rôznych zaťažovacích stavoch. Pre potreby práce sa uvažovalo so zaťažovacími stavmi vplyvom vlastnej tiaže potrubia (Empty weight - W1), vplyvom teploty (Expansion - T1) a vplyvom hmotnosti, pretlaku a teploty (Operating – W1+P1+T1).

1 EXPERIMENTÁLNE ZARIADENIE

Obrázok 1 znázorňuje blokovú schému navrhovaného zariadenia, ktoré bude pozostávať z:

1. Regulačnej jednotky JULABO na reguláciu teploty cirkulujúcej vody.
2. Meracej ústredne na snímanie povrchovej teploty potrubia pomocou kontaktného snímača teploty.
3. Počítača na spracovanie a vyhodnotenie údajov z meracej ústredne.
4. Z prirodzeného, resp. axiálneho kompenzátora, na ktorých sa budú simulovať vplyvy tepelnej dilatácie. Tieto budú tvoriť komplexné kompenzačné úseky, ktoré budú obsahovať doplňujúce prvky ako manometer, odvzdušňovací ventil, meradlá na vizuálne odčítanie dilatačných posunov, pevné body a klzné uloženia pre uloženie dilatačného úseku na tabuli so stojanom.

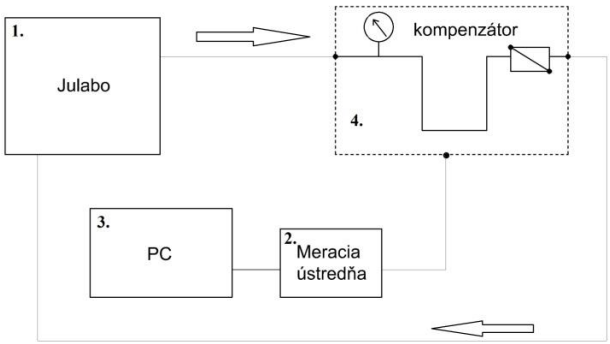

Obr. 1. Bloková schéma experimentálneho zariadenia

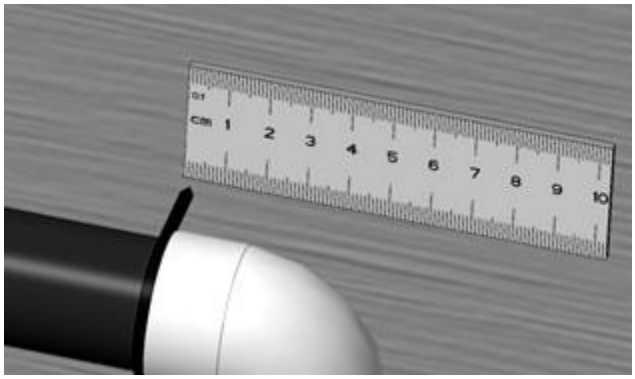

Obr. 2. Detail meradla

Na obr. 3 je zobrazený 3D model navrhovaného zariadenia vo variante s prirodzeným „U“ kompenzátorom. Julabo FP35-HL predstavuje vykurovacie obehové čerpadlo s rozsahom pracovných teplôt - 35 °C až +150 °C, s vykurovacou kapacitou 2 kW. To bude spojené s vetvou kompenzačného úseku pomocou flexibilných hadíc na vodu, ako prívod a odvod cirkulujúcej vody. Meracia ústredňa bude slúžiť na snímanie povrchovej teploty potrubia cez vstup pre kontaktný snímač Pt100. Úlohu odvzdušňovania okruhu bude vykonávať odvzdušňovací ventil DISCALSLIM Caleffi pre horizontálne potrubia, s maximálnym prevádzkovým tlakom 5bar a teplotou 110 °C. Veľkosť dĺžkových zmien v dilatačných úsekoch bude znázornená pomocou rysky umiestnenej na konci úseku a dĺžkového meradla (obr. 2).

2 NUMERICKÉ VÝPOČTY

V časti numerických výpočtov boli vykonané výpočty dilatácií jednotlivých materiálov pre potrubia s dĺžkou 2 m, spolu s výpočtami rozmerov prirodzených kompenzátorov „U“, „Z“ a „L“.

Pri výpočte tepelnej dilatácie sa vychádzalo zo základného vzťahu [8]:

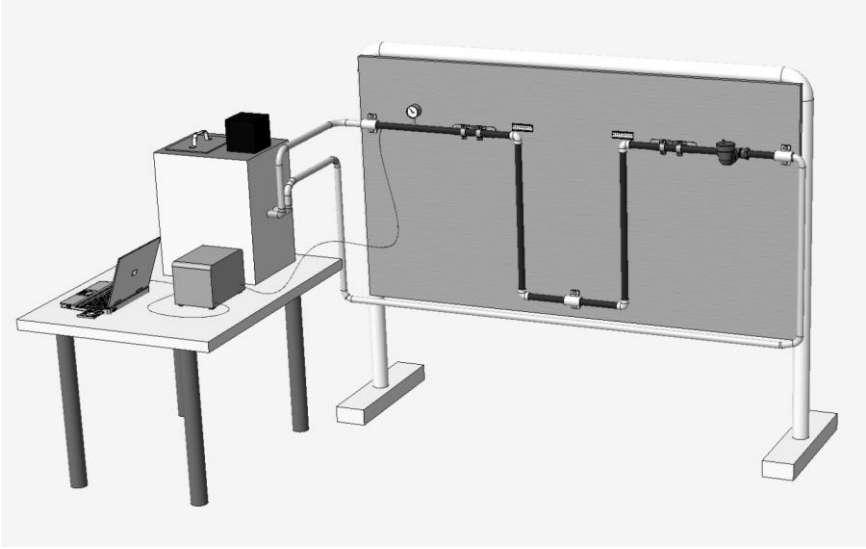

Obr. 2. 3D model experimentálneho zariadenia – „U“ kompenzátor

$$\Delta L = L \cdot \alpha \cdot \Delta T \text{ [mm]} \quad (1)$$

Pre súčiniteľ teplotnej rozťažnosti α sa uvažovalo s hodnotami zobrazenými v tab. 1.

Tab. 1. Hodnoty súčiniteľov teplotnej rozťažnosti

Materiál	Súčiniteľ teplotnej rozťažnosti [K^{-1}]
oceľ	$1{,}2 \cdot 10^{-5}$
meď	$1{,}8 \cdot 10^{-5}$
PE	$18 \cdot 10^{-5}$

Pri výpočtoch rozmerov prirodzených kompenzátorov sa vychádzalo zo vzťahu pre výpočet dĺžky voľného ramena, zároveň jednotlivé označenia rozmerov sú objasnené na obr. 4 [8]:

$$L_1 = C \cdot \sqrt{D \cdot \Delta T} \quad \text{[mm]} \quad (2)$$

$$L_U \geq \frac{L_1}{2} \quad \text{[mm]} \quad (3)$$

Získané rozmery kompenzačného ramena sú znázornené v tab. 3, pre tri druhy materiálov pri

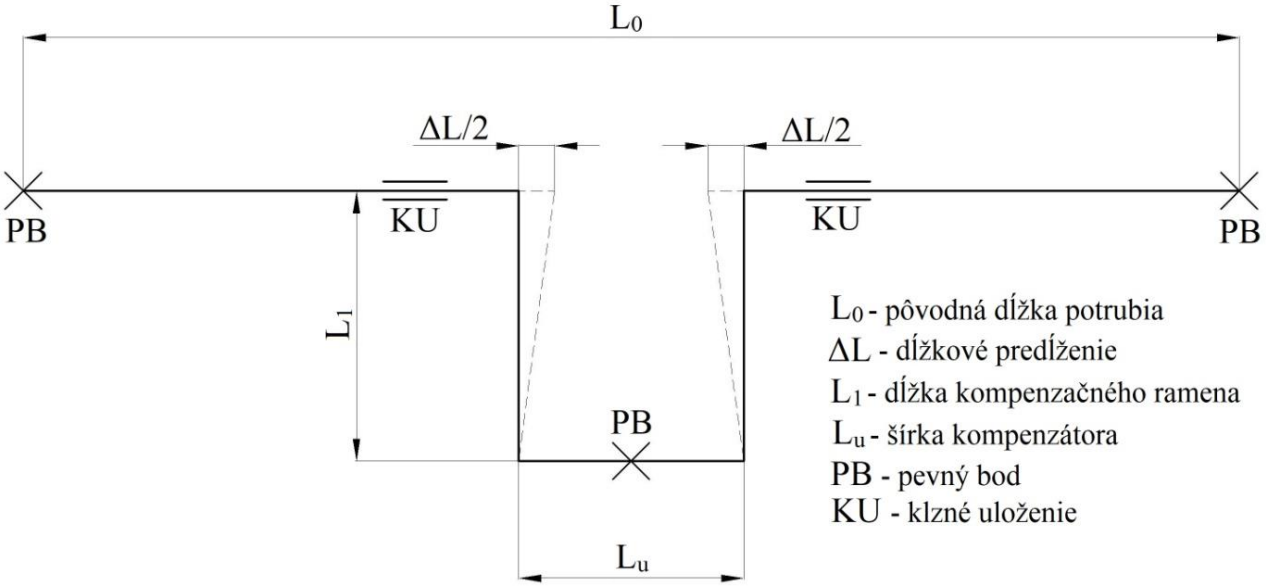

Obr. 4. Rozmery „U“ kompenzátora

Pre účely tohto článku bol zo všetkých uvažovaných kompenzátorov vybraný variant „U“ kompenzátora ako príklad, keďže princíp výpočtov prirodzených kompenzátorov bol totožný vo všetkých vybraných typoch. Pre tieto typy kompenzátorov sa počítalo s vonkajším priemerom potrubia D = 32 mm.

Pomocou spomínaného vzťahu (1) boli vypočítané dĺžkové predĺženia potrubia s dĺžkou 2 m, pri rôznych teplotných zmenách. V práci sa neskôr pri návrhoch zariadenia a výpočtoch v programovom prostredí CAE Pipe uvažovalo s teplotnou zmenou ΔT = 50 *K*. Získané výsledky teplotných predĺžení sú znázornené v tab. 2.

Tab. 2. Teplotné predĺženie pre rúry 2 m

ΔL pre 2 m potrubia [mm]	PE	Oceľ	Meď
ΔT = 10 K	3,6	0,24	0,36
ΔT = 20 K	7,2	0,48	0,72
ΔT = 30 K	10,8	0,72	1,08
ΔT = 40 K	14,4	0,96	1,44
ΔT = 50 K	18	1,2	1,8

rôznych teplotných zmenách.

Veľkosť kompenzačného ramena závisí od mechanických vlastností použitých materiálov, ako aj od hodnoty súčiniteľa teplotnej rozťažnosti. Čím vyššiu hodnotu vykazuje, tým sa kladú väčšie priestorové nároky na konštrukciu prirodzeného kompenzátora, čo vyplýva aj z tab. 3.

Tab. 3. Rozmery kompenzačného ramena L_1

L_1 [mm]	PE	Oceľ	Meď
ΔT = 10 K	290	100	54
ΔT = 20 K	410	141	77
ΔT = 30 K	502	173	94
ΔT = 40 K	580	200	109
ΔT = 50 K	648	223	121

3 ANALÝZA VÝPOČTOV V PROGRAME CAE PIPE

Získané návrhy kompenzačných prvkov z numerických výpočtov boli zadávané ako modely do výpočtového programu CAE Pipe. Pre potreby práce sa pracovalo s programovou verziou CAE Pipe

EVAL 10.10 (študentská verzia voľne dostupná na: <https://www.sstusa.com/piping-software-download.php>). Tá v dostatočnej miere ponúkla možnosť analýzy dilatačných posunov prirodzených kompenzátorov a veľkosti síl na pevné body, v zaťažovacích stavoch:

- Empty weight (W1) – vplyvom vlastnej tiaže potrubia.
- Expansion (T1) – vplyvom teploty.
- Operating (W1+P1+T1) – vplyvom tiaže, tlaku a teploty.

Pri axiálnom kompenzátore sa skúmali sily na pevné body spolu so stlačením kompenzátora, pričom účinky kompenzátora na potrubný úsek boli porovnávané s rovnou vetvou potrubia s dĺžkou 2m bez kompenzátora, uloženou pomocou dvoch pevných bodov.

Tab. 4. Použité materiály a vstupné údaje výpočtov

	PE	Pozinkovaná oceľ	Meď
Materiál	EN 15494	EN 1.0425 (P265GH)	EN 1057
Prac. teplota	65 °C		
Prac. tlak	5 bar		

Obrázok 5 znázorňuje animáciu dilatácie jednoduchého potrubného úseku „U“ kompenzátora, uloženého pomocou troch pevných bodov a dvoch osových vedení. Analýza bola vykonaná na základe vstupných údajov a materiálov podľa tab. 4.

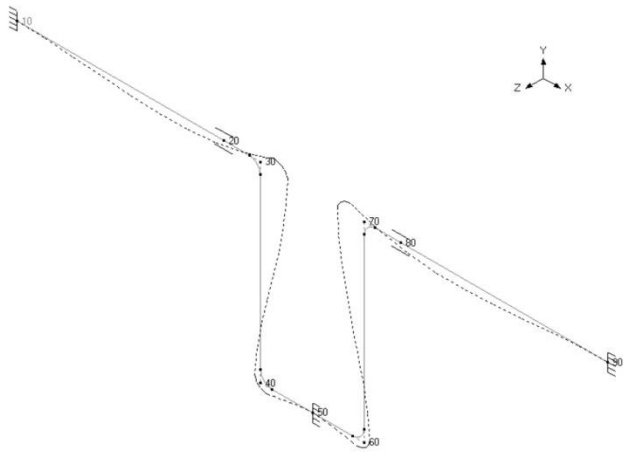

Obr. 5. Dilatácia potrubného úseku

Výsledky dilatačných posunov a uhlových vychýlení v sebe zahŕňali hodnoty nadobudnuté v troch rovinách *X*, *Y*, *Z*, čo dodalo výsledkom reálnejšiu predstavu o správaní sa potrubného úseku v praxi, vplyvom rôznych zaťažovacích stavov.

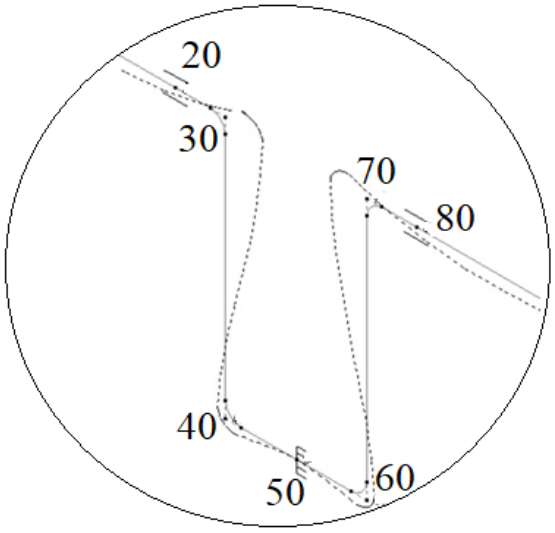

Obr. 6. Detail „U“ kompenzátora

Na obr. 6 je znázornený detail ohybov „U“ kompenzátora z obr. 5, ktoré podľa predpokladov vykazovali najväčšie hodnoty dilatačných posunov. Jednotlivé označenia prvkov potrubného úseku prislúchajú k označeniam vyjadreným v tab. 5, ktorá obsahuje maximálne hodnoty posunov v osi *X* a *Y* [mm], a hodnoty uhlových vychýlení [°] pre materiály PE, pozinkovaná oceľ a meď, v troch zvolených zaťažujúcich stavoch.

Tab. 5. Hodnoty maximálnych posunov a uhlových vychýlení

	Uzol	*FX* [N]	*FY* [N]	*MZ* [Nm]
PE	**10**	-16	-10	-2
	50	0	-165	0
	90	16	-10	2
OCEĽ	**Uzol**	***FX* [N]**	***FY* [N]**	***MZ* [Nm]**
	10	-670	-79	-20
	50	0	-1945	0
	90	670	-79	20
MEĎ	**Uzol**	***FX* [N]**	***FY* [N]**	***MZ* [Nm]**
	10	-1447	-56	-14
	50	125	-1458	1
	90	1322	-51	13

Tabuľka 6 obsahuje výsledné hodnoty síl na pevné body pre materiály PE, pozinkovaná oceľ a meď, v zaťažujúcom stave Operating.

Pri porovnaní dosiahnutých výsledkov dilatácií numerickým výpočtom a výpočtom v programe, hodnoty vykazujú značnú odchýlku. Je to spôsobené najmä tým, že výpočtový program CAE Pipe počítal s reálnymi podmienkami zaťažovacích stavov a namáhaniami vo všetkých smeroch, tzn. s axiálnym a laterálnym zaťažením potrubného úseku.

Rozloženia napätí pôsobiacich na jednotlivé potrubné úseky sú znázornené na obr. 7, 8 a 9. Najväčšie hodnoty vykazovalo potrubie z ocele a naopak najnižšie potrubie z PE, pre svoje dobré elastické vlastnosti. Nevýhodou tohto druhu potrubia však je veľká miera teplotnej rozťažnosti a s ňou spojené priestorové nároky na uloženie potrubia, resp. kompenzáciu dilatácie.

Tab. 6. Veľkosti síl na pevné body v zaťažovacom stave Operating

PE		Empty weight (W1)		Expansion (T1)		Operating (W1+P1+T1)	
		#	Hodnota	#	Hodnota	#	Hodnota
X [mm]	Min	30	-0,010	70	-6,890	70	-6,880
	Max	70	0,010	30	6,890	30	6,880
Y [mm]	Min	40	-0,033	60	-1,720	60	-1,753
	Max	10	0,000	30	2,647	30	2,614
ZZ [°]	Min	30	-0,016	70	-1,381	70	-1,365
	Max	70	0,016	30	1,381	30	1,365
OCEĽ		**Empty weight (W1)**		**Expansion (T1)**		**Operating (W1+P1+T1)**	
		#	Hodnota	#	Hodnota	#	Hodnota
X [mm]	Min	30	0,000	70	-0,464	70	-0,464
	Max	70	0,000	30	0,464	30	0,464
Y [mm]	Min	10	0,000	60	-0,004	60	0,000
	Max	30	0,000	30	0,141	30	0,141
ZZ [°]	Min	80	0,000	40	-0,154	40	-0,154
	Max	20	0,000	60	0,154	60	0,154
MEĎ		**Empty weight (W1)**		**Expansion (T1)**		**Operating (W1+P1+T1)**	
		#	Hodnota	#	Hodnota	#	Hodnota
X [mm]	Min	30	0,000	70	-0,656	70	-0,656
	Max	30	0,000	30	0,645	30	0,646
Y [mm]	Min	10	0,000	10	0,000	10	0,000
	Max	30	0,000	30	0,206	30	0,206
ZZ [°]	Min	80	-0,001	30	-0,369	30	-0,369
	Max	20	0,001	70	0,359	70	0,359

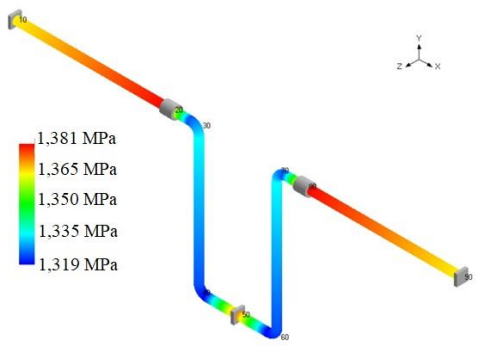

Obr. 7. Rozloženie napätí v potrubí z PE

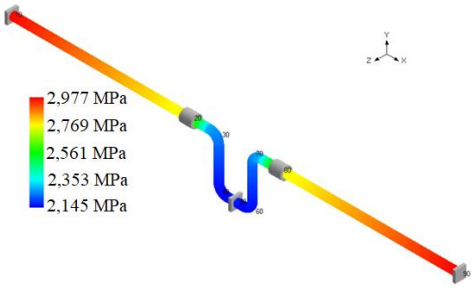

Obr. 8. Rozloženie napätí v potrubí z ocele

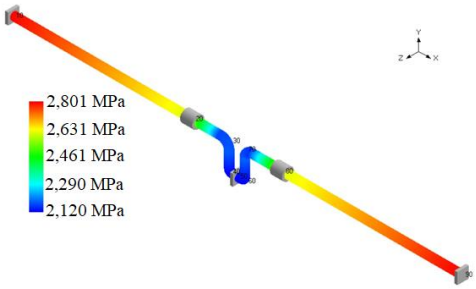

Obr. 9. Rozloženie napätí v potrubí z medi

ZÁVER

Aj keď je otázka dilatácie potrubia v praxi dlhodobo komplexne objasnená, dá sa o navrhovanom experimentálnom zariadení tvrdiť, že ako učebná pomôcka na akademickej pôde splní svoj účel. Študenti budú môcť vďaka tomuto zariadeniu pozorovať vplyv tepelnej dilatácie na potrubnú sústavu a analyzovať jej správanie pri rôznych simulovaných podmienkach. Ako najvhodnejší variant spomedzi navrhovaných v práci sa javí zariadenie s prirodzenými kompenzátormi z PE, pre vysokú mieru tepelnej rozťažnosti materiálu v porovnaní s oceľou alebo meďou. To umožní pozorovateľom vidieť zmeny dĺžkových rozmerov potrubia aj voľným okom. Vďaka takej skúsenosti sa môžu ich nadobudnuté vedomosti viac prehĺbiť a pre tých, ktorých daná téma osloví, sa otvárajú ďalšie možnosti v podobe zdokonaľovania sa vo výpočtových programoch pre danú problematiku, ako napríklad program CAE Pipe využitý v tejto práci.

ZOZNAM SKRATIEK A ZNAČIEK

A_0	efektívna plocha kompenzátora	[m^{-2}]
c	tuhosť kompenzačného prvku	[$N \cdot mm^{-1}$]
C	materiálová konštanta	[-]
D	vonkajší priemer rúry	[m]
DN	svetlosť potrubia	[mm]
F_C	celková osová sila do pevného bodu	[N]
F_D	sila vplyvom dilatácie potrubia	[N]
F_H	sila od tiaže potrubia	[N]
F_P	sila od pretlaku v potrubí	[N]
F_T	sila od trenia ostatných uložení	[N]

g	gravitačné zrýchlenie	[m·s^{-2}]
L	dĺžka potrubného úseku	[m]
L_m	montážna dĺžka (po predopnutí)	[m]
L_u	šírka kompenzátora	[m]
L_v	voľná dĺžka kompenzátora (pôvodná)	[m]
L_1	dĺžka kompenzačného ramena	[m]
m_p	nominálna hmotnosť potrubia	[kg·m^{-1}]
m_{pCELK}	nominálna hmotnosť potrubia	[kg·m^{-1}]
p_{max}	maximálny pretlak v sústave	[Pa]
T_{max}	maximálna teplota média	[°C]
T_{min}	minimálna teplota média	[°C]
T_{mon}	montážna teplota	[°C]
α	súčiniteľ teplotnej rozťažnosti	[K^{-1}]
Δ	predpätie kompenzátora	[mm]
ΔL	dĺžková zmena materiálu vplyvom teploty	[m]
ΔT	teplotný gradient	[K]
λ	celková kompenzačná schopnosť kompenzátora	[mm]
μ	súčiniteľ trenia v uložení	[-]

Poďakovanie

Táto práca vznikla za podpory projektov KEGA 038ŽU-4/2019 "Potrubné systémy v zásobovaní teplom" a VEGA 1/0233/19 " Konštrukčná modifikácia horáka na spaľovanie tuhých palív v malých zdrojoch tepla".

LITERATÚRA

[1] NECKÁŘOVÁ, J. - DOSKOČIL, L. (1972): *Potrubí a armatury.* Vysoké učení technické v Praze, Fakulta strojní. Vydavatelství ČVUT, Praha 1, Husova 5, 1972, 137 s.

[2] BHATIA, P. - JHA, A. (2014): *Analytical calculation for piping thickness and stress.* [online]. 2020, [cit. 2020-09-25]. Dostupné na internete: <http://ijmcr.com/wpcontent/uploads/2015/05/Paper 21640-643.pdf>.

[3] BOKAIAN, A. (2004): *Thermal expansion of pipe-in-pipe systems.* [online]. [cit. 2020-09-25]. Dostupné na internete: <https://www.sciencedirect.com/science/article/pii/S 0951833904000929>.

[4] SCHEINER, S. - PICHLER, B. - HELLMICH, CH. - EBERHARDSTEINER, J. (2020): *Loading of soil-covered oil and gas pipelines due to adverse soil settlements – Protection against thermal dilatation-induced wear, involving geosynthetics.* .[online]. [cit. 2020-09-25]. Dostupné na internete: <https://www.sciencedirect.com/science/article/pii/S 0266352X06000851>

[5] GERLACH, T. - ACHMUS, M. - TERCEROS, M. (2018): *Numerical investigation on district heating pipelines under combined axial and lateral loading.*[online]. [cit. 2020-09-25]. Dostupné na internete: <https://www.sciencedirect.com/science/article/pii/S 1876610218305046>.

[6] LENHARD, R. - KADUCHOVÁ, K. - PAPUČÍK, Š. - JANDAČKA, J. (2014): *Utilization of heat pipes for transfer heat from the flue gas into the heat transfer medium*. EPJ web of conferences [online]. 2014, 67, 02067 [cit. 2020-09-25]. ISSN 2101-6275.

[7] NESLUŠAN, M. - TRŠKO, L. - MINÁRIK, P. - ČAPEK, J. - BRONČEK, J., - PASTOREK, F. - ČÍŽEK, J. - MORAVEC, J. (2018): *Non-Destructive Evaluation of Steel Surfaces after Severe Plastic Deformation via the Barkhausen Noise Technique*, Metals 2018, 8 1029 doi: 10.3390/met 8 12029, ISSN 2075-4701 (10%)

[8] POSPÍŠIL, P. (2020): *Kompenzace délkových změn potrubí.* [online]. 2020, [cit. 2020-09-25]. Dostupné na internete: <https://adoc.tips/kompenzace-delkovych-zmn-potrubi.html>.

Určenie tlakovej straty tlmičov hluku vo vzduchotechnike experimentálne a pomocou CFD metód

Šimon Kubas, Ing.*
Katedra energetickej techniky, Strojnícka fakulta,
Žilinská univerzita v Žiline,
Univerzitná 1, 010 26 Žilina, Slovenská republika.
E-mail: simon.kubas@fstroj.uniza.sk, Tel.: + 421 917 847 379

Andrej Kapjor, doc. Ing., PhD.
Katedra energetickej techniky, Strojnícka fakulta,
Žilinská univerzita v Žiline,
Univerzitná 1, 010 26 Žilina, Slovenská republika.
E-mail: andrej.kapjor@fstroj.uniza.sk, Tel.: + 421 908 593 408

Martin Vantúch, Ing., PhD.
Katedra energetickej techniky, Strojnícka fakulta,
Žilinská univerzita v Žiline,
Univerzitná 1, 010 26 Žilina, Slovenská republika.
E-mail: martin.vantuch@fstroj.uniza.sk, Tel.: + 421 915 865 749

Determination of the local pressure loss coefficient experimentally and using CFD methods

Abstract: When designing air conditioning systems, it is necessary to pay attention to the level of noise generated during the operation of such a system. Each of the components of the air conditioning system either absorbs or generates noise. Noise in pipes and fittings can be reduced to the required level by dimensioning the pipes. However, noise generated by the fan itself must be eliminated in another way. To eliminate fan noise, silencers are used in the duct just behind the air handling unit. For the correct design of the silencer, it is necessary to pay attention not only to its acoustic attenuation, but also to the pressure loss. If the pressure drop of the muffler is too high, noise will occur directly in the muffler. The pressure losses of the dampers are determined mainly experimentally. Based on the performed measurement, a CFD model of the selected damper was constructed, where the influence of various parameters on the value of the pressure loss of the selected damper was investigated.

ÚVOD

V súčasnosti sa kladie veľký dôraz na znižovanie hluku spojeného s prevádzkou klimatizačných systémov, preto sú do potrubnej siete zabudované komponenty, ktorých úlohou je tento hluk tlmiť a absorbovať. Pre správny návrh systému je však potrebné poznať tlakovú stratu jednotlivých komponentov potrubnej siete. Pri praktickom navrhovaní tlmiča sa často zabúda na pokles tlaku tejto súčasti a hodnotí sa iba jej akustické tlmenie zvuku.

Dnes je neoddeliteľnou súčasťou rôznych meraní a experimentov výpočtový model konštruovaný pomocou metód CFD. Vytvorený výpočtový model musí byť overený meraním. Tento overený model môže výrazne uľahčiť ďalšie experimenty, pretože sa dá použiť na riešenie podobných úloh.

1 ÚTLM HLUKU VO VZDUCHOTECHNIKE

Systémy vzduchotechniky musia spĺňať prísne hygienické normy, ktoré určujú maximálne hodnoty hluku v priestore. Preto je nevyhnutné eliminovať hluk a vibrácie šíriace sa zo zdrojov do ostatných konštrukcií. Zariadenia je nutné opatriť rôznymi tlmičmi, vložkami a pod., keďže čiastočný prirodzený útlm hluku v potrubiach a tvarovkách nie je postačujúci [1].

Okrem tlmenia hluku pomocou rôznych prvkov slúžiacich na útlm hluku je možné využiť aj tzv. pasívne prvky. Tie sa delia do nasledujúcich kategórií:

- Redukcia zdroja – hodnota akustického hluku ventilátora je závislá od otáčok ventilátora, preto je nutné ventilátor správne navrhnúť.

- Dispozícia – je potrebné dbať na rozmiestnenie jednotlivých zdrojov hluku.
- Zvukové izolácie – odizolovaním zariadenia a skvalitnením akustických vlastností konštrukcií, ktoré oddeľujú zdroje hluku od chránených priestorov.
- Zvuková pohltivosť – materiály s dobrými absorpčnými vlastnosťami, použitých ako napr. obklady alebo antivibračné nátery zvyšujú pohltivosť konštrukcie [2].

1.1 Tlmiče hluku

Za účelom zníženia prenášanej akustickej energie sú do potrubnej siete vkladané tlmiče hluku. Tieto obsahujú materiály schopné pohlcovať hluk. Funkciou tlmiča je zníženie hluku, ktoré je dosiahnuté rozdielom hladín akustického výkonu pred a za tlmičom. Tlmič hluku ako taký sám spôsobuje aj tvorbu hluku. Táto vlastnosť je nazývaná vlastný akustický výkon tlmiča a je závislá hlavne od rýchlosti prúdenia vzduchu v tlmiči, ako aj od iných parametrov tlmiča. Optimálna rýchlosť prúdenia vzduchu v tlmiči hluku je do 5 $m \cdot s^{-1}$ [1].

Akustika rozdeľuje tlmiče hluku na reflexné a absorpčné. Avšak reflexné tlmiče nemajú vo vzduchotechnike veľké použitie. Pre dodržanie nízkej prietočnej rýchlosti vzduchu v tlmiči je potrebné zväčšovať prierez tlmiča, tým pádom rastie aj jeho cena. Poznáme rôzne prevedenia absorpčných tlmičov [1].

1.2 Kulisové tlmiče

Sú zložené z kulís, ktoré sú vyhotovené najčastejšie z minerálnej vlny. Samotný tlmič pozostáva zo štvorhranného potrubia, ktoré je po stenách obložené tlmiacimi vložkami, alebo sú do neho vložené kulisy v rôznom počte a šírke (obr. 1). Voľbou počtu a rozmerov vložených kulís je možné regulovať akustický výkon daného tlmiča hluku [2].

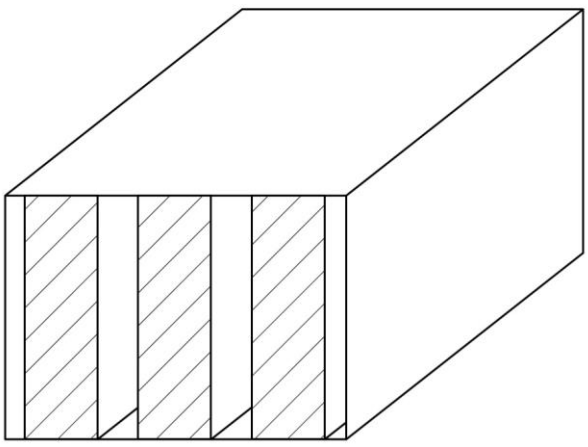

Obr. 1. Kulisový tlmič

2 TLAKOVÉ STRATY

Odpor proti prúdeniu je spôsobený jednak trením tekutiny o steny potrubia (straty trením), ako aj zmenou geometrie alebo zmenou smeru prúdenia (miestne straty). Hydraulické straty sa vyjadrujú ako násobok kinetickej energie jednotkou hmotnosti tekutiny.

Za predpokladu, že každý hydraulický odpor sa prejavuje nezávisle na účinku ostatných odporov. Celková tlaková strata je tým pádom daná súčtom jednotlivých strát [3].

2.1 Tlakové straty trením

Tlakové straty trením v potrubí je možné vypočítať pomocou Darcy-Waisbachovej rovnice (1):

$$e_{z,t} = \Lambda \cdot \frac{l}{d} \cdot \frac{v^2}{2} \ [\mathrm{J \cdot kg^{-1}}] \tag{1}$$

Na vyjadrenie tlakovej straty, môžeme túto rovnicu napísať v tvare (2):

$$p_{z,t} = \Lambda \cdot \frac{l}{d} \cdot \frac{v^2}{2} \cdot \rho \ [\mathrm{Pa}] \tag{2}$$

Súčiniteľ trenia Λ je vo všeobecnosti daný funkciou (3). Sú v ňom zahrnuté vlastnosti dopravovaného média ako aj vlastnosti potrubia:

$$\Lambda = f\left(v, \nu, d, l, k\right) \tag{3}$$

Pri dostatočne dlhých potrubiach dĺžka potrubia neovplyvňuje tento faktor, z dôvodu lineárnej závislosti. Pre rôzne veľkosti potrubí ako aj pre rôzne rýchlosti sa funkčná závislosť koeficientu trenia vyjadruje pomocou Reynoldsového čísla a pomeru medzi drsnosťou a priemerom (4) [3]:

$$\Lambda = f\left(Re, k/d\right) \tag{4}$$

2.2 Drsnosť steny potrubia

Všeobecne sa drsnosť určuje výškou výstupkov nerovnomerností povrchu. Označuje sa k. Poznáme viac druhov drsnosti potrubia.

Absolútna drsnosť je výška výstupku nerovnosti povrchu. Pre výpočet však nie je možné túto hodnotu dobre využiť, keďže výška jednotlivých výstupkov nie je rovnaká.

Stredná drsnosť sa určuje ako stredná hodnota výšky výstupkov na povrchu. Bola zavedená ako hodnota pre výpočty.

Pomerná drsnosť je určená ako pomer medzi strednou hodnotou drsnosti a priemerom potrubia. Táto hodnota lepšie vystihuje vplyv drsnosti na súčiniteľ trenia ako samotná stredná hodnota drsnosti [3].

2.3 Súčiniteľ trenia pre kruhové potrubia

Spočiatku bol súčiniteľ trenia považovaný za konštantný. Avšak postupne sa ukázalo, že je závislý od hodnoty strednej rýchlosti prúdenia. Jeho hodnota je ovplyvnená hlavne typom prúdenia a veľkosťou Reynoldsového čísla. Keďže neexistuje univerzálny vzorec na výpočet tohto koeficientu, je nutné poznať hodnotu *Re*.

2.4 Miestne tlakové straty

Príčinou vzniku týchto strát je lokálne narušenie prúdu. Pri takomto narušení dochádza k deformácií rýchlostného profilu prúdenia. Dôsledkom takéhoto narušenia sa prúd zvykne odtrhnúť od steny, takže vznikajú vírové oblasti. Jednotlivé víri sú potom prúdom odnášané v smere prúdenia, postupne sa rozpadajú na menšie, až sa celkom rozplynú. Ich kinetická energia sa pri rozpade mení na teplo.

Tlaková strata sa určuje podľa Bordovho vzťahu miestnych strát (5). Avšak výpočet miestnych tlakových strát pomocou tohto vzorca sa veľmi často líši od skutočných hodnôt zistených experimentálne. Táto metóda výpočtu je odvodená od rozdielu rýchlostí pred a za prvkom, ktorý miestnu tlakovú stratu spôsobuje:

$$p_z = \frac{\rho}{2} \cdot \left(v_1 - v_2\right)^2 \quad \text{[Pa]} \tag{5}$$

Spôsob výpočtu tlakových strát pomocou Bordovho vzťahu, je najpresnejší pri skúmaní miestneho odporu pri náhlom rozšírení alebo zúžení prúdu, kde je rozdiel rýchlostí najvýraznejší.

Najspoľahlivejšou metódou určenia miestnych tlakových strát komponentov systému je na základe zistenia súčiniteľa miestnych tlakových strát ξ.

Súčiniteľ ξ sa vždy vzťahuje na rýchlosť prúdenia, ktorá je daná plochou prierezu potrubia. Ak vychádzame z podmienky, že tlaková strata sa nemení, je možné prepočítať tento koeficient na iný prierez potrubia. Daný prepočet vychádza zo vzťahu (6):

$$\xi_1 \cdot \frac{v_1^2}{2} \cdot \rho = \xi_2 \cdot \frac{v_2^2}{2} \cdot \rho \tag{6}$$

V súčiniteli miestneho odporu ja väčšinou obsiahnutá aj tlaková strata trením alebo strata dynamického tlaku. Pri zisťovaní koeficientu miestnej tlakovej straty býva prvok vložený do potrubia, tým pádom je v súčiniteli ξ obsiahnutá aj tlaková strata vyrovnaním rýchlostného profilu.

Prvky radené bezprostredne za sebou so známym koeficientom miestnej tlakovej straty sa navzájom ovplyvňujú. Z toho vyplýva, že výsledná hodnota tlakovej straty sa nebude rovnať jednoduchému súčtu tlakových strát týchto vložených odporov [4].

2.5 Súčiniteľ miestnych tlakových strát

Hodnota tohto súčiniteľa je závislá od geometrie miestneho odporu a od rýchlosti prúdenia tekutiny. Jeho určenie prebieha experimentálne a je platný len v rovnakých podmienkach, pri ktorých bol určený, alebo vo fyzikálne podobných prípadoch [4].

3 MODELOVÝ TLMIČ HLUKU

Pre určenie koeficientu miestnej tlakovej straty je navrhnutý modelový tlmič hluku.

Vonkajší plášť tlmiča je štvorhranné potrubie z pozinkovaného plechu ukončené prírubami.

Rám vložky tlmiča je vyrobený z pozinkovaného plechu. Vložená absorpčná výplň je vyrobená z nehorľavého, zvukovo-izolačného materiálu, obojstranne potiahnutá laminovanou, hygienicky nezávadnou látkou. Vložená minerálna vlna je hygienicky nezávadná, odolná proti hnilobe a odpudzuje vlhkosť. Pri navrhovanej dĺžke kulisy sa izolácia stabilizuje výstužou. Závesy sú pripevnené k plášťu potrubia nitmi.

3.1 Konštrukcia a rozmery

Tlmič hluku bude pozostávať zo šiestich kulís osadených v hranatom potrubí. Rozmery potrubia sú uvedené na obr. 2. Nezaplnený prierez tlmiča bude pozostávať zo siedmych medzier medzi kulisami. Rozostupy medzi jednotlivými kulisami budú o dĺžke 66 mm, pričom rozstup medzi vonkajšími stenami potrubia a kulisami bude 33 mm.

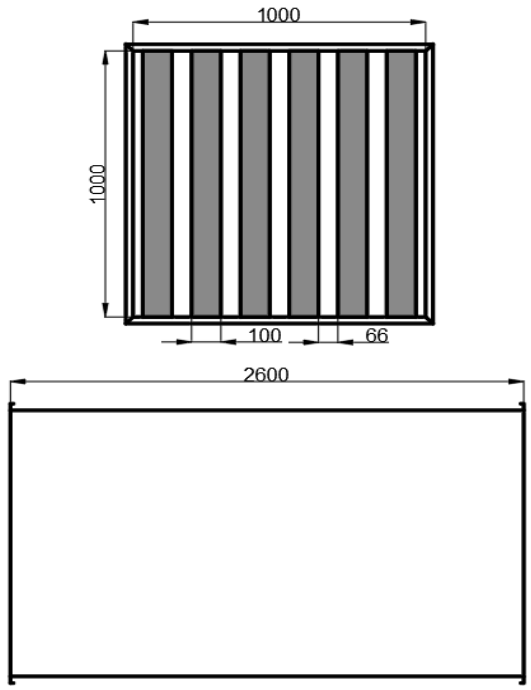

Obr. 2. Priečny rez modelovaným tlmičom hluku

Každá z osadených kulís bude o potrubie pripevnená pomocou nitov. Rozmery kulisy sú uvedené na

obr. 3. V našom prípade bude v tlmiči osadených šesť tlmiacich kulís.

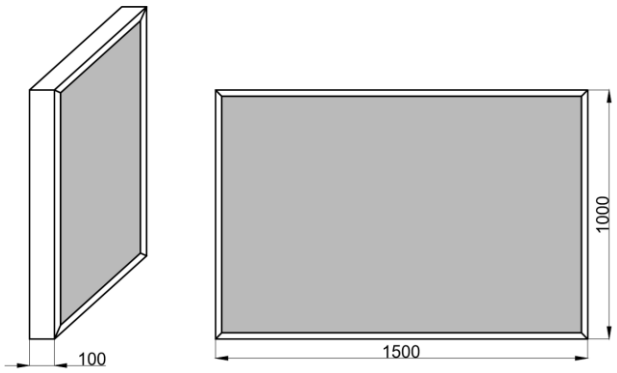

Obr. 3. Kulisa vložená v tlmiči hluku

Prívod vzduchu do systému bude zabezpečený pomocou potrubného axiálneho ventilátora, ktorý bude dopojený na potrubie s rozmerom 500x500 mm. Dĺžka prípojného potrubia bude v tomto prípade 1500 mm. Samotný tlmič hluku je osadený v potrubí s rozmermi 1000x1000 mm, ktoré je z prívodným potrubím spojené pomocou symetrického prechodu pre štvorhranné potrubia s uhlom 45°. Za osadenými kulisami bude pokračovať potrubie s rovnakými rozmermi aby došlo k ustáleniu prúdenia. Celá skonštruovaná zostava je zobrazená na obr. 4.

4.1 Meranie modelového tlmiča hluku

Meranie sa uskutočnilo na skutočnom tlmiči, skonštruovanom tak, ako je znázornené na obr. 4. Experiment pozostával z merania poklesu tlaku, teploty a prietoku. Prietok sa tiež meral pomocou Wilsonovej mriežky s tlakovým prevodníkom Airflow PTSXR-K, aby sa zvýšila presnosť merania.

Jednotlivé meracie prístroje boli spojené tak, ako je to znázornené na obr. 5.

Prívod vzduchu k meranej klapke je zabezpečený pomocou axiálneho potrubného ventilátora s maximálnym prietokom vzduchu 9000 $m^3 \cdot h^{-1}$. Objemový prietok ventilátora bol regulovaný pomocou frekvenčného meniča. Ventilátor bol pripojený k potrubiu s rozmermi 500x500 mm. Samotný meraný tlmič je namontovaný v potrubí s rozmermi 1000x1000 mm, ktoré je pripojené k prívodnému potrubiu potrubným priechodom.

4.2 Postup merania

Boli vykonané jednotlivé merania pre rôzne hodnoty objemového prietoku. Regulácia prietoku sa uskutočňovala pomocou frekvenčného meniča.

Meranie tlakového rozdielu sa uskutočňovalo podľa obr. 5 v bodoch 1 a 2.

Výsledná rýchlosť sa určila ako aritmetický priemer merania na Wilsonovej mriežke a priemerná hodnota

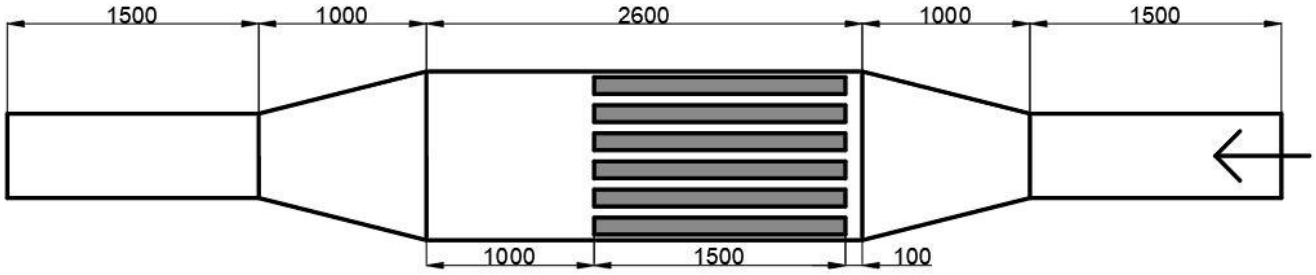

Obr. 4. Pozdĺžny rez modelovaným tlmičom hluku

4 MODELOVÝ TLMIČ HLUKU

Vykonaný experiment bol navrhnutý na základe normy STN EN ISO 7235. Na stanovenie koeficientu lokálnej tlakovej straty je potrebné vykonať najmenej päť rôznych meraní pri rôznych objemových prietokoch.

Modelovaná zostava a zariadenie na meranie strednej hodnoty statického tlaku na oboch stranách skúšobného objektu a celého jeho poklesu tlaku musia byť také, ako je to znázornené na obr. 5. Tlak v potrubí sa musí merať kalibrovaným manometrom.

nameraná pomocou rýchlostnej sondy ALMEMO. Namerané a priemerné hodnoty rýchlosti sa vzťahujú na prierez potrubia s rozmermi 500x500 mm.

Z nameraných hodnôt rýchlosti sa následne pomocou rovnice (7) stanovil objemový prietok potrubím:

$$Q = S \cdot v \cdot \rho \tag{7}$$

Hodnota koeficientu miestnej tlakovej straty ξ sa vypočíta podľa rovnice (6). Pretože samotný tlmič je umiestnený v potrubí s rozmermi 1000x1000 mm, na stanovenie koeficientu lokálnej tlakovej straty ξ pre tlmič sme museli prepočítať nameranú rýchlosť na hodnotu v danom priereze. Táto premena sa uskutočnila pomocou rovnice kontinuity:

$$S_1 \cdot v_1 = S_2 \cdot v_2 \quad (8)$$

Výsledná hodnota činiteľa ξ, ako aj rýchlosť prúdenia v širšej časti potrubnej zostavy je uvedená v tab. 1.

Ďalším krokom bolo vyhotovenie rozdelenia modelu na prvky pomocou metódy konečných objemov. Bola zvolená sieť pozostávajúca z pyramídových elementov v kombinácii s prvkami v tvare kvádra pred a za potrubným prechodom. Vytvorená sieť

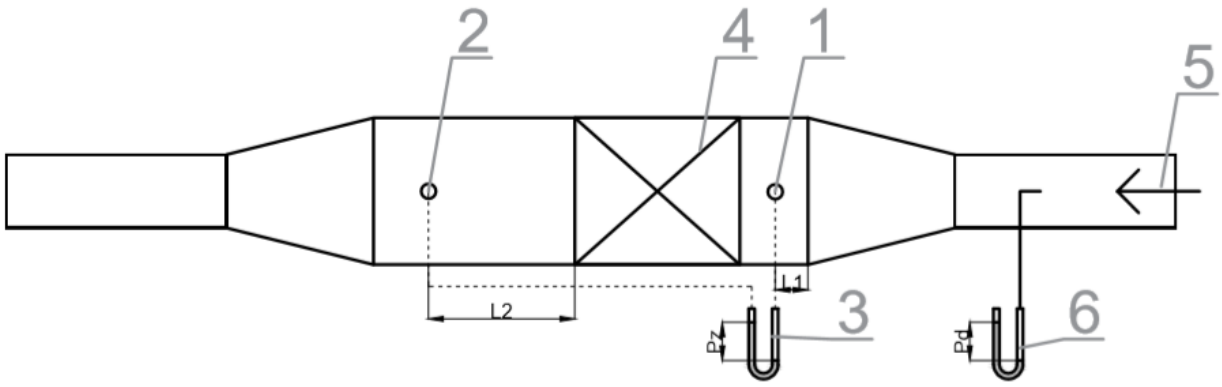

Obr. 5. Schéma merania tlakovej straty podľa STN EN ISO 7235 (1-meranie statického tlaku proti prúdeniu pred skúšaným objektom, 2-meranie statického tlaku po prúde za skúšaným objektom, 3-manometer, 4-kulisový tlmič, 5-smer prúdenia, 6- meranie prietoku)

Tab. 1. Výsledky merania

Frekvencia ventilátora [Hz]	v_1 [m.s^{-1}]	v_2 [m.s^{-1}]	ξ
20	4.40	1.10	6.2
22	4.85	1.21	5.8
24	5.30	1.33	6.2
26	5.74	1.44	7.2
28	6.16	1.54	8.9
30	6.64	1.66	8.9
32	7.08	1.77	8.9
34	7.44	1.86	8.9
36	7.99	2.00	6.9
38	8.40	2.10	6.9
40	8.82	2.21	7.5
Aritmetický priemer			**7.48**

5 CFD Model

Na základe reálne zostrojeného tlmiča hluku bol zostrojený CFD model pomocou softvéru Ansys Fluent.

Účelom tohto modelu bolo vypočítať tlakovú stratu a zároveň zistiť, aký výpočtový model je najvhodnejší pre danú aplikáciu.

Pre použitie numerických metód na výpočet tlakovej straty bolo nutné zostrojiť trojrozmerný model reálneho tlmiča hluku, na ktorom bolo vykonané meranie.Geometria bola vyhotovená pomocou softvéru Ansys Design Modeler.

bola zahustená v oblasti vstupu a výstupu z medzier medi jednotlivými kulisami tlmiča hluku.

Spomedzi modelov turbulencie ponúkaných programom Fluent sme zvolili štyri modely. Každý z týchto modelov turbulencie je založený na princípe Reynoldsového časového stredovania. Ide o modely *k-ε* RNG, *k-ε* Realizable, *k-ω* Standard a *k-ω* SST [5].

Pre každý zo zvolených modelov turbulencie bolo vykonaných jedenásť výpočtov, pre rovnaké objemové prietoky ako boli zistené pri meraní.

Z vypočítaných hodnôt pomocou CFD bol vytvorený aritmetický priemer pre koeficient miestnej tlakovej straty (obr. 6).

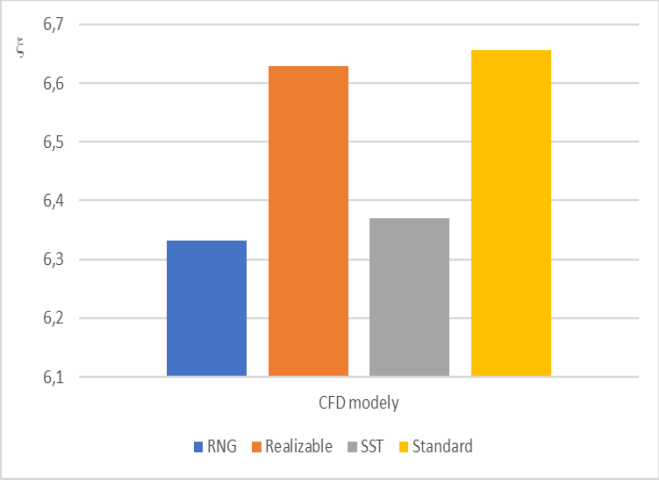

Obr. 6. Graf priemernej hodnoty koeficientu ξ

ZÁVER

V súčasnosti sa kladie veľký dôraz na tlakové straty komponentov vzduchotechniky. Práca sa venuje problematike stanovenia tlakovej straty tlmičov hluku pri určovaní koeficientu miestnej tlakovej straty. Časť práce je venovaná popisu tlakových strát. Tieto straty sú spôsobené buď trením kvapaliny o steny potrubia, alebo miestnymi odpormi, ktoré sú spôsobené buď obídením prekážky, alebo zmenou smeru prúdenia.

Výsledkom tejto práce je overenie vytvoreného CFD modelu pre stanovenie tlakových strát pomocou experimentu. Takto vytvorený a overený výpočtový model bude možné použiť aj použiť aj na stanovenie tlakových strát kulisových tlmičov hluku s inými rozmermi.

Poďakovanie

Táto práca vznikla za podpory projektov KEGA 038ŽU-4/2019 Potrubné systémy v zásobovaní teplom.

LITERATÚRA

[1] CHYSKÝ, J. (1993): *Větrání a klimatizace*. Praha, SNTL, ISBN 04-217-73.

[2] GEBAUER, G. - RUBINOVÁ, O. - HORKÁ, H. (2007): *Vzduchotechnika*. Brno, Vydavatelství ERA, ISBN 978-80-7366-091-8.

[3] SZÉKYOVÁ, M. - FERSTL, K. - NOVÝ, R. **(**2004): *Vetranie a klimatizácia*. Bratislava, Jaga group, ISBN 80-8076-000-4.

[4] IDELCHIK, I. E. (2008): *Handbook of Hydraulic Resistance, 4th Edition*. New York: US, ISBN 978-1-56700-251-5

[5] PATSCH M. - PILAT, P. (2018): *Simulation of Combustion Air Flow in the Gasification Biomass Boiler*, 21st International Scientific Conference on The Application of Experimental and Numerical Methods in Fluid Mechanics and Energy (AEaNMiFMaE), APR 25-27, 2018.

Možnosti úpravy tvaru roztavenej oblasti zvaru pri simulácií oblúkového zvárania v programe SYSWELD

Radoslav Koňár, Ing., PhD.*
Katedra technologického inžinierstva, Strojnícka fakulta,
Žilinská univerzita v Žiline,
Univerzitná 1, 010 26 Žilina, Slovenská republika.
E-mail: radoslav.konar@fstroj.uniza.sk, Tel.: + 421 41 513 2799

Lukáš Petričko, Ing.
SvarExpert s.r.o.,
Krištofova 1443/27, Ostrava, Česká republika.
E-mail: petricko@svarexpert.cz

Possibilities of adjusting the arc welding molten weld area shape in simulation software SYSWELD

Abstract: The article is focused on modifying the shape of the molten area in the simulation of arc welding in the Sysweld program. The shape of the molten zone in the Sysweld program, depends on the set input parameters, namely on the parameters of the Goldak model and the definition of finite elements through which heat is distributed to the model. The possibilities of changing the shape of the molten area are illustrated on a single-layer weld made by submerged arc welding technology.

ÚVOD

Definovanie tepelného zdroja pri simulácií zvárania je jedným z najdôležitejších krokov pre dosiahnutie správnych výsledkov numerickej simulácie zvárania. Správne definovanie tepelného zdroja pre simuláciu je veľakrát zložitým časovo náročným procesom. Základným krokom kontroly správnej definície tepelného zdroja pre simuláciu je porovnanie vypočítanej roztavenej oblasti s reálnou oblasťou získanou z makroštruktúry zvaru.

Pre definovanie tepelného zdroja pre numerickú simuláciu je možné použiť rôzne typy matematických modelov. Pre procesy oblúkového zvárania je využívaný Goldakov model zdroja tepla, ktorým je možné najpresnejšie popísať pohyblivý zdroj tepla pri zváraní vytvorený elektrickým oblúkom.

Článok je zameraný na možnosti ovplyvňovania roztavenej oblasti zvaru vstupnými parametrami simulácie a to parametrami Goldakovho modelu, polohou jeho centra a tiež definovaním konečných prvkov, cez ktoré bude nadefinovaná tepelná energia vnesená do modelu pri výpočte. Proces definovania zdroja tepla a jeho tvaru je popísaná na simulácií návaru vytvoreného zváraním pod tavivom.

Simulácia zváracích procesov je v dnešnej dobe bežným prostriedkom využívaným pre analýzy zvarových spojov, a to buď pri optimalizácií technologických postupov, alebo pri riešení problémov vyskytujúcich sa vo výrobe.

1 SIMULAČNÝ PROGRAM SYSWELD

Program SYSWELD patrí medzi moderné simulačné programy. Je zameraný na oblasť zvárania a tepelného spracovania. Ide o program, pracujúci na základe metódy konečných prvkov (MKP), čo dovoľuje riešiť konštrukčne a technologicky náročné úlohy z oblasti zvárania. Z matematického hľadiska je metóda MKP využívaná k nájdeniu aproximovaného riešenia parciálnych diferenciálnych a integrálnych rovníc (napr. rovnica vedenia tepla) pomocou PC.

Programom SYSWELD možno riešiť oblúkové (MMA, MIG/MAG, TIG, ZPT), odporové (bodové, švové zváranie), vysokoenergetické (laserový, elektrónový lúč), trecie spôsoby zvárania, ako aj tepelné spracovanie materiálov. Po vhodnom zadefinovaní vstupných dát, geometrie a okrajových podmienok, možno po procese simulácie získať výsledky ako deformácie, zvyškové napätia, tvrdosť HV, rozloženie materiálových fáz, veľkosť a tvar teplom ovplyvnenej oblasti.

Simulačný program SYSWELD umožňuje definovať tri typy tepelných zdrojov:

- Trojrozmerný dvojelipsoidný Goldakov model.
- Trojrozmerný kónický Gaussov model.

- Dvojrozmerný Gaussov model.

Ako už bolo spomenuté, pre matematické definovanie tepelných zdrojov vznikajúcich pri oblúkových spôsoboch zvárania je najvhodnejšie použiť dvojelipsoidný Goldakov model.

Definovanie správnych parametrov Goldakovho modelu je potrebné vykonať pred spustením výpočtu tepelno-metalurgickej analýzy (teplotné polia, zmeny a rozloženie štruktúry), kde je tepelné zaťaženie jedným zo základných výpočtových vstupov. Po teplotne-metalurgickej analýze nasleduje mechanická analýza (zvyškové napätia, deformácie) ktorej presnosť výsledkov závisí od tepelne-metalurgickej analýzy.

Definovanie tepelného zdroja je možné rozdeliť do nasledujúcich krokov:

1. Definovanie základných rozmerových parametrov a pozície centra Goldakovho modelu z makroštruktúry zvaru.
2. Nadefinovanie MKP prvkov pre distribúcie tepla do modelu.
3. Overenie správnosti definovania parametrov pomocou čiastkového výpočtu.

Jediným zaťažujúcim účinkom pri numerickej simulácii zvárania je rozloženie teplotných polí v jednotlivých časových okamihoch. Teplota pri zváracom procese je funkciou súradníc a času:

$$T = f\left(x, y, z, t\right) \tag{1}$$

kde T [°C] – teplota,

x, y, z [m] – súradnice,

t [s] – čas.

Goldakov dvojelipsoidný model najdôveryhodnejšie popisuje pohyblivý zdroj tepla, pôsobiaci pri oblúkových metódach zvárania. Matematicky možno tento dvojelipsoidný zdroj tepla popísať dvomi rovnicami:

$$q\left(x,y,z,t\right) = \frac{6\cdot\sqrt{3}\cdot f_f \cdot Q}{b\cdot c\cdot a_f \cdot \pi\cdot\sqrt{\pi}} \cdot e^{\frac{-3\cdot x^2}{b^2}} \cdot e^{\frac{3\cdot z^2}{c^2}} \cdot e^{\frac{-3\cdot\left[y-v\cdot\left(\tau-t\right)\right]^2}{a_f^2}} \tag{2}$$

$$q\left(x,y,z,t\right) = \frac{6\cdot\sqrt{3}\cdot f_r \cdot Q}{b\cdot c\cdot a_r \cdot \pi\cdot\sqrt{\pi}} \cdot e^{\frac{-3\cdot x^2}{b^2}} \cdot e^{\frac{-3\cdot z^2}{c^2}} \cdot e^{\frac{-3\cdot\left[y-v\cdot\left(\tau-t\right)\right]^2}{a_r^2}} \tag{3}$$

$$f_f + f_r = 2 \tag{4}$$

kde q [W·m^{-2}] – tepelný tok do materiálu

a_f, a_r, b, c [m] – rozmery roztavenej oblasti,

f_f, f_r – konštanty ovplyvňujúce rozloženie intenzity toku energie do materiálu [1],

τ [s] – celkový čas zvárania.

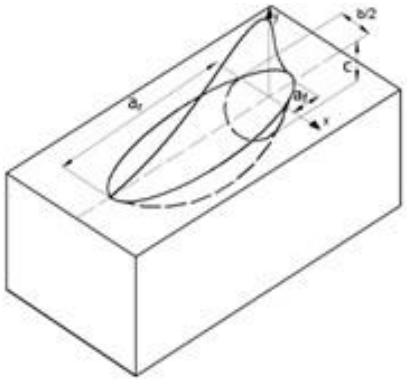

Obr. 1. Goldakov model zdroja tepla

Pre použitie dvoj-elipsoidného modelu je treba poznať veľkosti natavenej oblasti. Tieto parametre sú zisťované na základe rovníc pre dvoj a troj-rozmerné teplotné pole alebo na základe vykonaných experimentov. Parametre zisťované z reálnych experimentov možno odčítať z makroštruktúry zvaru.

2 DEFINÍCIA GOLDAKOVHO TEPELNÉHO ZDROJA V SIMULAČNOM SYSTÉME SYSWELD

Ako podklad pre vytvorenie simulácie a poukázanie na možnosti modifikácie roztavenej oblasti pri simulácií v programe Sysweld bol vytvorený experimentálny návar technológiou zvárania pod tavivom na oceľový plech S355J2G3 s rozmermi 300x300x30 mm. Návar s dĺžkou 100 mm bol vytvorený v strede experimentálnej vzorky. Rýchlosť zvárania bola v_z = 0,4 m·min^{-1}, parametre zvárania U_z = 30 V, I_z = 400 A. Makroštruktúra návaru je na obr. 2.

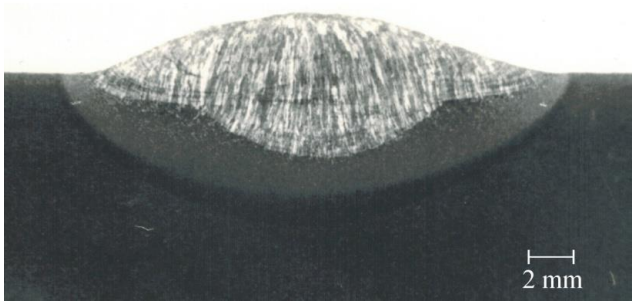

Obr. 2. Makroštruktúra návaru [5]

Pre proces simulácie bol vytvorený polovičný symetrický 3D MKP model s rozmermi reálnej vzorky. Rovina symetrie modelu prechádzala cez os zvaru a bola orientovaná kolmo na povrch vzorky. 3D MKP odel tvorilo 33 542 3D elementov a 31 656 uzlových bodov.

Pre simuláciu bola použitá materiálová databáza ocele S355, ktorá je priamo súčasťou systému Sysweld. Pre

odvod tepla zo vzorky bola vytvorená povrchová 2D sieť. Rýchlosť odvodu tepla bola nadefinovaná pre ochladzovanie vzduchom s hodnotou 25,0 $W \cdot m^{-2} \cdot K^{-1}$. Schéma 3D modelu je na obr. 3.

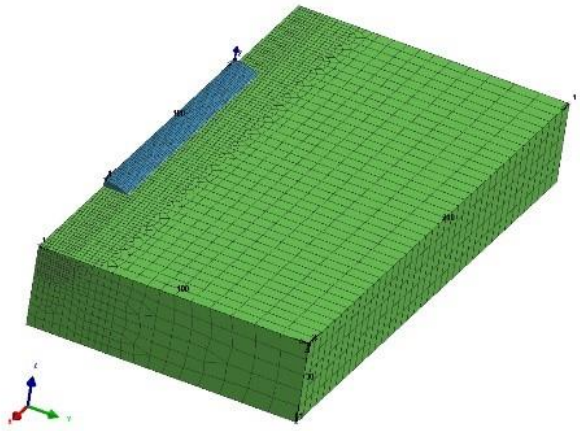

Obr. 3. 3D model pre simuláciu

Stanovenie základných parametrov Goldakovho modelu vychádzalo z merania rozmerov makroštruktúry. V prípade prvotného stanovenia parametrov je dôležité stanoviť šírku zvaru a hĺbku prievaru. Tieto dve hodnoty sú parametrami b a c Goldakovho modelu (obr. 1). Dĺžka modelu $a_f + a_r$ bola zvolená na 10,0 mm. Túto dĺžku je možné tiež stanoviť z geometrie koncového krátera zvaru. Geometrické parametre definujú tvar Goldakovho modelu a sú pomernými hodnotami tvaru Goldakovho modelu. Znamená to, že ak budeme meniť tepelný príkon, tak pomery jednotlivých osí modelu zostanú rovnaké, zmení sa iba mohutnosť zdroja. Mohutnosť zdroja je definovaná tepelným príkonom Q [W]. Centrum zdroja bol pri simulácií posunutý v smere hrúbky o 1,5 mm nad povrch vzorky.

Pomocou týchto nadefinovaných parametrov je možné stanoviť približný tvar simulovanej roztavenej oblasti, avšak tvar bude pravidelný a bude kopírovať tvar elipsy. V prípade aj je tvar roztavenej oblasti nepravidelný, je potrebné pre definovanie roztavenej oblasti zdroja použiť vybranú skupinu konečých prvkov, cez ktoré bude pri výpočte vnesená zadefinovaná tepelná energia. Táto skupina prvkov sa nazýva „LOAD“. Sú to 3D prvky umiestnené v blízkosti zvaru, cez ktoré sa pri pohybe tepelného zdroja pri simulácií teplo vnáša do modelu. Podľa rozloženia týchto prvkov je teda možné do určitej miery ovplyvňovať tvar roztavenej oblasti.

Príklad použitých prvkov pre nadefinovanie nepravidelného tvaru roztavenej oblasti pre návar je na obr. 4.

Overenie správnosti definovania jednotlivých parametrov je na základe vykonania čiastkového výpočtu a porovnania vypočítanej roztavenej oblasti s reálnou makroštruktúrou. Ak sa výsledky nezhodujú, je potrebné ich upraviť a znovu vykonať výpočet.

Pre simuláciu tepelno-metalurgickej analýzy boli použité nasledovné parametre Goldakovho modelu a_f = 3,3 mm, a_r = 6,7 mm, b = 10,0 mm, c = 3,0 mm, Z_0 = -1,5 mm, v_z = 0,4 $m \cdot min^{-1}$, Q = 980,0 W. Výsledok výpočtu roztavenej oblasti je na obr. 5.

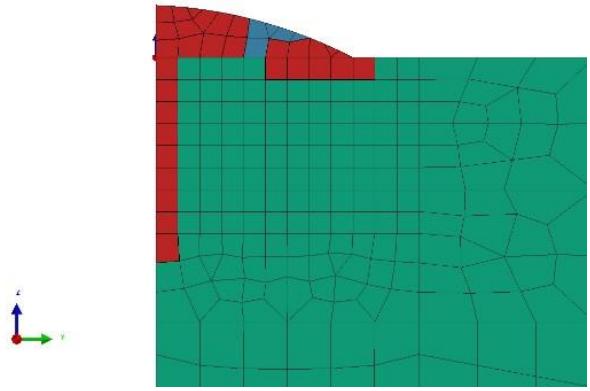

Obr. 4. „LOAD“ prvky

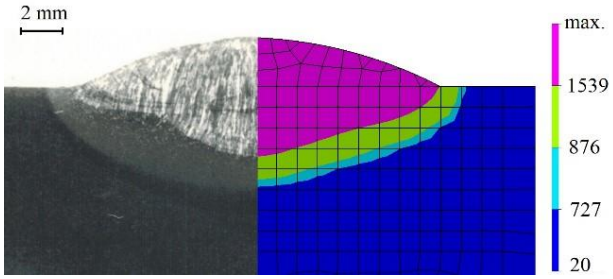

Obr. 5. Porovnanie vypočítanej a skutočnej roztavenej oblasti

Výpočet teplotných polí počas zvárania pre nadefinovaný zdroj tepla je uvedený na obr. 6.

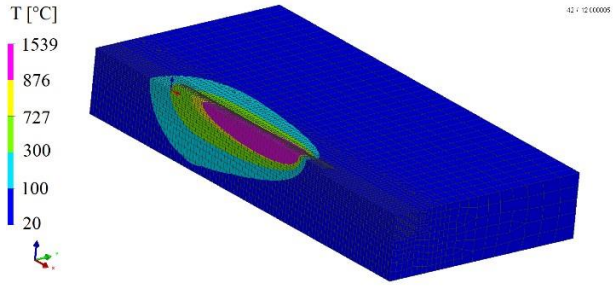

Obr. 6. Teplotné polia počas zvárania

Z výsledkov teplotne-metalurgickej analýzy je tiež možné získať priebeh teplotných cyklov pre ktorýkoľvek uzlový bod, výpočet tvrdosti a zmeny štruktúry počas a po zváraní.

ZÁVER

Článok popisuje problematiku definovania a modifikácie tvaru roztavenej oblasti pri simulácií

zvárania oblúkovými technológiami v programe Sysweld. V článku je popísaný postup definície teplotného zdroja za účelom dosiahnutia uspokojivého tvaru roztavenej oblasti pri simulácií zvárania.

Presnosť definovania tepelného zdroja pri procese simulácie zvárania je jedným z najvýraznejších faktorov ovplyvňujúcich presnosť výsledkov nielen tepelno-metalurgickej, ale aj nadväznej mechanickej analýzy.

LITERATÚRA

[1] WU, C. S. - WANG, H. G. - ZHANG, Y. M. (2006): *A New Heat Source Model for Keyhole Plasma Arc Welding in FEM Analysis of Temperature Profile.* In: Welding Journal, 85(12), 2006, pp. 284-29, ISSN 0043-2296.

[2] TSAI, N. S. - EAGAR, T. W. (1984): *Changes of Weld Pool Shape by Variations in The Distribution of Heat source in Arc Welding.* In: Modelling of casting and Welding Processes II, J.A. Dantzig and J.T. Berry, eds., AIME, New York, p. 317, 1984.

[3] MESKO, J. - RADEK, N. - ZRAK, A. (2014): *Technology of laser forming.* Manufacturing technology, Vol. 14, no.3, s. 428-431. ISSN 1213-2489.

[4] MICIAN, M. - PATEK, M. - SLADEK, A. (2014): *Concept of Reapiring Branch Pipes on High-pressure Pipelines by Using split Sleeve.* In: *Manufacturing technology,* Vol. 14, No. 3, pp. 60-66. ISSN 1212-2489.

[5] WINCZEK, J. et al. (2019): *Theoretical and Experimental Investigation of Temperature and Phase Transformation During SAW Overlaying*. In: Applied Science, Vol. 9, No. 7, Article No. 1472, ISSN 20763417.

Pokročilé pohonné systémy elektromobilov

Laura Lachvajderová, Ing.
Ústav manažmentu, priemyselného a digitálneho inžinierstva, Strojnícka fakulta,
Technická univerzita v Košiciach,
Park Komenského 9, 042 00 Košice, Slovenská republika.
E-mail: laura.lachvajderova@tuke.sk, Tel.: + 421 55 602 2724

Jaroslava Kádárová, doc. Ing., PhD.
Ústav manažmentu, priemyselného a digitálneho inžinierstva, Strojnícka fakulta,
Technická univerzita v Košiciach,
Park Komenského 9, 042 00 Košice, Slovenská republika.
E-mail: jaroslava.kadarova@tuke.sk, Tel.: + 421 55 602 3242

Michal Puškár, doc. Ing., PhD.*
Katedra konštrukčného a dopravného inžinierstva, Ústav konštrukčného inžinierstva a mechaniky,
Strojnícka fakulta, Technická univerzita v Košiciach,
Park Komenského 9, 042 00 Košice, Slovenská republika.
E-mail: michal.puskar@tuke.sk, Tel.: + 421 55 602 2360

Advanced propulsion systems of electric vehicles

Abstract: The paper deals with the propulsion system, respectively electric motors, which are used in modern electric vehicles. The introductory part of the article briefly deals with the reasons for the introduction of electromobility and shortly describes the most used electric motors and their main requirements. The aim of this article focuses on individual types of electric motors, describe different concepts and specify advantages and disadvantages. In the final part, the paper focuses on integrated electric drives used in today's modern electric vehicles. The output is a comparison, evaluation of the issue and possible prospects for the future.

ÚVOD

V posledných desiatich rokoch sa automobiloví výrobcovia pod tlakom verejnosti čoraz viac prikláňajú k alternatívnym zdrojom energie akým je napríklad aj elektrický pohon. Popularita elektromobilov sa postupne zvyšuje, a to nielen vďaka snahe zníženia škodlivých emisií unikajúcich do ovzdušia, ale hlavne kvôli zníženiu závislosti od fosílnych zdrojov energie. Každoročne pribúdajú nové a nové modely a vznikajú nové spoločnosti zaoberajúce sa vývojom a výrobcov elektromobilov. Jednoznačne ide o zaujímavé technológie, ktoré však zatiaľ trpia mnohými nedostatkami, akými sú napríklad neprimerane krátky jazdný dosah, vysoká kúpna cena a nedostatočný počet dobíjacích staníc výrazne spomaľujúcich ich rozšírenie. Najmä z týchto dôvodov je počet elektromobilov na Slovensku a aj v Českej republike minimálny. Na druhej strane majú množstvo výhod, o ktorých nie všetci bežný ľudia vedia. Medzi ich jednoznačné výhody patria nízke prevádzkové náklady, tichosť chodu, dobrý priebeh točivého momentu a ďalšie. Ide o niekoľko stoviek kusov, takže stretnúť elektromobil na našom území je v súčasnosti pomerne zriedkavý jav. Je zrejmé, že elektromobily v dnešnej dobe, aj napriek štátnym dotáciám, predstavujú drahú a luxusnú záležitosť.

1 ELEKTROMOTORY

Elektromobily sa skladajú zo štyroch základných častí, ktorými sú elektrický motor, regulátor, batérie a systém dobíjania batérií. Elektromotor je elektrické zariadenie, ktoré na rozdiel od konvenčného spaľovacieho motora využíva na vytvorenie mechanického pohybu elektromagnetické javy. Veľkou výhodou elektromotora je fakt, že ide o veľmi jednoduché zariadenie, ktoré sa skladá iba z dvoch vzájomne integrujúcich prvkov. Týmito prvkami sú stator a rotor. Ďalšou výhodou elektromotora je jeho vlastnosť, že svojím správaním pripomína generátor, z čoho vyplýva možnosť tzv. rekuperácie. Princíp rekuperácie sa uplatňuje pri brzdení a spomaľovaní vozidla a umožňuje navracať energiu späť do batérie, a tým ju dobíjať. Hlavným rysom elektrického motora v automobiloch je schopnosť dosiahnuť maximálny krútiaci moment takmer od nulových otáčok a vďaka veľkému rozpätiu pracovných otáčok nepotrebnosť konvenčnej viacstupňové prevodovky, ktorú nahrádza reduktor [1]. Elektromotory môžeme deliť do viacerých kategórií podľa druhu privádzaného prúdu na jednosmerné a striedavé. Striedavé motory ďalej delíme na synchrónne a asynchrónne (indukčné) [2].

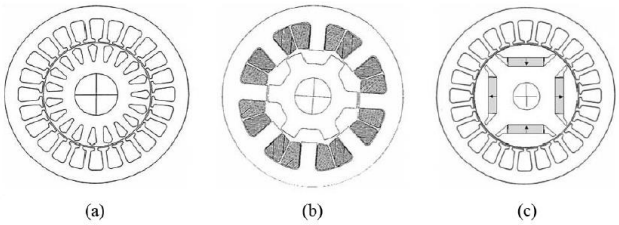

Obr. 1. Najpoužívanejšie elektromotory (a) indukčný motor (b) reluktančný motor (c) synchrónny motor s permanentnými magnetmi [3]

Medzi najobľúbenejšie motory (obr. 1) patria motory s permanentným magnetom, ktoré dominujú svojimi vlastnosťami. Problém pri tomto type motora nastáva v obmedzenom množstve vzácnych permanentných magnetov na zemi. Riešením sa zdajú byť indukčné a reluktančné motory, ktoré neobsahujú permanentné magnety a v súčasnosti sú najviac vyvíjané [4, 5].

Hlavné požiadavky elektromotorov:

- Vysoký okamžitý a merný výkon.
- Vysoký krútiaci moment aj v malých rýchlostiach.
- Rýchly nástup výkonu.
- Vysoká spoľahlivosť a účinnosť.
- Priaznivá cena.

1.1 Synchrónny motor

Synchrónne motory sa používajú najčastejšie v kombinácii s permanentnými magnetmi (PMSM), ktoré sú umiestnené buď na povrchu alebo vo vnútri rotora (obr. 2).

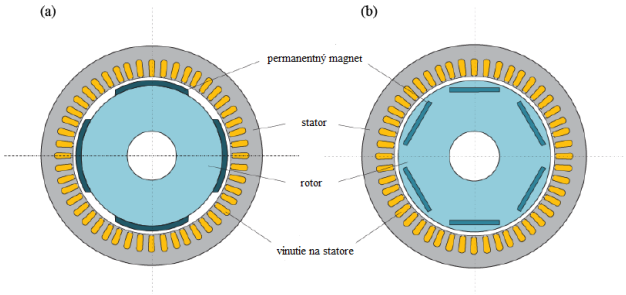

Obr. 2. Priečny rez motorov s permanentnými magnetmi (rôzne uloženia magnetu) (a) permanentné magnety na povrchu rotora, (b) permanentné magnety vo vnútri rotora [7]

Magnety používané v synchrónnych motoroch sú prevažne neodymové [4]. Tieto motory, ako už názov napovedá, sú charakteristické pre synchrónny pohyb rotora a statora. Konštrukcia bez magnetu obsahuje rotor s budiacim vinutím, ktoré vyžaduje stály prívod prúdu pre vytvorenie magnetického poľa. Stator sa skladá z plechov, v ktorého drážkach je uložené trojfázové vinutie produkujúce magnetické pole pod striedavým napätím [6, 7]. V statore sa pomocou striedavého trojfázového prúdu tvorí rotujúce magnetické pole. Konštantné magnetické pole rotora spôsobené permanentnými magnetmi integruje s indukovaným poľom statora, a tým sa motor otáča. Pre rozbeh tohto typu motora sa často používa tzv. Rozbehová klietka, ktorá je hlavnou časťou indukčných motorov [7].

Výhody PMSM:

- Rotor nepotrebuje prívod napätia.
- Vysoký merný výkon vďaka silným magnetom.
- Nízka hlučnosť a vibrácie.
- Výkonnejší než indukčný motor.

Nevýhody PMSM:

- Vysoká cena magnetov.
- Citlivé na pracovnú teplotu.

1.2 Asynchrónny (indukčný) motor

Indukčný motor bol vynájdený v roku 1882 Nicolom Teslom a je to najpoužívanejší elektromotor skrz všetky oblasti priemyslu. Jeho obľúbenosti prispieva fakt, že je možné tento motor napájať striedavým prúdom bez meniča, a tým dodávať konštantné otáčky. V elektromobile sa k zmenám rýchlosti otáčok používa menič. Tento typ motora sa skladá zo statora s trojfázovým vinutím a rotora v tvare klietky (anglicky squirrel-cage) (obr. 3) [5].

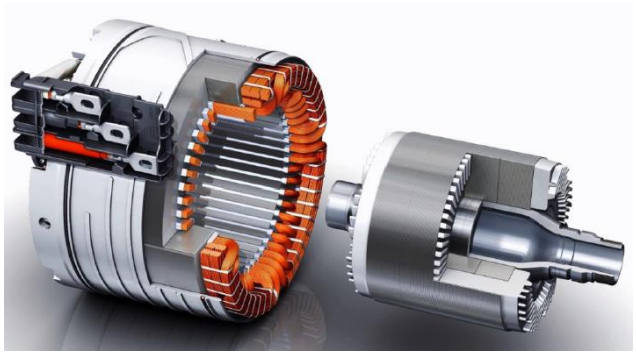

Obr. 3. Trojfázový asynchrónny motor Audi [9]

V statore sa pomocou striedavého trojfázového prúdu tvorí rotujúce magnetické pole, ktoré indukuje prúd na uzavretej klietke rotora. Tento indukovaný prúd vyvolá v rotore magnetický tok, ktorý integruje so statorom a spôsobí žiaduce otáčania rotora. Toto otáčanie sa však nikdy nemôže vyrovnať rýchlosti otáčania magnetického poľa v statore [6, 7, 8].

Výhody asynchrónneho motora:

- Vysoká spoľahlivosť a nízka cena.
- Minimálne nároky na údržbu.
- Nie je obmedzený teplotou.

Nevýhody asynchrónneho motora:

- Malý rozsah otáčok.
- Malý krútiaci moment zo štartu.

1.3 Spínaný reluktančný motor

Ďalším zo sľubných kandidátov pre použitie v elektromobiloch je spínaný reluktančný motor (SRM). Ako už môže názov napovedať, pre svoj princíp využíva magnetický odpor - reluktanciu. Tento motor má relatívne dlhú históriu a prvé zmienky o ňom môžeme nájsť už v roku 1923, kedy J. K. Kocky v článku "Polyphase Reaction Synchronous Motors" predstavuje koncept reluktančného motora a jeho potenciál [10]. Aj napriek veľkému potencionálu tohto typu motora v minulosti nebol používaný kvôli jeho náročnosti pri riadení frekvenčnými meničmi. Medzi hlavné prednosti reluktančného stroja patrí jednoduchá konštrukcia, nízke výrobné náklady, veľké rozpätie otáčok a výborný výkon. Práve tieto vlastnosti robia z reluktančného motora vhodného kandidáta na použitie v elektrických vozidlách. Naopak, medzi hlavné nevýhody môžeme zaradiť vyššiu hlučnosť a nutnosť použitia elektroniky na sledovanie polohy rotora. Za ďalšiu nevýhodu možno tiež považovať použitie meniča pre správne napájanie vinutia na statore [8].

SRM má na rozdiel od konvenčnej synchrónnej verzii tohto motora póly na rotore aj statore. Stator nesie na každom póle vinutie, zatiaľ čo rotor je bez akéhokoľvek vinutia či permanentných magnetov. Na rotore sa pri zavedení prúdu do zodpovedajúcich pólov statora tvorí magnetické pole. Následne sa rotor snaží dostať na miesto s čo najmenším magnetickým odporom a tým sa roztočí. Ďalej je prúd posielaný do ďalších pólov na statore a tento proces sa opakuje. Počet pólov na rotore býva spravidla menší ako na statore (obr. 4) kvôli zamedzeniu tzv. mŕtveho bodu, t. j. poloha pri ktorej by motor nemal žiaden krútiaci moment [3, 11].

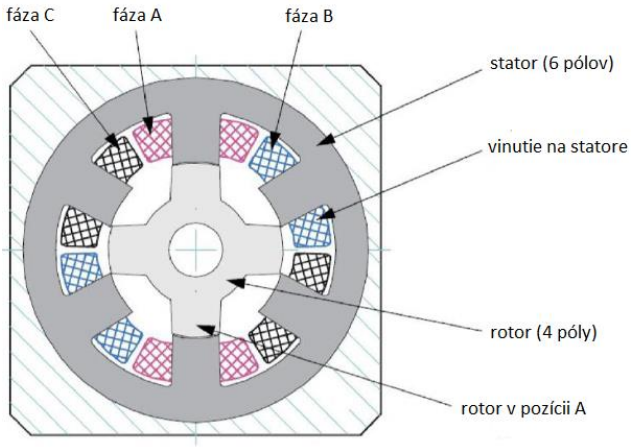

Obr. 4. Schéma reluktančného motora [12]

Výhody reluktančného motora:

- Jednoduchá konštrukcia.
- Nízke výrobné náklady.
- Vysoký merný výkon.
- Účinnosť až 95 %.
- Pracuje aj pri vysokých teplotách.
- Široké rozpätie otáčok.

Nevýhody reluktančného motora:

- Vyššia hlučnosť.
- Zložité riadenie.
- Náročné na presnosť.
- Cena.

2 INTEGROVANÉ ELEKTRICKÉ POHONY

E-axle (electric axle) je kompaktné a nákladovo atraktívne riešenie elektrického pohonu pre akumulátorové elektrické vozidlá a hybridné aplikácie. Elektromotor, výkonová elektronika a prevodovka sú spojené v kompaktnom celku, ktorý priamo poháňa nápravu vozidla. To pomáha robiť elektrické pohony menej zložitými a jednoduchšími. Okrem toho sa pohonná jednotka stáva lacnejšou, kompaktnejšou a efektívnejšou. Medzi hlavné výhody týchto kompaktných pohonných jednotiek môžeme zaradiť prijateľnú cenu, nízku hmotnosť a univerzálnosť pre rôzne použitie [13]. Priekopníkom vo vývoji tejto technológie sa stala spoločnosť GKN, ktorá ako prvá v roku 2014 začala so sériovou výrobou v spolupráci s automobilkou BMW. Práve BMW použilo ich E-axle v hybridnom automobile BMW i8. Toto riešenie je pre automobilky veľmi atraktívne z dôvodu ľahkého zabudovania E-axlu a možnosti prepracovať existujúce modely na elektrické verzie.

Najnovším produktom výrobcu GKN (obr. 5) je E-axle eTwinsterX disponujúci dvojstupňovou koaxiálnou prevodovkou, synchrónnym motorom s permanentnými magnetmi, diferenciálom a dvoma spojkami. Tento systém bol predstavený v spolupráci s automobilkou Jeep na modeli Renegade. Prevodové pomery sú 17 a 9,5, výkon elektromotora 120 kW, krútiaci moment až 3 500 Nm a maximálne otáčky 18 000 min^{-1}. Značku GKN a jej verzie E- axle je možné nájsť napríklad v automobiloch BMW, Volvo alebo Porsche [14].

Obr. 5. E–axle GKN eTwinsterX [14]

Ďalším silným hráčom na poli elektromobility je nemecký gigant Bosch so svojim riešením (obr. 6) obsahujúcim elektromotor, prevodovku a výkonovú elektroniku. E-axle značky Bosch je veľmi variabilný a zákazník si môže vybrať rôzne výkonné motory od 50 kW pre malé automobily alebo hybridy až po 300 kW pre čisto elektrické automobily. Krútiaci moment je v rozmedzí 1 000 až 6 000 N·m [15].

Obr. 6. E-axle spoločnosti Bosch [15]

Nemecký výrobca Schaeffler predstavil svoj variant E-axlu (obr. 7). Za zmienku určite stojí E-axle spoločnosti Schaeffler a použitie planétového diferenciálu, ktorý nahrádza tradičný kužeľový. Toto riešenie je veľmi kompaktné a jeho malé rozmery v radiálnom smere nechávajú viac priestoru pre motor samotný. Prevodovka je tiež planétová a jej prevodový pomer je 15. Elektromotor je synchrónny s permanentnými magnetmi disponujúci výkonom 150 kW, maximálnym krútiacim momentom 3 750 N·m a maximálnymi otáčkami až 18 200 min^{-1}. Hmotnosť celého systému v spomínanej konfigurácii je 75 kg [16].

Obr. 7. E-axle spoločnosti Schaeffler [16]

ZÁVER

Elektromotory sú nenahraditeľnou súčasťou elektromobilu, na druhej strane, ich jednoduchá konštrukcia sa už zrejme nedočká, na rozdiel napríklad od batérií, žiadneho veľkého prelomu. Elektromobily používajú najčastejšie synchrónne motory s permanentnými magnetmi, ktoré ponúkajú ideálny pomer medzi dodávaným krútiacim momentom a účinnosťou. Hlavným problémom týchto motorov a dôvod pre hľadanie iných riešení je nutnosť použitia drahých permanentných magnetov. V súčasnej dobe sú jedinou možnou alternatívou indukčné motory. Jednosmerné motory (DC) patrili medzi obľúbené, avšak v súčasnej dobe sa už v elektromobiloch často nepoužívajú. Zaujímavou možnosťou môže byť použitie reluktančných motorov, ktoré majú, vďaka svojim vlastnostiam, veľký potenciál presadiť sa a nahradiť používané elektromotory v súčasnosti.

Poďakovanie

Tento dokument bol vypracovaný s podporou grantového projektu KEGA 009TUKE-4/2020 „Prenos digitalizácie do vzdelávania v študijnom programe Podnikové hospodárstvo a ekonomika“. Táto práca bola podporená Agentúrou na podporu výskumu a vývoja na základe Zmluvy č. APVV-19-0328.

LITERATÚRA

[1] ŠKODA Storyboard (2020): *Jak funguje elektrický motor*. [online]. [cit. 12.10.2020]. Dostupné na internete: <https://www.skoda-storyboard.com/cs/e-mobilita-cs/jak-funguje-elektricky-motor-10-otazek-a-odpovedi/>.

[2] KRÁLOVÁ, M. (2020): *Elektromotory*. [online]. Plzeň, Techmania Science Center, [cit. 12.10.2020]. Dostupné na internete: <https://edu.techmania.cz/de/node/1713 >.

[3] ZHU, Z. - HOWE, D. (2007): *Electrical Machines and Drives for Electric, Hybrid, and Fuel Cell Vehicles.* Proceedings of the IEEE, Institute of Electrical and Electronics Engineers (IEEE), 95(4), 746-765. DOI: 10.1109/jproc.2006.892482. ISSN 0018 9219. Dostupné na interete: <https://dx.doi.org/10.1109/JPROC.2006.892482>.

[4] CHAN, C. (2002): *The state of the art of electric and hybrid vehicles.* Proceeding of the IEEE, 90(2), 247-275. DOI: 10.1109/5.989873. ISSN 1558-2256.

[5] NIKOWITZ, M. (2016): *Advanced hybrid and electric vehicles*. System optimization and vehicle integration, Springer International Publishing. ISBN 978-1 4471-6781-5.

[6] EHSANI, M. - GAO, Y. - LONGO, S. - et al. (2018): *Modern electric, hybrid electric and fuel cells vehicles.* Third edition. Boca Raton: CRC Press, ISBN 978-1-4987-6177-2.

[7] EMADI, A. (2017): *Advanced electric drive vehicles.* Boca Raton: CRC Press, ISBN 978- 113-8072-855.

[8] HASHEMNIA, N. - ASAEI, B. (2008): *Comparative study of using different electric motors in the electric vehicles.* In: 2008 18th International conference of electrical machines. IEEE, s. 1-5. DOI: 10.1109/icelmach.2008.4800157. Dostupné na internete: <https://dx.doi.org/10.1109/ICELMACH.2008.4800157>.

[9] AUDI (2020): *Asynchronous motor*. [online]. Ostfildren, [cit. 12.10.2020]. Dostupné na internete: <https://www.audi mediacenter.com/en/photos/detail/asynchronous-motor-70267>.

[10] ANDERSON, A. (2001): *Development history.* Newnes Power Engineering Series. Oxford: Newnes, s. 6-33. DOI: https://doi.org/10.1016/B978075065073-1/50004-3. ISBN 978-0-7506-5073-1. Dostupné na internete:<http://www.sciencedirect.com/science/article/pii/B9780750650731500043>.

[11] HUGHES, A. - DRURY, B. (2013): *Electric Motors and Drives.* DOI: 10.1016/C2011-0-07555-5.

[12] KOPECKÝ, L. (2008): *Reluktanční motor a elektromobil*. In: Free-energy. [online]. [cit. 13.10.2020]. Dostupné na internete: <http://free-energy.xf.cz/inventions/srm.pdf>.

[13] HOLMES, F. (2018): *Integrated e-axles create flexible e-powertrains.* Automotive World, Veľká Británia. [online]. [cit. 14.10.2020]. Dostupné na internete: <https://www.automotiveworld.com/articles/integrated-e axles-create-flexibile-epowertrains/>.

[14] SMITH, D. (2019): *GKN demos eTwinster* Birmingham. [online]. [cit. 14.10.2020]. Dostupné na internete: <https://www.sae.org/news/2019/03/gkn-etwinster-bev-e-axle-debut>.

[15] BOSCH (2020): *EAxle*. [online]. Nemecko: Bosch [cit. 14.10.2020]. Dostupné na internete: <https://www.bosch-mobility-solutions.com/en/products and-services/passenger-carsand-light-commercial-vehicles/powertrain-systems/electric-drive/eaxle/>.

[16] SHAEFFLER (2018): *Electric axle drive*. In: Schaeffler [online]. Nemecko: Schaeffler. [cit. 14.10.2020]. Dostupné na internete: <http://schaeffler events.com/symposium/lecture/h8/index.html>

Nový obraz budúcnosti a trendy v globálnej trhovej ekonomike v 21. storočí, adaptácia podniku na budúci vývoj – organizačný rozvoj podniku

Ivan Litvaj, Ing., PhD.*
Katedra elektroenergetiky a elektrických pohonov, Fakulta elektrotechniky a informačných technológií,
Žilinská univerzita v Žiline,
Univerzitná 8215/1, 010 26 Žilina, Slovenská republika.
E-mail: ivan.litvaj@feit.uniza.sk, Tel.: + 421 41 513 2168

A new picture of the future and trends in the global market economy in the 21st century, an adaptation of a company to future development - organizational development of a company

Abstract: Budúcnosťou, teda možným a predpokladaným budúcim vývojom trhovej ekonomiky, sa môžeme a vieme do určitej miery zaoberať, odhadovať však tento možný budúci vývoj je veľmi, skutočne veľmi náročné, o tom ani nik nepochybuje. Môžeme sa o to pokúsiť napr. na základe poznania doterajšieho vývoja v predmetnej oblasti a na tomto základe vieme do určitej miery predpovedať alebo predpokladať budúci vývoj, pozorovaním situácie vieme odhadnúť možný budúci vývoj, dôkladným sledovaním, analyzovaním a hodnotením jednotlivých symptómov v ekonomike, v spoločnosti a pod. tiež vieme predpokladať budúci stav. V tomto príspevku sa na vymedzenom priestore zaoberám budúcnosťou podnikov v globálnom charaktere, v globálnej trhovej ekonomike, vývojom ktorý sa v budúcnosti predpokladá, že sa uskutoční, tiež sa zaoberám trendami pri riadení podnikov, to je nie menej dôležitá časť môjho príspevku. Je to veľmi ťažká úloha písať o budúcnosti, je to ťažká a zložitá téma. Veď už P. Drucker povedal: „Pokúšať sa predpovedať budúcnosť je ako pokúšať a šoférovať po poľnej ceste s vypnutými svetlami pozerajúc sa len cez zadné okno.“

ÚVOD

V posledných rokoch sa vo vyspelých aj rozvojových krajinách, hlavne v odborných a podnikateľských kruhoch intenzívne diskutuje aktuálna závažná a potrebná téma - budúcnosť manažmentu. Hľadajú sa odpovede na otázky typu - Aký vlastne bude manažment v budúcnosti? Ako sa budú podniky riadiť v 21. storočí? Akými metódami a postupmi budeme riadiť podniky v 21. storočí? Aké budú podniky v 21. storočí? K týmto témam sa vyjadrujú mnohé vplyvné osobnosti z viacerých oblastí, ktorí píšu o zmenách v manažmente v 21. storočí. Veľa významných autorov, väčšina autorov sa však zhoduje na určitých záveroch, napr. na tom, že manažment v 21. storočí bude odlišný, skutočne odlišný, bude založený na iných princípoch, ako mal manažment v 20. storočí. V manažmente vznikajú nové trendy, paradigmy, ako reakcia na vývoj v ekonomike, v globálnej trhovej ekonomike. Tieto zmeny si vyžadujú zmenu prístupu manažmentu a všetkých zamestnancov v podniku, a to z dôležitého dôvodu, aby podnik aj v meniacich sa podmienkach globálnej, trhovej ekonomiky, aby podnik v súčasnej turbulentnej globálnej ekonomike ostal aj naďalej konkurencieschopný, životaschopný. Uvedomujem si pritom, keď chcem písať na tomto vymedzenom priestore o budúcom vývoji a trendoch v globálnej ekonomike reálnu nemožnosť úplne, dostatočne a komplexne predpovedať a popisovať budúcnosť vonkajšieho ekonomického a spoločenského prostredia.

Súčasnej globálnej ekonomike môžeme dať tento prívlastok - turbulentná, a preto jednou z najdôležitejších, rozhodujúcich úloh pre manažmenty v podnikoch, v organizáciách aj v rôznych inštitúciách je monitorovať prostredie a adaptovať sa na zmenené, na neustále sa meniace prostredie, byť, ostať aj v novom, zmenenom prostredí konkurencieschopný. Treba to zdôrazniť, lebo platí nasledovné - manažment v podnikoch by mal mať takú internú stratégiu, aby sa dokázal adaptovať na zmenené a neustále sa meniace vonkajšie ekonomické prostredie (zmeny sú napr. hyperkonkurencia, nárast neurčitosti na trhu, diskontinuita vývoja trhu, atď.), pričom platí, že frekvencia zmien narastá. Mnohí významní autori písali a píšu aj v omnoho širších súvislostiach nielen o budúcnosti manažmentu, píšu o ďalekosiahlejších, historických zmenách v spoločnosti, ktoré

sa postupne rysujú a sú nevyhnutné, zmeny sú nevyhnutné a nemajú alternatívu. Mnohí autori o tom píšu, ale taká je aj nálada v spoločnosti, myslím si, som o tom presvedčený. Autori píšu o transformácii v spoločnosti, širšej transformácii v spoločnosti, je to reakcia, prirodzená reakcia na nevyhovujúci dlhodobo už neudržateľný stav súčasnej spoločnosti vo viacerých oblastiach v mnohých demokratických krajinách. Áno, je to reakcia na dlhodobý, dlhoročný vývoj v spoločnosti v mnohých krajinách. Autori sa venujú témam ako sú napríklad kritika politických a ekonomických elít, morálna kríza, kritika previazanosti politiky a biznisu, priama demokracia, obrovská majetková nerovnosť, ktorá je realitou, silnejúca nedôvera občanov k politickým elitám, k vládam, k politickému systému, kritika súčasného ekonomického a spoločenského zriadenia. Pomaly ale neustále silnie tlak verejnosti na zvyšovanie transparentnosti v politickom a spoločenskom živote, ale neustále silnie tlak jednotlivcov, rôznych združení, zoskupení, tretieho sektora aj verejnosti na dodržiavanie morálnych princípov v politike, v ekonomike, v štátnej a lokálnej správe, narastá odpor verejnosti voči korupcii. Ja tieto zmeny podporujem, tiež si myslím, že sú nevyhnutné. Nebývalý rozmach zaznamenávajú sociálne siete a diskusie k témam, ktoré som uviedol vyššie. Toto sú samozrejme len niektoré spomenuté kvalitatívne zmeny, trendy v spoločnosti, ktoré sa dejú a myslím si, že sa budú aj naďalej diať a budú pokračovať. Výraznejšie zmeny sa prejavujú a budú sa ďalej uskutočňovať aj v manažmente samotnom. V minulom storočí sa považovali za nevyhnutné predpoklady konkurenčnej úspešnosti podniku - kapitál, investície, technológie, produktivita, kvalita. V 21. storočí nastáva zmena, významná zmena, ťažisko sa od uvedených predpokladov konkurencieschopnosti podnikov presúva, presúva sa napr. ku „ekonomike vedomostí“, ku inováciám. A toto sú zásadné zmeny. Toto konštatovanie má širšie súvislosti aj zdôvodnenie. Globalizácia neustále postupuje, globalizácia predstavuje v súčasnosti spolu s informačnými a komunikačnými technológiami, technológiami ako takými a ich rozmachom tie najdôležitejšie trendy, mega trendy vo svetovej civilizácii, prirodzene so všetkými svojimi výhodami a nevýhodami, aj hrozbami. Pre 21. storočie je mnohými odborníkmi z oblasti manažmentu predpovedané obdobie kríz, latentných kríz v globálnej ekonomike, sú tu neurčitosť, nerovnováha, neustále zmeny na trhu, ktoré sa ešte zrýchľujú. To sú znaky súčasnej a budúcej trhovej ekonomiky, tak ako to predpovedal P. Drucker „prichádza vek diskontinuity.“ V súčasnom období má čoraz väčší význam pre podniky prekonávanie prekážok na rýchlo sa meniacom globálnom trhu. Stanovovanie strategických cieľov manažmentom podniku musí zohľadniť súčasný a predpokladaný vývoj, prijať zmeny v podnikateľskom modeli podniku, tieto zmeny vyvolávajú tlak na podniky napr. tlak na inovácie výrobkov ale aj inovácie manažérskych metód a stratégií. Áno, nehovorme čisto len o inováciách výrobkov, zaiste sú nevyhnutné a prirodzené, to je fakt, že sú nevyhnutnou podmienkou, ak si chce podnik udržať svoju konkurencieschopnosť, o tom nikto nepochybuje. Ale tak isto je nevyhnutné tiež hovoriť o inováciách manažmentu, a to z toho dôvodu, lebo zmena samotná sa stáva základom, jadrom manažmentu. Preto musí manažment inovovať svoje prístupy ku riadeniu podniku. Turbulentné zmeny v globálnej ekonomike, nárast rizík a neurčitostí si inovácie v manažmente jednoducho vyžadujú, sú nevyhnutné, ak chce podnik dlhodobo konkurovať a dlhodobo prosperovať v prostredí globálnej konkurencie. Manažment podniku musí tento fakt akceptovať a stotožniť sa s ním. Tak, ako sa mení všetko okolo nás, menia sa aj ciele, princípy, zásady, metódy a nástroje riadenia podnikov, to je pravda, je to dané vývojom trhu, ekonomiky a celkovým vývojom spoločnosti. Ku inováciám manažmentu môžeme priradiť zmeny funkcií samotných manažérov, zmeny organizačných štruktúr, nové užitočné manažérske systémy aplikované v podniku a pod. Sú to mnohokrát práve inovácie manažmentu, ktoré zmenili na nepoznanie už stagnujúce podniky a premenili ich na prosperujúce. Je potrebné zvyšovať tempo inovácií manažmentu v podniku, zvyšovať tempo uplatňovania nových doteraz nepoužívaných manažérskych stratégií a systémov, zvyšovať tempo celkovej obnovy v podniku. Nemôžete riadiť podnik v 21. storočí stále tými istými metódami, ako ste ho riadili v 20. storočí. Vyššie sme písali o súčasnom svete a o trendoch v ňom, napr. o globalizácii, o zmenách v manažmente ktoré sa dejú a budú diať, o zmenách na trhu, zmenách v podnikoch, v spoločnosti a pod. Tiež píšeme, že mnohí autori píšu širšie o ďalekosiahlejších zmenách, o postupnej transformácii v spoločnosti, ktorá je na pulze doby. Jednou z týchto zmien je transformácia a prechod ekonomiky na znalostnú ekonomiku, tak ako o tom písal napríklad P. Drucker, významný americký a celosvetový odborník na manažment.

1 TRANSFORMÁCIA AKO PRECHOD K SPOLOČNOSTI ZNALOSTI

Podľa P. Druckera je prebiehajúca transformácia ďalšou z radu transformácií, ktoré pravidelne nastávajú v histórii západu v priebehu niekoľkých storočí. Takúto transformáciu charakterizuje proces, keď počas niekoľkých krátkych desaťročí spoločnosť pretvára samu seba - mení sa jej pohľad na svet, základné hodnoty, sociálna a politická štruktúra,

umenie, kľúčové inštitúcie a po 50-tich rokoch je tu celkom nový svet. My sami, hovorí Drucker, teraz žijeme v čase takejto transformácie, keď sa tvorí post-kapitalistická spoločnosť. Prebiehajúca transformácia však nie je obmedzená iba na západnú spoločnosť, ale ide o transformáciu celej civilizácie. Táto dnešná transformácia sa neskončí skôr ako v roku 2010 alebo 2020, ale už dokázala zmeniť politickú, ekonomickú, sociálnu a mravnú tvar sveta. Podľa Druckera je v podstate isté, že prvotným zdrojom budú znalosti.

To, že znalosti sú dnes aplikované na poznanie, je tretí a možno aj posledný krok v transformácii poznania. Manažment je potom poskytovanie znalostí o tom, ako môže byť dnešné poznanie čo najlepšie využité, aby prinášalo výsledky. Okrem toho sú znalosti využívané na systematické inovovanie. Túto tretiu zmenu v dynamike poznania nazýva Drucker manažérskou revolúciou. Rozšírenie manažérskej revolúcie po celom svete trvalo menej ako 50 rokov, kým revolúcii produktivity to trvalo 70 rokov a priemyselnej revolúcii 100 rokov. Prínos, ktorý určitá krajina alebo firma získava zo znalostí, sa nepochybne musí v stále významnejšej miere stávať určujúcim faktorom ich konkurencieschopnosti. A o ich ekonomickom a sociálnom úspechu a ich celkovej výkonnosti bude čoraz viac rozhodovať produktivita znalostí. Mnohé krajiny, ktoré majú nízku produktivitu znalostí, majú aj ekonomické problémy a naopak, krajiny, ktoré majú vysokú produktivitu znalostí, sú vysoko konkurencieschopné [1].

2 SÚČASNÉ TRENDY V TEÓRII A PRAXI MANAŽMENTU

Súčasné trendy v teórii a praxi manažmentu. Ako ich môžeme stručne opísať? Treba povedať, že zatiaľ čo 80. roky 20. storočia boli poznamenané najmä snahou účinne reagovať na japonskú výzvu, ďalšie roky boli silno poznamenané nástupom globalizácie a jej dôsledkami. Vo vyspelých krajinách nasýtenosť trhu spomaľuje rast potrieb, to vyvoláva potrebu prechodu od „trhu dodávateľov“ k „trhu zákazníkov. Rastie tlak na konkurencieschopnosť, tlak na potrebu vyrábať lacno a kvalitne, rýchlo inovovať, poskytovať vysokú úroveň služieb. Rýchlo sa rozvíjajú informačné technológie a neustále rastú možnosti ich využitia. Globalizácia trhu prináša nové výzvy a nové možnosti, no na druhej strane rozpory a ohrozenia. Posilňuje sa vplyv nadnárodných spoločností, ktoré najmä po pádu socializmu expandujú do nových krajín. Zmena dynamiky externého prostredia prináša okrem príležitostí aj nečakané riziká a hrozby. Z toho všetkého vyplývajú nové problémy a nové požiadavky na ich riešenie. Do popredia manažérskej teórie a praxe sa dostávajú také témy, ako nové koncepcie v strategickom manažmente, manažment zmeny, reinžiniering, projektový manažment, manažment kvality, benchmarking, rozvoj marketingu, informačný manažment, informatizácia spoločnosti, lean (štíhly) manažment, zvýšenie hospodárnosti a efektívnosti, dôraz na pridanú hodnotu, nové trendy rozvoja a využívania ľudských zdrojov, zmeny v prístupe k vedeniu ľudí, a pod.

Zdroje a východiská súčasného manažmentu sú, myslím si veľmi výstižne, popísané na nasledovnom obr. 1.

Obr. 1. Vplyvy na súčasný manažment [2]

Nepochybne je faktom, že v globálnej ekonomike pozorujeme zmeny vonkajšieho prostredia, niektoré z nich som stručne na vymedzenom priestore popisoval vyššie. Tieto zmeny sa zákonite prejavujú aj v mikroekonomike. Treba na tomto mieste tiež podotknúť, že pochopenie rozsahu a rýchlosti vonkajším zmien sa prejavuje rôzne v jednotlivých podnikoch a organizáciách. Aj adaptácia podnikov na tieto zmeny sa prejavuje rozdielne v jednotlivých podnikoch, toto má potom prirodzene za následok aj rôznu úroveň konkurencieschopnosti jednotlivých podnikov a organizácií. Napríklad inovácie sú chápané ako nevyhnutný predpoklad konkurencieschopnosti podniku, inovácie produktov, ale aj inovácie v manažmente podnikov, to sú dôležité oblasti zmien v podnikoch. Súčasnosť a ešte viac budúcnosť si bude vyžadovať, aby všetci zamestnanci mali byť upovedomení a stotožnení s tým, že podnik sa zbavuje zabehnutých návykov a stereotypov. Takto, týmto smerom by mala byť nastavená podniková kultúra. Je to filozofia manažmentu, filozofia manažmentu zmeny a cieľom týchto zmien je zlepšenie systému riadenia v podniku a udržanie, prípadne zlepšovanie konkurencieschopnosti podniku. Platí nasledovné, zamestnanci majú schopnosť uvažovania nad rámec zabehnutého systému riadenia v podniku. Tvorivosť a iniciatíva sú prirodzené ľudské vlastnosti, to je nesporným faktom. Je však úplne bežné v podnikovej praxi, že podniky pracujú stále rovnako. Ale situácia sa pre podnikanie mení, pre 21. storočie je charakteristická - zmena, zmeny, narastajúca rýchlosť a frekvencia zmien, ako som už písal. A preto budú musieť podniky učiť zamestnancov a podporovať ich aby uvažovali

nad rámec súčasných, zabehnutých pomerov, boli iniciatívni a inovatívny. Pri zlepšovaní, pri zdokonaľovaní v podniku, nič nie je posvätné a nedotknuteľné. Podnik je inovatívny, inovuje nielen výrobky, ale aj používané manažérske stratégie a metódy pri riadení podniku, lebo nemenia sa len výrobky, ale aj princípy v riadení podnikov a používané manažérske systémy, ktoré reflektujú dynamiku vývoja externého prostredia, reflektujú zmeny na trhu a pomáhajú podnikom úspešne sa na tieto zmeny adaptovať. Ak používate autoritatívny prístupu v riadení, je to prežitok, nahraďte ho spoluprácou, participáciou na riadení lebo autoritatívny prístup v riadení podniku sa nevypláca, na druhej strane nechajte zamestnancom dostatočnú autonómiu pri plnení úloh, vyplatí sa. Akokoľvek schopný je majiteľ alebo manažér, jednoducho nie je schopný obsiahnuť všetky potrebné vedomosti nevyhnutné pre efektívne riadenie podniku. Hlavný zmysel akejkoľvek inovácie v manažmente je zmena, užitočná zmena v systéme riadenia v podniku alebo nová manažérska stratégia s cieľom zvýšiť efektívnosť procesov a zvýšenie konkurencieschopnosti podniku. Doteraz nebývalý rozvoj a rozmach vedy, techniky a nových technológií je iba jedným (i keď veľmi významným) z množstva ďalších faktorov ktoré rozhodujú a budú rozhodovať o úspechu či neúspechu podniku v konkurenčnom boji. Tými ďalšími faktormi sú napr. inovácie, inovácie či už výrobkov alebo v systéme riadenia podniku.

3 KONKURENCIESCHOPNOSŤ A ROZVOJ PODNIKU V BUDÚCNOSTI

Súčasný podnik, jeho konkurencieschopnosť, jeho schopnosť inovácií, jeho prosperita a celkový rozvoj sú podmienené aj jeho schopnosťou správne, adekvátne a rýchlo reagovať interne v podniku na externé prostredie a zmeny v tomto externom prostredí na trhu, ktoré sú, ako som už písal v tomto článku, stále väčšie a rýchlejšie. Podnik, ak chce byť obchodne a ekonomicky úspešný, musí sa adaptovať na trh, zmeny na trhu, musí sa adaptovať, správne reagovať na tieto zmeny. Tieto zmeny sú výzvou pre podnik. Toto treba podnikom zdôrazniť, toto si musia manažéri, ktorí riadia podniky uvedomiť, s týmto faktom sa musia stotožniť. Podniky musia prejsť prechodom, musia sa vydať na cestu organizačného rozvoja. Tak, ako o tom píše napríklad M. Antošová: „Organizačný rozvoj ako reakcia na zmeny je súčasťou prechodu od priemyselnej spoločnosti do spoločnosti založenej na znalostiach, ktorej ekonomickou základňou je tvorba a výmena tovarov nemateriálnej povahy a služieb“ [3].

3.1 Organizačný rozvoj podniku

Organizačný rozvoj sa týka plánovania a realizácie programov zlepšovania efektívnosti fungovania organizácie a jej reakcií na zmeny. Cieľom je zabezpečiť plánovitý a premyslený prístup k zlepšovaniu efektívnosti organizácie. Za efektívnu možno považovať takú organizáciu, ktorá plní svoj účel tým, že uspokojuje priania a potreby všetkých, ktorí sú na nej zainteresovaní, prispôsobuje svoje zdroje príležitostiam, pružne sa adaptuje na zmeny prostredí a vytvára kultúru, ktorá zvyšuje oddanosť, kreativitu a vzájomnú dôveru. Ak chápeme organizačný rozvoj ako proces, nie štruktúru, rozhodujúcou otázkou je postup - t. j. AKO, nie ČO robiť. Proces sa týka spôsobu, akým ľudia konajú a navzájom na seba pôsobia. Je to záležitosť rolí, ktoré ľudia hrajú, aby zvládli udalosti a situácie, ktorých sa zúčastňujú iní ľudia a aby sa adaptovali na meniace sa okolnosti.

Organizačný rozvoj je rozsiahly a všeobecnejší termín pre prístupy smerujúce k zmene procesov, kultúry a správania sa v organizácii ako celku alebo v niektorej jej časti. Tieto zmeny sa sústreďujú na správanie sa skupín a jednotlivcov, ale vždy v súvislosti s organizáciou a s tým, čo je potrebné urobiť pre zlepšenie jej efektívnosti [3].

Podľa M. Armstronga tieto prístupy zahŕňajú:

- Rozvoj organizácie.
- Riadenie zmeny.
- Transformáciu organizácie.
- Komplexné riadenie kvality.
- Riadenie pracovného výkonu zamestnancov.
- Profesijné vzdelávanie a rozvoj zamestnancov.
- Podnikovú kultúru a jej zmenu.
- Reeingineering podnikových procesov [4].

Rozvoj organizácie je chápaný ako súčasť organizačného rozvoja a je najčastejšie reakciou na zmenu, stratégiou zameranou na zmenu presvedčenia, postojov, hodnôt ľudí a štruktúry organizácie tak, aby sa mohla lepšie prispôsobiť novým technológiám, trhom, výzvam a rýchlosti samotnej zmeny. Je to plánovaný systematický proces. Organizácia je často donútená k svojej transformácii v dôsledku vzniknutých problémov, nových výziev, či vonkajších tlakov.

Riadenie zmeny predpokladá proces, ktorý začína uvedomením si potreby zmeny. Analýza takejto situácie a faktorov, ktoré ju spôsobili, vedie k diagnóze jej špecifických charakteristík a k určeniu smeru, ktorým budú podniknuté ďalšie kroky. Ďalej je nutné rozhodnúť aké cesty budú zvolené, aby sa organizácia dostala do žiaducej situácie. Práve obdobie prechodu je kritickou fázou procesu zmeny, keď sa objavujú problémy zavádzania zmien

týkajúce sa napr. odporu niektorých ľudí k zmenám, nízkej stability, vysokej miery stresu, energie zameranej nesprávnym smerom, vzniku konfliktov, straty podnetov a podobne. Tí ľudia v organizácii, ktorí chcú zmenu, musia byť dostatočne pevní vo svojich cieľoch, ale aj dostatočne pružní, ak ide o prostriedky.

Transformácia všeobecne predpokladá zmenu tvaru, štruktúry, či povahy niečoho. Transformácia organizácie je procesom, ktorý zabezpečí, že organizácia môže vytvárať a realizovať programy hlavných zmien s cieľom strategicky reagovať na nové požiadavky a trvalo efektívne fungovať v dynamickom prostredí, v ktorom pôsobí. Aktivity transformácie organizácie sa môžu týkať radikálnych zmien štruktúry, kultúry a procesov v organizácii. Predpokladom jeho úspešnej realizácie je líder, ktorý dokáže aktivizovať a získať ostatných zamestnancov, aby sa usilovali o dosiahnutie spoločných vyšších cieľov.

Komplexné riadenie kvality je intenzívne, dlhodobé úsilie smerujúce k vytvoreniu a udržaniu vysokej úrovne kvality výrobkov a služieb, ktorú očakávajú zákazníci. V organizácii môže mať značný vplyv na vytváranie kultúry a procesov v nej. Cieľom je významne zvýšiť povedomie všetkých zamestnancov o tom, že kvalita je životne dôležitá pre úspešnosť organizácie a jej budúcnosť. Podnik musí byť premenený na niečo, čo existuje preto, aby uspokojovalo potreby zákazníkov čo najlepším spôsobom.

Riadenie pracovného výkonu zamestnancov v modernej organizácii sa považuje za dôležité východisko na zdokonalenie jej fungovania. Pracovný výkon vždy bol a je podstatným ukazovateľom efektívnosti a konkurenčnej schopnosti. Neodmysliteľnými faktormi v tomto procese sú pracovné, resp. zamestnanecké vzťahy a s nimi súvisiaci štýl vedenia uplatňovaný na pracovisku, ako aj prvky komunikácie. Moderný prístup manažmentu ľudských zdrojov zdôrazňuje potrebu vytvárania pracovných úloh a pracovných miest tak, aby čo najviac vyhovovali schopnostiam a preferenciám každého zamestnanca. Riadenie pracovného výkonu sa tak týka navzájom súvisiacich procesov práce, riadenia, rozvoja a odmeňovania. Je nástrojom dosahovania lepších výsledkov podniku, tímov a jednotlivcov pochopením a riadením výkonu v dohodnutom rámci plánovaných cieľov, noriem a požadovaných kompetencií. Na tomto základe sú vytvárané pracovné úlohy, hodnotený zamestnanec a jeho výkon, prebieha odmeňovanie, realizuje sa vzdelávanie a rozvoj personálu [5].

Profesijné vzdelávanie a rozvoj zamestnancov je ďalším z predpokladov zvládnutia nových úloh náročného podnikateľského prostredia. Vzdelanosť patrí dnes k základným cieľom, ale zároveň aj k dôsledkom modernej spoločnosti. Požiadavky na vedomosti a zručnosti človeka v modernej spoločnosti sa neustále menia a aby človek mohol fungovať ako pracovná sila, musí neustále prehlbovať a rozširovať svoje vedomosti a zručnosti. Dnes už nežijeme v dobe, keď človek počas svojej ekonomickej aktivity vystačil s tým, čo sa naučil v priebehu prípravy na povolanie. Vzdelávanie a formovanie pracovných schopností sa v dnešnej modernej spoločnosti stáva celoživotným procesom, musí byť permanentné a zohľadňovať všetky aktuálne potreby vyvolané realitou zmien. A v tomto procese zohráva stále väčšiu úlohu podnik a ním organizované vzdelávacie aktivity. Dnes si už čoraz viac zamestnávateľov uvedomuje, že základom úspechu v každom druhu podnikania je správne vybratý a odborne zdatný personál. Keďže vývoj, vzťahy v spoločnosti, podmienky trhu a ďalšie faktory výrobného a obchodného procesu, vrátane služieb podliehajú neustálym zmenám, je nevyhnutné v predstihu, či priebežne s týmito zmenami počítať a všetkých zamestnancov systematicky vzdelávať. Plnenie úloh organizácie, ktorej cieľom je uspokojenie potrieb zákazníka v akejkoľvek oblasti podnikania predpokladá mať dokonale pripravený personál [5].

Podniková kultúra prestáva už byť pre slovenských manažérov neznámym pojmom, mnohí ju chápu ako dôležitý faktor výkonnosti a konkurencieschopnosti organizácie, stáva sa neoddeliteľnou súčasťou moderného manažmentu. Predstavuje niečo zjavne existujúce, čo sa nedá nariadiť, často ani vysvetliť, ale výrazne ovplyvňuje fungovanie subjektu. Podchytiť a využiť túto problematiku v riadení však nie je jednoduché. Základom každej podnikovej kultúry je adekvátny kvalitný pracovný potenciál, t. j. dostatočný počet zamestnancov vo vyhovujúcej štruktúre, ale aj ich talent, vedomosti a schopnosti. Kvalita personálu, jeho strategicky podporované prístupy, postoje, aktivita, spôsoby konania a správania sú predpokladom vytvárania a rozvíjania silných stránok a konkurenčných výhod. Organizačný rozvoj predpokladá riadené formovanie podnikovej kultúry, resp. jej prípadnú zmenu, čo možno realizovať napr. modelom kľúčových kompetencií organizácie, ktorý spája tri úrovne - strategickú, úroveň vedenia a rozvoja ľudí a úroveň výsledku u zákazníka. Takýto model umožní presne špecifikovať merateľné premenné a teda aj vyhodnocovať rozvoj podnikovej kultúry. Nevyhnutnosťou je pridržať sa jasne formulovaných kľúčových kompetencií a ich prejavov na všetkých týchto úrovniach, ako aj podporiť celý proces kvalitnou internou, aj externou komunikáciou.

Reeingineering podnikových procesov je v súčasnom manažmente jedna z najradikálnejších

metód zmien. Znamená zásadné prehodnotenie a radikálnu rekonštrukciu podnikových procesov tak, aby mohlo byť dosiahnuté dramatické zdokonalenie z hľadiska kritických mier výkonnosti, ako sú náklady, kvalita, služby a rýchlosť. Úvodom je potrebné hľadať nový zmysel a účel práce celého podniku (rethinking), zásadne prehodnotiť model podnikového riadenia (redefinition) a preprojektovať kľúčové a pomocné podnikové procesy (redesign). Reeingineering využívajú podniky, ktoré majú veľké problémy a nemajú inú možnosť prežitia, t. j. majú vysoké náklady, nízku úroveň kvality, odliv zákazníkov, a pod. [6].

V novom svete podnikania sa konkuruje podnikateľským modelom. Toto konštatovanie Ash Maurya je závažné, ale myslím si že pravdivé a správne, pretože, keď sa zamyslíme a pochopíme podnik a jeho fungovanie v trhovom prostredí, v súčasnom trhovom prostredí, potom odsúhlasíme tento výrok, pretože produkt je v skutočnosti výstupom z kvalitných, dobre nastavených, riadených a neustále zlepšovaných podnikových procesov, podnikateľský model spoločnosti má také atribúty ako napr. efektívnosť všetkých procesov a činností, inovácie a manažérstvo zlepšovania, kvalita ako spokojnosť zákazníka a ostatných zainteresovaných strán atď., ktoré v celku tvoria podnikateľský model podniku.

ZÁVER

Cieľ tohto príspevku bol nasledovný, na vymedzenom priestore sa zamerať na budúcnosť v súvislosti s podnikmi, podnikaním, riadením podnikov, zameral som sa stručne aj na trendy, ktoré v týchto oblastiach už pozorujeme dlhodobejšie, trendy ktoré sa naplnili, trendy, ktoré sú predpokladané že sa budú napĺňať. Je to dôležitá problematika, trendy vývoja ekonomiky, globálnej ekonomiky, vplyv vývoja v ekonomike na manažment. na riadenie podnikov, na podniky samotné, na ich konkurencieschopnosť, na ich perspektívu. Informácií a literatúry o trendoch v podnikaní v globálnej ekonomike je naozaj veľa a sú prístupné, veľa je kvalitných autorov a ich hodnotných diel, ktoré sa venujú tejto problematike. Tieto fakty ohľadne budúcnosti ekonomiky a tým pádom prirodzene aj podnikov naberajú na význame ako postupuje globalizácia rastie vonkajší vplyv na podniky, rastie práve z hľadiska stále väčších zmien, neurčitostí a turbulencií na trhu v globálnej ekonomike. Tieto zmeny sú závažné, tak hlboké, ich frekvencia stále narastá a to do takej miery, že zmena samotná sa stáva jadrom manažmentu. Podľa P. Druckera: „Existujeme v turbulentnom prostredí neustálych zmien... a Druckerovou odpoveďou je, že „Treba riadiť inovatívne.“ Inovácie sú motorom, ktorý bude hnať firmy dopredu. Zmeny, ktoré sa v globálnej ekonomike a spoločnosti dejú, znamenajú nové podmienky pre podniky a ich adaptáciu na tieto zmeny, je to pre podniky rozhodne výzva, výzva adaptovať sa na meniace podmienky v globálnej ekonomike. Tieto zmeny okrem iného znamenajú, že jednotlivé krajiny budú tvoriť v budúcnosti a nie tak vzdialenej hyperkonkurenčný globálny trh, kde budú mať dôležitú úlohu informačné a komunikačné technológie. Štruktúra novej globálnej ekonomiky vyspelých krajín sa vyvíja a bude vyvíjať v priamej závislosti na vývoji nových technológií. Nová ekonomika sa postupne vytvára a môžeme povedať, že bude sieťová, digitálna, informačná a znalostná, bude turbulentná a plná neurčitostí. Globálna sieťová ekonomika je už dnes realitou, globálna sieťová ekonomika vytvára nový konkurenčný priestor. Konkurenčnú výhodu budú mať tí, tie podniky, ktoré budú schopné využívať a rozvíjať ľudský kapitál (znalosti, schopnosť realizácie, kreativitu, inovácie a pod.), podniky, ktoré budú vedieť rýchlo, pružne reagovať na trh a jeho potreby, jeho zmeny. Dominantnou štruktúrou globálnej ekonomiky budú nadnárodné korporácie. Zmeny v organizovaní a riadení podnikov, vývoja a výroby vedú postupne k tomu, že sa budú vytvárať virtuálne podniky, ktoré budú schopné s malým množstvom zamestnancov dosahovať obrovské obraty. Ekonomický rast vyspelých krajín v 21. storočí, tak ako to potvrdzuje vývoj z konca 20. storočia až doteraz, môže pochádzať len z rastúceho využitia jediného zdroja, v ktorom majú tieto štáty ešte stále konkurenčnú výhodu - znalostí resp. nových znalostí, resp. využitie vedomostných pracovníkov, teda zamestnancov, ktorí sú vybavení potrebnými znalosťami a tieto vedia prakticky používať pre rozvoj podniku.

LITERATÚRA

[1] KLINEC. I. (2005): *Futurológia - Veda o budúcnosti*. Teoreticko-metodologické aspekty. Študijný materiál.

[2] *Zdroje a východiská súčasného manažmentu.* Dostupné na : http://fsi.uniza.sk/kkm/old/publikacie/ma/ma_02.pdf

[3] ANTOŠOVÁ, M. (2010): *Manažment ľudských zdrojov a organizačný rozvoj ako východisko znalostného manažmentu.* In: Acta Montanistica Slovaca, Vol. 15, No. 1, ISSN 1335-1788.

[4] ARMSTRONG, M. (2002): *Řízení lidských zdroju*. Grada, Praha 2002, ISBN 80-247-0469-2.

[5] ANTOŠOVÁ, M. (2008): *Manažment ľudských zdrojov v praxi*. ES F BERG, Košice, ISBN 978-80-553-017-7.

[6] MAJTÁN, M. (2008): *Manažment.* Sprint, Bratislava, ISBN 978-80-89085-72-9.

Aplikácia CAD programov pri tvorbe počítačového modelu pre zníženie emisií hluku prevodoviek

Samuel Sivák, Ing.*
Katedra konštrukčného a dopravného inžinierstva, Ústav konštrukčného inžinierstva a mechaniky,
Strojnícka fakulta, Technická univerzita v Košiciach,
Letná 9, 042 00 Košice, Slovenská republika.
E-mail: samuel.sivak@tuke.sk, Tel.: + 421 55 602 2355

Silvia Maláková, doc. Ing., PhD.
Katedra konštrukčného a dopravného inžinierstva, Ústav konštrukčného inžinierstva a mechaniky,
Strojnícka fakulta, Technická univerzita v Košiciach,
Letná 9, 042 00 Košice, Slovenská republika.
E-mail: silvia.malakova@tuke.sk, Tel.: + 421 55 602 2372

Matúš Lavčák, Ing.
Katedra konštrukčného a dopravného inžinierstva, Ústav konštrukčného inžinierstva a mechaniky,
Strojnícka fakulta, Technická univerzita v Košiciach,
Letná 9, 042 00 Košice, Slovenská republika.
E-mail: matus.lavcak@tuke.sk, Tel.: + 421 55 602 3364

Application of CAD programs for making a computer model aimed at lowering gearboxes sound emissions

Abstract: Noise emissions in automobile gearboxes are affected by a significant degree by vibration in gearboxes. Modern methods for investigating vibrations include the finite element method. The FEM is a numerical method for solving a wide range of engineering problems. The first step is to create a geometric model of the investigated gears.

ÚVOD

Medzi popredné problémy automobilového priemyslu patrí hluk. Tie sa konštruktéri snažia odstrániť a hlučnosť znížiť na možné minimum. Čím je menšia hlučnosť, tým je jazda v aute príjemnejšia. V niektorých kladných prípadoch má takéto úsilie za následok aj zvýšenie výkonu motora, zníženie spotreby paliva ale hlavne zníženie emisií hluku.

Negatívny vplyv dopravného hluku a ochrana proti nemu naberajú celosvetovo na vážnosti. Dopravný hluk nie je len rušivým javom, ale je štatisticky dokázaná priama súvislosť celkovej nemohúcnosti obyvateľov s hlukovými pomermi ich obydlí. Emisie hluku zasahujú okolité prostredie, ale aj osoby nachádzajúce sa vo vnútornom prostredí automobilov. Podľa zákona Národnej rady SR povolená hladina hluku automobilov je 74 dB. Konštruktéri musia dbať na to, aby pri zachovaní zvýšenej výkonnosti automobilu pri zníženej emisii a spotrebe paliva klesla aj hladina hluku, a to pod daný limit. Zároveň je nutné dodržiavať limity hluku podľa predpisu EHK (Európska hospodárska komisia) č. 51. Predpis sa zameriava na podmienky udelenia homologizácie z hľadiska externého hluku.

Zvýšeným legislatívnym tlakom vystupuje do popredia hľadisko ekológie týkajúce sa hlučnosti automobilov. Táto skutočnosť vedie k potrebe identifikácie zdrojov hlučnosti a ich kvantitatívnemu ohodnoteniu. Značný podiel na hlučnosti automobilov tvorí hlučnosť automobilových prevodoviek. Za najvýznamnejšiu príčinu hlučnosti je považovaná tzv. chyba prevodu (Transmission Error), ktorá súvisí s tuhosťou ozubenia a s kinematickou presnosťou.

Prevodovky, ktoré fungujú niekoľko rokov s relatívne nízkymi vibráciami, môžu začať vykazovať vysoké vibrácie. Tento nárast vibrácií je často včasným varovaním, že porucha prevodovky môže nastať za niekoľko týždňov. Vibrácie vo vozidlách alebo lietadlách nie sú vítané - aj keď sú prevody schopné fungovať dlho bez poruchy. Vibrácie indukované v úzko prepojenom mechanickom systéme môžu spôsobiť predčasné zlyhanie krehkých súčastí, ako sú prístroje, ovládacie mechanizmy, malé motory alebo dokonca skrutky (pri niektorých

skrutkových spojoch môže dôjsť k uvoľneniu skrutiek) [1].

1 VIBRÁCIE A ICH MERANIE

Ak sa vibrácie zmerajú v jednom zo štyroch rohov prevodovej skrine, tak výsledkom merania bude malý pohyb kmitajúci tam a späť pri vysokej frekvencii. Charakter tohto pohybu má tvar sínusovej vlny. Obrázok 1 zobrazuje sínusový charakter vibrácie v určitom okamihu. Na obr. 1 je radiálny posun vektorová vzdialenosť *d*. Veľkosť tohto vektora je určená bodom pohybujúcim sa po kružnici rýchlosťou ω, pre radiány za sekundu.

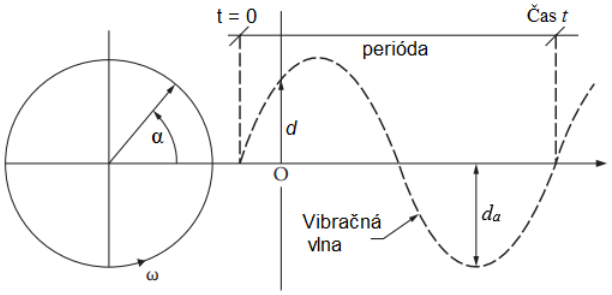

Obr. 1. Schéma vlny vibrácie

Meranie vibrácií zahŕňa snímacie zariadenie, ktoré detekuje amplitúdu, záznamové zariadenie, ktoré zaznamenáva signály zo snímacieho zariadenia a zariadenie na spracovanie údajov, ktoré prevádza prvotné údaje na analytické údaje vo forme množstva vibrácií pri rôznych frekvenciách. Prístroj, ktorý sníma, sa všeobecne považuje za prevodník. Výstupom meniča je elektrický signál, ktorý prechádza vodičmi do dátového záznamníka. Záznamník dát môže tieto signály zaznamenávať na magnetickú pásku. Taktiež je možné mať záznamník údajov, ktorý okamžite spracuje prichádzajúce signály a poskytne údaje o intenzite vibrácií. Zariadenie na spracovanie údajov môže zaznamenať zaznamenané údaje a poskytnúť maximálne vibrácie napríklad pre každú tretinu oktávového pásma. Spracovateľské zariadenie bude mať zvyčajne schopnosť prijímať signál v jednom z troch vibračných režimov (amplitúda, rýchlosť a zrýchlenie) a prevádzať tento signál na ďalšie dva režimy. Pri premene na údajov na zvyšné dve nemerané veličiny sa predpokladá, že vibračná vlna má jednoduchý harmonický pohyb.

Pri meraní vibrácií na prevodovke sa zvykne zvoliť viacero miest. Na začiatku sa bežne meria v troch smeroch. Tie sú zvyčajne horizontálne, vertikálne, a axiálne. Neskôr, keď je nameraná história vibrácií, je možné vykonať merania iba na jednom alebo dvoch miestach, a iba v jednom alebo dvoch smeroch a stále si byť dostatočne istý, či sú vibračné charakteristiky uspokojivé alebo nie.

Údaje o vibráciách sú obzvlášť užitočné pri monitorovaní prevodoviek v prevádzke, ktoré môžu byť náchylné na zlyhanie. Závažná chyba v geometrii alebo kvalite metalurgie sa môže prejaviť aj po rozsiahlych a presných kontrolách kvality. Kontrola vibrácií v prevádzke je poslednou šancou na zistenie chyby skôr, ako dôjde k závažnej poruche [1, 2].

2 ZDROJE HLUČNOSTI PREVODOVKY

Vo všeobecnosti je prevodovka akusticky uzatvorený systém, z ktorého sa hluk šíri najmä vibráciami povrchu skrine alebo pripojenými agregátmi, vrátane základnej konštrukcie. Za najvýznamnejšiu príčinu hlučnosti je považovaná tzv. chyba prevodu

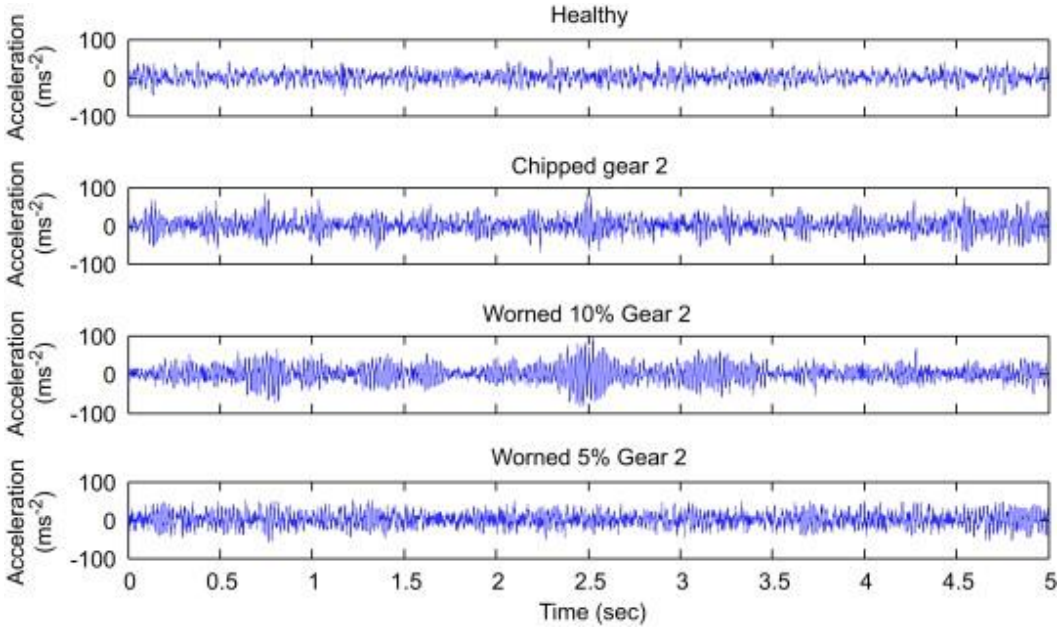

Obr. 2. Názorná ukážka merania vibrácií od ozubených kolies, Healthy – nepoškodené kolesá, Chipped – hlava zuba je poškodená, Worned 10 % - odobratých 0,5 mm hrúbky zuba, Worned 5 % - odobratých 0,3 mm hrúbky zuba [4]

(Transmission Error), ktorá súvisí s tuhosťou ozubenia a s kinematickou presnosťou ozubenia [3].

Pri zábere ozubených kolies sú vibrácie prenášané na obal prevodovky sú najvýznamnejším zdrojom hlučnosti. Z fyzikálneho hľadiska je príčinou vibrácií dynamická sila, ktorá môže meniť svoju amplitúdu, smer alebo pôsobisko. V evolventnom ozubení je najvýznamnejšia zmena amplitúdy, ktorej hlavnou príčinou je premenlivá tuhosť ozubenia a rázy pri vstupe zubov do záberu vplyvom deformácií, odchýlok rozstupu a profilu zubov voči teoretickými rozstupmi. Na obr. 2 je možné vidieť ako opotrebenie zubov vplýva na hlučnosť prevodovky.

V zábere ozubených kolies vplýva na vibrácie mnoho ďalších skutočností, napríklad vibrácie prídavnými dynamickými silami, ktoré majú za následok zvyšovanie vibrácií).

Obsahom prevodovky sú komponenty, ktoré môžu byť samy o sebe zdrojom hluku a vibrácií, alebo vibrácie vybudia, prípadne prenášajú a zosilňujú. Patria sem napríklad pomocné prvky, ako napríklad prvky riadenia, ložiská a hriadele. Najvýraznejšie sa z týchto prvkov prejavujú ložiská, ktoré sú druhým najvýznamnejším zdrojom hluku po ozubení. Vibrácie vznikajú odvaľovaním valivých prvkov ložiska po vnútornej a vonkajšej dráhe. Ich frekvencia je daná nerovnosťami povrchu (pitting) alebo nepravidelnosťou funkčných plôch, ktoré vznikajú opotrebovaním alebo pri výrobnom procese (deformácie vplyvom upnutia).

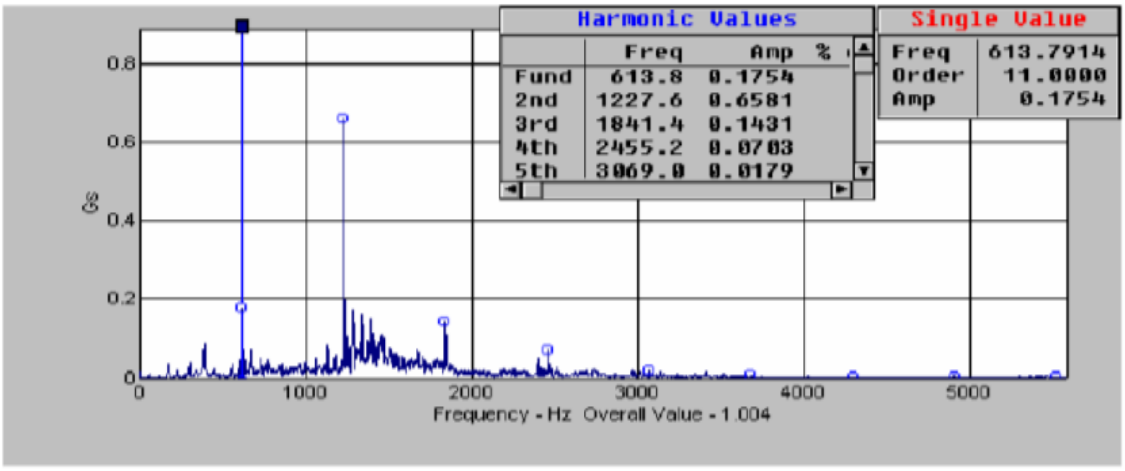

Obr. 3. Ukážka merania vibrácií na použitej prevodovke [5]

prenášané do ozubenia z hnacieho alebo hnaného agregátu, kmitanie hriadeľov a ložísk. Všetky uvedené javy sa podieľajú na zväčšovaní amplitúdy v ozubení. Celková energia vyžarovaného hluku sa postupne zvyšuje.

Medzi špecifické zdroje hluku patrí vznik rázov vplyvom axiálnej a bočnej (zubovej) vôle ozubených kolies so šikmým ozubením. Vzniká predovšetkým u málo zaťažených ozubených kolesách (napríklad pri voľnobežných otáčkach spaľovacieho motora), alebo naopak pri veľmi zaťažených ozubených kolesách s malými otáčkami. K tomu prispieva nepravidelný chod hnacieho agregátu a dochádza k torznému kmitaniu (zmena uhlového zrýchlenia behom jednej otáčky) [6]. Tento hluk je označovaný ako rinčanie a klepkanie (zvonenie, chrastenie, ...). V tejto dobe sa motory moderných aut vybavujú dvojhmotovým zotrvačníkom a spojky zase s tlmičmi záberu.

Ďalšími javmi spôsobujúcimi hluk pri zábere ozubenia patrí tzv. Air Pocketing (súvisiaci so vzduchovými kapsami v mazive) a Lubricant Entrainment (vplyvom malých vôlí nie je prebytočné mazivo vytlačené zo záberu a namáha ozubenie Veľkým podielom na hlučnosť prevodových skríň má však skoro vždy budenie vibrácií v zábere ozubených kolies. Na obr. 3 je príklad celkového hodnotenia hluku použitej automobilovej prevodovke [3].

3 METÓDA ODOBRANÍM

Ďalšia metóda modelovania v CAD programoch používa Booleovské operácie ako napr. Vyrezanie na odstránenie materiálu, v tomto prípade sa odstráni z obrobku objem a tvar nástroja v závislosti na vzájomnom pohybe, prebiehajúcom po malých krokoch, ktorým sa simuluje skutočná výroba ozubeného kolesa. Táto metóda využíva postupy, ktoré sa používajú v reálnej výrobe a preto pri jej použití vznikajú modely, ktoré môžu byť aj neanalytického typu. Zároveň vzhľadom na relatívne pozície ozubeného kolesa a nástroja, sú pri modelovaní možné akékoľvek typy posunov profilu.

Nevýhodou tejto metódy je že potrebuje veľa času na vytvorenie modelu, a to aj pre jednoduché profily. Generovanie ozubených kolies takouto metódou môže na obyčajných počítačoch trvať hodiny a v niektorých extrémnych prípadoch aj dni. Avšak

ak nie je potrebná vysoká precíznosť generovaných CAD modelov, tak je možné znížiť čas generovania na minúty. CAD modely ozubených kolies so zníženou precíznosťou môžu byť kľudne použité vo vizuálnych simuláciách, pre sledovanie pohybu, ale na presné skúmanie kontaktov, tvorbu siete konečných prvkov a následnú simuláciu zaťaženia sú tieto modely takmer nepoužiteľné.

Červené časti na obr. 4 boli získané pri 2° krokoch otáčania, žlté časti pri 1°, modré pri 0,5° a azúrové (najvyššia presnosť, avšak ich nevidno, lebo sa nachádzajú pod zvyšnými troma) boli získané pri 0,2° krokoch otáčania. Z toho vyplýva že pri znižovaní stupňov otáčania pre každý krok sa zvyšuje presnosť tvaru evolventy ozubenia a tým pádom aj plochy ktoré vytvorí. Pričom generovanie ozubeného kolesa trvalo pre 2° kroky 21 s a pre 0,2° kroky 2900 s [7].

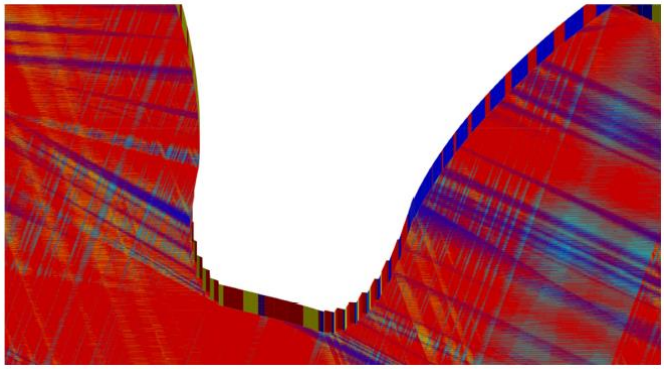

Obr. 4. Profil zuba metódou odobraním [7]

4 ZLOŽENÁ METÓDA

Ďalšou metódou modelovania ozubených kolies je zložená metóda modelovania (mixed modeling method), a tá začína diskretizovaním rezných profilov nástroja, rozdeľovaním profilov do priamok a oblúkov vo vzdialenostiach špecifikovanými užívateľom (pozri obr. 5).

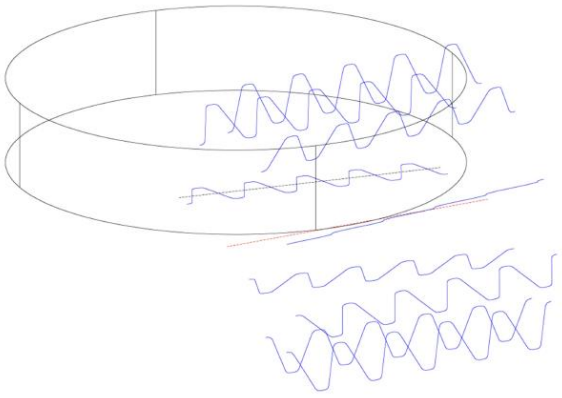

Obr. 5. Schéma nástroja a ozubeného kolesa

Následne sú dané profily nahradené 3D entitami (obr. 6), s vrcholmi ktoré obsahujú rozdeľovacie body. Pri modelovaní sa hýbe len nástroj a modelované ozubené koleso je fixované. Metóda spočíva v tom že nástroj vytvorí podľa svojej geometrie body na ktorých sa následne vytvoria plochy profilov ozubenia. V ďalšom kroku sú z telesa odstránené objemy vytvorené plochami medzi zubami a tým vzniká presný a rýchlo generovaný tvar ozubenia a ozubeného kolesa.

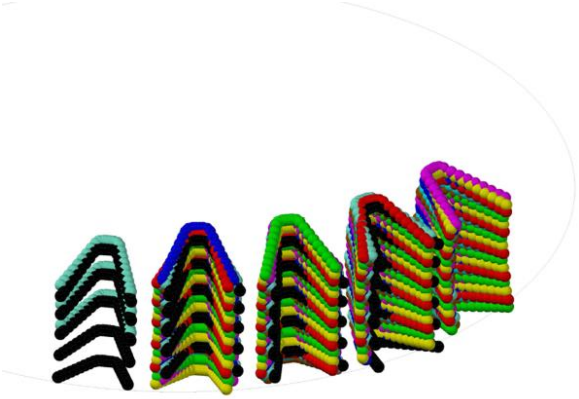

Obr. 6. Body tvoriace zubové medzery [7]

5 PARAMETRICÁ METÓDA

Táto metóda je použiteľná ako pre čelné ozubenie tak aj pre kužeľové ozubenie a zároveň aj pre rovné a šikmé zuby. Princípom tejto metódy je v prvom rade výpočet hodnôt ozubeného kolesa a ozubenia a následne na to sa vytvorí evolventná krivka a prechodová krivka v CAD programe pomocou funkcie parametrická krivka. Ozubenie sa vytvorí tak ako pri ostatných metódach formou odobrania profilu, ktorý tvorí zubovú medzeru. Následným skopírovaním tohto profilu po obvode ozubeného kolesa v rovnakých rozstupoch vznikne celkové ozubenie.

Rozstupová kružnica tvorí základ pre vytvorenie ozubenia. Je to myslená kružnica, ktorá slúži na výpočet modulu ozubenia a rozstupu medzi dvoma bodmi susedných zubov. Zároveň rozstupové kružnice pastorka a ozubeného kolesa vytvárajú pomyselné valce, ktorými sa v kinematike nahrádzajú príslušné ozubené kolesá a vďaka tomu je zachovaná podmienka stáleho prevodového pomeru.

Základná kružnica je myslenou kružnicou, z ktorej sa pri parametrickej metóde odvádzajú rovnice pre evolventu, ako aj pre prechodovú krivku.

Uhol α je záberový uhol definovaný ako uhol nachádzajúci sa medzi záberovou priamkou, ktorá je kolmá na rozstupovú os a spoločnou dotyčnicou rozstupových kružníc. Pre nekorigované čelné ozubenie je tento uhol normalizovaný, a to $\alpha = 20°$.

V CAD programoch ktoré disponujú nástrojom na tvorenie rovníc je možné zadať vstupné parametre a následne napísať všeobecné rovnice s premennými. Tieto rovnice vypočíta program a do modelu sa vkladajú už len označenia rovníc. Takýto nástroj

umožňuje užívateľovi ľubovoľne a rýchlo upravovať daný model len zmenou vstupných parametrov. V prípade ak CAD program takýmto nástrojom nie je vybavený je potrebné do modelu vkladať vypočítané hodnoty.

Pri modelovaní sa začína s hlavovou kružnicou a tá je následne vytiahnutá do priestoru v danej hrúbke ozubeného kolesa. Je vhodné aby bolo teleso vyťahované do priestoru symetricky, čím sa umožní ľahšia manipulácia s modelom v procese skladania zostavy, pohybovej štúdie alebo metódy konečných prvkov. Týmto krokom sa získa prvotné 3D teleso, ktoré bude ďalej formované do požadovaného tvaru. Ďalším krokom je vytvorenie evolventy zuba. V tomto prípade sa škicuje na jednej z rovných plôch 3D telesa a vychádza sa zo základnej kružnice. Avšak v tejto škici budú v ďalších krokoch potrebné aj rozstupová kružnica a pätná kružnica.

Parametrická krivka môže byť teoreticky vytvorená ako je na obr. 7. Čiastočný výsek *B* je pripojený k valcu *A*, okolo ktorého je obtočená myslená šnúra def. Tá je v bode f pevne pripevnená. Bod b na myslenej šnúre znázorňuje bod, ktorý leží na evolvente a obtáčaním alebo odtáčaním myslenej šnúry má jeho dráha tvar evolventy. Krivka evolventy je v tomto prípade daná bodmi *AC*. Polomer zaoblenia evolventy sa priebežne mení podľa množstva odtočenia tento myslenej šnúry a to tak že v bode a je bod b totožný s bodom a a polomer zaoblenia je nulový. V bode c je polomer zaoblenia maximálny avšak bod c je od stredu valca A vzdialený v hodnote polomeru hlavovej kružnice, a tým pádom je ďalšie vyšetrovanie evolventy pre tvorbu zuba zbytočné. Z tohto obrázku vyplýva že bod b stále rotuje okolo bodu e a tým pádom priamka de je kolmá na evolventu v každom bode b a zároveň stále dotyčnicou valca *A*.

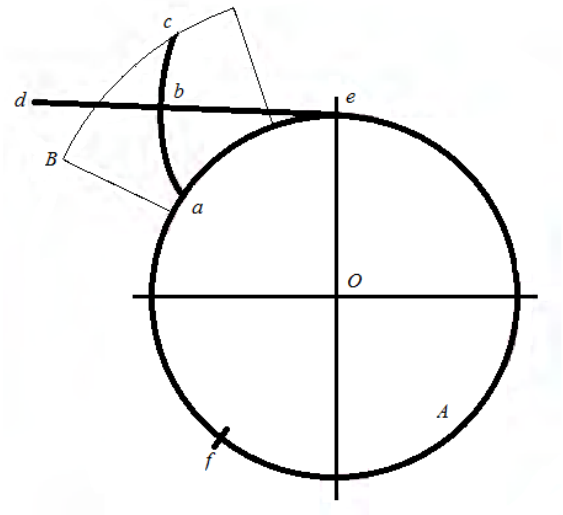

Obr. 1 Schéma tvorby evolventy

Zvolením funkcie krivka daná rovnicou a následným upresnením danej rovnice na parametrickú a nie explicitnú, sa namodeluje evolventa, a to nasledujúcimi rovnicami (1) a (2) podľa [2]:

$$x = r_b \cdot \left[\cos(t) + t \cdot \sin(t)\right], \quad (1)$$

$$y = r_b \cdot \left[\sin(t) - t \cdot \cos(t)\right]. \quad (2)$$

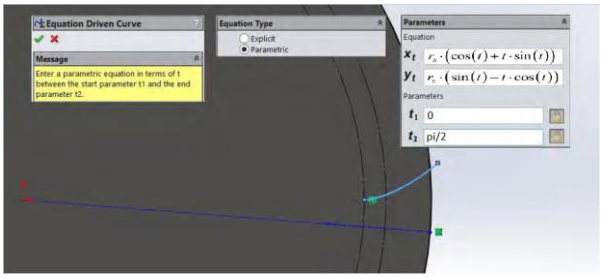

Obr. 8. Parametrické modelovanie evolventy

Na obr. 8 je príklad parametrického modelovania evolventy. Pre parametre t_1 a t_2 je vhodné zvoliť 0 a $\pi/2$.

Profil evolventného ozubenia je tvorený nielen evolventou, ale aj prechodovou krivkou, avšak tá už nie je potrebná pre správny záber ozubených kolies. Geometria tejto krivky má značný vplyv na ohybové napätie zuba. Vzniká ako následok výrobného procesu, kde priamková časť nástroja končí tvorbu evolventy a zaoblená časť pri otáčaní kolesa začne vytvárať prechodovú krivku (obr. 9), a to v mere od pätnej kružnice. Primárna trochoida je totožná s dráhou relatívneho pohybu stredu nástroja obr. 9. Prechodová krivka sa vytvorí zo sekundárnej trochoidy, čo je rovnaká krivka ako primárna trochoida, avšak je od nej vzdialená v konštantnom rozostupe, ktorý je polomer zaoblenia nástroja, čiže je ekvidištantná. Z tohto vyplýva že geometria a typ nástroja udáva tvar prechodovej krivky. Pri prevádzkovom použití je v mieste prechodovej krivky koncentrované maximálne napätie, čiže tvar a rozmery tejto krivky ovplyvňujú ohybovú pevnosť zuba.

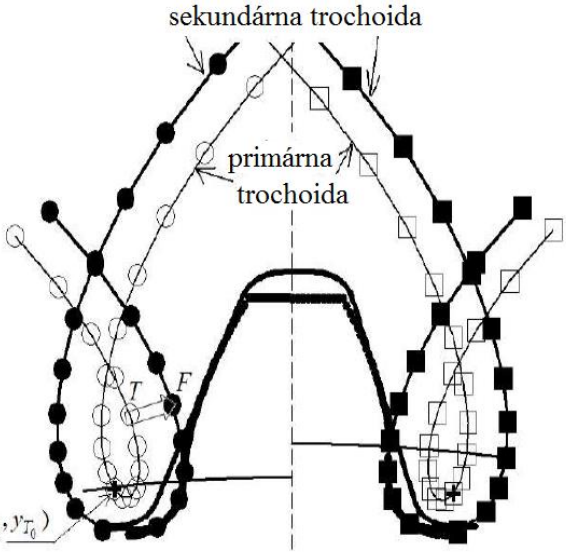

Obr. 2 Schéma prechodových kriviek [8]

Súradnice bodov primárnej trochoidy sú vyjadrené rovnicami (3) a (4):

$$x_T = -r \cdot \sin\varphi + \left(r\varphi + x_{T0}\right) \cdot \cos\varphi + y_{T0} \cdot \sin\varphi, \quad (3)$$

$$y_T = r\left(1 - \cos\varphi\right) - \left(r\varphi + x_{T0}\right) \cdot \sin\varphi + y_{T0} \cdot \cos\varphi \quad (4)$$

Následne sa sekundárna trochoida vyjadrí rovnicami (5) a (6) ako:

$$x_F = x_T + \rho\left[\sin\left(\gamma - \varphi\right)\right], \quad (5)$$

$$y_F = y_T + \rho\left[\cos\left(\gamma - \varphi\right)\right], \quad (6)$$

kde γ je daná vzťahom (7):

$$\gamma = \operatorname{arctg}\left(\frac{y_{T0}}{r\varphi + x_{T0}}\right). \quad (7)$$

Ďalším krokom je odstránenie prebytočných kriviek funkciou Trim, a to tých, ktoré netvoria bočný profil zuba.

Medzi posledné kroky patrí odzrkadlenie krivky bočného profilu zuba cez polovicu zubovej medzery, čím vznikne profil zubovej medzery. Ten sa následne použije vo funkcii Cut alebo Lofted Cut (podľa modelovaného ozubeného kolesa). Vzniknutá zubová medzera sa namnoží po celom obvode v danom počte zubov.

ZÁVER

Zvyšovaním výkonov a zlepšovaním zaťažení strojov s ozubeným prevodom vedie k rastu technickej úrovne strojov, ale to vedie k zhoršovaniu kvality životného prostredia. Medzi takýto kvalitatívny faktor, ktorý zhoršuje životné prostredie patrí práve hluk.

Pre konštruktérov je dôležité, aby mohli vopred navrhovať a zlepšovať navrhnuté komponenty prevodoviek s požiadavkou na zníženie hluku. Takýto proces sa začína už pri tvorbe geometrických modelov, ktoré musia byť presné a rýchle, čo umožňuje užívateľom kvalitnejšie kontroly daných častí. Čím viac sa model priblíži geometrii reálnemu výrobku, tým bude kontrola na vibrácie pomocou MKP užitočnejšia.

Poďakovanie

Táto práca bola podporená Agentúrou na podporu výskumu a vývoja na základe Zmluvy č. APVV-19-0328.

Príspevok vznikol s podporou projektov: KEGA 006TUKE-4/2020 „Implementácia poznatkov z výskumu zameraného na redukciu emisií motorových vozidiel do edukačného procesu.“

LITERATÚRA

[1] RADZEVICH, S. P. (2016): *Dudley's handbook of practical gear design and manufacture*. CRC Press, Taylor & Francis Group, ISBN 9781498753104.

[2] BRIANZA, G. - GONZÁLEZ, G. R. (2017): *Parametric Geometric Modeling of a Spur Gear Using SolidWorks.* Gear Solution, pp. 31-36.

[3] NEMČEKOVÁ, M. - BOŠANSKÝ, M. - VEREŠ, M. (2006): *Možnosti znižovania hlučnosti prevodoviek.* Acta Mechanica Slovaca, Roč.10, č. 4-B, pp. 257-262.

[4] GHARAVIAN, M. H. - ALMAS GANJ, F. – OHADI, A. R. - HEIDARI BAFROUI, H. (2013): *Comparison of FDA-based and PCA-based features in fault diagnosis of automobile gearboxes*. Neurocomputing, 121, pp. 150-159.

[5] *Měření vibrací automobilových převodovek.* (2012): Liberec, Technická zpráva. Technická Univerzita v Liberci. 54 s.

[6] CHEN, Z. - SHAO, Y. (2013): *Mesh stiffness of an internal spur gear pair with ring gear rim deformation*. Mechanism and Machine Theory. 69, pp. 1-12.

[7] TOLVALY-ROSCA, F. - FORGÓ, Z. - MÁTÉ, M. (2015): *Evaluation of a Mixed CAD Gear Modeling from Time and Precision Point of View*. Procedia Technology, 19, pp. 28-33.

[8] SU, X. - HOUSER, D, R. (2000): *Characteristics of trochoids and their application to determining gear teeth fillet shapes*. Mechanism and Machine Theory. Pergamon, pp. 1-14.

Návrh výpočtového modelu pre analýzu stavu napätosti na povrchu zvaru s reálnou geometriou

Peter Kopas, Ing., PhD.*
Katedra aplikovanej mechaniky, Strojnícka fakulta,
Žilinská univerzita v Žiline,
Univerzitná 8215/1, 010 26 Žilina, Slovenská republika.
E-mail: peter.kopas@fstroj.uniza.sk, Tel.: + 421 41 513 2955

Marián Handrik, Ing., PhD.
Katedra aplikovanej mechaniky, Strojnícka fakulta,
Žilinská univerzita v Žiline,
Univerzitná 8215/1, 010 26 Žilina, Slovenská republika.
E-mail: marian.handrik@fstroj.uniza.sk, Tel.: + 421 41 513 2984

Milan Sága, prof. Dr. Ing.
Katedra aplikovanej mechaniky, Strojnícka fakulta,
Žilinská univerzita v Žiline,
Univerzitná 8215/1, 010 26 Žilina, Slovenská republika.
E-mail: milan.saga@fstroj.uniza.sk, Tel.: + 421 41 513 2500

Milan Vaško, doc. Ing., PhD.
Katedra aplikovanej mechaniky, Strojnícka fakulta,
Žilinská univerzita v Žiline,
Univerzitná 8215/1, 010 26 Žilina, Slovenská republika.
E-mail: milan.vasko@fstroj.uniza.sk, Tel.: + 421 41 513 2981

Pavol Novák, Ing., PhD.
Katedra aplikovanej mechaniky, Strojnícka fakulta,
Žilinská univerzita v Žiline,
Univerzitná 8215/1, 010 26 Žilina, Slovenská republika.
E-mail: pavol.novak@fstroj.uniza.sk, Tel.: + 421 41 513 2968

Milan Uhríčik, Ing., PhD.
Katedra materiálového inžinierstva, Strojnícka fakulta,
Žilinská univerzita v Žiline,
Univerzitná 8215/1, 010 26 Žilina, Slovenská republika.
E-mail: milan.uhricik@fstroj.uniza.sk, Tel.: + 421 41 513 2615

Design of a computational model for the analysis of the state of stress on the weld surface with real geometry

Abstract: The paper presents the procedure of creating a geometric model of the weld surface from 3D scan data. The geometric model is used to calculate the stress concentration on the real weld surface. The stress concentration on the weld surface affects the fatigue properties of the welds and the initiation of damage from the weld surface. In MATLAB, the 3D scan data of the weld surface is processed and the file with geometry for program ADINA is created. Next step is stress concentration analysis in the weld in the software ADINA.

ÚVOD

Pri zváraní dochádza k lokálnemu roztaveniu materiálu v mieste zvaru. Pri jeho opätovnom tuhnutí dochádza k vzniku charakteristického povrchu zvaru. Na povrchu zvaru môžu vzniknúť aj tvary, ktoré sú charakterizované ako chyby zvaru. Mikroskopický a makroskopický tvar povrchu konštrukcie je jedným z dôležitých kritérií, ktoré určuje únavové vlastnosti konštrukcie. Geometrické imperfekcie na povrchu spôsobujú koncentráciu

napätí. Miesta so zvýšenými hodnotami napätí na povrchu sú spravidla oblasti inicializácie trhlín. V príspevku prezentujeme postup vytvorenia reálneho geometrického modelu povrchu zvaru a následnej analýzy stavu napätosti v zvare. Vytvorené algoritmy sú implementované v programe Matlab, ktoré generujú geometrický model pre program Adina [1]. Pre testovanie vytvorených algoritmov je v programe Matlab vygenerovaný tvar povrchu definovaním bodov na povrchu. Pri skenovaní reálneho povrchu zvaru použitím laserového skeneru získame súradnice bodov na povrchu. Vytvorené algoritmy je teda možné použiť na generovanie geometrie získanej 3D skenovaním povrchu zvaru [2-5].

1 VPLYV POVRCHU ZVARU S REÁLNOU GEOMETRIOU NA ÚNAVOVÉ VLASTNOSTI MATERIÁLU

Mechanické vlastnosti konštrukčného materiálu sú výsledkom sofistikovaného výrobného režimu, ktorým sa riadi kinetika metalurgických procesov [6,7]. Nech aplikujeme do tohto procesu akýkoľvek dodatočný tepelno-deformačný proces, tento akt sa jednoznačne prejaví na výsledných vlastnostiach materiálu. Dnes už vieme, že zvarový spoj je tvorený zvarovým kovom, ktorý predstavuje skryštalizovanú taveninu základného a prídavného materiálu. Zvarový spoj je ďalej tvorený aj teplom ovplyvnenou oblasťou, kde sa teplom aktivoval jeden alebo viacero mechanizmov spevnenia a zároveň táto oblasť úzko nadväzuje na pôvodný (základný) materiál. Vo všeobecnosti sa dá povedať, že zmena metalurgického stavu materiálu po zváraní je tým výraznejšia, čím zložitejší bol režim výroby zvarového spoju.

A práve v závislosti od reálnych podmienok namáhania môžu nadobúdať z pohľadu hodnotenia bezpečnosti resp. životnosti takejto konštrukcie význam jednotlivé oblasti teplom ovplyvnenej zóny.

Kvalita povrchu zváraných konštrukcií má pri cyklickom zaťažovaní veľmi často zásadný význam pre zabezpečenie požadovaných únavových charakteristík [8]. Je zrejmé, že vytvorené zvarové spoje majú veľkú nevýhodu v porovnaní so základným materiálom a to v podobe zmeny svojho tvaru s častým prevýšením oproti hrúbke prierezu zváraného materiálu. Táto zmena pri zaťažovaní spôsobuje v miestach prechodu základného materiálu so zvarovým kovom zvýšenú koncentráciu napätí. Tá ďalej spôsobí nerovnomernosť v rozložení zaťaženia v priereze zvaru. Z tohto je možné usúdiť, že každá zmena tvaru prierezu konštrukcie bude spôsobovať vrubový účinok [9,10]. Okrem tohto geometrického účinku vrubu musíme brať do úvahy aj technologický vplyv vrubu. Ten sa prejaví vo forme metalurgického spojenia zvarového kovu so základným materiálom, čo je znázornené na obr. 1.

Z tohto pohľadu by zväčšenie absolútnych rozmerov priečneho prierezu vo zvarovom spoji malo podstatne znížiť medzu únavy. Z pohľadu súčasného vnímania tohto javu sa za ideálny zvarový spoj považuje spoj bez prevýšenia, kde je splynutie zvaru so základným materiálom plynulé. Tento spôsob spájania materiálov je možný len pri niektorých mechanizovaných spôsoboch zvárania, čo pri ručnom spôsobe zvárania nepripadá do úvahy. Rovnako pri náročnejších spôsoboch zvárania je nereálne očakávať, aby zvar nespôsoboval vrubový účinok. Dá sa povedať, že chyby vo zvarových spojoch sú neoddeliteľnou súčasťou vyhotovovania týchto zvarov. Na proces vytvárania zvaru vplýva množstvo faktorov, ktoré sa podieľajú i na vzniku defektov. Jedným z kritérií rozdelenia chýb zvarových spojov je situovanie chyby na povrch zvarového spoja alebo do jeho vnútra. Podľa toho môžeme rozdeliť chyby na vonkajšie a vnútorné.

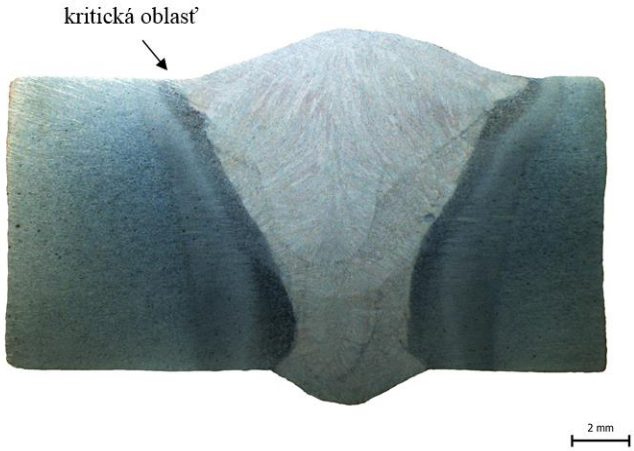

Obr. 1. Oblasť nepriaznivého tvaru zvaru

Na únavovú životnosť zváraných konštrukcií majú spravidla významný vplyv aj nedokonalosti tvaru zvarového spoja, ďalej makro vruby napríklad vo forme krycích húseníc zvaru alebo veľké koreňové neprievary. Prostredníctvom napäťovej analýzy priečneho rezu kútového spoja bolo dokázané, že súčiniteľ koncentrácie napätia v úpätí zvaru pri zaťažovaní naprieč zvarom je približne rovnaký ako súčiniteľ zodpovedajúci osamelej diere v platni. Malé rozdiely sú spôsobené len zmenou geometrie úpätia zvaru, ktorá je zložitejšia ako jednoduchá diera. V úpätí zvarov sa tiež nachádzajú zápaly vo forme nadmerného prevýšenia povrchového profilu zvaru, čo spôsobí lokálne zvýšenie koncentrácie napätia v tomto mieste [11-13].

Okrem toho sa v úpätí zvaru často nachádzajú drobné nespojitosti, ktoré svojou povahou predstavujú prítomnosť trhlín respektíve vtrúsenín. Opakovaná prítomnosť týchto porúch po dĺžke zvaru znemožňujú presnejšie stanoviť hodnotu súčiniteľa napätia. V praxi to predstavuje ešte väčšie zníženie únavových vlastností celej konštrukcie akoby bola táto konštrukcia bola hodnotená len z pohľadu prítomnosti zvarov. Ďalšou príčinou zmien v lokálnej koncentrácii napätí je prítomnosť neprievarov zvarových spojov v oblasti koreňa zvaru. V závislosti od veľkosti a geometrie neprievaru koreňa zvaru môžu byť tieto vruby oveľa nebezpečnejšie ako predchádzajúce uvedené chyby [14,15].

Dnešnou úlohou konštruktérov a technológov je snaha zmierniť vrubový účinok týchto chýb vo zvaroch. Nie je to vždy jednoznačná úloha. Prevýšenie v mieste zvarového spoja ako krycích tak aj koreňových húseníc zapríčiní na jednej strane zväčšenie prierezu zvaru a tým nárast koncentrácie napätia ale na druhej strane sa tým zvýši aj pevnosť zváraného dielca. Tento problém je v dnešnej dobe vyriešený správnou voľbou prídavného materiálu tak, aby pevnostne zodpovedal úrovni základného materiálu.

Existencia zvarových spojov súvisí s takmer bezpodmienečnou prítomnosťou koncentrátorov napätí, čo spôsobuje lokálne zvyšovanie napätosti v prierezoch, ktoré sú kritické pre vznik lomovej plochy. Ak k tejto skutočnosti pripočítame ešte aj pôsobenie reziduálnych napätí za predpokladu, že materiál už nemá prebytok plastických vlastností, alebo patrí medzi ťažkozvaritelný materiál, prítomné zvyškové napätia môžu vyvolať vznik prasklín. Okrem toho zvyškové napätia, ktoré pôsobia na ťah vyvolávajú aj rozmerovú nestabilitu zváraných dielcov a tým nepriaznivo ovplyvňujú aj únavovú životnosť takejto konštrukcie. Je potrebné ale podotknúť, že je možné vytipovať aj také oblasti zaťažovania, kde sa tieto napätia môžu prejaviť aj pozitívne [16, 17].

2 PRÍPRAVA GEOMETRICKÉHO MODELU POVRCHU ZVARU

Pri vytváraní algoritmov sme vychádzali z predpokladu, že tvar reálnej geometrie zvaru bude popísaný prostredníctvom súradníc bodov na povrchu zvaru. Súradnice bodov na povrchu zvaru je možné získať 3D laserovým skenovaním povrchu zvaru. V čase prípravy výpočtových modelov neboli k dispozícii dáta zo skenovania reálneho tvaru povrchu zvaru, preto sme ich nahradili vygenerovaním súradníc bodov v programe Matlab. Na generovanie bodov sme použili funkciu PEAKS. Vygenerované súradnice bodov sme v smere kolmom k rovine *x*-*y* 10-násobne zmenšili a vytvorili maticu bodov, v ktorej riadok zodpovedal bodu na povrchu a stĺpce obsahovali postupne *x*, *y* a z súradnicu bodu (obr. 2).

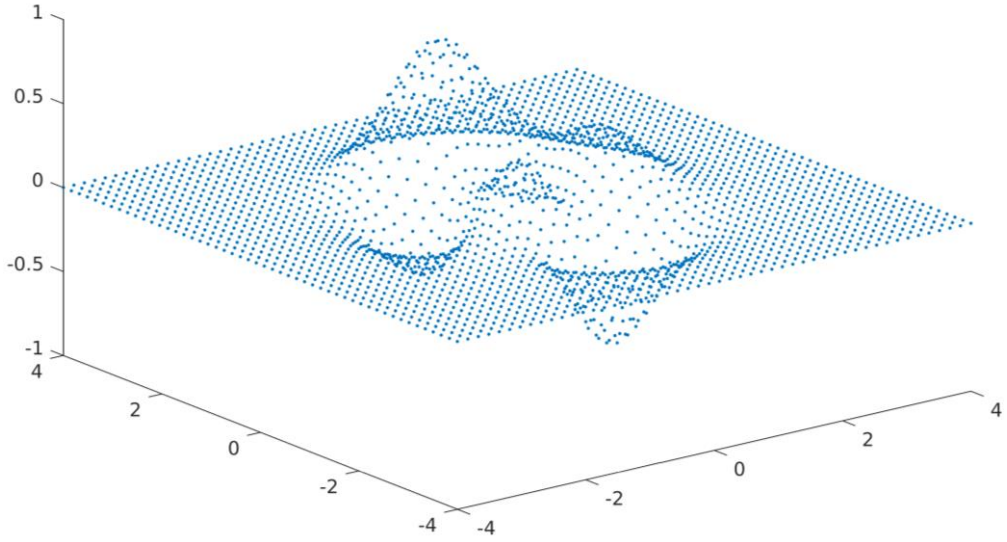

Obr. 2. Tvar vygenerovaného povrchu zvaru

Pri vytváraní modelu budeme používať v MKP programe Adina modul Adina-M. Modul Adina-M je modelár, ktorý pracuje s grafickým formátom parasolid. Umožňuje import geometrie v formáte iges, a import mraku bodov. Pri importe mraku bodov sme získali geometrický model, kde kopce aj krátery tvorili objemové telesá, a preto import bodov rozmiestnených na povrchu bol nepoužiteľný.

Modul Adina-M umožňuje vytvorenie uzavretej hraničnej čiary plochy a následné vygenerovanie plochy použitím hranice. Pri tomto vytváraní plôch je obmedzenie, vytváraná plocha musí byť priamkovou plochou. Následne je možné vytvorené telesá s jednou plochou zlúčiť do jedného telesa s veľkým počtom plôch pre zjednodušenie práce s takýmto telesom.

Pri vytváraní programov pre generovanie geometrie používame vyššie uvedený možnosti modelovania v module Adina-M. Postup generovania geometrického modelu reálnej plochy je nasledovný:

- Vytvorenie siete trojuholníkov v rovine *x*-*y*. Na vytvorenie siete použijeme delaunay triangularizáciu v programe Matlab. Pri triangularizácii použijeme iba *x* a *y* súradnice bodov. Získame sieť trojuholníkov, ktorá vytvára trojuholníky zo susedných bodov bez toho, aby sa niektoré trojuholníky navzájom prekrývali.
- Vygenerovanie príkazu programu Adina, v ktorom sú zapísané súradnice všetkých bodov na vytváranej ploche.
- Vygenerovanie príkazov na vytvorenie jednotlivých hraničných čiar segmentov vytváranej plochy. Vytvoria sa čiary typu polyline.
- Vygenerovanie príkazov na vytvorenie plôch z jednotlivých hraničných čiar. Pri generovaní plôch sa používa vytváranie telesa typu sheet.
- Zlúčenie jednotlivých telies, ktoré tvoria segmenty vytváranej plochy do jedného telesa typu sheet. Používa sa vytváranie telesa metódou sewn.

Vytvorený algoritmus generovania modelu reálnej plochy je rýchly. Generovanie modelu pre plochu popísanú bodmi v rastri 50x50 trvá rádovo niekoľko sekúnd. Načítanie vytvoreného modelu do programu Adina je výrazne časovo náročnejšie a trvá niekoľko minút. Vytvorené teleso typu sheet je zobrazené na obr. 3.

Po vytvorení telesa je potrebné doplniť ostatné plochy, ktoré budú vytvárať geometrický model zvarového spoja (obr. 4).

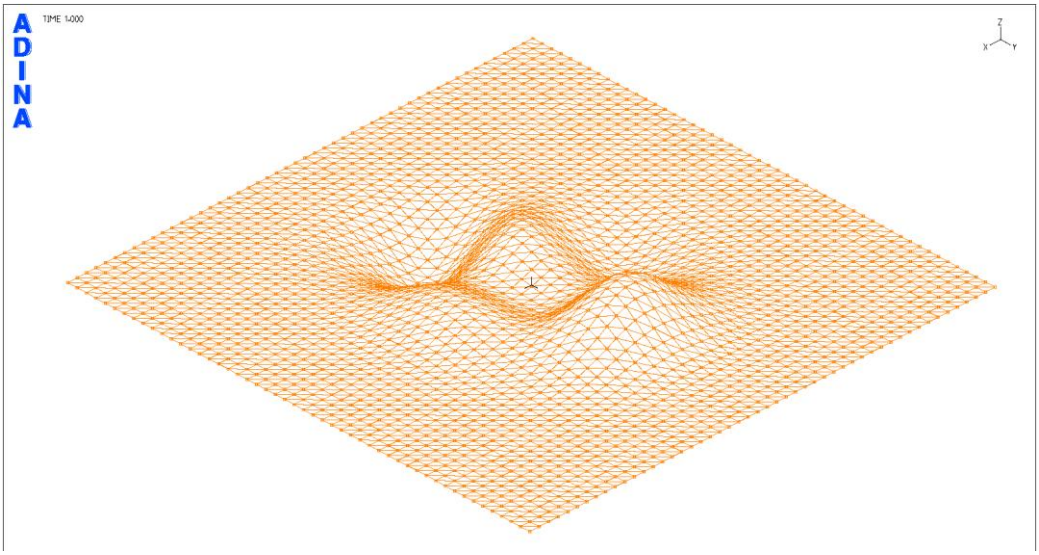

Obr. 3. Vytvorená geometria povrchu zvaru

3 ANALÝZA STAVU NAPÄTOSTI

Vytvorené algoritmy boli testované na modeli s maximálnou hĺbkou krátera 0,65 mm. Celková hrúbka materiálu bola vo vytvorenom modeli 4 mm. V mieste krátera je hrúbka materiálu menšia o cca 16 %. Vytvorený geometrický model zobrazený na obr. 5 ja zaťažený jednoosím stavom napätosti v smere osi *x*. Veľkosť zaťaženia je 100 MPa.

V mieste tvarovej zmeny povrchu sú použité elementy veľkosti 0,1 mm a v ostatných častiach modelu sú elementy veľkosti 0,3 mm. V modeli je použitých cca 1 milión elementov a cca 180 tisíc uzlových bodov. Sieť konečných prvkov je tvorená lineárnymi tetrahedrónmi. Pre zrealizovanie výpočtu bol použitý elastický materiálový model Youngov modul pružnosti s hodnotou $E = 210$ GPa, aplikovaná hodnota Poissonovho čísla bola $\mu = 0{,}3$.

Maximálna vypočítaná hodnota napätí pre napätia v smere zaťaženia je 203 MPa (obr. 5).

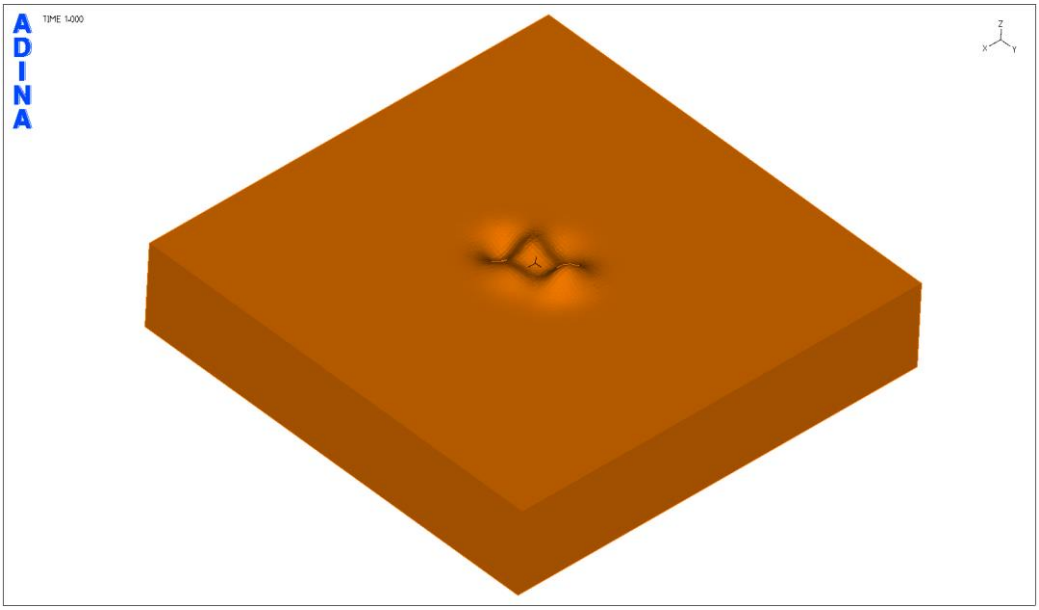

Obr. 4. Geometrický model zvarového spoja s geometriou povrchu zvaru

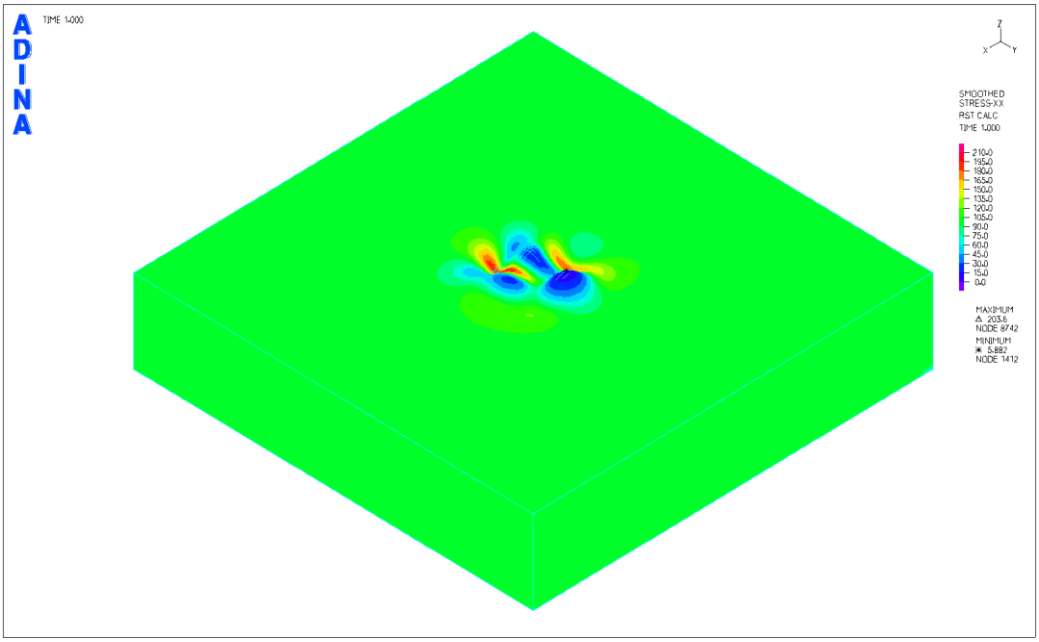

Obr. 5. Rozloženie napätí v smere zaťaženia v smere osi x

ZÁVER

Navrhnuté výpočtové modely a algoritmy umožňujú analýzu stavu napätosti na povrchu reálnej geometrie zvaru. Reálnu geometriu tvaru zvaru je možné získať 3D laserovým skenovaním. Prezentovaný výsledok testovacieho príkladu ukazuje, že pri 16 % zmenšení hrúbky materiálu v mieste zvaru došlo k 100 % zvýšeniu napätia. Tieto výsledky poukazujú na potrebu hlbšieho výskumu v oblasti vplyvu tvaru povrchu reálneho zvaru na rozloženie napätosti v zvare. Zvýšené hodnoty napätia v mieste zvaru s reálnou geometriou povrchu zvaru môžu mať zásadný vplyv na únavové vlastnosti zvarového spoja.

Poďakovanie

Poďakovanie Ministerstvu školstva, vedy, výskumu a športu Slovenskej republiky v súvislosti s realizáciou projektu „Výskum inteligentných systémov a procesov s použitím princípov Industry 4.0 so zameraním na spájanie ťažko spojiteľných materiálov vysoko-koncentrovanými zdrojmi energie - laserom a elektrónovým lúčom“, č. zmluvy MŠSR 1227/2018.

LITERATÚRA

[1] ADINA, http://www.adina.com

[2] MATLAB, http://www.mathworks.com

[3] KREJSA, M. - BROZOVSKY, J. - MIKOLASEK, D. - PARENICA, P. - FLODR, J. -MATERNA, A. - HALAMA, R. - KOZAK, J. (2018): *Numerical modeling of steel fillet welded joint.* Advances in Engineering Software 117, pp. 59-69. DOI: 10.1016/j.advengsoft.2017.03.013.

[4] KUBIAK, M. - DOMANSKI, T. - DEKYS, V. - SAPIETOVA, A. (2017): *Measurement of strain during tension test of welded joint using multi-camera 3D correlation system*. XXI Polish-Slovak Scientific Conference Machine Modeling and Simulations MMS 2016. Procedia Engineering 117, pp. 107-113. DOI: 10.1016/

j.proeng.2017.02.197.

[5] PERZ, P. - MALUJDA, I. - WILCZYNSKI, D. - TARKOWSKI, P. (2017): *Methods of controlling a hybrid positioning system using LabVIEW*. In: XXI Polish-Slovak Scientific Conference Machine Modeling and Simulations MMS 2016. Procedia Engineering 177, pp. 339-346. DOI: 10.1016/j.proeng.2017.02.235.

[6] WALESA, K. - MALUJDA, I. - TALASKA, K. (2018): *Butt Welding Of Round Drive Belts*. Acta Mechanica et Automatica 12 (2), pp. 115-126. DOI: 10.2478/ama-2018-0019.

[7] MACKO, M. - SZCZEPAŃSKI, Z. - MIKOŁAJEWSKA, E. - NOWAK, J. - MIKOŁAJEWSKI, D. (2017): *Repository of 3D images for education and everyday clinical practice purposes.* Bio-Algorithms and Med-Systems 13 (2), pp. 111-116, p-ISSN: 1895-9091, e-ISSN: 1896-530X.

[8] VAŠKO, A - BELAN, J. - KUCHARIKOVA, L. - TILLOVA, E. (2017): *Low And High Frequency Fatigue Tests Of Nodular Cast Irons*. Metalurgija 56(1-2), pp. 25-28.

[9] IŽDINSKÁ, Z. - EMMER, Š.- GONDÁR, E. (2006): *Strojárske materiály*. STU Bratislava.

[10] NĚMEC, J. (1973): *Spolehlivá životnosť svařovaných částí.* Vydavatelství ČVUT, Praha.

[11] SENUMA, T. (2001): *Physical Metallurgy of Modern High Strength Steel Sheets*. ISIJ International, Vol. 41 (6), pp. 520-532.

[12] SCHIJVE, J. (2003): *Fatigue of structures and materials in the 20th century and the state of the art*. International Journal of Fatigue 25, pp. 679-702.

[13] SCHIJVE, J. (2009): *Fatigue of Structures and Materials.* Springer Science+Business Media, B.V., p. 613.

[14] MADDOX, S. J.(2002): *Fatigue strength of welded structures.* Abigton Publishing.

[15] FRICKE, W. (2012): *Guideline for the Assessment of Weld Root Fatigue*. International Instite of Welding. IIW-Doc. XIII-2380r3-11/XV-1383r3-11.

[16] IŽDINSKÁ, Z. (2001): *Požiadavky na akosť zvarových spojov z hľadiska bezpečnosti potrubí*. Slovgas, 6, s. 9-11.

[17] BULEJ, V. - STANCEK, J. - KURIC, I. (2018): *Vision Guided Parallel Robot and its Application for Automated Assembly Task*. Advances in Science And Technology-Research Journal 12 (2), pp. 150-157. DOI:10.12913/

22998624/91887.

NDT skúška umelých srdcových chlopní BSCC

Milan Sapieta, Ing., PhD.*
Katedra aplikovanej mechaniky, Strojnícka fakulta,
Žilinská univerzita v Žiline,
Univerzitná 8215/1, 010 26 Žilina, Slovenská republika.
E-mail: milan.sapieta@fstroj.uniza.sk, Tel.: + 421 41 513 2974

Vladimír Dekýš, doc. Ing., PhD.
Katedra aplikovanej mechaniky, Strojnícka fakulta,
Žilinská univerzita v Žiline,
Univerzitná 8215/1, 010 26 Žilina, Slovenská republika.
E-mail: vladimir.dekys@fstroj.uniza.sk, Tel.: + 421 41 513 2954

Peter Weis, Ing., PhD.
Katedra konštruovania a častí strojov, Strojnícka fakulta,
Žilinská univerzita v Žiline,
Univerzitná 8215/1, 010 26 Žilina, Slovenská republika.
E-mail: peter.weis@fstroj.uniza.sk, Tel.: + 421 41 513 2965

NDT test of artificial heart valves BSCC

Abstract: The subject of investigation is a set of four artificial heart valves made of electrically conductive material, namely the alloy Ti-6Al-4V. Notches of defined geometry with gradually increasing depth were formed on these BSCC (Bjork-Shiley Convexo-Concave) valves. These defects are created on the so-called output strut, which serves as a support mechanism for the controlled movement of the so-called occluder disc and they have been investigated. The method which was used is ultrasonic infrared thermography, where the object was excited by the UTVIS EDEVIS ultrasonic system and the response was detected by the FLIR SC 7200 infrared camera. The postulate for the use of this method is that the excitation signal may be periodically pulsate or in any other way modulated by certain amplitude frequencies, called "lock-in frequency". Lock-in thermography is a type of active lock-in method. The results of damage detection on these relatively complicated objects are compared and discussed.

ÚVOD

V systéme riadenia kvality výrobného procesu zohráva dôležitú úlohu nedeštruktívne skúšanie materiálov (NDT). Umožňuje včasné odhalenie vnútorných chýb výrobku alebo polotovaru, ktoré by mohli po určitej dobe prevádzky zabrániť jeho efektívnemu použitiu alebo spôsobiť nehodu. Na detekciu a kvantifikáciu zistených chýb v oblasti nedeštruktívneho testovania používame množstvo metód využívajúcich rôzne fyzikálne princípy.

Výhodou nedeštruktívnych metód oproti deštruktívnym je skutočnosť, že produkt po testovaní zostane nezmenený a môže sa ďalej použiť. Skúšobné metódy NDT pre jednotlivé druhy polotovarov a výrobkov sú predpísané v príslušných normách a predpisoch. Z tohto hľadiska je obvykle rozhodujúca požiadavka zákazníka, ktorá určuje, podľa ktorej normy alebo predpisu má byť výrobok posudzovaný pre NDT.

1 LOCK-IN TERMOGRFIA

Predpokladom pre použitie tejto technológie je, že budiaci signál môže periodicky pulzovať alebo byť akokoľvek inak amplitúdovo menený určitou frekvenciou, nazývanou "lock-in frekvencia" $f_{lock\text{-}in}$. V niektorých prípadoch je táto zmena súčasťou experimentu, napríklad experimenty s cyklickým mechanickým zaťažovaním. Najelegantnejším spôsobom ako tento amplitúdovo menený signál vytvoriť je ovládať generátor elektronicky, voľbou vhodného trigrovania.

Proces digitálnej lock-in korelácie pozostáva z priemerovania výsledkov nameraných hodnôt F_k a zo sústavy váhových faktorov K_k až do celkového počtu nameraných hodnôt M:

$$S = \frac{1}{M} \cdot \sum_{k=1}^{M} F_k \cdot K_k \,, \tag{1}$$

potom S je výstupný signál.

Keď je budiaci signál harmonický, potom je najvýhodnejšou korelačnou funkciou tiež

harmonická (sínusová, kosínusová) funkcia. Tento typ lock-in korelácie sa nazýva sin/cos alebo úzkopásmová korelácia. Dalo by sa to dosiahnuť buď zúžením šírky pásma zaznamenaného signálu, alebo využitím množstva harmonických funkcií pre K_k vo vzorci (1) [1].

Hlavnou výhodou korelácie sin/cos je to, že umožňuje užívateľovi zohľadniť fázu signálu po vyhodnotení (off-line), keď sa použije dvojkanálová korelácia. Zámerom dvojkanálovej korelácie je, že boli použité dva druhy váhových faktorov, jeden aproximuje funkciu sin a druhý aproximuje funkciu cos. Korelácia sa prenáša dvakrát paralelne s oboma druhmi váhových faktorov [1-5]:

$$K^0(t) = 2 \cdot \sin(2 \cdot \pi \cdot f_{lock-in} \cdot t), \quad (2)$$

$$K^{\pi/2}(t) = 2 \cdot \cos(2 \cdot \pi \cdot f_{lock-in} \cdot t). \quad (3)$$

Prvý kanál ďalej meria zložku vo fáze s funkciou sin a druhý kanál meria zložku vo fáze s funkciou cos, ktorá je π/2 fázovo posunutá k funkcií sin [13].

Ak sa do vzorca (1) zadajú vzorce (2, 3), potom je výsledok dvoch korelácií za celý počet snímkov [5-10]:

$$S^0 = \frac{1}{n} \cdot \sum_{i=1}^{n} F_i \cdot K_i^0, \quad (4)$$

$$S^{\frac{\pi}{2}} = \frac{1}{n} \cdot \sum_{i=1}^{n} F_i \cdot K_i^{\frac{\pi}{2}}, \quad (5)$$

kde je S^0 sa nazýva fázový signál a $S^{\frac{\pi}{2}}$ je zvyčajne označovaný ako amplitúdový signál. Oba signály môžu byť pozitívne alebo negatívne [10-18].

2 UTVIS EDEVIS

Ultrazvuková lock-in termografia je účinnou metódou merania na zisťovanie indikácií trhlín, nehomogenít alebo delaminácií.

UTVIS je založený na digitálnych vysoko výkonných ultrazvukových generátoroch a prevodníkoch ako zdrojov excitácie a používa vysoko citlivú infračervenú kameru.

Ultrazvuková termografia (alebo vibrotermografia) využíva na detekciu materiálových chýb interakciu mechanických a tepelných vĺn. Ak porucha v súčiastke absorbuje vysoko-energetické vlny vysokej energie, ohreje sa lokálne (selektívna metóda defekčného tmavého poľa). Výsledný teplotný gradient na povrchu vzorky sa meria pomocou infračervenej kamery, ktorá vizualizuje rozptýlenú energiu. V závislosti na aplikácii existujú dve možnosti tejto metódy: veľmi rýchla analýza fázou rozpadu a citlivá Lock-in metóda. V obidvoch prípadoch hodnotenie počíta časové oneskorenie medzi priatou energiou a tepelnou odozvou, čo vedie k robustnej a spoľahlivej technike, ktorá je konštantná voči povrchovým vlastnostiam alebo ultrazvukovej distribúcii [19].

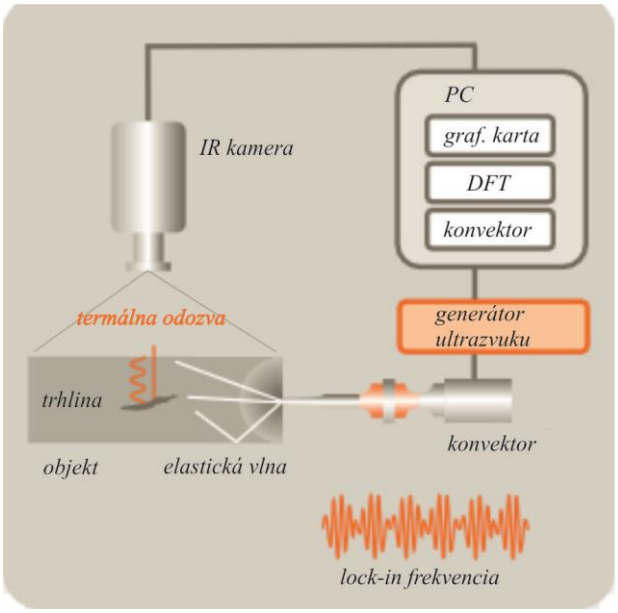

Obr. 1. Schematické znázornenie princípu UTVIS, skratka DST znamená diskrétna Fourierova transformácia [19]

2.1 Meranie

Ako vzorky boli vybrané 4 umelé srdcové chlopne vyrobené z elektricky vodivého materiálu, konkrétne zo zliatiny Ti-6Al-4V. Tri vzorky boli poškodené rezaním, boli vytvorené zárezy s postupne sa zväčšujúcou hĺbkou. Vzorka bola umiestnená pod ultrazvukový budič a je podložená vhodným tvarom držiaka (obr. 2).

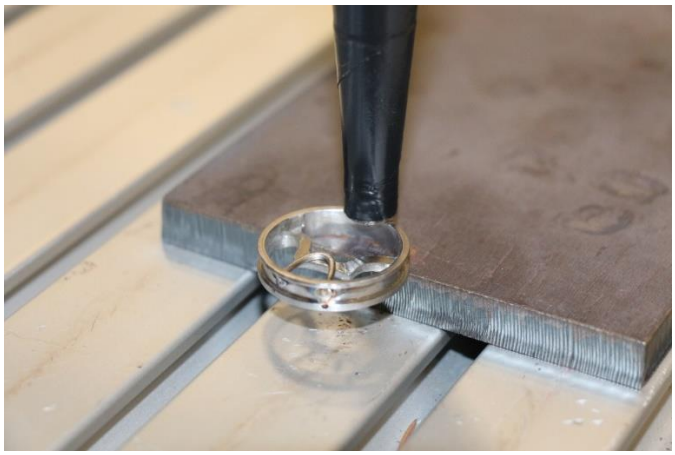

Obr. 2. Vzorka pod ultrazvukovým budičom

Potom bola vzorka vybudená zvolenou modulovanou frekvenciou, pokiaľ nebola zobrazená chyba. Celý priebeh budenia bol zaznamenaný infračervenou kamerou (obr. 3). Nastavenie infračervenej kamery bola rovnaké pre každé jednotlivé budiace frekvencie. Na infračervenej kamere bola zvolená snímkovacia frekvencia 50 Hz. Hodnota emisivity bola v softvérovom prostredí zvolená ako 1, pretože táto veličina neovplyvňuje výsledok merania.

Program, ktorý sa používal na vyhodnotenie každého jedného obrázka, sa nazýva DisplayImg a bol dodaný spolu s budiacim zariadením. Tento program využíva teoretické základy techniky lock-in, ako je vysvetlené v prvej časti tohto článku.

Obr. 3. Proces záznamu infračervenej kamery na excitáciu vzorky

Ako prvá forma excitácie bola zvolená plynulá excitácia. Toto je typ budenia, ktoré prechádza celou oblasťou modulovaných frekvencií. Predpokladá sa, že vykoná celý proces budenia a potom zvolí najvhodnejšiu modulovanú frekvenciu, pri ktorej sa zistia poškodenia meraného subjektu.

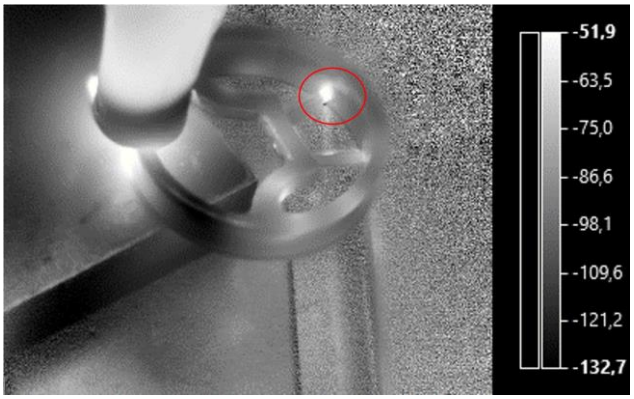

Obr. 4. Prvá vzorka po excitácii, frekvencia excitácie je 0,03 Hz

Ďalej sa hodnotili iba zobrazenia vo fáze. V prvej vzorke možno pozorovať poškodenie zobrazené svetlou oblasťou s budiacou frekvenciou 0,03 Hz (obr. 4). Na druhej vzorke je možné vidieť poškodenie, keď je budiaca frekvencia 0,006 Hz (obr. 5). Tretia vzorka bola excitovaná frekvenciou 0,065 Hz, pri ktorej sa zobrazilo poškodenie (obr. 6).

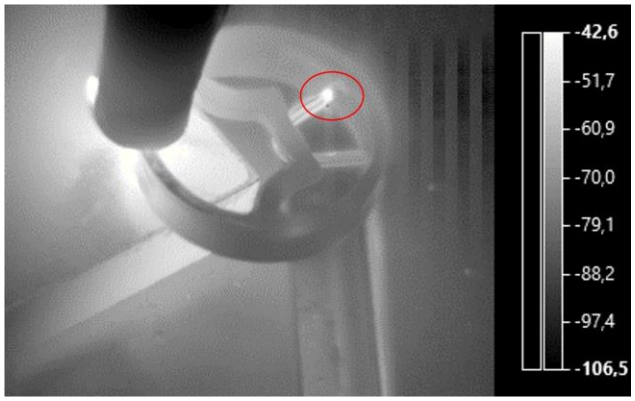

Obr. 5. Druhá vzorka po excitácii, frekvencia excitácie je 0,006 Hz

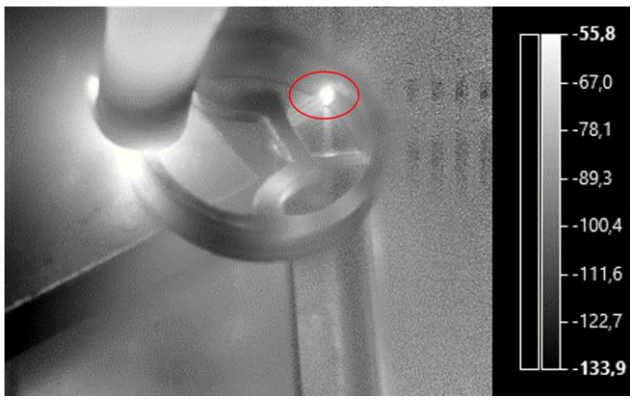

Obr. 6. Tretia vzorka po excitácii, frekvencia excitácie je 0,065 Hz

ZÁVER

Za účelom tohto merania sa uskutočnilo nedeštruktívne testovanie materiálu. Ako vzorky boli vybrané štyri umelé srdcové chlopne vyrobené z elektricky vodivého materiálu, konkrétne zo zliatiny Ti-6Al-4V. Na chlopniach boli vytvorené poškodenia definovanej geometrie. Tieto poškodenia majú čoraz väčšiu hĺbku. Ako budiace zariadenie na testovanie vzoriek sa použilo zariadenie s ultrazvukovým budením UTVIS. Najskôr sa uskutočnilo ultrazvukové budenie cez celú oblasť modulovanej frekvencie, pomocou ktorého sa nasledovne vybrala modulovaná frekvencia, ktorá dokázala nájsť chyby na vzorkách.

Za dôležitý fakt možno považovať poznatok, že vplyvom kmitania (ak je modifikovaná frekvencia budiacej oblasti, potom keď zodpovedá frekvencia budenia vlastnej frekvencií objektu vzniká rezonancia) a tohto druhu budenia (ultrazvuk) je reakcia v infračervenom poli závislá od okamžitých premenných signálu excitácie.

Na interpretovaných obrázkoch bol defekt zobrazený svetlými poľami čo bolo spôsobené obmenou radiačnej štruktúry. Táto metóda sa dá považovať za vhodnú metódou na riešenie testovania NDT na identifikáciu chýb srdcových chlopní.

Poďakovanie

Tento príspevok bol podporený VEGA grant No.1/0141/20 a VEGA grant No. 1/0510/20.

LITERATÚRA

[1] SAPIETA, M. - SULKA, P. - SVOBODA, M. (2017): *Localization of delamination in composite test specimen.* XXII SLOVAK-POLISH SCIENTIFIC CONFERENCE ON MACHINE MODELLING AND SIMULATIONS 2017, Book Series: MATEC Web of Conferences, Vol. 157, Article Number: 01015.

[2] DODOK T. - ČUBOŇOVÁ N. - KURIC I. (2017): *Workshop programming as a part of technological preparation of production*. Advanced in Science and Technology Research Journal. Volume 11, issue 1, pages 111-116, ISSN: 2299-8624.

[3] KRAWIEC, P. - DOMEK, G. - WARGUŁA, Ł. - WALUŚ, K. - ADAMIEC, J (2018): *The application of the optical system ATOS II for rapid prototyping methods of non-classical models of cogbelt pulleys.* MATEC Web of Conferences, Vol. 157, art. no 01010.

[5] KRAWIEC, P. - MARLEWSKI, A. (2016): *Profile design of noncircular belt pulleys.* Journal of Theoretical and Applied Mechanics, 54 (2), pp. 561-570.

[6] SÁGA, M. - KOPAS, P. - UHRIČIK, M. (2012): *Modeling and experimental analysis of the aluminium alloy fatigue damage in the case of bending - torsion loading*. Procedia Engineering 48, pp. 599-606.

[7] KOPAS, P. - BLATNICKÝ, M. - SÁGA, M. - VAŠKO, M. (2017): *Identification of mechanical properties of weld joints of AlMgSi07.F25 aluminium alloy*. Metalurgija, Vol. 56, No. 1-2, pp. 99-102.

[8] SAGA, M. - VASKO, M. - SAGOVA, Z. - HANDRIK, M. (2018): *Effective algorithm for structural optimiza-tion subjected to fatigue damage and random excitation*. Scientific journal of Silesian University of Technology – Series Transport, Vol. 99, pp. 149-161.

[9] VAŠKO, M. - BLATNICKÝ, M. - KOPAS, P. - SÁGA, M. (2017): *Research of weld joint fatigue life of the AlMgSi07.F25 aluminium alloy under bending-torsion cyclic loading*. Metalurgija, Vol. 56, No. 1-2, pp. 94-98.

[10] JAKUBOVIČOVÁ, L. - SÁGA, M. - VAŠKO, M. (2014): *Numerical study of influence of mutual slewig of roller bearing rings on the principal stresses at contact area.* Scientific journal of Silesian University of Technology – Series Transport, Vol. 84, pp. 83-91.

[11] DEKÝŠ, V. - SAPIETOVÁ, A. - ŠTEVKA, O. (2013): *Understanding of the dynamical properties of ma-chines based on the interpretation of spectral measurements and FRF*. Conference: 51st International Scientific Conference on Experimental Stress analysis (EAN 2013) Location: Litomerice, Czech Republic, June 11-13.

[12] SAPIETOVÁ, A. - PETRECH, R. - PETROVIČ, M. (2014): *Analysis of the dynamical effects on housing of the axial piston hydromotor.* NOVEL TRENDS IN PRODUCTION DEVICES AND SYSTEMS Book Series: Applied Mechanics and Materials, Vol. 474, pp. 357-362.

[13] KEKEZ, M - RADZISZEWSKI, L - SAPIETOVA, A. (2015): *Fuel type recognition by classifiers developed with computational intelligence methods using combustion pressure data and the crankshaft angle at which heat release reaches its maximum*. 20th INTERNATIONAL CONFERENCE MACHINE MODELING AND SIMULATIONS, MMS 2015, Book Series: Procedia Engineering, Vol. 136.

[14] STALMACH, O. - DEKYS, V. - NOVAK, P. - SAPIETA, M. (2019): *Processing of results from a thermal fem analysis using the lock-in method and comparison with experiment.* Scientific Journal of Silesian University of Technology - Series Transport. Vol. 104, pp. 159-168.

[15] DEKÝŠ, V. - STANKOVIČOVÁ, Z. - NOVÁK, P. - STALMACH, O. (2018): *The contribution to the modal analysis using an infrared camera*. MATEC Web of Conferences, Vol. 157.

[16] DEKYS, V. - STALMACH, O. - SOUKUP, J. - SAPIETOVA, A. - RYCHLIKOVA, L. (2018): *Detection of composite damage by IR NDT using ultrasonic and optic excitation*. XXIII POLISH-SLOVAK SCIENTIFIC CONFERENCE ON MACHINE MODELLING AND SIMULATIONS (MMS 2018), Book Series: MATEC Web of Conferences, Vol. 254.

[17] SAPIETA, M. - DEKYS, V. - PASTOREK, P. (2014): *Using of active thermography and lock-in method with ultrasound excitation for detection of material defects.* SCIENTIFIC REPORTS, 7, Article No.: 1386.

[18] JURKOVIC, M. - KALINA, T. - JANCOSEK, L. - KADNAR, R. - GORZELANCZYK, P. - JERABEK, K. (2019): *Proposal of Conversion the Tugboat Engines to Diesel - LNG Operation* ADVANCES IN SCIENCE AND TECHNOLOGY-RESEARCH JOURNAL Vol. 13, No. 4, pp. 129-142.

[19] EDEVIS Homepage: https://www.edevis.com/content/en/ultrasound_thermography.php

Vplyv excentricity zváracej trajektórie a predohrevu na deformáciu a zvyškové napätia hliníkovej zliatiny zváranej elektrónovým lúčom

Pavol Novák, Ing., PhD. *
Katedra aplikovanej mechaniky, Strojnícka fakulta,
Žilinská univerzita v Žiline,
Univerzitná 8215/1, 010 26 Žilina, Slovenská republika.
E-mail: pavol.novak@fstroj.uniza.sk, Tel.: + 421 41 513 2968

Peter Kopas, Ing., PhD.
Katedra aplikovanej mechaniky, Strojnícka fakulta,
Žilinská univerzita v Žiline,
Univerzitná 8215/1, 010 26 Žilina, Slovenská republika.
E-mail: peter.kopas@fstroj.uniza.sk, Tel.: + 421 41 513 2984

Milan Vaško, doc. Ing., PhD.
Katedra aplikovanej mechaniky, Strojnícka fakulta,
Žilinská univerzita v Žiline,
Univerzitná 8215/1, 010 26 Žilina, Slovenská republika.
E-mail: milan.vasko@fstroj.uniza.sk, Tel.: + 421 41 513 2981

Marián Handrik, Ing., PhD.
Katedra aplikovanej mechaniky, Strojnícka fakulta,
Žilinská univerzita v Žiline,
Univerzitná 8215/1, 010 26 Žilina, Slovenská republika.
E-mail: marian.handrik@fstroj.uniza.sk, Tel.: + 421 41 513 2955

Milan Sága, prof. Ing. Dr.
Katedra aplikovanej mechaniky, Strojnícka fakulta,
Žilinská univerzita v Žiline,
Univerzitná 8215/1, 010 26 Žilina, Slovenská republika.
E-mail: milan.saga@fstroj.uniza.sk, Tel.: + 421 41 513 2500

Influence of eccentricity of welding trajectory and preheating on deformation and residual stresses of aluminium alloy welded by electron beam

Abstract: The aim of this paper is to investigate the influence of technological parameters of the welding process on the level of the residual stresses, distortions, and phase proportions. The preheating temperature and the eccentricity of the weld path are taken into account. The Visual Weld tool from ESI Group was used for simulation.

ÚVOD

Vykonanie numerických simulácií zvarových spojov nám umožňuje zistiť vplyv technologických parametrov zvárania na veľkosť zvyškových napätí, percentuálneho zastúpenia fáz a veľkosti pretvorenia výrobkov. To je spojené so znižovaním nákladov spojených so správnym návrhom technológie výroby zvarového spoja. Simulácie tvorby zvarových spojov je možné vykonávať s rôznym stupňom zohľadnenia prebiehajúcich fyzikálnych dejov počas zvárania. Autori v práci [1] simulujú pri ohreve materiálu pomocou lasera komplexný problém šírenia tepla a prúdenia materiálu v roztavenej oblasti zvarového spoja. Je to zložitý fyzikálny problém vyžadujúci veľa vstupných parametrov a zložité numerické metódy pre simulovanie pohybujúceho sa rozhrania tavenina-kov. Preto si mnohé softvéry zjednodušujú simulácie procesov zvárania tak, že reálne simulujú len procesy prebiehajúce v tuhej fáze. Takto postupuje aj

program Sysweld, ktorý sa používa ako riešič v prostredí Visual Weld. Program Sysweld umožňuje simulovať zmenu skupenstva pomocou zadaného skupenského tepla a teplotnej závislosti všetkých vstupných materiálových vlastností. Ďalšie zjednodušenie a zrýchlenie simulácie v prostredí Visual Weld je možnosť riešiť najskôr tepelno-metalurgickú analýzu a až následne štrukturálnu analýzu. Tento postup je presný, keď môžeme zanedbať teplo vzniknuté pri plastickej deformácii materiálu, čo platí pre drvivú väčšinu technológií zvárania. Riešenie tepelno-metalurgickej analýzy je výrazne rýchlejšie. To sa veľmi často využíva na naladenie zdrojov tepla pre daný spôsob zvárania, rozmery a tvary zvarových húseníc ako aj rozmery a tvary zváraných dielcov. Na kvalitné naladenie tepelného zdroja je potrebné vykonať experimentálne meranie a z neho získať „makrá“ zvarového spoja a merať teplotné cykly procesu zvárania. Takto naladený tepelný zdroj potom bude zabezpečovať, že veľkosť a tvar roztavenej oblasti zvarového spoja, ako aj veľkosť a tvar tepelne ovplyvnenej oblasti sa budú zhodovať s experimentom. V [2] je uvedený spôsob modelovania tepelného zdroja pre laserový lúč použitý na rezanie materiálu a vplyvu jeho parametrov na kvalitu rezových plôch ako aj na teplotné namáhanie materiálu. Rozmery roztavenej oblasti a tepelne ovplyvnenej oblasti spolu s teplotnými cyklami vplývajú na veľkosť a rozloženie zvyškových napätí, pretvorení a zmene percentuálneho zastúpenia fáz v blízkosti zvarovej húsenice. V [3] autori skúmajú vplyv zvarového spoja na mechanické vlastnosti zliatiny hliníka.

1 MODELOVANIE ZVÁRANIA HLINÍKOVÝCH ZLIATIN TRIEDY 5000

Pri zváraní hliníkových zliatin triedy 5000 simulujeme fázové zmeny prebiehajúce medzi štyrmi fázami. Fáza číslo jeden predstavuje pôvodný materiál dielcov. Ide o mechanicky spevnený materiál.

Fáza číslo dva má veľmi nízke mechanické vlastnosti a reálne tepelné vlastnosti. Používa sa na počiatočnú náhradu zvarových húseníc, lebo konečnoprvková sieť musí už na začiatku analýzy obsahovať aj prvky modelujúce húsenice, ktoré však vznikajú až v procese zvárania. Počas procesu zvárania sa účinkom prechádzajúceho tepelného zdroja táto pomocná fáza premení na reálnu fázu s reálnymi tepelnými aj mechanickými vlastnosťami. Táto premena je popísaná pomocou ARA diagramu zliatiny, ktorý je súčasťou materiálových dát.

Fáza číslo tri má vlastnosti hliníkovej zliatiny s daným chemickým zložením, ktorá bola roztavená.

Fáza číslo štyri predstavuje rekryštalizovaný materiál – materiál s nižšími pevnostnými vlastnosťami ako mala fáza číslo jedna – pôvodný materiál dielcov.

Fázové transformácie sú popísané pomocou Leblondovho modelu fázových transformácií.

2 POPIS NUMERICKÉHO MODELU ZVAROVÉHO SPOJA

V článku uvádzame príklad zvarového spoja tvaru *T*, ktorého geometria spolu s použitou sieťou konečných prvkov je na obr. 1.

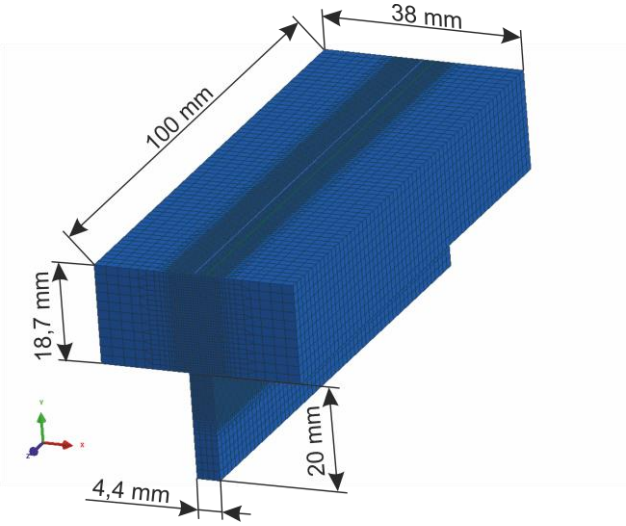

Obr. 1. Geometria simulovaného zvarového spoja typu *T*

Hliníkové platne tvoriace T spoj sú pred samotným procesom zvárania spojené pomocou bodových zvarov na obidvoch koncoch a v strede platní. Počas prvých 200 s je zvarový spoj uchytený ako je uvedené na obr. 2. Uchytenie simuluje upevnenie hrubšej platne v čeľustiach zveráku. Toho je dosiahnuté odobratím všetkých možných posunutí uzlov konečnoprvkovej siete v miestach označených červenými bodkami.

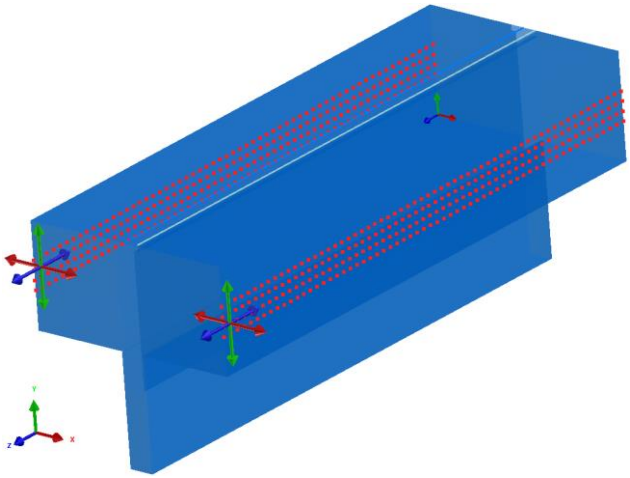

Obr. 2. Uchytenie zvarového spoja počas prvých 200 s zvárania

Následne je zvarový spoj uvoľnený zo zveráka a voľne položený na pracovnom stole až do

vychladnutia, t. j. do času 7200 s. Tento spôsob uchytenia je modelovaný pomocou staticky určitého uchytenia ako je uvedené na obr. 3.

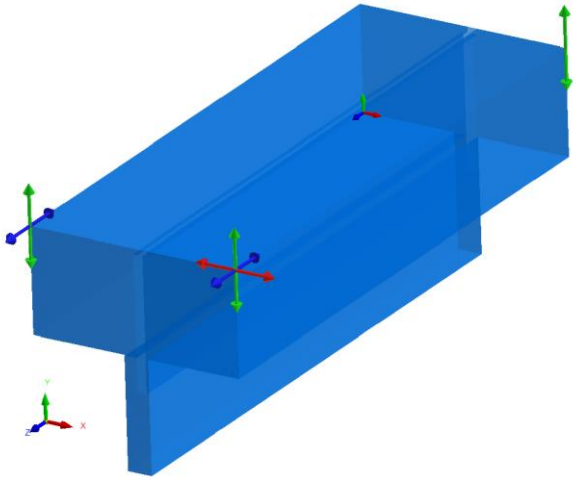

Obr. 3. Uchytenie zvarového spoja v časovom intervale 200 – 7200 s (do vychladnutia)

Použitá sieť konečných prvkov pozostáva z 302 684 prvkov a 278 886 uzlov. V roztavenej oblasti zvarového spoja a v tepelne ovplyvnenej oblasti je použitá jemná mapovaná sieť osemstenových prvkov z dôvodu zachytenia tu vznikajúcich gradientov zvyškových napätí, teplotných gradientov a s tým súvisiacimi zmenami fáz. V ostatných oblastiach je z dôvodu efektivity výpočtu použitá hrubšia sieť.

Percentuálny obsah legujúcich prvkov v simulovanej hliníkovej zliatine je uvedený v tab. 1.

Tab. 1. Chemické zloženie legujúcich prvkov hliníkovej zliatiny

Chemický prvok	Percentuálny podiel
Si	0,25
Fe	0,4
Cu	0,1
Mn	0,5-1,0
Mg	2,4-3,0
Cr	0,05-0,2
Zn	0,25
Ti	0,2

Pre simulovanie zvárania pomocou elektrónového lúča bol použitý kónický tepelný zdroj kombinovaný s tepelným zdrojom Gaussovho typu.

Pri simulácii bola predpísaná vnesená tepelná energia na jednotku dĺžky $Q = 650\ \mathrm{J \cdot mm^{-1}}$, rýchlosť zvárania $v = 8\ \mathrm{mm \cdot s^{-1}}$, vrchný priemer kónického zdroja tepla 2,2 mm, spodný priemer kónického zdroja tepla 2,0 mm a penetrácia zvaru 23 mm.

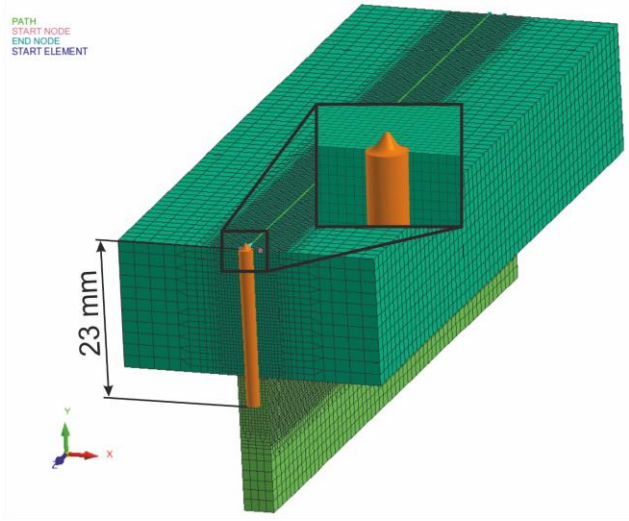

Obr. 4. Tvar použitého tepelného zdroja

Pri výpočtoch boli simulované tri hodnoty excentricity trajektórie zvarového spoja: 0,1 mm, 0,2 mm a 0,3 mm. Rovnako boli simulované tri hodnoty predohrevu a to 50 °C, 100 °C a 150 °C.

3 VÝSLEDKY SIMULÁCIÍ

3.1 Vplyv excentricity trajektórie zvaru

Obrázok 5 ukazuje, že excentricita trajektórie zvaru nemá vplyv na maximálne a minimálne hodnoty posunutí zvarenca po vychladnutí. Tieto hodnoty vymedzujú objem, v ktorom sa bude zvarenec nachádzať. Ich zmena je v tisícinách milimetra.

Excentricita však vplýva na hodnoty zvyškových napätí vo zvarenci (obr. 6). Hodnota redukovaného napätia podľa Misesa s excentricitou rastie. Výraznejšie pre excentricitu väčšiu ako 0,2 mm. Maximálna hodnota prvého hlavného napätia však s excentricitou rastie veľmi nevýrazne. Prvé hlavné napätie predstavuje maximálne ťahové napätie, ktoré bude vo vzorke pôsobiť a mohlo by byť hnacou silou šírenia trhlín. Hodnota tretieho hlavného napätia pri excentricite 0,2 mm poklesne voči hodnote pri excentricite 0,1 mm, ale potom opäť výrazne stúpne pri excentricite 0,3 mm.

3.2 Vplyv teploty predohrevu materiálu

Obrázok 7 reprezentuje vplyv teploty predohrevu na maximálne a minimálne hodnoty posunutí bodov zvarenca. Maximálna hodnota posunutia v smere osi *y* mierne klesá a minimálna hodnota posunutia v smere osi z v absolútnej hodnote rastie: Ostatné posunutia sa menia nevýrazne. Obrázok 8 znázorňuje vplyv predohrevu zvarenca na pokles jeho zvyškových napätí.

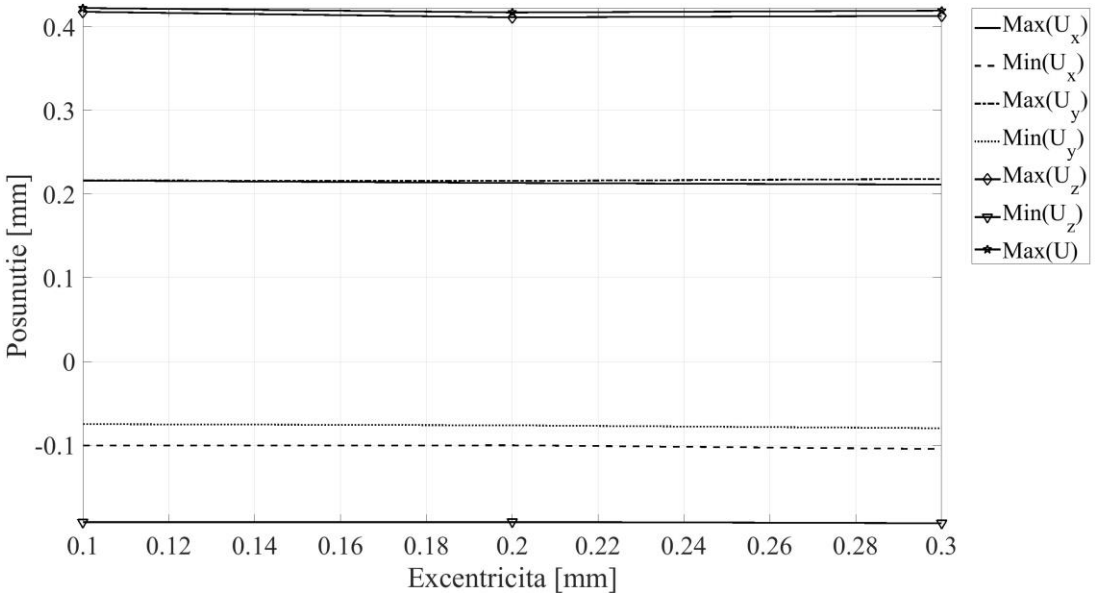

Obr. 5. Vplyv excentricity na posunutia bodov zvarenca

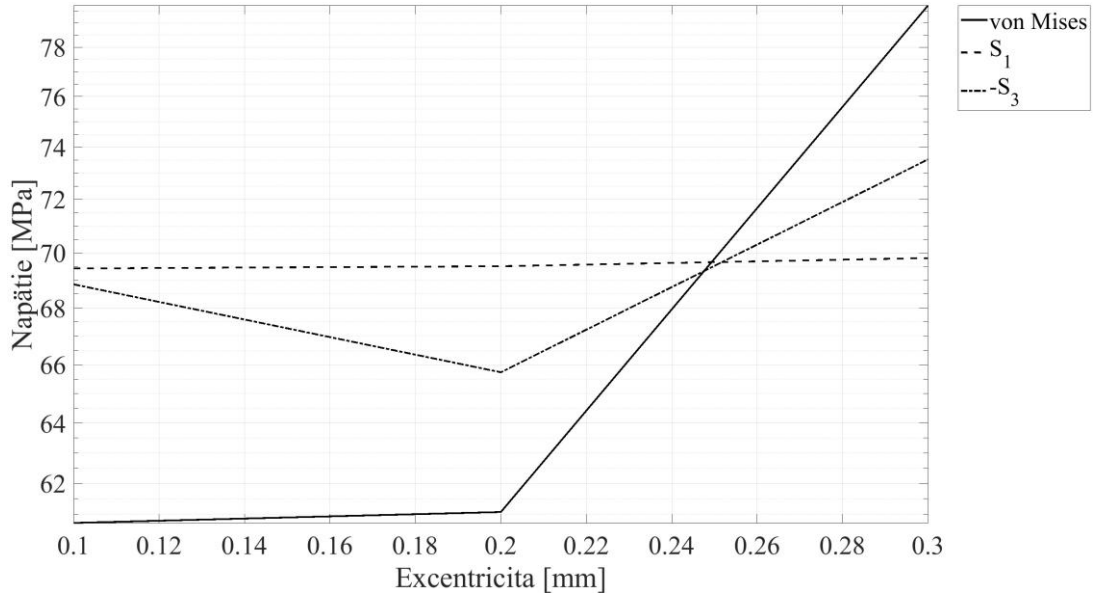

Obr. 6. Vplyv excentricity na hodnoty zvyškových napätí zvarenca

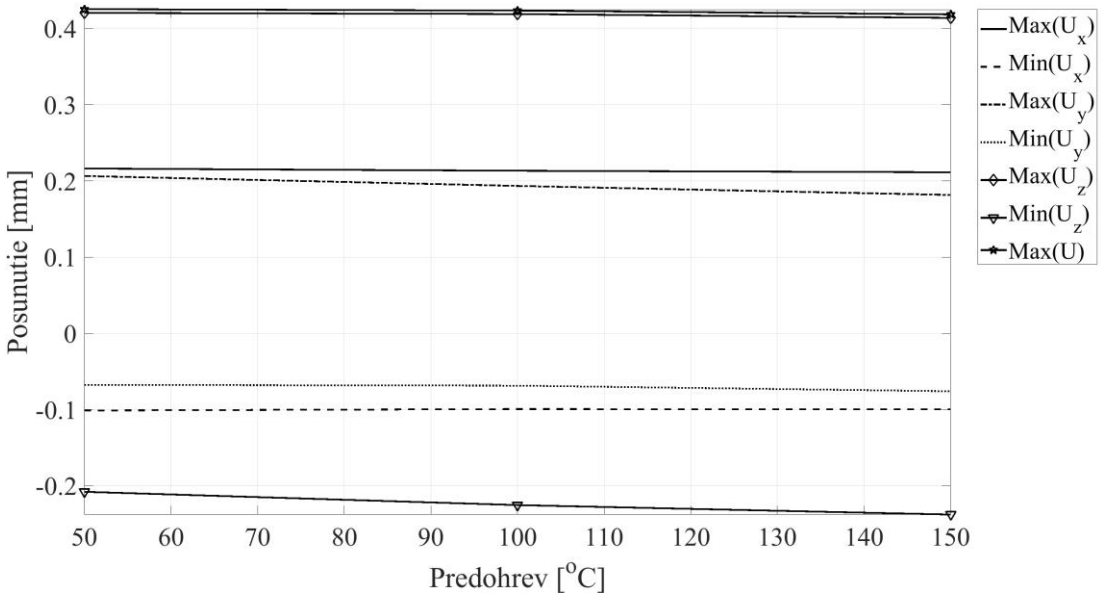

Obr. 7. Vplyv teploty predohrevu zvarenca na posunutia bodov

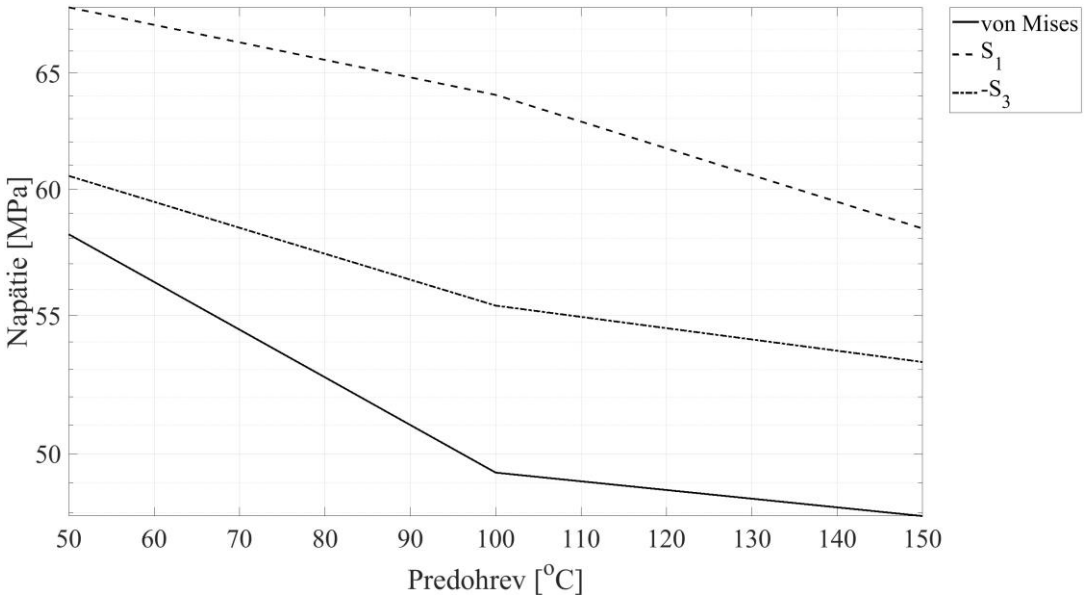

Obr. 8. Vplyv teploty predohrevu zvarenca na hodnoty zvyškových napätí

ZÁVER

Z prezentovaných výsledkov vyplýva, že s rastúcou hodnotou excentricity rastie hodnota zvyškových napätí vo zvarenci a s rastúcou hodnotou predohrevu hodnota zvyškových napätí vo zvarenci klesá. Pokles zvyškových napätí vo zvarenci so zvyšujúcou sa hodnotou predohrevu je spôsobený poklesom percentuálneho zastúpenia fázy číslo jeden vo zvarenci.

Poďakovanie

Poďakovanie Ministerstvu školstva, vedy, výskumu a športu Slovenskej republiky v súvislosti s realizáciou projektu Výskum inteligentných systémov a procesov s použitím princípov Industry 4.0 so zameraním na spájanie ťažko spojiteľných materiálov vysokokoncentrovanými zdrojmi energie -laserom a elektrónovým lúčom, č. Zmluvy MŠSR 1227/2018.

LITERATÚRA

[1] KUBIAK, M. (2019): *Prediction of microstructure composition in steel plate heated using high power Yb: YAG laser radiation.* In: Malujda, I; Dudziak, M; Krawiec, P. (eds.) MMS 2018, MATEC Web of Conferences, Vol. 254, pp. 1–13.

[2] SATERNUS, Z. - PIEKARSKA, W. - KUBIAK, M. - DOMANSKI, T. - GOSZCZYNSKA-KROLISZEWSKA, D. (2019): *Numerical modeling of cutting process of steel sheets using a laser beam.* In: Malujda, I; Dudziak, M; Krawiec, P. (eds.) MMS 2018, MATEC Web of Conferences, Vol. 254, pp. 22-28.

[3] KOPAS, P. - BLATNICKÝ, M. - SÁGA, M. VAŠKO, M. (2017): *Identification of mechanical properties of weld joints of AlMgSi07.F25 aluminium alloy*. Metalurgija, Vol. 56, No. 1-2, pp. 99-102.

Porovnanie spôsobov umiestnenia meracej techniky pri použití optickej lock-in termografie

Ondrej Štalmach, Ing., PhD.*
Katedra aplikovanej mechaniky, Strojnícka fakulta,
Žilinská univerzita v Žiline,
Univerzitná 8215/1, 010 26 Žilina, Slovenská republika.
E-mail: ondrej.stalmach@fstroj.uniza.sk, Tel.: + 421 41 513 2965

Vladimír Dekýš, doc. Ing., CSc.
Katedra aplikovanej mechaniky, Strojnícka fakulta,
Žilinská univerzita v Žiline,
Univerzitná 8215/1, 010 26 Žilina, Slovenská republika.
E-mail: vladimir.dekys@fstroj.uniza.sk, Tel.: + 421 41 513 2954

Václav Straka, Ing.
TMV SS spol. s r. o.
Studánková 395, 14000, Praha.
E-mail: vaclav.straka@tmvss.cz, Tel.: +420 272 942 720

Comparison of methods of positioning measuring system using optical lock-in thermography

Abstract: Optical lock-in thermography is a non-destructive testing method. The surface of the sample is excited using the thermal waves and the response is recorded by the thermal camera. This image thermal sequence is processed using the image processing method named lock-in method. Optical lock-in thermography can be used to detect cracks and damages in metal or composite material. Two position modes are used: the reflection and the transmission mode. In this paper, are compared these two modes. An experiment is carried out on a printed composite plane with the square blinded holes placed in the different depths below the surface. The phase images are created using the lock-in method for both position modes. The results are compared, and the advantages and the disadvantage of these position modes find out.

ÚVOD

Za posledných 20 rokov sa termografia rozvinula na dva hlavné smery: na aktívnu a pasívnu termografiu. V súčasnosti sa vedci zameriavajú hlavne na vývoj nových metód v oblasti aktívnej termografie. Aktívna termografia sa líši od pasívnej termografie tým, že meraný objekt musí byť excitovaný externým zdrojom, napr. pomocou tepelnej vlny. Následne sa odozva na dané budenia meria pomocou termokamery. Aktívna termografia sa využíva na rôzne typy meraní ako napr. nedeštruktívne testovanie (NDT) pomocou termografických systémov [1-4], termoelastická napäťová analýza [5-9], metódy na hodnotenie únavy materiálov [10-16] atď.

Najznámejšie metódy v oblasti aktívnej termografie sú:

- Termoelastická napäťová analýza TSA.
- Pulzná termografia.
- Lock-in termografia.
- Vibrotermografia.
- Rýchla metóda stanovenia medze únavy.

1 LOCK-IN METÓDA

V prípade modulovaného ohrevu povrchu telesa frekvenciou *f* sa v podpovrchovej oblasti šíri tlmená a rozptýlená tepelná vlna. V rovinných vrstvách telesa je možné pomocou vzťahu (1) vyhodnotiť teplotu *T* v hĺbke *z* pod povrchom telesa a v čase *t* [17]:

$$T(z,t) = T_0 \cdot e^{-\frac{z}{\mu}} \cdot \cos\left(\frac{2 \cdot \pi \cdot z}{\lambda} - 2 \cdot \pi \cdot f \cdot z\right), \qquad (1)$$

kde μ je hĺbka prieniku tepelnej vlny, pri ktorej teplota klesne na $\frac{1}{e^{T_0}}$,

T_0 je povrchová teplota telesa.

Rovnica pre výpočet μ je nasledujúca [17]:

$$\mu = \sqrt{\frac{\kappa}{\pi \cdot f \cdot \rho \cdot c_p}}, \qquad (2)$$

kde κ je súč. tepelnej vodivosti [W. m^{-1}. K^{-1}],
ρ je hustota [kg. m^{-3}],
c_p je merná tep. kapacita [J. kg^{-1}. K^{-1}],
λ je tepelná vlnová dĺžka [m],
f je frekvencia [Hz].

Lock-in termografia je založená na tepelných vlnách generovaných vo vnútri meraného objektu pomocou periodického (sínusového) budiaceho signálu. Periodický budiaci signál má frekvenciu nazývanú lock-in frekvencia f_L. Tepelná vlna (zvyčajne sínusová) preniká do meraného objektu a pri anomálii v štruktúre sa odráža späť smerom k povrch. Na povrchu objektu dochádza k interferencii vyžarovaného a dopadajúceho infračerveného žiarenia. Vďaka tomu sú snímané termogramy na danom mieste modifikované vracajúcou sa tepelnou vlnou z vnútra meraného objektu. Odozva sa pre vybrané f_L získa z hĺbky μ pod povrchom meraného objektu. Týmto spôsobom je teoreticky možné získať odozvu v celom rozsahu hrúbky materiálu pomocou rôznych hodnôt f_L.

Hlavnou myšlienkou lock-in termografie je predpoklad, že keď má budiaci signál sínusový charakter s frekvenciou f_L, zaznamenaná odozva bude mať tiež sínusový charakter s rovnakou frekvenciou. Z toho vyplýva, že rovnicu odozvy je možné napísať nasledovne:

$$\begin{aligned} s(t) &= A\cdot\sin\left(2\cdot\pi\cdot f_L\cdot t+\varphi\right)= \\ &= A\cdot\cos\varphi\cdot\sin\left(2\cdot\pi\cdot f_L\cdot t\right)+ \\ &+A\cdot\sin\varphi\cdot\cos\left(2\cdot\pi\cdot f_L\cdot t\right)= \\ &= a\cdot\cos\left(2\cdot\pi\cdot f_L\cdot t\right)+b\cdot\sin\left(2\cdot\pi\cdot f_L\cdot t\right) \end{aligned} . \quad (3)$$

Odhad parametrov a, b je určený odhadmi a_{cos}, b_{sin} pomocou vzťahov diskrétnej Fourierovej transformácie nasledovne:

$$a_{\cos}=\sum_{i=1}^{N}S_i\cdot\cos\left(2\cdot\pi\cdot f_L\cdot t_i\right),. \quad (4)$$

$$b_{\sin}=\sum_{i=1}^{N}S_i\cdot\sin\left(2\cdot\pi\cdot f_L\cdot t_i\right),. \quad (5)$$

kde N je počet snímkov z termokamery,
S_i je i-ty snímok,
t_i je čas, kedy bol i-ty snímok nasnímaný.

Následne pre fázu harmonickej funkcie $s(t)$ platí rovnica:

$$\varphi=\arctan\frac{a_{\cos}}{b_{\sin}}. \quad (6)$$

2 EXPERIMENTÁLNE MERANIE

Experimentálne meranie bolo vykonané v spolupráci so spoločnosťou TMVSS s.r.o. Spoločnosť zapožičala pre dané meranie optický budiaci systém OTvis, potrebnú termokameru InfraTec ImageIR a priestory v jej budove.

Pred meraním bolo potrebné navrhnúť a vyrobiť testovaciu vzorku. Vzorka bola navrhnutá ako platnička s rozmermi 120x120 x5 mm. Bola vyrobená z kompozitného materiálu Onyx pomocou 3D tlačiarne Mark TWO. Vzorka obsahoval 9 defektov so štvorcovým prierezom so stranami 10x10 mm (obr. 1). Defekty boli navrhnuté ako slepé diery s rôznou hĺbkou (od 0,5 do 4,5 mm, s prírastkom 0,5 mm).

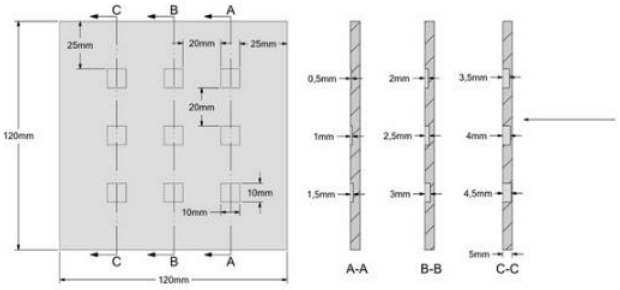

Obr. 1. Rozmery skúšobnej vzorky

Testovacia vzorka sa merala pomocou optickej lock-in termografie. Použité boli dva spôsoby rozloženia meracej techniky: reflexná metóda a transmisná metóda. Ako zdroj budenia bola použitá halogénová lampa s výkonom 2,5 kW. Na zaznamenávanie odozvy bola použitá termokamera InfraTec ImageIR s rozlíšením 640x480 pixelov. Na spracovanie nameraných údajov a vyhodnotenie fázových obrazov sa použil softvér DisplayIMG.

Pre reflexnú aj transmisnú metódu bolo nameraných desať záznamov. Boli použité rôzne lock-in frekvencie s cieľom získať odozvu na desiatich rôznych miestach pod povrchom. Lock-in frekvencie sa vypočítali pomocou materiálových vlastností nasledovne:

$$f_L=\frac{\kappa}{\pi\cdot\rho\cdot c_p\cdot\mu^2}=\frac{\alpha}{\pi\cdot\mu^2}. \quad (7)$$

Pretože súč. tepelnej vodivosti κ a merná tep. kapacita c_p nie sú definované výrobcom materiálu Onyx, ich hodnoty bolo možné približne vyjadriť pomocou zmiešavacieho pravidla (pretože bol známy percentuálny pomer jednotlivých zložiek). Onyx sa skladá z 93 % nylonu a 7 % uhlíka, a preto je možné κ a c_p vyjadriť nasledovne:

$$\begin{aligned} c_{p-onyx} &= 0,93\cdot c_{p-nylon}+0,07\cdot c_{p-uhlík}= \\ &= 0,93\cdot 1510+0,07\cdot 717=1454,5\left[\mathrm{J\cdot kg^{-1}\cdot K^{-1}}\right] \end{aligned}. \quad (8)$$

$$\begin{aligned} \kappa_{onyx} &= 0,93\cdot\kappa_{nylon}+0,07\cdot\kappa_{uhlík}= \\ &= 0,93\cdot 0,23+0,07\cdot 1,7=0,33\left[\mathrm{W\cdot m^{-1}\cdot K^{-1}}\right] \end{aligned}. \quad (8)$$

V tab. 1 sú vypočítané lock-in frekvencie pre zadané hĺbky μ pod povrchom.

Počas merania bola testovacia doska pripevnená k polystyrénovej doske 1000x1000x50 mm, na ktorý sa aplikoval čierny emisný sprej. Uprostred polystyrénovej platne bol urobený otvor 100x100 mm. Testovaná vzorka bola pripevnená tak, aby na každej strane vzorky bolo 20 mm prekrytie s polystyrénovou doskou. Cieľom tohto riešenia bolo homogenizovať prostredie okolo testovacej platne.

Tab. 1. Lock-in frekvencie zodpovedajúce príslušným hĺbkam μ pod povrchom

	1.	**2.**	**3.**	**4.**	**5.**
μ [mm]	0,25	0,5	0,75	1,0	1,25
f_L [Hz]	0,968	0,242	0,108	0,06	0,039
	6.	**7.**	**8.**	**9.**	**10.**
μ [mm]	1,5	1,75	2,0	2,25	2,5
f_L [Hz]	0,027	0,02	0,015	0,012	0,01

Termokamera a halogénová žiarovka boli umiestnené vo vzdialenosti 1 m od meranej vzorky v uhle približne 40°. Výkon žiarovky bol nastavený na 50 % výkonu a dĺžka záznamu bola nastavená na štyri budiace periódy.

3 REFLEXNÁ METÓDA

Reflexná metóda spočíva v tom, že termokamera a zdroj budenia (halogénová lampa) sú umiestnené vedľa seba a oproti je umiestnený meraný objekt (obr. 2).

Obr. 2. Reflexná metóda

Na obr. 3 sú znázornené fázové obrazy pre jednotlivé odozvy z hĺbky μ pod povrchom vzorky. Vzorka bola navrhnutá tak, aby prvý defekt (defekt v ľavom dolnom rohu) bol umiestnený 0,5 mm pod povrchom a každý ďalší defekt bol umiestnený o 0,5 mm nižšie. Zároveň takéto umiestenie defektov umožňovalo overiť správnosť vypočítaných materiálových vlastností súč. tepelnej vodivosti κ (8) a mernej tep. kapacity c_p (9).

Pretože, ak by boli hodnoty κ a c_p boli vypočítané správne, defekty by sa mali zobrazovať postupne pri 2. (μ = 0,5 mm), 4. (μ = 1 mm), 6. (μ = 1,5 mm), 8. (μ = 2 mm), 10. (μ = 2,5 mm), fázovom obraze (6 a 7).

Na obr. 3 je vidieť, že prvý defekt (v ľavom dolnom rohu) je zobrazený v hĺbke μ = 0,5 mm a druhý defekt je zobrazený v μ = 1 mm. Tretia chyba sa zobrazuje v hĺbke μ = 1,5 mm. Štvrtý defekt sa mierne zobrazuje už v hĺbke μ = 1,75 mm. Piaty defekt sa zobrazuje iba minimálne v hĺbke μ = 2,5 mm.

Z daných výsledok merania sa dá predpokladať, že vypočítané materiálové vlastnosti súč. tepelnej vodivosti κ a merná tep. kapacita c_p boli vypočítané správne.

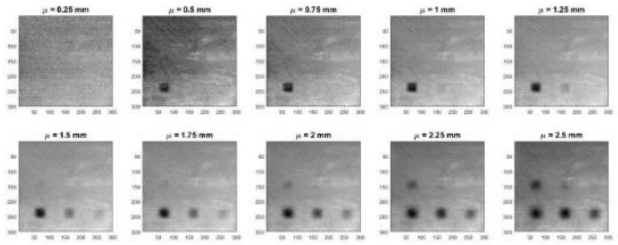

Obr. 3. Reflexná metóda: fázové obrazy

4 TRANSMISNÁ METÓDA

Transmisná metóda sa líši od reflexnej metódy v tom, že meraný objekt je umiestnený medzi termokamerou a zdrojom excitácie. Termokamera meria odozvu na prednej/meracej ploche objektu a zdroj excitácie excituje jeho zadnú stranu (pozri obr. 4).

Obr. 4. Transmisná metóda

Termokamera bola umiestnená vo vzdialenosti 1 m tak ako pri reflexnej metóde a halogénová lampa sa umiestnila 1 m od zadnej plochy polystyrénovej platne. Nastavený výkon na 50 % a dĺžka záznamu štyri periódy zostali nezmenené.

Na obr. 5 sú znázornené fázové obrazy z daného merania. Je vidieť, ako sa výsledky daných metód výrazne líšia.

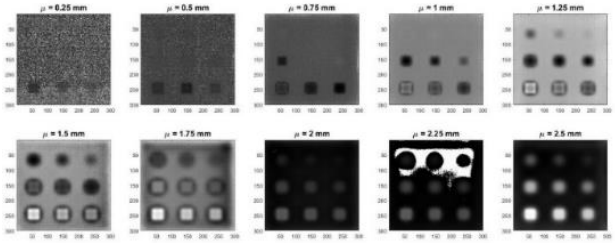

Obr. 5. Transmisná metóda: fázové obrazy

Z nameraných údajov je zrejmé, že je možné detegovať poruchy skôr, ako by sa mali zobrazovať podľa teórie tepelných vĺn. Z fázových obrazov možno pozorovať, že je možné zistiť prítomnosť všetkých deväť defektov. Kvalita zobrazenia fázového obrazu sa postupne zvyšuje až do hĺbky μ = 1,5 mm. Následne kvalita obrazu klesá a v hĺbke μ = 2,25 mm je fázový obraz poškodený v dôsledku saturácia detektora termokamery.

ZÁVER

Z nameraných údajov je zrejmé, že každá z metód (reflexia aj transmisná) má svoje výhody a nevýhody. Výhodou reflexnej metódy je, že sa riadi teóriou tepelných vĺn. Z tohto dôvodu umožňuje získať informácie o prítomnosti defektu v meranom objekte a najmä v akej hĺbke pod povrchom sa nachádza. Na druhej strane nevýhodou je, že hĺbka, z ktorej je možné získať odozvu, je pre kompozitný materiál Onyx približne 2,5 mm. Z tohoto dôvodu bolo možné pri experimentálnom meraní zistiť prítomnosť iba päť z deviatich defektov na testovacej vzorke. Nevýhodou taktiež bolo, že fázový obraz získaný z väčšej hĺbky pod povrchom mal zhoršenú schopnosť zobrazovať skutočný tvar defektov.

Transmisná metóda nedodržiava štandardné pravidlá teórie tepelných vĺn, pretože defekty sa zobrazovali skôr, ako mali. Preto nebolo možné získať odozvu z konkrétnej hĺbky pod povrchom meraného objektu (nebolo možné definovať, v akej hĺbke pod povrchom sa defekty nachádzajú). Výhodou oproti reflexnej metóde je však to, že bolo možné zistiť prítomnosť všetkých deväť defektov.

Transmisná metóda má vyššiu schopnosť detegovať prítomnosť defektov (kvalitatívne hodnotenie), zatiaľ čo reflexná metóda poskytuje informácie o morfológii/tvare a polohe defektov (kvantitatívne hodnotenie).

Ďalším cieľom príspevku bolo overiť, či boli hodnoty materiálových parametrov κ a c_p vypočítané správne pomocou zmiešavacieho pravidla (8) (9). Z výsledkov meraní pomocou reflexnej metódy môžeme pozorovať, že poruchy sa zobrazujú pri lock-in frekvenciách, pri ktorých by sa mali zobrazovať podľa teórie tepelných vĺn. Preto môžeme považovať vypočítané materiálové parametre κ a c_p za správne.

Poďakovanie

Tento príspevok bol podporený projektom VEGA 1/0510/20 a VEGA 1/0141/20.

LITERATÚRA

[1] STANKOVICOVA, Z. - DEKYS, V. - NOVY, F. - NOVAK, P. (2017): *Nondestructive testing of metal parts by using infrared camera STFT*. Procedia Engineering, Vol. 177, pp. 562-567.

[2] DEKYS, V. - KOPAS, P. - SAPIETA, M. - STEVKA, O. (2014): *A detection of deformation mechanisms using infrared thermography and acoustic emission*. Applied Mechanics and Materials, Vol. 474, pp. 315-320.

[3] JAKUBOVICOVA, L. - VASKO, M. - SAGA, M. - KOPAS, P. (2018): *Experimental and computational comparative study of the specimens loaded by bending and torsion*. MATEC Web of Conferences, Vol. 157.

[4] SAPIETA, M. - DEKYS, V. - PASTOREK, P. (2014): *Using of active thermography and lock-in method with ultrasound exication for detection of material defects*. Scientific Journal of Silesian University of Technology-Series Transport, Vol. 84, pp. 119-124.

[5] SAPIETA, M. - SAPIETOVA, A. - DEKYS, V. (2017): *Comparison of the thermoelastic phenomenon expressions in strainless steels during cyclic loading*. Metalurgija, Vol. 56, pp. 203-206.

[6] SAPIETA, M. - DEKYS, V. - SAPIETOVA, A. (2016): *Thermal-stress analysis of beam loaded by 3-point bending.* Procedia Engineering, Vol. 136, pp. 216-219.

[7] SAPIETOVA, A. - NOVAK, P. - SAGA, M. - SULKA, P. - SAPIETA, M. (2019): *Dynamic and Stress Analysis of a Locking Mechanism in the Ansys Workbench Software Environment.* Advances in Science and Technology-Research Journal, Vol. 13, pp. 23-28.

[8] STANKOVICOVA, Z. - DEKYS, V. - NOVAK, P. (2016): *Time average synchronization in thermoelastic stress analysis*. Procedia Engineering, Vol. 136, pp. 204-210.

[9] HONNER, M. - HONNEROVA, P. (2015): *Survey of emissivity measurement by radiometric methods.* Applied Optics, Vol. 54, pp. 669-683.

[10] STANKOVICOVA, Z. - DEKYS, V. - UHRICIK, M. - NOVAK, P. - STRNADEL, B. (2018): *Fatigue limit estimation using IR camera*. MATEC Web of Conferences, Vol. 157.

[11] DEKYS, V. - KRISKA, P. - LIETAVA, L. - KOPAS, P. - STALMACH, O. (2018): *Simplified estimate of fatigue damage based on dynamic analysis*. Scientific Journal of Silesian University of Technology-Series Transport, Vol. 99, pp. 15-23.

[12] KOPAS, P. - SAGA, M. - NOVY, F. - LEITNER, B. (2018): *Low-cycle fatigue behaviour of laser welded high-strength steel DOMEX 700 MC*. MATEC Web of Conferences, Vol. 157.

[13] SAGA, M. - VASKO, M. - KOPAS, P. - PIEKARSKA, W. - DOMANSKI, T. - KUBIAK, M. (2018): *Contribution to fatigue damage prediction of thin shell finite element models.* MATEC Web of Conferences, Vol. 157.

[14] SAGA, M. - KOPAS, P. - UHRICIK, M. (2012): *Modeling and Experimental Analysis of the Aluminium Alloy Fatigue Damage in the case of Bending - Torsion Loading.* Procedia Engineering, Vol. 48, pp. 599-606.

[15] SAPIETA, M. - SULKA, P. - SVOBODA, M. (2018): *Monitoring the fatigue crack on the test specimen during the cyclic loading*. MATEC Web of Conferences, Vol. 157.

[16] SAPIETA, M. - SAPIETOVA, A. - GAJDOS, L. (2017): *Determine the fatigue life of flange of bearings test station.* Procedia Engineering, Vol. 177, pp. 548-553.

[17] KREIDL, M. - SMID, R. (2006): *Technická diagnostika.* BEN - technická literatúra, Vol. 1, ISBN 80-7300-158-6.

Kinematická analýza priestorovej viazanej mechanickej sústavy

Alžbeta Sapietová, prof. Ing., PhD.*
Katedra aplikovanej mechaniky, Strojnícka fakulta,
Žilinská univerzita v Žiline,
Univerzitná 8215/1, 010 26 Žilina, Slovenská republika.
E-mail: alzbeta.sapietova@fstroj.uniza.sk, Tel.: + 421 41 513 2950

Vladimír Dekýš, doc. Ing., CSc.
Katedra aplikovanej mechaniky, Strojnícka fakulta,
Žilinská univerzita v Žiline,
Univerzitná 8215/1, 010 26 Žilina, Slovenská republika.
E-mail: vladimir.dekys@fstroj.uniza.sk, Tel.: + 421 41 513 2954

Ondrej Štalmach, Ing., PhD.
Katedra aplikovanej mechaniky, Strojnícka fakulta,
Žilinská univerzita v Žiline,
Univerzitná 8215/1, 010 26 Žilina, Slovenská republika.
E-mail: ondrej.stalmach@fstroj.uniza.sk, Tel.: + 421 41 513 2974

Milan Sapieta, Ing., PhD.
Katedra aplikovanej mechaniky, Strojnícka fakulta,
Žilinská univerzita v Žiline,
Univerzitná 8215/1, 010 26 Žilina, Slovenská republika.
E-mail: milan.sapieta@fstroj.uniza.sk, Tel.: + 421 41 513 2974

Kinematic analysis of a spatial multibody system

Abstract: The aim of this paper is to present a method of computer formulation and solution of equations of kinematics of spatial mechanical systems. The method of the vector closed loop is generally known way how to build the constraint equations. This method is recommended for planar kinematics. This paper shows the way how to take advantage of the vector cross product, vector magnitude and scalar product of two vectors for getting the constraint equations for spatial mechanism.

ÚVOD

Cieľom výpočtových metód v kinematike a dynamike mechanizmov je vytvoriť metodiku riešení a vhodný počítačový softvér, ktorý inžinierovi umožní zadávať údaje, ktoré špecifikujú mechanické vlastnosti viazaných mechanických systémov. Mali by tu byť automaticky formulované väzobné rovnice kinematiky, automaticky riešené nelineárne rovnice kinematickej odozvy a poskytovaný počítačový grafický výstup výsledkov simulácií a to na analýzu, vyhodnotenie i komunikáciu výstupov s konštruktérom alebo analytikom. Podstatou tohto cieľa je maximálne využiť výkon digitálneho počítača na rýchlu a presnú manipuláciu s dátami a numerickými výpočtami, čím sa inžinier zbaví zdĺhavých riešení náchylných na chyby [1, 2]. Ako naznačujú pokroky v počítačovej analýze pružných telies, pomocou metódy konečných prvkov a analýze elektronických obvodov, na implementáciu výpočtov v používateľsky orientovanom počítačovom programe, je potrebný systematický prístup k formulovaniu a riešeniu rovníc kinematiky a dynamiky mechanických systémov [3-6].

Na konci 60. a začiatkom 70. rokov [7-9] bolo vyvinutých niekoľko počítačových programov pre kinematickú a dynamickú analýzu použijúc medzi telesami relatívne súradnice. Tieto programy sú vhodné pre mnohé aplikácie. Koncom 70. rokov bola predstavená alternatívna metóda formulovania väzobných obmedzení a pohybových rovníc z hľadiska globálnych karteziánskych súradníc [10–12], ktorá obišla topologickú analýzu a uľahčila používateľovi dodávať obmedzenia a väzobné rovnice. Tento prístup vedie k univerzálnemu počítačovému programu, ktorý prakticky nemá nijaké obmedzenie týkajúce sa typu mechanizmu alebo stroja, ktorý je možné analyzovať. Nevýhodou

je však rozsiahlejší systém rovníc, ktoré sa majú vyriešiť [13, 14]. V tomto článku sú v oblasti výpočtovej kinematiky uvedené konkrétne možnosti alternatívnych a kompromisných opatrení.

1 TEORETICKÉ VÝCHODISKÁ

1.1 Vlastnosti geometrických vektorov

Geometrický vektor $\bar{\boldsymbol{a}}$ začínajúci v bode *A* a končiaci v bode *B* je definovaný ako orientovaná úsečka od *A* do *B*. Veľkosť vektora $\bar{\boldsymbol{a}}$ je jeho dĺžka *a* je označená znakom *a* alebo $|\bar{\boldsymbol{a}}|$. Jednotkový vektor, to znamená vektor s veľkosťou 1 jednotky.

Násobenie vektora $\bar{\boldsymbol{a}}$ skalárom $c > 0$ je definované ako vektor v rovnakom smere, ale s veľkosťou $c \cdot a$. Násobenie vektora $\bar{\boldsymbol{a}}$ skalárom $c < 0$ je vektor s veľkosťou $c \cdot a$, ale opačným smerom ako $\bar{\boldsymbol{a}}$.

Skalárny súčin dvoch vektorov $\bar{\boldsymbol{a}}$ a $\bar{\boldsymbol{b}}$ je definovaný ako súčin absolútnych hodnôt vektorov a kosínusu uhla medzi nimi (1):

$$\bar{\boldsymbol{a}} \cdot \bar{\boldsymbol{b}} = \boldsymbol{a} \cdot \boldsymbol{b} \cdot \cos\theta\left(\bar{\boldsymbol{a}}, \bar{\boldsymbol{b}}\right). \tag{1}$$

O dvoch nenulových vektoroch sa hovorí, že sú ortogonálne, ak je ich skalárny súčin nulový. Pre skalárny súčin platia nasledovné vzťahy:

$$\begin{aligned} \bar{\boldsymbol{a}} \cdot \bar{\boldsymbol{i}} &= \boldsymbol{a}_x \\ \bar{\boldsymbol{a}} \cdot \bar{\boldsymbol{j}} &= \boldsymbol{a}_y \\ \bar{\boldsymbol{a}} \cdot \bar{\boldsymbol{k}} &= \boldsymbol{a}_z \end{aligned}, \tag{2}$$

$\bar{\boldsymbol{i}}$, $\bar{\boldsymbol{j}}$ a $\bar{\boldsymbol{k}}$ sú jednotkové vektory, ktoré ležia v smere pozdĺž osí *x, y* a *z*:

$$\bar{\boldsymbol{a}} \cdot \bar{\boldsymbol{b}} = \boldsymbol{a}_x \cdot \boldsymbol{b}_x + \boldsymbol{a}_y \cdot \boldsymbol{b}_y + \boldsymbol{a}_z \cdot \boldsymbol{b}_z, \tag{3}$$

$$\boldsymbol{a} = \sqrt{\bar{\boldsymbol{a}} \cdot \bar{\boldsymbol{a}}}. \tag{4}$$

Vektorový súčin dvoch vektorov $\bar{\boldsymbol{a}}$ a $\bar{\boldsymbol{b}}$ je definovaný ako vektor $\bar{\boldsymbol{c}}$, ktorý spĺňa nasledujúce podmienky:

- Nositeľka vektora $\bar{\boldsymbol{c}}$ je priamka kolmá na rovinu ktorú tvoria vektory vektorov $\bar{\boldsymbol{a}}$ a $\bar{\boldsymbol{b}}$.
- Veľkosť $\bar{\boldsymbol{c}}$ je súčinom absolútnych hodnôt $\bar{\boldsymbol{a}}$ a $\bar{\boldsymbol{b}}$ a sínusu uhla θ tvoreného medzi $\bar{\boldsymbol{a}}$ a $\bar{\boldsymbol{b}}$.

Máme teda $\boldsymbol{c} = \boldsymbol{a} \cdot \boldsymbol{b} \cdot \sin\theta$. Orientáciu vektora $\bar{\boldsymbol{c}}$ poznáme tak, že osoba nachádzajúca sa na špičke $\bar{\boldsymbol{c}}$ bude pozorovať rotáciu predpokladaného pohybu prvého vektora k druhému po kratšej ceste v proti smeru hodinových ručičiek.

Vektorový súčin dvoch vektorov je reprezentovaný matematickým výrazom:

$$\begin{aligned} \bar{\boldsymbol{c}} = \bar{\boldsymbol{a}} \times \bar{\boldsymbol{b}} = &\left(\boldsymbol{a}_y \cdot \boldsymbol{b}_y - \boldsymbol{a}_z \cdot \boldsymbol{b}_z\right) \cdot \bar{\boldsymbol{i}} + \\ &+ \left(\boldsymbol{a}_z \cdot \boldsymbol{b}_x - \boldsymbol{a}_x \cdot \boldsymbol{b}_z\right) \cdot \bar{\boldsymbol{j}} + \left(\boldsymbol{a}_x \cdot \boldsymbol{b}_y - \boldsymbol{a}_y \cdot \boldsymbol{b}_x\right) \cdot \bar{\boldsymbol{k}} \end{aligned}. \tag{5}$$

2 KINEMATICKÉ VÄZOBNÉ ROVNICE

Poloha a orientácia telesa v priestore môže byť definovaná troma bodmi *A, B* a *C*, respektíve dvoma vektormi $\bar{\boldsymbol{r}}_{BA}$ a $\bar{\boldsymbol{r}}_{CA}$ (možné sú aj ďalšie kombinácie). Akákoľvek množina premenných, ktorá jedinečným spôsobom určuje polohu a orientáciu všetkých telies v mechanizme, to znamená konfiguráciu mechanizmu, sa nazýva množina zovšeobecnených súradníc. Zovšeobecnené súradnice môžu byť nezávislé alebo závislé. Zovšeobecnené súradnice sú v tomto článku označené stĺpcovým vektorom:

$$\boldsymbol{q} \equiv \left[\boldsymbol{q}_1, \boldsymbol{q}_2, ..., \boldsymbol{q}_{nc}\right]^T, \tag{6}$$

kde $n \cdot c$ je celkový počet zovšeobecnených súradníc použitých na opis konfigurácie systému.

Telesá mechanizmu sú vzájomne prepojené väzbami a existujú obmedzovacie rovnice, ktoré sa týkajú zovšeobecnených súradníc. Keď sú tieto väzobné podmienky vyjadrené ako algebraické rovnice v zmysle zovšeobecnených súradníc, nazývajú sa tieto holonómne väzobné kinematické rovnice. Systém holonómnych kinematických väzobných rovníc, ktorý nezávisí výslovne od času, možno vyjadriť ako:

$$\boldsymbol{\Phi}^K(\boldsymbol{q}) = \left[\boldsymbol{\Phi}_1^K(\boldsymbol{q}), \boldsymbol{\Phi}_2^K(\boldsymbol{q}), ..., \boldsymbol{\Phi}_{nh}^K(\boldsymbol{q})\right]^T. \tag{7}$$

Rovnice obmedzenia prezentujú geometriu väzby. Ak sú väzobné rovnice 7 konzistentné a nezávislé, potom sa hovorí, že systém má $n \cdot c - n \cdot h$ stupňov voľnosti DOF. Ak sú pre kinematickú analýzu špecifikované obmedzenia nezávislých DOF, označia sa:

$$\boldsymbol{\Phi}^D(\boldsymbol{q}, t) = \boldsymbol{0}. \tag{8}$$

Potom je možné určiť konfiguráciu systému ako funkciu času. To znamená, že kombináciou obmedzovacích rovníc 7 a 8:

$$\boldsymbol{\Phi}(\boldsymbol{q}, t) = \begin{bmatrix} \boldsymbol{\Phi}^K(\boldsymbol{q}) \\ \boldsymbol{\Phi}^D(\boldsymbol{q}, t) \end{bmatrix} = \boldsymbol{0} \tag{9}$$

možno vyriešiť kinematické parametre pre $\boldsymbol{q}(t)$. Hovoríme, že takýto systém je kinematicky poháňaný [14].

3 KINEMATICKÁ ANALÝZA PRIESTOROVÉHO MECHANIZMU

3.1 Väzobné kinematické rovnice vo forme použiteľnej pre MATLAB

Jeden zo spôsobov, ako získať rovnice kinematických väzieb (9), je uvedený v nasledujúcom príklade. Využívame vlastnosti geometrických vektorov.

Obrázok 1 zobrazuje trojrozmerný štvorčlenný mechanizmus RSCR (Revolute-Sferical-Cylindrical-Revolute) modelovaný s prirodzenými súradnicami

[14]. Tento mechanizmus má tri pohyblivé jednotkové vektory; to znamená dvanásť závislých karteziánskych súradníc a jeden stupeň voľnosti. Tiež bol zavedený vstupný uhol ψ ako ďalšia externe poháňaná súradnica.

- Vstupné konštanty:

$\boldsymbol{I}_{BA}$, $\boldsymbol{I}_{CB}$, $\boldsymbol{I}_{DE}$, φ_2, φ_3, φ_4 a φ_5 a jednotkové vektory $\boldsymbol{u}_A$ a $\boldsymbol{u}_E$. Vektor $\boldsymbol{r}_{A0}$ je v rovine *xy*. Súradnice bodov *A* a *E*.

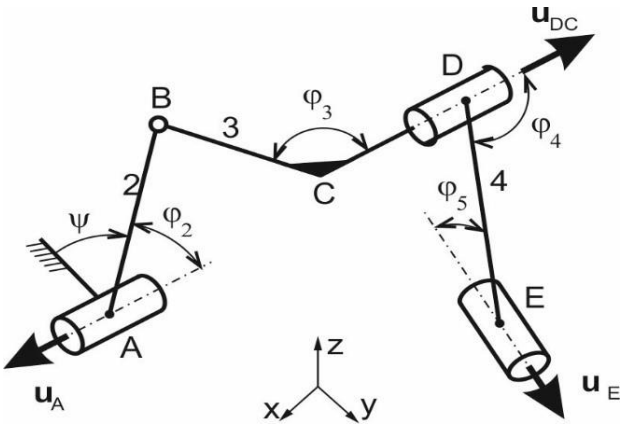

Obr. 1. Trojrozmerný štvorčlenný mechanizmus RSCR

Najskôr napíšeme rovnice pre jednotkový vektor $\boldsymbol{r}_{A0}$:

- Iba dve neznáme konštanty:

$$\boldsymbol{r}_{A0} = \left(\boldsymbol{r}_{A0x}, \boldsymbol{r}_{A0y}, 0\right). \tag{10}$$

- Vektor $\boldsymbol{r}_{A0}$ musí byť kolmý na $\boldsymbol{u}_A$:

$$\boldsymbol{r}_{A0} \cdot \boldsymbol{u}_A^T = 0. \tag{11}$$

- $\boldsymbol{r}_{A0}$ je jednotkový vektor:

$$\left|\boldsymbol{r}_{A0}\right| - \boldsymbol{1} = \boldsymbol{0}. \tag{12}$$

Máme dve rovnice pre dve neznáme zložky $\boldsymbol{r}_{A0}$.

Prvok 2 sa otáča okolo osi opísanej vektorom $\boldsymbol{u}_A$. Jeho pohyb je úplne definovaný:

- Väzobná rovnica ψ:

$$-\boldsymbol{r}_{A0} \cdot \boldsymbol{r}_{BA}^T - \boldsymbol{I}_{A0} \cdot \cos\psi = \boldsymbol{0}. \tag{13}$$

- Rotačná väzba, uhol φ_2 je konštantný:

$$\boldsymbol{u}_A \cdot \boldsymbol{r}_{BA}^T \cdot \cos\varphi_2 = \boldsymbol{0}. \tag{14}$$

- Vzdialenosť bodov *A* a *B* je konšt. $\boldsymbol{I}_{BA}$:

$$\boldsymbol{r}_{BA} \cdot \boldsymbol{r}_{BA}^T - \boldsymbol{I}_{BA}^2 = \boldsymbol{0}. \tag{15}$$

Pohyb prvkov 3 a 4 je úplne definovaný:

- Vzdialenosť bodov *B* a *C* je konštantná $\boldsymbol{I}_{CB}$:

$$\boldsymbol{r}_{CB} \cdot \boldsymbol{r}_{CB}^T - \boldsymbol{I}_{CB}^2 = \boldsymbol{0}. \tag{16}$$

- Člen 3 je zalomený, uhol φ_3 je konštantný:

$$\boldsymbol{u}_{DC} \cdot \boldsymbol{r}_{CB}^T - \boldsymbol{I}_{CB}^2 \cdot \cos\varphi_3 = \boldsymbol{0}. \tag{17}$$

- $\boldsymbol{u}_{DC}$ je jednotkový vektor:

$$\boldsymbol{u}_{DC} \cdot \boldsymbol{u}_{DC}^T - 1 = \boldsymbol{0}. \tag{18}$$

- Vzdialenosť bodov *D* a *E* je konštantná $\boldsymbol{I}_{DE}$:

$$\boldsymbol{r}_{DE} \cdot \boldsymbol{r}_{DE}^T - \boldsymbol{I}_{DE}^2 = \boldsymbol{0}. \tag{19}$$

- Rotačný kĺb, uhol φ_4 je konštantný:

$$\boldsymbol{u}_{DC} \cdot \boldsymbol{r}_{DE}^T - \boldsymbol{I}_{DE}^2 \cdot \cos\varphi_4 = \boldsymbol{0}. \tag{20}$$

- Rotačný kĺb, uhol φ_5 je konštantný:

$$\boldsymbol{u}_E \cdot \boldsymbol{r}_{DE}^T - \boldsymbol{I}_{DE}^2 \cdot \cos\varphi_5 = \boldsymbol{0}. \tag{21}$$

- Rotačný kĺb, uhol φ_6 je konštantný:

$$\boldsymbol{u}_E \cdot \boldsymbol{r}_{DC}^T - \boldsymbol{I}_{DC}^2 \cdot \cos\varphi_6 = \boldsymbol{0}. \tag{22}$$

- Cylindrické spojenie, vektory $\boldsymbol{u}_{DC}$ a $\boldsymbol{r}_{DC}$ sú závislé:

$$\boldsymbol{r}_{DC} \times \boldsymbol{u}_{DC} = \boldsymbol{0}. \tag{23}$$

Vektorový súčin (23) predstavuje tri skalárne rovnice, z ktorých iba dve sú nezávislé.

Vektory v rovniciach (10 - 23) možno formulovať pomocou troch bodov *B*, *C* a *D* (9 neznámych premenných) a jedného jednotkového vektora $\boldsymbol{u}_{DC}$ (tri neznáme premenné). Máme dvanásť nelineárnych rovníc pre dvanásť neznámych premenných.

Rovnica (9) má pre náš príklad tvar (24):

$$\boldsymbol{\Phi}(\boldsymbol{q},t) = \begin{bmatrix} \boldsymbol{r}_{A0} \cdot \boldsymbol{r}_{BA}^T - \boldsymbol{I}_{A0} \cdot \cos\psi \\ \left\|\boldsymbol{r}_{BA}\right\| - \boldsymbol{I}_{BA} \\ \boldsymbol{u}_A \cdot \boldsymbol{r}_{BA} - \boldsymbol{I}_{BA} \cdot \cos\varphi_2 \\ \left\|\boldsymbol{r}_{CB}\right\| - \boldsymbol{I}_{CB} \\ \boldsymbol{u}_{DC} \cdot \boldsymbol{r}_{CB} - \boldsymbol{I}_{CB} \cdot \cos\varphi_3 \\ \left\|\boldsymbol{r}_{DC}\right\| - \boldsymbol{1} \\ \left\|\boldsymbol{r}_{DE}\right\| - \boldsymbol{I}_{DE} \\ \boldsymbol{u}_{DC} \cdot \boldsymbol{r}_{DE} - \boldsymbol{I}_{DE} \cdot \cos\varphi_4 \\ \boldsymbol{u}_E \cdot \boldsymbol{r}_{DE} - \boldsymbol{I}_{DE} \cdot \cos\varphi_5 \\ \boldsymbol{u}_E \cdot \boldsymbol{u}_{DC} - \cos\varphi_6 \\ ry_{DC} \cdot uz_{DC} - rz_{DC} \cdot uy_{DC} \\ rz_{DC} \cdot ux_{DC} - rx_{DC} \cdot uz_{DC} \\ \psi - \psi(t) \end{bmatrix} = \boldsymbol{0} \cdot \tag{24}$$

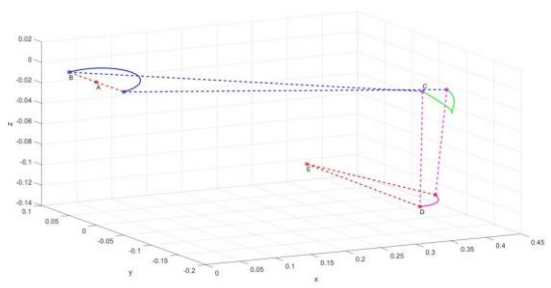

Obr. 2. Polohy mechanizmu

4 MATLAB súbory

4.1 Main script

```
% vstupné parametre
l = [1,0.05,0.4,0.15];     % vektor
konštantných dĺžok, [l_AO, l_BA,
l_CB, l_DE]
gfi = [0,90,90,90,95,15]*pi/180;  %
vektor konštantných uhlov, [blank,
fi_2, fi_3, fi_4, fi_5, fi_6]
om_psi = 30;  % [rad/s] uhlová
rýchlosť člena 2
xA=[0,0,0];
xE=[0.3,0,-0.1];    % súradnice
bodov A, E
u_A=[-0.13,0,1];
u_A=u_A/norm(u_A); % jednotkový
vektor - os rotácie v bode A
u_E=[0.1,0,1 ];
u_E=u_E/norm(u_E);% jednotkový
vektor - os rotácie v bode E
if u_A(2)==0
   r_A0=[0,1,0];
else
    r_A0=[1,-u_A(1)/u_A(2),0];  %
jednotkový vektor - nulová priamka
- nulová priamka pre uhol <;/
    r_A0=r_A0/norm(r_A0);
end
% prvá aproximácia neznámych
súradníc pre nelineárne riešenie v
prvej polohe
xB0=[0.00, 0.05, 0.00];
xC0=[0.30,-0.16, 0.00];
xD0=[0.35,-0.12, 0.11];
uDC0=[-0.10,-0.16,1];
uDC0=uDC0/norm(uDC0);
x_0=[xB0,xC0,xD0,uDC0]; % neznámy
vektor pre rovnicu 20
v_psi=(90:3:450)*pi/180;     %
vector nezávislých premenných rp
pre riešený interval
sp=size(v_psi);
s_psi=sp(2); % riešené pozície
mechanizmu
for kp = 1:s_psi     % hlavná slučka
riešenia_psi(kp);
xp=fsolve(@mech3Dr,x_0,[],psi,r_A0,
xA,xE,u_A,u_E,l,gfi);
    xB(kp,1:3)=xp(1:3);
    xC(kp,1:3)=xp(4:6);
    xD(kp,1:3)=xp(7:9);
    u_DC(kp,1:3)=xp(10:12);
    x_0=xp; % aproximácia neznámych
súradníc pre nasledujúcu hodnotu
psi
end
```

4.2 Function fsolve

```
function
y=mech3Dr(x,psi,r_A0,xA,xE,u_A,u_E,
l,gfi)
% vyjadrenie vektorov pre rovnice
9-19
y=zeros(1,12);
r_BA=x(1,1:3)-xA;
r_CB=x(1,4:6)-x(1,1:3);
r_DC=x(1,7:9)-x(1,4:6);
r_DE=x(1,7:9)-xE;
u_DC=x(1,10:12);
y(1) = -r_BA*r_A0'-cos(psi)*l(2);
y(2) = r_BA*r_BA'-l(2)^2;
y(3) = u_A*r_BA'-cos(gfi(2))*l(2);
y(4) = r_CB*r_CB'-l(3)^2;
y(5)=u_DC*r_CB'-l(3)*cos(gfi(3));
y(6)=u_DC*u_DC'-1;
y(7)=r_DE*r_DE'-l(4)^2;
y(8)=u_DC*r_DE'-l(4)*cos(gfi(4));
y(9)=u_E*r_DE'-l(4)*cos(gfi(5));
y(10)=u_E*u_DC'-cos(gfi(6));
yp=cross(r_DC,u_DC);
y(11:12)=yp(1:2);
```

ZÁVER

Záverom treba povedať, že rovnice 10 a 11 môžu byť nahradené jednou rovnicou, ktorá explicitne určuje vektor. Rovnice 12 a 14 je lepšie nahradiť explicitný vzťah pomocou rotačnej transformačnej matice. Tieto zlepšenia nám prinášajú znižovanie počtu nelineárnych rovníc.

Poďakovanie

Tento príspevok bol podporený projektom VEGA grant No.1/0141/20 a VEGA grant No. 1/0510/20.

LITERATÚRA

[1] PIEKARSKA, W. - KUBIAK, M. - VAŠKO, M. (2017): *Numerical estimation of the shape of weld and heat affected zone in laser-arc hybrid welded joints.* Procedia Engineering, Vol. 177, pp. 114-120, DOI: 10.1016/j.proeng.2017.02.198.

[2] JAKUBOVIČOVÁ, L. - SÁGA, M. - VAŠKO,

M. (2014): *Numerical study of influence of mutual slewing of roller bearing rings on the principal stresses at contact area.* Scientific journal of Silesian University of Technology – Series Transport, Vol. 84, pp. 83-91.

[3] KOPAS, P. - SÁGA, M. - BANIARI, V. - VAŠKO, M. - HANDRIK, M. (2017): *A plastic strain and stress analysis of bending and torsion fatigue specimens in the low-cycle fatigue region using the finite element methods.* Procedia Engineering, Vol. 177, pp. 526-531, DOI: https://10.1016/j.proeng.2017.02.256.

[4] JAKUBOVICOVA, L. - VASKO, M. - SAGA, M. - KOPAS, P. - NOVAK, P. - HANDRIK, M. (2019): *Design and stress analysis of wheeled compactor construction.* MATEC Web of Conferences, Vol. 254, pp. 1-10, DOI:ttps://doi.org/10.1051/matecconf/20192540201.

[5] KUKUCA, P. - BARTA, D. - DIZO, J. - CABAN, J. (2018): *Piston kinematics of a combustion engine with unconventional crank mechanism.* MATEC Web of Conferences, Vol. 244, pp. 1-7, DOI: 10.1051/matecconf/201824403006.

[6] VAVRO, J. Jr. - VAVRO, J. - KOVACIKOVA, P. - BEZDEDOVA, R. (2017): *Kinematic and dynamic analysis of planar mechanisms by means of the Solid Works software.* Procedia Engineering, Vol. 177, pp. 476-481, DOI: 10.1016/j.proeng.2017.02.248.

[7] PAUL, B. - KRAJCINOVIC, D. (1970): *Computer Analysis of Machines with Planar Motion-Part I: Kinematics., Part II: Dynamics*. Journal of Applied Mechanics, Vol. 37, pp. 697-712.

[8] CHACE, M. A - SMITH, D. (1971): *DAMN-A Digital Computer Program for the Dynamic Analysis Of Generalized Mechanical Systems.* SAE International, Vol. 80, No. 2, pp. 969-991.

[9] SHETH, P. N. - UICKER, J. J., Jr. (1972): *IMP (Integrated Mechanisms Program).* A Computer Aided Design Analysis for Mechanisms and Linkages. Journal of Engineering for Industry, Vol. 94, pp. 454-464.

[10] ORLANDEA, N. - CHACE, M. A. - CALAHAN, D. A. (1977): *A Sparsity-Oriented Approach to the Dynamic Analysis and Design of Mechanical Systems - Parts I and II*. Journal of Engineering for Industry, Vol. 99, pp. 773-784.

[11] WEHAGE, R. A. - HAUG, E. J. (1982): *Generalized Coordinate Partitioning for Dimension Reduction in Analysis of Constrained Dynamic Systems.* Journal of Mechanical Design, Vol. 104, No. 1, pp. 247-255.

[12] CHUNG, I. S. - CHANG, CH. O. - HUNG, E. - WEHAGE, R. A. - BECK, R. R. (1981): *Dynamic Analysis of Three Dimensional Constrained Mechanical Systems Using Euler Parameters.* Technical Report 81-11, Center for Computer Aided Design.

[13] DE JALON, G. - J. G., BAYO, J. - EDUARDO (1993): *Kinematic and Dynamic Simulation of Multibody Systems.* 2. Edn. Springer-Verlag, Springer-Verlag, New York.

[14] HAUG, E. J. (1989): *Computer-Aided Kinematics and Dynamics of Mechanical systems.* 1. Edn. Allyn and Bacon, Massachusetts.